

UC Irvine

UC Irvine Electronic Theses and Dissertations

Title

Preparation, Conjugation, and Stabilization of Amyloid- β Peptides

Permalink

<https://escholarship.org/uc/item/2n66n7xf>

Author

Zhang, Sheng

Publication Date

2021

Peer reviewed|Thesis/dissertation

UNIVERSITY OF CALIFORNIA,
IRVINE

Preparation, Conjugation, and Stabilization of Amyloid- β Peptides

DISSERTATION

submitted in partial satisfaction of the requirements
for the degree of

DOCTOR OF PHILOSOPHY

in Chemistry

by

Sheng Zhang

Dissertation Committee:
Professor James S. Nowick, Chair
Professor Jennifer A. Prescher
Professor David Van Vranken

2021

DEDICATION

To my girlfriend, Fangfei Huo. Thank you for your love and support in the last ten years.

TABLE OF CONTENTS

LIST OF FIGURES	iv
LIST OF TABLES	viii
ACKNOWLEDGEMENTS	x
CURRICULUM VITAE	xii
ABSTRACT OF THE DISSERTATION	xviii
CHAPTER 1: An Efficient Method for the Expression and Purification of A β _(M1-42)	1
CHAPTER 2: Expression of N-Terminal Cysteine A β ₄₂ and Conjugation to Generate Fluorescent and Biotinylated A β ₄₂	48
CHAPTER 3: Preparation and Studies of a Disulfide-Stapled A β that Forms Dimers but Does Not Form Fibrils	132
CHAPTER 4: Structure-Based Drug Design of an Inhibitor of the SARS-CoV-2 Main Protease	186

LIST OF FIGURES

	Page
Figure 1.1 Sequences of A β ₍₁₋₄₂₎ and A β _(MC1-42)	2
Figure 1.2 Purification and characterization of A β _(M1-42)	6
Figure 1.3 MALDI mass spectra and NMR spectra of unlabeled and ¹⁵ N-labeled A β _(M1-42)	8
Figure 1.4 Molecular cloning strategy for constructing recombinant plasmids of A β _(M1-42) containing familial mutations	9
Figure 1.5 MALDI mass spectra and typical yields of A β peptides	10
Figure 1.S1 HPLC trace of filtered urea-solubilized A β _(M1-42) and silver-stained SDS-PAGE gel of HPLC fractions	22
Figure 1.S2 UV absorption spectra of A β _(M1-42) at different pH	25
Figure 1.S3 Design of the DNA sequences for A β _(M1-42) mutants	29
Figure 1.S4 Analytical HPLC and MALDI-MS traces of A β _(M1-42)	35
Figure 1.S5 Analytical HPLC and MALDI-MS traces of ¹⁵ N-labeled A β _(M1-42)	37
Figure 1.S6 Analytical HPLC and MALDI-MS traces of A β _(M1-42/A21G)	39
Figure 1.S7 Analytical HPLC and MALDI-MS traces of A β _(M1-42/E22G)	41
Figure 1.S8 Analytical HPLC and MALDI-MS traces of A β _(M1-42/E22K)	44
Figure 1.S9 Analytical HPLC and MALDI-MS traces of A β _(M1-42/D23N)	46
Figure 2.1 Sequences of A β ₍₁₋₄₂₎ , A β _(MC1-42) , and A β _(C1-42)	50
Figure 2.2 Characterization of A β _(C1-42)	53
Figure 2.3 Conjugation of A β _(C1-42) with maleimide reagents and structures of labeled A β products	57
Figure 2.4 MALDI mass spectra of fluorophore and biotin labeled A β _(C1-42)	58
Figure 2.5 Analytical HPLC traces of purified fluorescent and biotin labeled A β _(C1-42)	59
Figure 2.6 UPLC-MS ^E total ion current chromatogram of 5-TAMRA-A β _(C1-42) digested with proteinase K	60

Figure 2.7	SDS-PAGE of labeled $A\beta_{(C1-42)}$ and $A\beta_{(M1-42)}$ at a range of concentrations, visualized by silver staining and fluorescence imaging	61
Figure 2.8	ThT fluorescence assays and fluorescence suppression assays of labeled $A\beta_{(C1-42)}$ and $A\beta_{(M1-42)}$	63
Figure 2.9	Transmission electron micrographs of fibrils formed by $A\beta$ peptides	64
Figure 2.10	Atomic force micrographs of fibrils formed by $A\beta$ peptides	65
Figure 2.11	Fluorescence micrographs of labeled $A\beta$ with mammalian cells and bacteria	67
Figure 2.S1	Design of the DNA sequence for $A\beta_{(MC1-42)}$	89
Figure 2.S2	Representative HPLC trace of filtered, unpurified $A\beta_{(C1-42)}$	95
Figure 2.S3	Representative HPLC trace of basified combined pure fractions of $A\beta_{(C1-42)}$	101
Figure 2.S4	Representative analytical HPLC trace of unpurified TAMRA-labeled $A\beta$	103
Figure 2.S5	Representative analytical HPLC trace of unpurified FAM-labeled $A\beta$	104
Figure 2.S6	Representative analytical HPLC trace of unpurified biotin-labeled $A\beta$	105
Figure 2.S7	Representative analytical HPLC trace of $A\beta_{(C1-42)}$	118
Figure 2.S8	Representative MALDI mass spectrum of $A\beta_{(C1-42)}$	119
Figure 2.S9	Representative MS/MS spectrum of $A\beta_{(C1-42)}$	120
Figure 2.S10	Representative analytical HPLC trace of 5-TAMRA- $A\beta_{(C1-42)}$	121
Figure 2.S11	Representative MALDI mass spectrum of 5-TAMRA- $A\beta_{(C1-42)}$	122
Figure 2.S12	Representative analytical HPLC trace of 6-FAM- $A\beta_{(C1-42)}$	123
Figure 2.S13	Representative MALDI mass spectrum of 6-FAM- $A\beta_{(C1-42)}$	124
Figure 2.S14	Representative analytical HPLC trace of PEG ₂ -biotin- $A\beta_{(C1-42)}$	125
Figure 2.S15	Representative MALDI mass spectrum of PEG ₂ -biotin- $A\beta_{(C1-42)}$	126
Figure 2.S16	ThT fluorescence assays and fluorescence suppression assays of labeled $A\beta_{(C1-42)}$ and $A\beta_{(M1-42)}$	127
Figure 2.S17	Fluorescence micrographs of labeled $A\beta$ with mammalian cells (low magnification views)	128
Figure 2.S18	Transmission electron micrographs of the fibrils formed by $A\beta$ peptides	129
Figure 2.S19	Atomic force micrographs of the fibrils formed by $A\beta$ peptides	130
Figure 3.1	Cartoons of covalent $A\beta$ dimer generated by intermolecular disulfide bridges and non-covalent $A\beta$ dimer generated by intramolecular disulfide bridges	133

Figure 3.2	Cartoons of mutant A β peptides that are constrained in β -hairpin conformation by intermolecular disulfide bridges	135
Figure 3.3	SDS-PAGE studies of the oligomerization propensities of the disulfide-stapled A β peptides	137
Figure 3.4	SDS-PAGE studies of A β _{C18C33} before and after TCEP reduction at various concentrations	138
Figure 3.5	SEC-MS studies of A β _{C18C33} peptide	140
Figure 3.6	IM-MS studies of A β _{C18C33} peptide	141
Figure 3.7	CD spectra of A β _{C18C33} and A β _(M1-42) in the absence or in the presence of SDS	142
Figure 3.8	CD spectra of A β _{C18C33} and A β _(M1-42) in the presence of DDM	144
Figure 3.9	ThT fluorescence assay results of A β _{C18C33} , A β _(M1-42) , and A β _{C18C33}	146
Figure 3.10	Transmission electron micrographs of A β peptides	147
Figure 3.11	Dynamic light scattering experiments of A β _{C18C33} and A β _(M1-42) peptides	148
Figure 3.S1	Design of the DNA sequences for A β _(MC1-42) mutants	163
Figure 3.S2	Molecular cloning strategy for constructing recombinant plasmids of A β _(MC1-42) mutants	164
Figure 3.S3	An analytical HPLC trace of A β _{C21C30} peptide	175
Figure 3.S4	An analytical HPLC trace of A β _{C21C32} peptide	176
Figure 3.S5	An analytical HPLC trace of A β _{C24C29} peptide	177
Figure 3.S6	An analytical HPLC trace of A β _{C21C31} peptide	178
Figure 3.S7	An analytical HPLC trace of A β _{C18C33} peptide	179
Figure 3.S8	MALDI-TOF mass spectra of A β _{C21C30} peptide	180
Figure 3.S9	MALDI-TOF mass spectra of A β _{C21C32} peptide	181
Figure 3.S10	MALDI-TOF mass spectra of A β _{C24C29} peptide	182
Figure 3.S11	MALDI-TOF mass spectra of A β _{C21C31} peptide	183
Figure 3.S12	MALDI-TOF mass spectra of A β _{C18C33} peptide	184
Figure 3.S13	Analytical ultracentrifugation studies of A β _{C18C33} peptide	185
Figure 4.1	Amide bond hydrolysis by a protease enzyme and binding of a protease to a polypeptide substrate	187
Figure 4.2	Proteolysis mechanism by the catalytic dyad of M ^{pro}	189

Figure 4.3	The interaction between the substrate and the active site of the protein	191
Figure 4.4	Building the cyclic peptide	193
Figure 4.5	Geometry optimization of the cyclic peptide inhibitor	195
Figure 4.6	Molecular docking of the geometry-optimized cyclic peptide inhibitor to SARS-CoV M ^{pro}	197
Figure 4.7	Molecular docking of the geometry-optimized cyclic peptide inhibitor to SARS-CoV-2 M ^{pro}	198

LIST OF TABLES

	Page
Table 1.1 Effect of different syringe filters on A β _(M1-42) recovery	4
Table 1.S1 M9 minimal media	19
Table 1.S2 A representative schedule for expression of A β _(M1-42)	25
Table 1.S3 A representative schedule for expression of ¹⁵ N-labeled A β _(M1-42)	25
Table 1.S4 Double-digestion of the pET- Sac A β _(M1-42) plasmid	29
Table 1.S5 SAP treatment of the vectors	30
Table 1.S6 Double-digestion of the inserts	31
Table 1.S7 T4 ligation of the inserts and the vectors	31
Table 2.S1 Restriction enzyme digestion of the pET- Sac A β _(M1-42) plasmid	88
Table 2.S2 rSAP treatment of the vector backbones	88
Table 2.S3 Restriction enzyme digestion of the A β _(MC1-42) DNA fragment	90
Table 2.S4 T4 ligation of the insert and the vector	91
Table 2.S5 Representative schedule for the expression, purification, and labeling of A β _(C1-42)	92
Table 2.S6 HPLC solvent gradient for the purification of A β _(C1-42)	96
Table 2.S7 Prep-HPLC column cleaning protocol	96
Table 2.S8 Reagent table for labeling A β _(C1-42) with maleimide-5-TAMRA	99
Table 2.S9 Recipe of making 750 mM sodium borate buffer (pH 9.0)	99
Table 2.S10 Titration of a 1.0 mL portion of the combined HPLC fractions of A β _(C1-42)	100
Table 2.S11 Basification of the remainder of the combined HPLC fractions of A β _(C1-42)	101
Table 2.S12 Analytical HPLC retention time	105
Table 2.S13 HPLC solvent gradient for the purification of labeled-A β _(C1-42)	106
Table 2.S14 Typical purities of labeled-A β _(C1-42) peptides	107
Table 2.S15 Typical yields of labeled-A β _(C1-42) peptides	108
Table 2.S16 Volumes of HFIP peptide solution per aliquot	109

Table 3.S1	Double-digestion of the pET- Sac A $\beta_{(M1-42)}$ plasmid	164
Table 3.S2	SAP treatment of the vectors	165
Table 3.S3	Double-digestion of the inserts	166
Table 3.S4	T4 ligation of the inserts and the vectors	166

ACKNOWLEDGEMENTS

I would like to express my deepest appreciation to my research advisor, Professor James S. Nowick. Even before starting at UCI, I hoped to have him as my research advisor. I am glad that I joined his group; that was one of the best decisions I have ever made. James is a phenomenal research advisor. I appreciate that he is so supportive of both my research and career development. He helped me learn how to think, work, and write like a Ph.D. scientist. Because he cares about science and his students so much, he made my life in his research group so enjoyable. I would not have made it to this point without his unconditional support.

I would like to thank my thesis committee members, Professor Jennifer A. Prescher and Professor David Van Vranken. Jennifer's Chem 219 lectures are so helpful and informative, which helped me build a solid foundation for my doctoral research in the field of chemical biology. I used to dread arrow pushing as tedious and opaque, but David made it such an informative experience through his Chem 201 lectures. Jennifer and David have also provided valuable advice during and after my advancement to candidacy exam. Thank you for your help throughout my doctoral studies.

I would like to thank my labmates. Dr. Adam Kreutzer is such an intelligent and friendly chemical biologist who has provided guidance and encouragement throughout my Ph.D. studies. Dr. Stan Yoo and I have worked closely to establish a protein expression and purification system for the first time in our research group. We started from generating a sterile area on our bench using a Bunsen burner, to providing our expressed and purified proteins to research groups around the world. Dr. Kevin Chen was my mentor when I joined the research group, and he made the first year of my Ph.D. studies so much easier. Tuan Samdin, Xing Li, and Maj Krumberger have always

been nice friends of mine to talk, vent, and cry to. It was a pleasant experience to work together with Chris Dickson in the last few months of my doctoral studies – I wish I could work with him for a longer time. My undergraduate and high-school mentees, Jonathan Lin, Hannah Jusuf, Grace Huizar, and Timothy Bierlein have always helped with my projects without hesitation. I would like to thank Dr. Hyunjun Yang, Gretchen Guaglianone, Sepehr Haerian, Dr. Michael Morris, Chelsea Parrocha, Dr. William Howitz, and many other current and previous lab members for their help and support.

I would like to thank my friends and helpers at UCI. Chao Gao has been an incredible friend; we went through many together in our doctoral studies. Ben Katz has kindly helped me with conducting mass spectrometry research and we have worked on many fascinating mass spectrometry-related projects. I would like to thank Dr. Dmitry Fishman, Dr. Li Xing, Dr. Jianguo Zheng, Dr. Felix Grun, Dr. Philip Dennison, Dr. Celia Goulding, and Dr. Rachel Martin for their advice and help. I would like to thank members of the Martin, Prescher, Tsai, Liu, Weiss, Goulding, and Spitale laboratories for providing helpful advice and access to equipment.

I would like to thank my parents, my grandparents, my aunt, my cousin, and other family members for their support.

Lastly, thank you, Fangfei, for your love and support in the last ten years.

CURRICULUM VITAE

Sheng Zhang

EDUCATION

Ph.D., Chemistry, **University of California Irvine** 2016–2021

Master's, Biotechnology **California State University Fresno** 2014–2016

B.S., Biotechnology **East China University of Science and Technology** 2010–2014

RESEARCH EXPERIENCE

2016–2021 Graduate Student Researcher with Professor James S. Nowick. University of California Irvine.

2014–2016 Graduate Student Researcher with Professor Qiao-Hong Chen. California State University Fresno.

2010–2014 Undergraduate Student Researcher with Professor Hui-Zhan Zhang. East China University of Science and Technology.

AWARDS

2021 Department of Chemistry Graduate Dissertation Fellowship

2020 Department of Chemistry Travel Award

2018 Peptide Therapeutics Symposium Travel Award

2016 Outstanding Graduate Student: Department of Chemistry

2016 Outstanding Graduate Student: Graduate Education Awareness and Recognition

2015 Liliane D. Wells Scholarship

2015 Faculty Sponsored Student Research Award

2015 Graduate Research Fellowship

2015 Associated Students, Inc. Research Grant

2015 California State University NSF Innovation Corps Grant

2015 College of Science and Mathematics Dean's Scholarship Tuition Waiver

PUBLICATIONS

10. **Sheng Zhang**, Stan Yoo, Benjamin Katz, Adam G. Kreutzer, and James S. Nowick*. A disulfide-stapled A β that forms dimers but does not form fibrils. In preparation for submission to *ACS Chemical Neuroscience* **2021**.

9. **Sheng Zhang**, Gretchen Guaglianone, Michael Morris, Stan Yoo, William J. Howitz, Hannah Jusuf, Grace Huizar, Jonathan Lin, Adam G. Kreutzer, and James S. Nowick*. Expression of N-terminal cysteine A β 42 and bioconjugation to generate fluorescent and biotinylated A β 42. *Biochemistry* **2021**, *60*, 1191–1200.

8. **Sheng Zhang**, Maj Krumberger[‡], Michael Morris[‡], Chelsea Parrocha, Adam Kreutzer, and James S. Nowick*. Structure-based drug design of an inhibitor of the SARS-COV-2 (COVID-19) main protease using free software: a tutorial for students and scientists. *European Journal of Medicinal Chemistry* **2021**, *218*, 11390.

7. Stan Yoo[‡], **Sheng Zhang**[‡] (co-first author), Adam G. Kreutzer, and James S. Nowick*. An efficient method for the expression and purification of A β (M1–42), *Biochemistry* **2018**, *57*, 3861–3866,

6. Bao Vue, **Sheng Zhang**, Andre Vignau, Guanglin Chen, Xiaojie Zhang, William Diaz, Qiang Zhang, Shilong Zheng, Guangdi Wang, and Qiao-Hong Chen*. O-Aminoalkyl-O-trimethyl-2,3-dehydrosilybins: synthesis and in vitro effects towards prostate cancer cells, *Molecules* **2018**, *23*: 3142.

5. Bao Vue, Xiaojie Zhang, Timmy Lee, Nandini Nair, **Sheng Zhang**, Guanglin Chen, Qiang Zhang, Shilong Zheng, Guangdi Wang, and Qiao-Hong Chen*. 5- or/and 20-O-Alkyl-2,3-dehydrosilybins: synthesis and biological profiles on prostate cancer cell models. *Bioorganic & Medicinal Chemistry* **2017**, *25*: 4845–4854.

4. **Sheng Zhang**, Bao Vue, Michael Huang, Xiaojie Zhang, Timmy Lee, Guanglin Chen, Qiang Zhang, Shilong Zheng, Guangdi Wang, and Qiao-Hong Chen*. 3-O-Alkyl-2,3-Dehydrosilibinins:

two synthetic approaches and in vitro effects toward prostate cancer cells, *Bioorganic & Medicinal Chemistry Letters* **2016**, *26*, 3226–3231.

3. Bao Vue, **Sheng Zhang**, Xiaojie Zhang, Konstantinos Parisi, Qiang Zhang, Shilong Zheng, Guangdi Wang, and Qiao-Hong Chen*. Silibinin derivatives as anti-prostate cancer agents: synthesis and cell-based evaluations. *European Journal of Medicinal Chemistry* **2016**, *109*, 36–46.

2. Bao Vue, **Sheng Zhang**, and Qiao-Hong Chen*. Flavonoids with therapeutic potential in prostate cancer. *Anti-Cancer Agents in Medicinal Chemistry* **2016**, *16*, 1205–1229.

1. Bao Vue, **Sheng Zhang**, and Qiao-Hong Chen*. Synergistic effects of dietary natural products as anti-prostate cancer agents. *Natural Product Communications* **2015**, *10*, 2179–2188.

CONFERENCE PROCEEDINGS

20. **Sheng Zhang**, Stan Yoo, Michael Morris, Gretchen E. Guaglianone, Hannah Jusuf, Grace Huizar, Jonathan Lin, Adam G. Kreutzer, James S. Nowick, Expression of N-terminal cysteine A β 42 and bioconjugation to generate fluorescent A β 42, The 260th American Chemical Society National Virtual Meeting & Exposition, August 17–20, 2020.

19. **Sheng Zhang**, Stan Yoo, Gretchen E. Guaglianone, Michael Morris, Hannah Jusuf, Grace Huizar, Jonathan Lin, Adam G. Kreutzer, James S. Nowick, An efficient expression and bioconjugation system for N-terminal fluorophore-labeled A β peptides, Gordon Research Conference: Chemistry and Biology of Peptides (GRC), Ventura, California, USA, February 9–14, 2020.

18. **Sheng Zhang**, Stan Yoo, Gretchen E. Guaglianone, Michael Morris, Hannah Jusuf, Grace Huizar, Jonathan Lin, Adam G. Kreutzer, James S. Nowick, An efficient expression and bioconjugation system for N-terminal fluorophore-labeled A β peptides, Gordon Research Seminar: Chemistry and Biology of Peptides (GRS), Ventura, California, USA, February 8–9, 2020.

17. Stan Yoo, **Sheng Zhang**, Adam G. Kreutzer, and James S. Nowick, Facile access to A β peptides and studies of stapled and labeled analogues, The 26th American Peptide Symposium, Monterey, California, USA, June 22–27, 2019.
16. **Sheng Zhang**, Stan Yoo, Adam G. Kreutzer, and James S. Nowick, The expression and Characterization of Disulfide-Bond Stabilized A β oligomers, The 13th Annual Peptide Therapeutics Symposium, La Jolla, California, USA, October 25–26, 2018.
15. Stan Yoo, **Sheng Zhang**, Adam G. Kreutzer, and James S. Nowick, An efficient method for the expression and purification of A β (M1–42) and N-terminal Cysteine A β (1–42), The 13th Annual Peptide Therapeutics Symposium, La Jolla, California, USA, October 25–26, 2018.
14. Bao Vue, **Sheng Zhang**, Andre Vignau, Guanglin Chen, Xiaojie Zhang, Qiaohong Chen, Nitrogen-containing derivatives of O-trimethyl-2, 3-dehydrosilybin: Design, synthesis, and in vitro evaluation in prostate cancer cell models, The 255th American Chemical Society National Meeting & Exposition, New Orleans, Louisiana, USA, March 18–22, 2018.
13. **Sheng Zhang**, Stan Yoo, Adam G. Kreutzer, and James S. Nowick, Expression and purification of wild type and beta-hairpin-pinched Amyloid beta proteins, OCACS meeting, Irvine, California, USA, September 28, 2017.
12. Bao Vue, **Sheng Zhang**, Xiaojie Zhang, Michael Huang, Timmy Lee, Guangli Chen, Qiaohong Chen, Potential of silibinin derivatives in prostate cancer managements, The 252nd American Chemical Society National Meeting & Exposition, Philadelphia, Pennsylvania, USA, August 21–25, 2016.
11. **Sheng Zhang**, Development of Silibinin Derivatives as Chemotherapeutics for Prostate Cancer (oral presentation), The 30th Annual California State University Student Research Competition, Bakersfield, California, USA, April 29, 2016.
10. **Sheng Zhang**, Bao Vue, Xiaojie Zhang, Timmy Lee, Michael Huang, and Qiao-Hong Chen, 2,3-dehydrosilibinin derivatives: design, synthesis, and biological evaluation in human prostate cancer cell models, The 251st American Chemical Society National Meeting & Exposition, San Diego, California, USA, March 13–17, 2016.

9. **Sheng Zhang**, Bao Vue, Xiaojie Zhang, Timmy Lee, and Qiao-Hong Chen, Nitrogen-containing derivatives of 2,3-Dehydrosilibinin as cytotoxic chemotherapeutics, The 28th Annual CSU Biotechnology Symposium, Garden Grove, California, USA, January 7–9, 2016.
8. **Sheng Zhang**, Timmy Lee, Bao Vue, Xiaojie Zhang, Francisco Leon, and Qiao-Hong Chen, 2,3-dehydrosilibinin derivatives: synthesis and anti-proliferative effects toward prostate cancer cells, The 28th Annual CSU Biotechnology Symposium, Garden Grove, California, USA, January 7–9, 2016.
7. **Sheng Zhang**, Xiaojie Zhang, Leyla Farshidpour, Yoshikazu Miura, Therapeutic uses of Curcumin analogs for treatment of prostate cancer (oral presentation), CSU Innovation Corps, The 28th Annual CSU Biotechnology Symposium, Garden Grove, California, USA, January 7–9, 2016.
6. **Sheng Zhang**, Michael Huang, Bao Vue, Xiaojie Zhang, Timmy Lee, and Qiao-Hong Chen, 3-O-Alkyl-2,3-dehydrosilibinins: synthesis and antiproliferative activity towards prostate cancer cells, The 45th Western Regional Meeting of the American Chemical Society, San Marcos, California, USA, November 6–8, 2015.
5. Bao Vue, **Sheng Zhang**, Xiaojie Zhang, Konstantinos Parisis, and Qiao-Hong Chen, Structure-activity relationships of Silibinin derivatives as anti-cancer agents, The 250th American Chemical Society National Meeting & Exposition, Boston, Massachusetts, USA, August 16–20, 2015.
4. **Sheng Zhang**, Bao Vue, Xiaojie Zhang, Konstantinos Parisis, and Qiao-Hong Chen, "Studies toward the development of silybin derivatives as potential chemotherapeutics, The 36th Annual Central California Research Symposium, Fresno, California, USA, April 22, 2015.
3. Bao Vue, **Sheng Zhang**, Xiaojie Zhang, Konstantinos Parisis, and Qiao-Hong Chen, Synthesis and characterization of silybin derivatives & anti-proliferative activity toward prostate cancer cells (oral presentation), The 36th Annual Central California Research Symposium, Fresno, California, USA, April 22, 2015.
2. Bao Vue, **Sheng Zhang**, Xiaojie Zhang, Konstantinos Parisis, and Qiao-Hong Chen, Silybin derivatives as anti-prostate cancer agents: synthesis and anti-proliferative activity, The 249th

American Chemical Society National Meeting & Exposition, Denver, Colorado, USA, March 22–26, 2015.

1. Bao Vue, **Sheng Zhang**, Xiaojie Zhang, Konstantinos Parisi, and Qiao-Hong Chen, Silybin derivatives as anti-prostate cancer agents: synthesis and anti-proliferative activity, The 27th Annual CSU Biotechnology Symposium, Santa Clara, California, USA, January 8–10, 2015.

ABSTRACT OF THE DISSERTATION

Preparation, Conjugation, and Stabilization of Amyloid- β Peptides

by

Sheng Zhang

Doctor of Philosophy in Chemistry

University of California, Irvine

2021

Professor James S. Nowick, Chair

Chapter 1 presents the development of an efficient method for the expression and purification of aggregation-prone amyloid- β (A β) peptides, including A β _(M1-42), ¹⁵N-labeled A β _(M1-42), and A β _(M1-42) familial mutants.

A β peptides are central to the pathogenesis of Alzheimer's disease. A β peptides are highly aggregation-prone, making them challenging to prepare and purify. Advances in amyloid research rely on improved access to A β peptides. Chemical synthesis of A β can lead to impurities, such as amino acid deletion products, that are difficult to eliminate during purification. Expression of A β ₍₁₋₄₂₎ peptide requires the generation of fusion protein and cleavage by protease to remove the N-terminal methionine group that originates from the translational start codon, which can make the preparation of A β costly and time-intensive.

In this chapter, I collaborated with fellow graduate student Stan Yoo to express $A\beta_{(M1-42)}$, a widely used form of $A\beta$ with properties comparable to those of the native $A\beta_{(1-42)}$ peptide. Expression of $A\beta_{(M1-42)}$ is simple to execute and avoids the expensive and difficult enzymatic cleavage step associated with expression and isolation of $A\beta_{(1-42)}$. We then developed an efficient method to afford $A\beta_{(M1-42)}$ and ^{15}N -labeled $A\beta_{(M1-42)}$ at around 19 mg per liter of bacterial culture with high purity using simple and inexpensive steps in three days. This method relies on the combination of protein biology tools such as bacterial expression and inclusion body solubilization, as well as peptide chemistry tools such as preparative HPLC purification of the solubilized inclusion bodies. This chapter also describes a simple method for the construction of recombinant plasmids and the preparation of $A\beta$ peptides containing familial mutations. These methods may enable experiments that would otherwise be hindered by insufficient access to $A\beta$, such as NMR experiments with ^{15}N -labeled $A\beta$. We anticipate that this method can be adjusted for the expression and purification of other amyloidogenic proteins.

Chapter 2 presents the preparation of $A\beta$ peptide with an N-terminal cysteine [$A\beta_{(C1-42)}$], the development of tailored chemical reaction conditions for the conjugation of aggregation-prone $A\beta_{(C1-42)}$ peptide with fluorophores or biotin, and the biophysical studies of labeled $A\beta$ peptides.

N-terminally functionalized $A\beta$ peptides are important in amyloid and Alzheimer's disease research. Site-specific labeling on the N-terminus of $A\beta$ minimizes perturbation in the structure and function of the peptide, as the central and C-terminal regions of $A\beta$ are more involved in fibril and oligomer formation. Although synthetic N-terminally functionalized $A\beta$ peptides are commercially available, these peptides are expensive and limited to biotin and a few common fluorophores. Expressed $A\beta$ peptides offer advantages over synthetic $A\beta$ because they are free from amino acid deletions and epimeric contaminants, and they have been found to be more

biological relevant because they aggregate more quickly and are more neurotoxic than synthetic A β .

The method of preparing A $\beta_{(C1-42)}$ relies on the hitherto unrecognized observation that the expression of the A $\beta_{(MC1-42)}$ gene yields the A $\beta_{(C1-42)}$ peptide, because the N-terminal methionine is endogenously excised by *E. coli*. This observation is significant, because it allows the preparation of a useful A $\beta_{(C1-42)}$ peptide without the additional N-terminal methionine that originates from the translational start codon. The A $\beta_{(C1-42)}$ peptide represents a minimal modification of native A $\beta_{(1-42)}$, and the addition of a single cysteine residue at the N-terminus enables labeling of the expressed A β with complete site specificity using widely available maleimide-based reagents.

The A β peptide is challenging to handle and label because of its strong propensity to aggregate. This chapter details the development of tailored chemical reaction conditions for handling and labeling of this aggregation-prone peptide. The labeling chemistry was optimized to be performed at pH 9 in HPLC fractions A $\beta_{(C1-42)}$, where A β remains mostly monomeric. Biophysical studies show that the labeled A β peptides behave like unlabeled A β and suggest that labeling of the N-terminus does not substantially alter the properties of the A β . This chapter also goes on to demonstrate the utility of the labeled A β peptides through fluorescence microscopy to visualize their interactions with mammalian cells and bacteria. Ready access to labeled A β bearing fluorophores will advance amyloid and Alzheimer's disease research by enabling experiments for investigating the pathogenic mechanism, transport, and clearance of A β , as well as for screening anti-A β antibodies.

Chapter 3 presents the introduction of intramolecular disulfide bonds to A β peptides that stabilizes A β into oligomeric state and the discovery of a disulfide-stapled peptide, A β _{C18C33}, that forms homogeneous dimers and does not fibrilize.

A β aggregates rapidly and exists as three different forms in equilibria: monomers, oligomers, and fibrils. Although A β fibrils are the most commonly found species in the brain tissue of patients with Alzheimer's disease, soluble A β oligomers are the toxic contributors to neurodegeneration. A β oligomers are heterogenous and metastable: they can rapidly aggregate into more thermodynamically stable fibrils, which makes it challenging to isolate them and study their structures and biological properties. No high-resolution structures of A β oligomers have been reported thus far. Filling this gap is necessary for an enhanced understanding of the molecular basis of Alzheimer's disease.

In this chapter, we aimed to generate stable, non-covalent A β oligomers by introducing intramolecular disulfide linkages to A β . The intramolecular linkages were designed to enforce a β -hairpin conformation, the key conformation that favors A β oligomer formation and disfavors fibrilization. We have designed, prepared, and studied a variety of mutant A β peptides containing intramolecular linkages. Among these mutant peptides, we discovered A β _{C18C33}, an A β peptide containing a disulfide bond between positions 18 and 33, that forms stable, homogeneous dimers and does not fibrilize, as evidenced by the results of a series of biophysical studies.

The A β dimer has been proposed to be the basic building block of many larger A β oligomers and is thought to be one of the most neurotoxic and pathologically relevant species in Alzheimer's disease. We thereby anticipate that the A β _{C18C33} peptide to serve as a stable, non-fibrilizing, and noncovalent A β dimer model for the exploration of the structure and pathogenesis of A β dimers, the generation of A β -specific antibodies, and the screening of A β -targeted drugs.

Our laboratory is exploring ways to obtain high-resolution structures of this dimeric A β model peptide, using techniques including cryo-EM, NMR, and X-ray crystallography.

Chapter 4 presents the structure-based design of a cyclic peptide inhibitor towards SARS-CoV-2 using free molecular modeling and docking software and publicly available X-ray crystallographic structures. When the COVID-19 pandemic forced the temporary closure of our laboratory in March 2020, we began working on the structure-based drug design of inhibitors against the SARS-CoV-2 virus main protease. These efforts resulted in the design of a cyclic peptide inhibitor, UCI-1. Working with other group members, I published a tutorial paper based to describe the structure-based drug design process and teach others how to do it using the publicly available software UCSF Chimera and AutoDock Vina.

SARS-CoV-2 is a highly infectious virus that causes COVID-19, a serious respiratory infection that has caused over 178 million infections and over 3.8 million deaths worldwide as of June 2021. Main protease is a crucial enzyme that SARS-CoV-2 utilizes for site-specifically cleaving the polyprotein that is translated from viral mRNA and generating mature proteins that are necessary for replication and infection. The essential role of main protease, as well as the success of HIV protease inhibitors in the treatment of AIDS, make main protease an attractive therapeutic target in the treatment of COVID-19.

This chapter begins with the analysis of the X-ray crystallographic structure of the main protease of the SARS coronavirus (SARS-CoV) bound to a peptide substrate. This chapter then describes the structural modification of the peptide substrate using the UCSF Chimera molecular modeling software to create a cyclic peptide inhibitor. Finally, this chapter presents the use of molecular docking software AutoDock Vina to show the interaction of the cyclic peptide inhibitor with both SARS-CoV main protease and the highly homologous SARS-CoV-2 main protease.

The supporting information section of this chapter provides an illustrated step-by-step protocol showing the inhibitor design process. These and other molecular modeling studies helped our laboratory decide to pursue the synthesis of the cyclic peptide and experimentally evaluate its promise as an inhibitor of SARS-CoV-2 main protease. The molecular modeling studies presented in this chapter may help students and scientists design their own drug candidates for COVID-19 and the coronaviruses that may cause future pandemics.

Chapter 1^a

An Efficient Method for the Expression and Purification of A β _(M1-42)

Introduction

Amyloid- β (A β) peptides, which include the highly neurotoxic 42-amino acid alloform A β ₄₂, are central to the pathology of Alzheimer's disease.¹⁻⁴ Ready access to experimental-scale quantities of pure A β peptides, including isotopically labeled A β and mutants associated with familial Alzheimer's disease, is essential to progress in research in Alzheimer's disease. A β peptides are highly aggregation-prone, making them challenging to prepare and purify. Expressing A β peptides overcomes the challenge of purification that arises as a result of chemical synthesis – elimination of amino acid deletion, addition, and epimerization byproducts – leading to products with superior fidelity and purity. Expressed A β peptides have also been reported to aggregate faster and be significantly more toxic toward neuronal cells than synthetic A β .⁵ Expression of A β ₍₁₋₄₂₎ peptide requires the generation of fusion protein and cleavage by protease to remove the N-terminal methionine group that originates from the translational start codon (Figure 1.1). This

^a This chapter is adapted from Yoo, S.[‡], Zhang, S.[‡], Kreutzer, A. G., and Nowick, J. S. *Biochemistry* 2018 57 (26), 3861–3866. Stan Yoo and I co-wrote the paper and published the paper as co-first authors. Stan Yoo has also included this chapter in his Ph.D. dissertation.

approach requires expression and purification of the protease and an affinity purification step, which can make the preparation of A β ₍₁₋₄₂₎ costly and time-intensive.⁵⁻⁷

Walsh and co-workers expressed A β ₍₁₋₄₂₎ as the A β _(M1-42) variants bearing the N-terminal methionine residue from the start codon (Figure 1.1).⁸ A β _(M1-42) is a widely used form of A β with properties comparable to those of the native A β ₍₁₋₄₂₎ peptide. The additional N-terminal methionine has little impact on aggregation properties, fibril structure, and neurotoxicity.⁹⁻¹⁶ The expression of A β _(M1-42) negates the need for the expensive and time-consuming protease cleavage and affinity purification steps, but the expression system reported by Walsh and co-workers only affords A β _(M1-42) with a yield of 1.7 mg per liter of bacterial culture.⁸

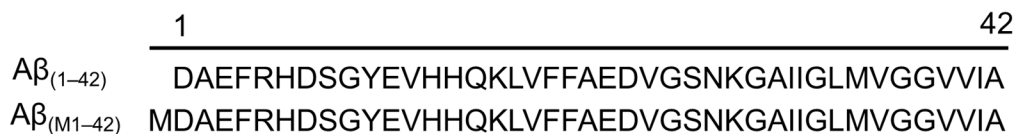


Figure 1.1. Sequences of A β ₍₁₋₄₂₎ and A β _(M1-42).

In this chapter, we report an efficient method for the expression and purification of A β _(M1-42) peptide and associated homologues, including the uniformly ¹⁵N-labeled peptide and familial mutants. This method relies on the combination of protein biology tools, such as bacterial expression and inclusion body solubilization, and peptide chemistry tools, such as preparative HPLC purification of the solubilized inclusion bodies. Our method bypasses cumbersome steps in previously reported A β preparation procedures and affords pure A β peptides in three days at ca. 19 mg/L of bacterial culture through simple and inexpensive steps. This chapter also reports a simple method for the construction of recombinant plasmids for the preparation of A β peptides containing familial mutations.

Results and Discussion

Expression of A β _(M1-42). To express A β _(M1-42), the pET-Sac-A β _(M1-42) plasmid is transformed into BL21(DE3)-pLysS competent *E. coli*. Expression is induced with isopropyl β -D-1-thiogalactopyranoside (IPTG). The expressed peptide is pelleted with the inclusion bodies, which are washed several times and then solubilized with 8 M urea. The yield of A β _(M1-42) depends on the extent of cell growth prior to IPTG induction, with an OD₆₀₀ of ca. 0.45 proving optimal for wild-type A β _(M1-42) production. Growth to substantially higher or lower OD₆₀₀ values gives lower yields of peptide.

Purification of A β _(M1-42). At this point in the procedure, the expressed peptide is handled like a synthetic peptide, and preparative HPLC is used to purify it. The solution of the inclusion bodies in 8 M urea is filtered to prevent damaging the HPLC column. Initially, a 0.22 μ m nylon syringe filter was used, but doing so resulted in a substantial loss of peptide. The hydrophobicity and propensity of A β to aggregate appear to make A β particularly prone to loss in filters. We screened several types of syringe filters to optimize peptide recovery, monitoring the relative concentrations of peptide by UV absorbance at 280 nm (Table 1.1).¹⁷ We found that a 0.22 μ m hydrophilic filter, such as hydrophilic polyvinylidene fluoride (PVDF) or poly(ether sulfone) (PES), provided satisfactory peptide recovery.

Table 1.1. Effect of different syringe filters on A β _(M1-42) recovery.

Filter type	UV absorbance at 280 nm	Peptide recovery
Nonfiltered A β sample	0.7279 \pm 0.0052	N/A
Millex-HV PES	0.6294 \pm 0.0001	86.5%
Fisher hydrophilic PVDF	0.6279 \pm 0.0009	86.3%
Millex-GV hydrophilic PVDF	0.5703 \pm 0.0003	78.3%
Fisher nylon	0.2907 \pm 0.0001	39.9%
Millex-GV MCE	0.2273 \pm 0.0001	31.2%

A typical HPLC trace of unpurified A β _(M1-42) shows three major peaks (Figure 1.2A). The first peak is the largest and contains mostly monomer, and the second and the third peaks appear to be oligomers (Figure 1.S1). For preparative HPLC, a reverse-phase silica-based C8 column is used as the stationary phase, and a gradient of water and acetonitrile containing 0.1% trifluoroacetic acid is used as the mobile phase. To enhance resolution and reduce peak tailing, it was necessary to heat the column. Without heating, the resolution and yield of the peptide are substantially lower. The A β _(M1-42) peptide monomer generally elutes at around 34% acetonitrile when the C8 column is heated to 80 °C in a water bath. HPLC fractions containing pure peptide were combined, and the purity was confirmed by analytical HPLC (Figure 1.2B). Acetonitrile was removed by rotary evaporation, and the aqueous solution of pure peptide was then frozen and lyophilized. These procedures typically yield ca. 19 mg of A β _(M1-42) as the trifluoroacetate salt per liter of bacterial culture.

This purification procedure does not require specialized equipment or costly reagents and is not time-consuming. It avoids the use of specialized and costly columns, such as cation exchange chromatography columns and size-exclusion chromatography columns. Another advantage of this

procedure is that it yields lyophilized powder as the final peptide product. Working with lyophilized peptide is convenient for subsequent studies as it can be dissolved in any appropriate buffer at a desired concentration.

The purity and composition of the $A\beta_{(M1-42)}$ peptide were further assessed via MALDI-MS and SDS-PAGE with silver staining. MALDI-MS confirms that the observed mass of $A\beta_{(M1-42)}$ matches the expected mass (Figure 1.2C). The silver-stained SDS-PAGE gel shows that at low concentrations, the $A\beta_{(M1-42)}$ peptide exists as a monomer. At higher concentrations, $A\beta_{(M1-42)}$ begins to form oligomers with molecular weights consistent with trimers and tetramers (Figure 1.2D).

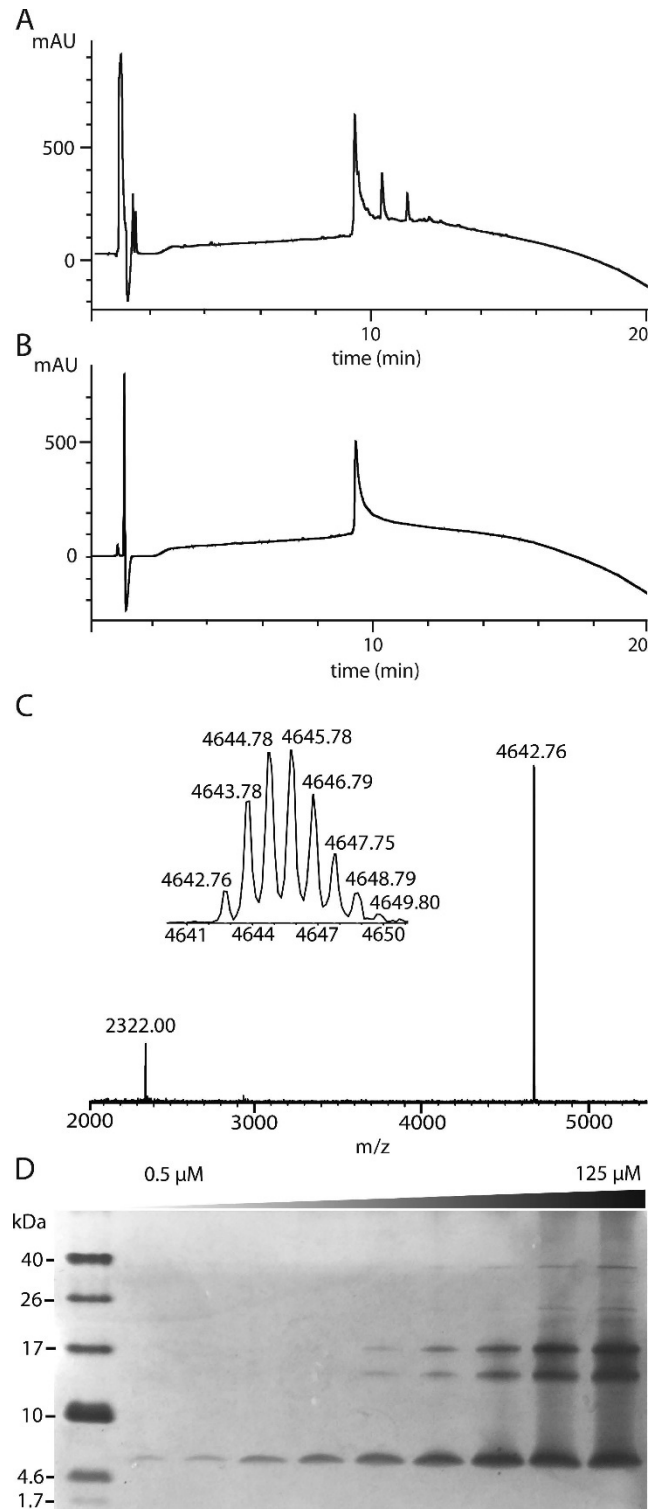


Figure 1.2. Purification and characterization of Aβ(M1-42). (A) Typical analytical HPLC trace of a filtered crude Aβ(M1-42) sample. (B) Typical analytical HPLC trace of purified Aβ(M1-42). (C) MALDI mass spectrum of purified Aβ(M1-42). (D) Silver-stained SDS-PAGE gel (16%)

polyacrylamide) of increasing concentrations of A β _(M1-42) from 0.5 to 125 μ M. A 12 μ L aliquot was loaded in each lane of the gel.

Sample Preparation for Biophysical and Biological Studies. The propensity of A β to aggregate necessitates the preparation of monomeric A β for subsequent studies.¹⁸ Without any sample preparation, studies are reported to be irreproducible.¹⁹ Fezoui and co-workers reported that treatment of A β with NaOH disrupts aggregates and generates A β that is monomeric or nearly monomeric.²⁰ This NaOH-treated A β is widely used in subsequent aggregation studies.¹⁸ We applied this procedure to each batch of expressed A β to generate aliquots for further studies. Thus, the lyophilized powder was dissolved in 2 mM NaOH, and the pH was adjusted, if necessary, by addition of 0.1 M NaOH, to give a pH 10.5 solution. The solution was sonicated for 1 min; the concentration was determined by UV absorbance at 280 nm, and the yield of A β _(M1-42) was calculated. The solution was then aliquoted in 0.0055 or 0.020 μ mol portions into small tubes, and these samples were frozen and lyophilized. The lyophilized aliquots were stored in a desiccator at -20 °C.

Expression of ¹⁵N-Labeled A β _(M1-42). ¹⁵N-labeled A β peptides are useful tools for NMR structural studies and for studying binding profiles of A β . For expression of ¹⁵N-labeled A β _(M1-42), *E. coli* cells are grown to an OD₆₀₀ of ca. 0.45 in LB medium, and then the LB medium is exchanged with M9 minimal medium containing ¹⁵NH₄Cl. Expression is induced in the ¹⁵N-enriched M9 medium for 16 h with IPTG. Purification and sample preparation of ¹⁵N-labeled A β _(M1-42) are identical to those of unlabeled A β _(M1-42). The composition of ¹⁵N-labeled A β _(M1-42) was assessed by MALDI-MS (Figure 1.3A). A ¹H-¹⁵N HSQC NMR spectrum of 160 μ M ¹⁵N-labeled A β _(M1-42) in 50 mM potassium phosphate buffer in 10% D₂O was recorded at 5 °C with a 500 MHz NMR spectrometer equipped with a cryogenic probe (Figure 1.3B). This spectrum matches the NMR spectrum reported by Macao and co-workers.⁹ The yield of the ¹⁵N-labeled

$A\beta_{(M1-42)}$ peptide is comparable to that of the unlabeled $A\beta_{(M1-42)}$ peptide, at ca. 19 mg/L of bacterial culture. Access to such amounts of the ^{15}N -labeled peptide at low cost enables the performance of SAR by NMR experiments.²¹

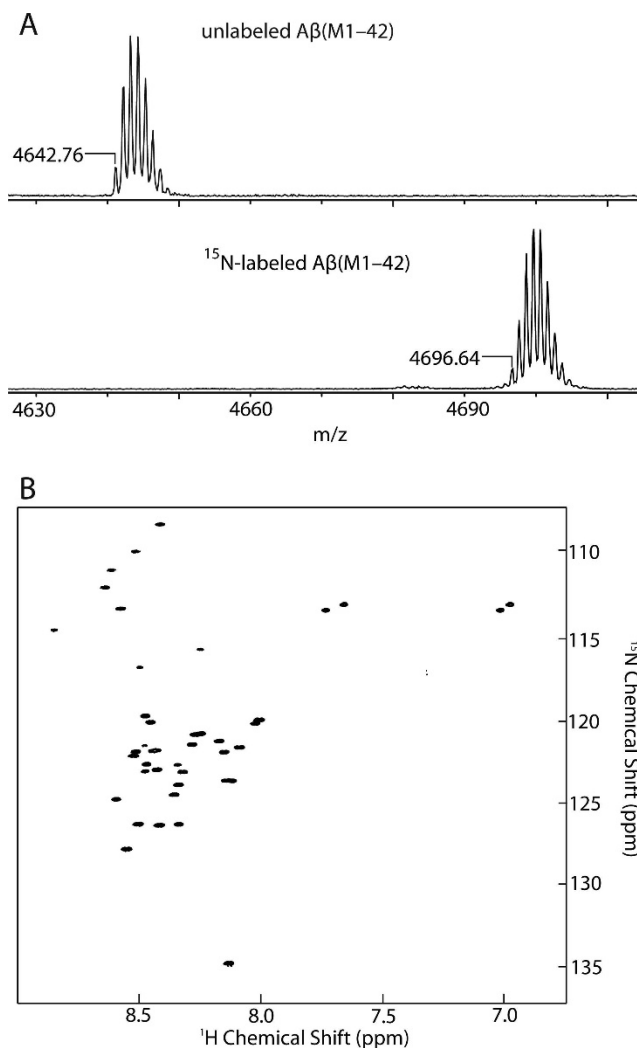


Figure 1.3. MALDI mass spectra and NMR spectra of unlabeled and ^{15}N -labeled $A\beta_{(M1-42)}$. (A) MALDI spectra of unlabeled $A\beta_{(M1-42)}$ and ^{15}N -labeled $A\beta_{(M1-42)}$ peptides. (B) ^1H - ^{15}N HSQC NMR spectrum of 160 μM ^{15}N -labeled $A\beta_{(M1-42)}$ peptide at 5 $^\circ\text{C}$ at 500 MHz equipped with a cryogenic probe.

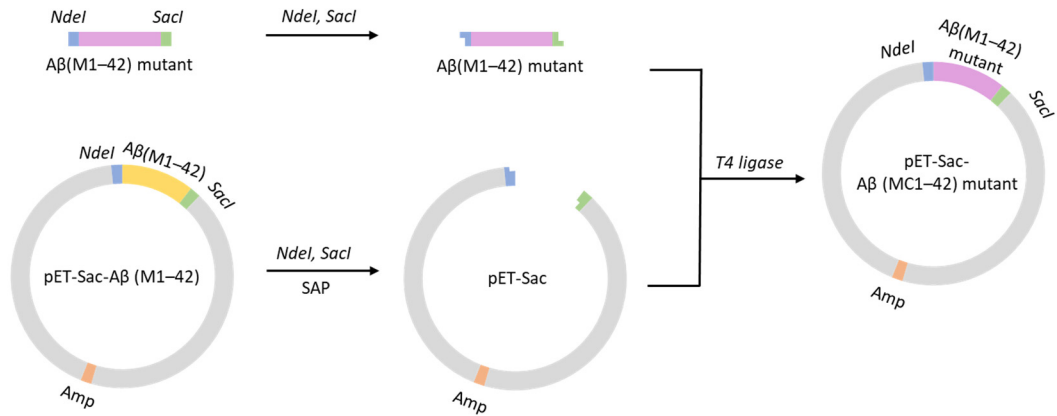
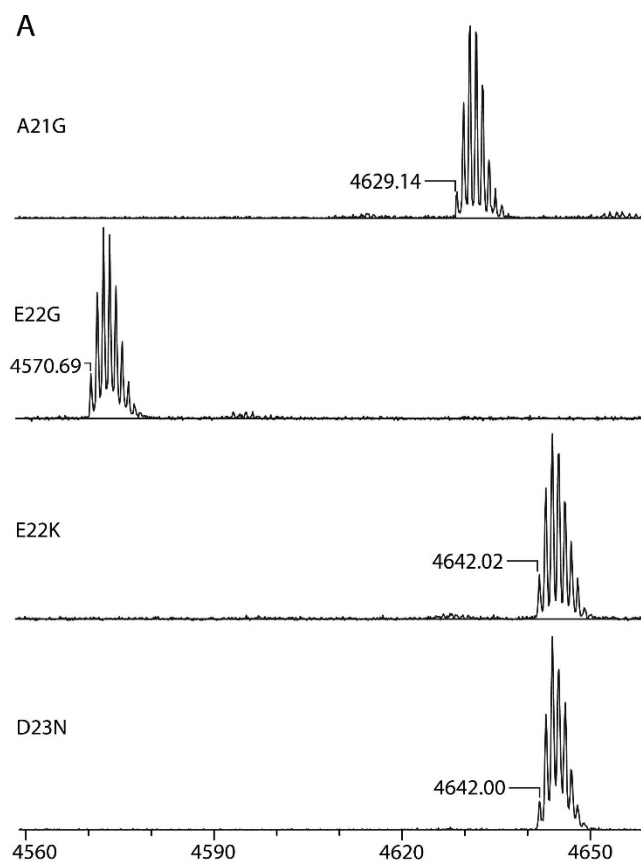


Figure 1.4. Molecular cloning strategy for constructing recombinant plasmids of $A\beta_{(M1-42)}$ containing familial mutations.



B

A β (M1-42) peptides	Yield (per liter of bacterial culture)
A β (M1-42)	19.4 mg
¹⁵ N-labeled A β (M1-42)	18.6 mg
A β (M1-42/D23N)	19.4 mg
A β (M1-42/E22K)	17.6 mg
A β (M1-42/E22G)	6.2 mg
A β (M1-42/A21G)	5.3 mg

Figure 1.5. MALDI mass spectra and typical yields of A β peptides. (A) MALDI mass spectra of A β _(M1-42) peptides with A21G, E22G, E22K, and D23N mutations. (B) Typical yields of A β _(M1-42), ¹⁵N-labeled A β _(M1-42), and mutant A β _(M1-42) peptides.

Construction of Recombinant Plasmids for Expression of Mutant A β _(M1-42) Peptides.

To express A β _(M1-42) peptides containing familial mutations, we construct recombinant plasmids by ligating enzymatically digested pETSac-A β _(M1-42) and DNA sequences that encode A β _(M1-42)

mutants (Figure 1.4). In this procedure, pET-Sac-A $\beta_{(M1-42)}$ is first digested with *NdeI* and *SacI* restriction enzymes to remove the wild-type A $\beta_{(M1-42)}$ sequence. Next, the digested pET-Sac vector is treated with shrimp alkaline phosphatase (rSAP) to remove the terminal phosphate groups. The digested vector is isolated by agarose gel electrophoresis purification using a commercially available kit. Synthetic DNA encoding each mutant A $\beta_{(M1-42)}$ is purchased and then digested with *NdeI* and *SacI* to generate the inset. The vector and insert are ligated using T4 ligase and then transformed into TOP 10 competent *E. coli*. *E. coli* cells transformed with ligated plasmid form colonies on agar containing carbenicillin. Plasmids are isolated from colonies, and the sequences are verified by DNA sequencing. In this section, we constructed five plasmids with familial mutations: A21G, E22G, E22K, E22Q, and D23N. This cloning strategy is inexpensive and is simpler to execute than site-directed mutagenesis. The entire cloning procedure takes 2 days, and many mutants can be generated concurrently. Another advantage of this strategy is that A $\beta_{(M1-42)}$ plasmids containing multiple point mutations can be prepared as easily as plasmids containing single point mutations.

The purification and preparation of A $\beta_{(M1-42)}$ containing familial mutations are identical to those of A $\beta_{(M1-42)}$. The composition of familial mutant A $\beta_{(M1-42)}$ peptides was assessed using MALDI-MS (Figure 1.5A). The expression levels and yields of the A $\beta_{(M1-42)}$ familial mutants varied because of different aggregation propensities of the peptides. Analytical HPLC traces of crude samples of the A21G and E22Q mutants showed smaller first peaks and larger second and third peaks, suggesting that more oligomers are formed after the inclusion bodies are dissolved. Figure 1.5B shows typical yields of the peptides. Our expression and purification procedures proved to be unsuitable for the E22Q mutant, which showed very little monomer in the HPLC trace.

Conclusion

The procedures described in this chapter provide an efficient method for the expression and purification of $A\beta_{(M1-42)}$, ^{15}N -labeled $A\beta_{(M1-42)}$, and $A\beta_{(M1-42)}$ containing several familial mutations. Our method employs the most convenient features of protein expression and peptide purification to provide ready access to good quantities of the pure peptides. We anticipate that our method will provide new opportunities for pilot experiments that require large amounts of $A\beta$. We also anticipate that this method can be adjusted for the expression and purification of other amyloidogenic proteins.

References

- (1) Benilova, I., Karran, E., and De Strooper, B. The toxic Abeta oligomer and Alzheimer's disease: an emperor in need of clothes. *Nat. Neurosci.* **2012**, *15*, 349–357.
- (2) Haass, C., and Selkoe, D. J. Soluble protein oligomers in neurodegeneration: lessons from the Alzheimer's amyloid betapeptide. *Nat. Rev. Mol. Cell Biol.* **2007**, *8*, 101–112.
- (3) Chiti, F., and Dobson, C. M. Protein Misfolding, Amyloid Formation, and Human Disease: A Summary of Progress Over the Last Decade. *Annu. Rev. Biochem.* **2017**, *86*, 27–68.
- (4) Jarrett, J. T., Berger, E. P., and Lansbury, P. T. The carboxy terminus of the beta amyloid protein is critical for the seeding of amyloid formation: Implications for the pathogenesis of Alzheimer's disease. *Biochemistry* **1993**, *32*, 4693–4697.
- (5) Finder, V. H., Vodopivec, I., Nitsch, R. M., and Glockshuber, R. The recombinant amyloid-beta peptide Abeta1–42 aggregates faster and is more neurotoxic than synthetic Abeta1–42. *J. Mol. Biol.* **2010**, *396*, 9–18.

- (6) Hortschansky, P., Schroeckh, V., Christopeit, T., Zandomenighi, G., and Fandrich, M. The aggregation kinetics of Alzheimer's beta-amyloid peptide is controlled by stochastic nucleation. *Protein Sci.* **2005**, *14*, 1753–1759.
- (7) Liao, Y. H., and Chen, Y. R. A novel method for expression and purification of authentic amyloid-beta with and without (15)N labels. *Protein Expression Purif.* **2015**, *113*, 63–71.
- (8) Walsh, D. M., Thulin, E., Minogue, A. M., Gustavsson, N., Pang, E., Teplow, D. B., and Linse, S. A facile method for expression and purification of the Alzheimer's disease-associated amyloid betapeptide. *FEBS J.* **2009**, *276*, 1266–1281.
- (9) Macao, B., Hoyer, W., Sandberg, A., Brorsson, A. C., Dobson, C. M., and Hard, T. Recombinant amyloid beta-peptide production by coexpression with an affibody ligand. *BMC Biotechnol.* **2008**, *8*, 82.
- (10) Silvers, R., Colvin, M. T., Frederick, K. K., Jacavone, A. C., Lindquist, S., Linse, S., and Griffin, R. G. Aggregation and Fibril Structure of AbetaM01–42 and Abeta1–42. *Biochemistry* **2017**, *56*, 4850–4859.
- (11) Sandberg, A., Luheshi, L. M., Sollvander, S., Pereira de Barros, T., Macao, B., Knowles, T. P., Biverstal, H., Lendel, C., Ekholm-Petterson, F., Dubnovitsky, A., Lannfelt, L., Dobson, C. M., and Hard, T. Stabilization of neurotoxic Alzheimer amyloid-beta oligomers by protein engineering. *Proc. Natl. Acad. Sci. U. S. A.* **2010**, *107*, 15595–15600.
- (12) Cohen, S. I., Linse, S., Luheshi, L. M., Hellstrand, E., White, D. A., Rajah, L., Otzen, D. E., Vendruscolo, M., Dobson, C. M., and Knowles, T. P. Proliferation of amyloid-beta42 aggregates occurs through a secondary nucleation mechanism. *Proc. Natl. Acad. Sci. U. S. A.* **2013**, *110*, 9758–9763.

- (13) Bertini, I., Gonnelli, L., Luchinat, C., Mao, J., and Nesi, A. A new structural model of Abeta40 fibrils. *J. Am. Chem. Soc.* **2011**, *133*, 16013–16022.
- (14) Colvin, M. T., Silvers, R., Ni, Q. Z., Can, T. V., Sergeyev, I., Rosay, M., Donovan, K. J., Michael, B., Wall, J., Linse, S., and Griffin, R. G. Atomic Resolution Structure of Monomorphic Abeta42 Amyloid Fibrils. *J. Am. Chem. Soc.* **2016**, *138*, 9663–9674.
- (15) Meisl, G., Yang, X., Hellstrand, E., Frohm, B., Kirkegaard, J. B., Cohen, S. I., Dobson, C. M., Linse, S., and Knowles, T. P. Differences in nucleation behavior underlie the contrasting aggregation kinetics of the Abeta40 and Abeta42 peptides. *Proc. Natl. Acad. Sci. U. S. A.* **2014**, *111*, 9384–9389.
- (16) Munke, A., Persson, J., Weiffert, T., De Genst, E., Meisl, G., Arosio, P., Carnerup, A., Dobson, C. M., Vendruscolo, M., Knowles, T. P. J., and Linse, S. Phage display and kinetic selection of antibodies that specifically inhibit amyloid self-replication. *Proc. Natl. Acad. Sci. U. S. A.* **2017**, *114*, 6444–6449.
- (17) Syringe filters with large pore sizes (0.45 μm) result in incomplete filtration of the peptide and risk damaging HPLC columns.
- (18) Teplow, D. B. Preparation of amyloid beta-protein for structural and functional studies. *Methods Enzymol.* **2016**, *413*, 20–33.
- (19) Wood, S. J., Maleeff, B., Hart, T., and Wetzel, R. Physical, morphological and functional differences between pH 5.8 and 7.4 aggregates of the Alzheimer's amyloid peptide Abeta. *J. Mol. Biol.* **1996**, *256*, 870–877.
- (20) Fezoui, Y., Hartley, D. M., Harper, J. D., Khurana, R., Walsh, D. M., Condron, M. M., Selkoe, D. J., Lansbury, P. T., Fink, A. L., and Teplow, D. B. An improved method of preparing the amyloid β -protein for fibrillogenesis and neurotoxicity experiments. *Amyloid* **2000**, *7*, 166–178.

(21) Shuker, S. B., Hajduk, P. J., Meadows, R. P., and Fesik, S. W. Discovering High-Affinity Ligands for Proteins: SAR by NMR. *Science* **1996**, *274*, 1531–1534.

Supporting Information

Table of Contents

Methods	18
Isolation of pET-Sac-A $\beta_{(M1-42)}$ plasmid	18
Bacterial expression of A $\beta_{(M1-42)}$	18
Table 1.S1. M9 minimal media	19
Cell lysis and inclusion body preparation	20
Peptide purification	20
Figure 1.S1. HPLC trace of filtered and urea-solubilized A $\beta_{(M1-42)}$ and silver-stained SDS-PAGE gel of HPLC fractions	22
NaOH treatment and peptide concentration determination	24
Figure 1.S2. UV absorption spectra of A $\beta_{(M1-42)}$ at different pH	25
Table 1.S2. A representative schedule for expression of A $\beta_{(M1-42)}$	25
Table 1.S3. A representative schedule for expression of ^{15}N -labeled A $\beta_{(M1-42)}$	25
Mass spectrometry	26
SDS-PAGE	26
NMR spectroscopy	27
Molecular cloning	28
Figure 1.S3. Design of the DNA sequences for A $\beta_{(M1-42)}$ mutants	29
Table 1.S4. Double-digestion of the pET-Sac-A $\beta_{(M1-42)}$ plasmids	29
Table 1.S5. SAP treatment of the vectors	30
Table 1.S6. Double-digestion of the inserts	31

Table 1.S7. T4 ligation of the inserts and the vectors	31
Characterization Data	33
Figure 1.S4. Analytical HPLC and MALDI-MS traces of A β _(M1-42)	35
Figure 1.S5. Analytical HPLC and MALDI-MS traces of ¹⁵ N-labeled A β _(M1-42)	37
Figure 1.S6. Analytical HPLC and MALDI-MS traces of A β _(M1-42/A21G)	39
Figure 1.S7. Analytical HPLC and MALDI-MS traces of A β _(M1-42/E22G)	41
Figure 1.S8. Analytical HPLC and MALDI-MS traces of A β _(M1-42/E22K)	44
Figure 1.S9. Analytical HPLC and MALDI-MS traces of A β _(M1-42/D23N)	46
References	47

Methods

Isolation of pET-Sac-A β _(M1-42) plasmid

We received the pET-Sac-A β _(M1-42) plasmid from Addgene as a bacterial stab and immediately streaked the bacteria onto a LB agar-plate containing carbenicillin (50 mg/L). Colonies grew in < 24h. Single colonies were picked and used to inoculate 5 mL of LB broth containing carbenicillin (50 mg/L). The cultures were shaken at 225 rpm overnight at 37°C. To isolate the pET-Sac-A β _(M1-42) plasmids, minipreps were performed using a Zymo ZR plasmid miniprep kit. The concentration of the plasmids was measured using a Thermo Scientific Nanodrop instrument.

Bacterial expression of A β _(M1-42)

Transformation and expression of A β _(M1-42)

All liquid cultures were performed in culture media (LB broth containing 50 mg/L carbenicillin and 34 mg/L chloramphenicol). For A β _(M1-42) wild-type and mutant peptides: Wild-type or mutant plasmids were transformed into BL21 DE3 PLYS Star Ca²⁺-competent *E. coli* through heat shock method. The cell cultures were spread on LB agar plates containing carbenicillin (50 mg/L) and chloramphenicol (34 mg/L). Single colonies were picked to inoculate 5 mL of culture media for overnight culture. (A glycerol stock of BL21 DE3 PLYS Star Ca²⁺-competent *E. coli* bearing the plasmids was made, and the future expressions were started by inoculating culture media with an aliquot of the glycerol stock). The next day, all 5 mL of the overnight culture were used to inoculate 1 L of culture media. After inoculation, the culture was shaken at 225 rpm at 37 °C until the cell density reached an OD₆₀₀ of approximately 0.45 (after

around 3 h 45 min). Protein expression was then induced by the addition of isopropyl β -D-1-thiogalactopyranoside (IPTG) to a final concentration of 0.1 mM, and the cells were shaken at 225 rpm at 37 °C for 4 h with IPTG. The cells were then harvested by centrifugation (4000 rpm, 4 °C, 25 min), and the cell pellets were stored at -80°C.

For ^{15}N -labeled $\text{A}\beta_{(M1-42)}$: Wild-type plasmids were transformed into BL21 DE3 PLYS Star Ca^{2+} -competent *E. coli* through heat shock method. The cell cultures were spread on LB agar plates containing carbenicillin (50 mg/L) and chloramphenicol (34 mg/L). Single colonies were picked to inoculate 5 mL of culture media for overnight culture. [A glycerol stock of BL21 DE3 PLYS Star Ca^{2+} -competent *E. coli* bearing the plasmids was made, and the subsequent expressions were started by inoculating culture media with an aliquot of the glycerol stock.] The next day, all 5 mL of the overnight culture were used to inoculate 1 L of culture media. After inoculation, the culture was shaken at 225 rpm at 37 °C until the cell density reached an OD_{600} of approximately 0.45–0.50 (after around 3 h 50 min). The cells were harvested by centrifugation in sterile 500-mL thick-walled centrifuge bottles (4000 rpm, 4 °C, 25 min). The cell pellets were then resuspended in sterile M9 minimal media supplemented with $^{15}\text{NH}_4\text{Cl}$, carbenicillin (50 mg/L), and chloramphenicol (34 mg/L) (Table 1.S1), and incubated for 1 h at 225 rpm at 37 °C. Protein expression was then induced by the addition of isopropyl β -D-1-thiogalactopyranoside (IPTG) to a final concentration of 0.1 mM, and the cells were shaken at 225 rpm at 25 °C for ~20 h with IPTG. The cells were then harvested by centrifugation (4000 rpm, 4 °C, 25 min), and the cell pellets were stored at -80°C.

Table 1.S1. M9 minimal media.

Reagents	Amount
----------	--------

5X M9 salts solution (34.0 g of Na ₂ HPO ₄ , 15.0 g of KH ₂ PO ₄ , and 2.5 g of NaCl in 1.0 L of H ₂ O)	200.0 mL
1.0 M MgSO ₄ ·7H ₂ O solution	2.0 mL
1.0 M CaCl ₂ solution	0.1 mL
¹⁵ NH ₄ Cl	1.0 g
D-Glucose	10.0 g
Carbenicillin (50 mg/mL)	1 mL
Chloramphenicol (34 mg/mL in EtOH)	1 mL
H ₂ O	Fill up to 1.0 L

Cell lysis and inclusion body preparation

To lyse the cells, the cell pellet was resuspended in 20 mL of buffer A (10 mM Tris/HCl, 1 mM EDTA, pH 8.0) and sonicated for 2 min on ice (50% duty cycle) until the lysate appeared homogenous. The lysate was then centrifuged for 25 min at 16,000 rpm at 4°C. The supernatant was removed, and the pellet was resuspended in buffer A, sonicated and centrifuged as described above. The sonication and centrifugation steps were repeated three times. After the fourth supernatant was removed, the remaining pellet was resuspended in 15 mL of freshly prepared buffer B (8 M urea, 10 mM Tris/HCl, 1 mM EDTA, pH 8.0), and was sonicated as described above, until the solution became clear.

Peptide purification

The solution (15 mL) was then diluted with 10 mL of buffer A and filtered through a Fisher Brand 0.22 µm non-sterile hydrophilic PVDF syringe filter (Catalog No. 09-719-00).

Analytical reverse-phase HPLC was performed to evaluate if expression of $A\beta_{(M1-42)}$ was successful. A 40- μ L sample of the above solution was injected onto an Agilent 1200 instrument equipped with a Phenomenex Aeris PEPTIDE 2.6u XB-C18 column with a Phenomenex SecurityGuard ULTRA cartridges guard column for C18 column. HPLC grade acetonitrile (ACN) and 18 M Ω deionized water, each containing 0.1% trifluoroacetic acid, were used as the mobile phase. The sample was eluted at 1.0 mL/min with a 5–100% acetonitrile gradient over 20 min, at 35 °C or 60 °C. Figure S1 shows an example HPLC trace of the crude $A\beta_{(M1-42)}$ solution.

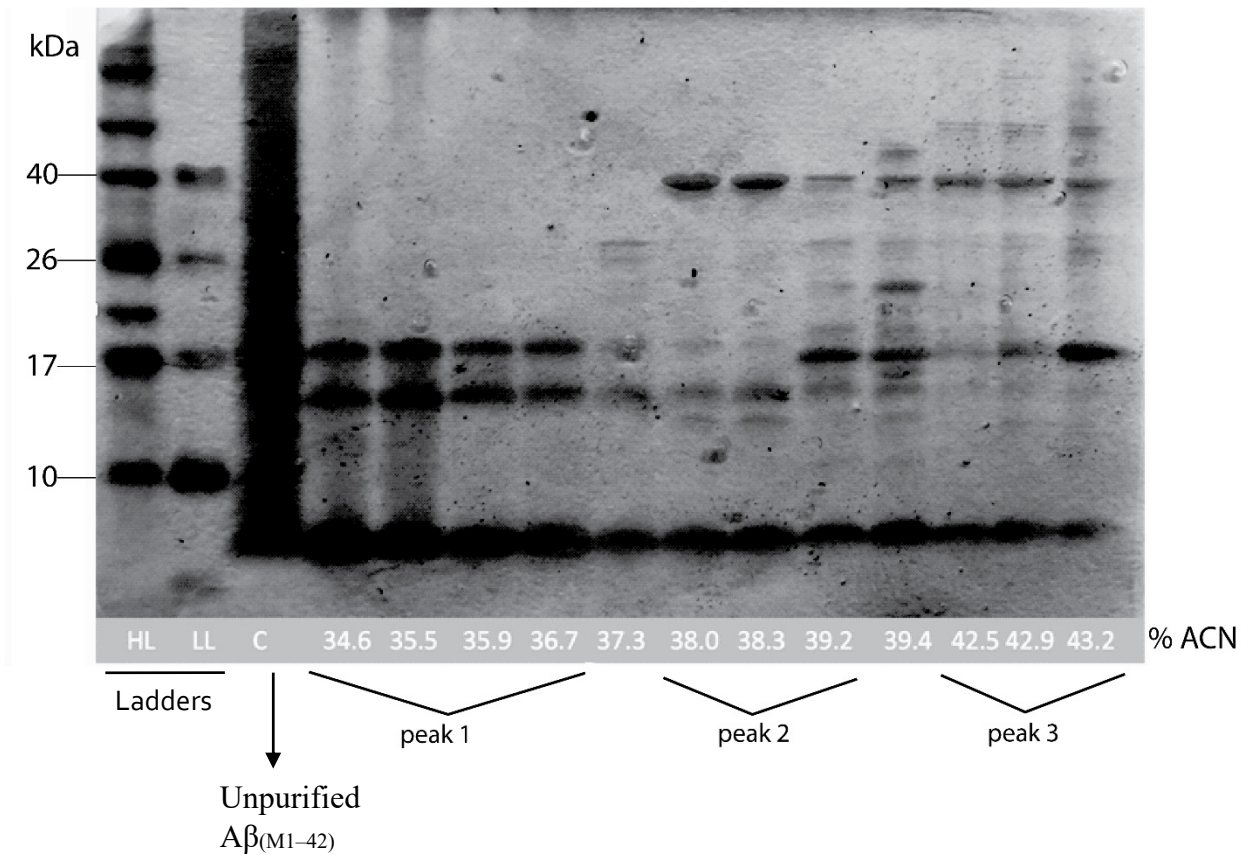
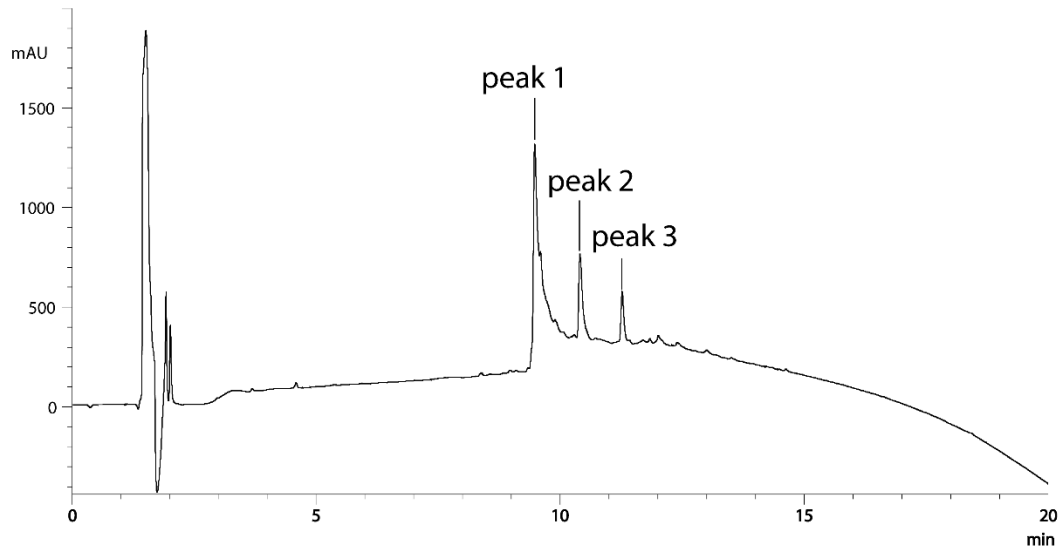


Figure 1.S1. HPLC trace of filtered urea-solubilized $A\beta_{(M1-42)}$ and silver-stained SDS-PAGE gel of HPLC fractions. HL: Precision Plus Protein Dual Color Standards from Bio-Rad; LL: Spectra Multicolor Low Range Protein Ladder from ThermoFisher.

A β _(M1-42) peptides were then purified by preparative reverse-phase HPLC equipped with an Agilent ZORBAX 300SB-C8 semi-preparative column (9.4 x 250 mm) with a ZORBAX 300SB-C3 preparative guard column (9.4 x 15 mm). The C8 column and the guard column were heated to 80 °C in a water bath. HPLC grade acetonitrile (ACN) and 18 M Ω deionized water, each containing 0.1% trifluoroacetic acid, were used as the mobile phase at a flow-rate of 5 mL/min. The peptide solution was split into three ~8 mL aliquots, and purified in three separate runs. The peptide was loaded onto the column by flowing 20% ACN for 10 min and then eluted with a gradient of 20–40% ACN over 20 min. Fractions containing the monomer generally eluted from 34% to 38% ACN. After the peptide was collected, the column was washed by injecting 5 mL of filtered buffer B (8 M urea, 10 mM Tris/HCl, 1 mM EDTA, pH 8.0) while flushing at 95% ACN for 15 minutes. This cleaning procedure ensures elution of all peptide that is retained in the column and avoids problems of cross-contamination between runs.

The purity of each fraction was assessed using analytical reverse-phase HPLC. A 40- μ L sample was injected onto the analytical HPLC. The sample was eluted at 1.0 mL/min with a 5–100% acetonitrile gradient over 20 min, at 35 °C or 60 °C. Pure fractions were combined and the purity of the combined fractions were checked using analytical HPLC. The combined fractions were concentrated by rotary evaporation to remove ACN, and then frozen with dry ice, liquid nitrogen, or a -80 °C freezer. [It is recommended to combine and freeze the purified fractions within 5 hours after purification to avoid oxidation of methionine.] The frozen sample was then lyophilized to give a fine white powder.

NaOH treatment and peptide concentration determination

The lyophilized peptide was then dissolved in 2 mM NaOH to achieve a concentration of ~0.5 mg/mL. The pH was adjusted (if necessary) by addition of 0.1 M NaOH to give a solution of pH ~10.5. The sample was sonicated in a water ultrasonic bath at room temperature for 1 min or until the solution became clear. When preparing samples, pH should not be near pH 5.5 where the peptide is prone to aggregate, and solution become opaque, giving inaccurate UV readings. pH should not be over 11, where tyrosine is mostly deprotonated, giving slightly different UV spectra (Figure 1.S2).

The concentration of $A\beta_{(M1-42)}$ was determined by absorbance at 280 nm using the extinction coefficient (ϵ) for tyrosine of $1490 \text{ M}^{-1}\text{cm}^{-1}$ ($c = A/1490$). The $A\beta_{(M1-42)}$ solution was then aliquoted into 0.0055 μmol or 0.020 μmol aliquots in 0.5 mL microcentrifuge tubes. The ^{15}N -labeled $A\beta_{(M1-42)}$ solution was aliquoted into appropriate volume that contains 0.5 mg in 1.6 mL Eppendorf tubes. The aliquots were lyophilized and then stored in a desiccator at $-20 \text{ }^\circ\text{C}$ for future use.

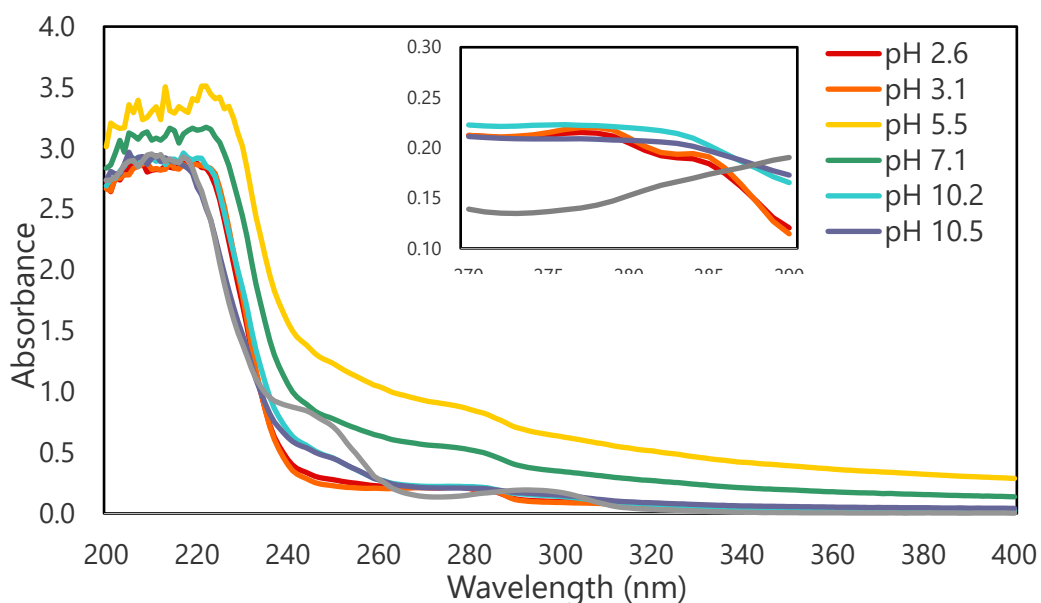


Figure 1.S2. UV absorption spectra of A β _(M1-42) at different pH.

Table 1.S2 shows a representative schedule for expression of A β _(M1-42). Table 1.S3 shows a representative schedule for expression of ¹⁵N-labeled A β _(M1-42).

Table 1.S2. A representative schedule for expression of A β _(M1-42).

Day	Time	Steps
Monday	Evening	Starter culture
	Morning	Daytime culture
Tuesday	Afternoon	IPTG Induced expression
	Evening	Cell pelleting
Wednesday	Morning	Sonication; urea extraction
	Afternoon	Purification by prep-HPLC Collecting pure fractions, freeze, and lyophilize
Thursday	Afternoon	NaOH treatment, freeze, and lyophilize

Table 1.S3. A representative schedule for expression of ¹⁵N-labeled A β _(M1-42).

Day	Time	Steps
Monday	Evening	Starter culture
	Morning	Daytime culture
Tuesday	Afternoon	Media exchange to ¹⁵ N-containing M9 media
	Evening	IPTG induction and incubation in 25 °C
Wednesday	Morning	Cell pelleting
	Morning	Sonication; urea extraction
	Afternoon	Purification by prep-HPLC; collecting pure fractions, freeze, and lyophilize

Mass spectrometry

MALDI mass spectrometry was performed using an AB SCIEX TOF/TOF 5800 System. 0.5 μL of 2,5-dihydroxybenzoic acid (DHB) was dispensed onto a MALDI sample support, followed by the addition of 0.5 μL peptide sample. The mixture was allowed to air-dry. All analyses were performed in positive reflector mode, collecting data with a molecular weight range of 2000–8000 Da.

SDS-PAGE

SDS-PAGE and silver staining were adapted from and in some cases taken verbatim from our previously reported procedure.² For the sample preparation, a 0.0055 μmol aliquot of A β peptide was dissolved in 11 μL of 20 mM HEPES buffer (pH 7.4) to give a 500 μM peptide stock solution, and serial diluted with 11 μL of 20 mM HEPES buffer (pH 7.4) to create 11 μL of peptide stock solutions with concentrations of 250 μM to 1.0 μM . The peptide stock solutions were then immediately diluted with 11 μL of 2X SDS-PAGE loading buffer (100 mM Tris buffer at pH 6.8, 20% (v/v) glycerol, and 4% w/v SDS) to give 11 μL of peptide working solutions with concentrations from 125 μM to 0.5 μM . A 12.0- μL aliquot of each working solution was run on a 16% polyacrylamide gel with a 4% stacking polyacrylamide gel. The gels were run at a constant 90 volts at room temperature.

Staining with silver nitrate was used to visualize peptides in the SDS-PAGE gel. Briefly, the gel was first rocked in fixing solution (50% (v/v) methanol and 5% (v/v) acetic acid in

deionized water) for 20 min. Next, the fixing solution was discarded and the gel was rocked in 50% (v/v) aqueous methanol for 10 min. Next, the 50% methanol was discarded and the gel was rocked in deionized water for 10 min. Next, the water was discarded and the gel was rocked in 0.02% (w/v) sodium thiosulfate in deionized water for 1 min. The sodium thiosulfate was discarded and the gel was rinsed twice with deionized water for 1 min (2X). After the last rinse, the gel was submerged in chilled 0.1% (w/v) silver nitrate in deionized water and rocked at 4 °C for 20 min. Next, the silver nitrate solution was discarded and the gel was rinsed with deionized water for 1 min (2X). To develop the gel, the gel was incubated in developing solution (2% (w/v) sodium carbonate, 0.04% (w/v) formaldehyde until the desired intensity of staining was reached (~1–3 min). When the desired intensity of staining was reached, the development was stopped by discarding the developing solution and submerging the gel in 5% aqueous acetic acid.

NMR spectroscopy

Approximately 0.5 mg of NaOH-treated, lyophilized ^{15}N -labeled $\text{A}\beta_{(\text{M1-42})}$ was dissolved in 0.6 mL of 50 mM potassium phosphate buffer containing the internal standard, 4,4-dimethyl-4-silapentane-1-ammonium trifluoroacetate (DSA) at a concentration of 30 μM and 10% D_2O (pH 7.4) to give a 160 μM peptide solution. The exact concentration of the peptide solution was determined by absorbance at 280 nm using the extinction coefficient for tyrosine of $1490 \text{ M}^{-1}\text{cm}^{-1}$. The NMR sample was prepared immediately prior to the NMR experiment. NMR was performed using a Bruker DRX500 500 MHz spectrometer equipped with a cryogenic probe. The temperature was maintained at 5 °C to reduce peptide aggregation. NMR data were processed using XWinNMR. ^1H - ^{15}N heteronuclear single quantum correlation (HSQC) spectra were acquired

using GARP decoupling. The number of points acquired in the direct dimension (^1H) was 2048, and the number of increments in the indirect dimension (^{15}N) was 256 experiments.

Molecular cloning

DNA sequences for $A\beta_{(M1-42)}$ familial mutant

DNA sequences for $A\beta_{(M1-42)}$ familial mutant peptides were ordered from Genewiz. Figure 1.S3 shows the design of the DNA sequences for $A\beta_{(M1-42)}$ mutants.

■ 3' and 5' overhangs ■ *NdeI* restriction site/start codon ■ stop codons
■ *SacI* restriction site ■ familial mutation

> $A\beta_{(M1-42)}$

GATATA CAT ATG GAC GCT GAA TTC CGT CAC GAC TCT GGT TAC GAA GTT CAC
CAC CAG AAG CTG GTG TTC TTC GCT GAA GAC GTG GGT TCT AAC AAG GGT GCT
ATC ATC GGT CTG ATG GTT GGT GGC GTT GTG ATC GCT TAA TAG GAGCTC
GATCCG

> $A\beta_{(M1-42/A21G)}$

GATATA CAT ATG GAC GCT GAA TTC CGT CAC GAC TCT GGT TAC GAA GTT CAC
CAC CAG AAG CTG GTG TTC TTC GGT GAA GAC GTG GGT TCT AAC AAG GGT GCT
ATC ATC GGT CTG ATG GTT GGT GGC GTT GTG ATC GCT TAA TAG GAGCTC
GATCCG

> $A\beta_{(M1-42/E22G)}$

GATATA CAT ATG GAC GCT GAA TTC CGT CAC GAC TCT GGT TAC GAA GTT CAC
CAC CAG AAG CTG GTG TTC TTC GCT GGT GAC GTG GGT TCT AAC AAG GGT GCT
ATC ATC GGT CTG ATG GTT GGT GGC GTT GTG ATC GCT TAA TAG GAGCTC
GATCCG

> $A\beta_{(M1-42/E22K)}$

GATATA CAT ATG GAC GCT GAA TTC CGT CAC GAC TCT GGT TAC GAA GTT CAC
CAC CAG AAG CTG GTG TTC TTC GCT AAG GAC GTG GGT TCT AAC AAG GGT GCT
ATC ATC GGT CTG ATG GTT GGT GGC GTT GTG ATC GCT TAA TAG GAGCTC
GATCCG

>A β _(M1-42/E22Q)

GATATA CAT ATG GAC GCT GAA TTC CGT CAC GAC TCT GGT TAC GAA GTT CAC
CAC CAG AAG CTG GTG TTC TTC GCT CAG GAC GTG GGT TCT AAC AAG GGT GCT
ATC ATC GGT CTG ATG GTT GGT GGC GTT GTG ATC GCT TAA TAG GAGCTC
GATCCG

>A β _(M1-42/D23N)

GATATA CAT ATG GAC GCT GAA TTC CGT CAC GAC TCT GGT TAC GAA GTT CAC
CAC CAG AAG CTG GTG TTC TTC GCT GAA AAC GTG GGT TCT AAC AAG GGT GCT
ATC ATC GGT CTG ATG GTT GGT GGC GTT GTG ATC GCT TAA TAG GAGCTC
GATCCG

Figure 1.S3. Design of the DNA sequences for A β _(M1-42) mutants.

Restriction enzyme digestion of pET-Sac-A β _(M1-42) and A β _(M1-42) familial mutant DNA sequences

The pET-Sac-A β _(M1-42) plasmid was digested using *SacI* and *NdeI* restriction enzymes. Table 1.S4 details the restriction reaction conditions. Reagents were added in the order they are listed.

Table 1.S4. Double-digestion of the pET- Sac A β _(M1-42) plasmid.

Reagents	Amount
pET-Sac A β _(M1-42)	20 μ L of 50 ng/uL plasmid solution (1.0 μ g in total)
10X CutSmart buffer	5.0 μ L

H ₂ O	23.0 μ L
<i>Nde</i> I restriction enzyme	1.0 μ L (1 U)
<i>Sac</i> I-HF restriction enzyme	1.0 μ L (1 U)
Total	50.0 μ L
<hr/>	
Time	1.0 h
Temperature	37.0 $^{\circ}$ C

Next, to prevent backbone self-ligation, the digested plasmid was treated with shrimp alkaline phosphatase (rSAP). Table 1.S5 details the rSAP reaction conditions.

Table 1.S5. SAP treatment of the vectors.

Reagents	Amount
Double-digestion mixture	50.0 μ L
rSAP	1.0 μ L (1U)
Total	51.0 μ L
<hr/>	
Time	0.5 h
Temperature	37.0 $^{\circ}$ C
Heat inactivation	65.0 $^{\circ}$ C for 20 min

After the rSAP reaction and heat inactivation were complete, the reaction mixture was mixed with DNA loading buffer and loaded onto a 1% agarose gel containing ethidium bromide (5 μ L per 100 mL gel). The agarose gel was run at 100 V for ~30 min. A UV box was used to visualize the digested pET-Sac vector (~4500 bp), which was excised from the gel using a razor blade. The digested pET-Sac vector was purified from the agarose gel using a Zymoclean Gel DNA Recovery Kit. The concentration of the vector after purification was measured using a

Thermo Scientific Nanodrop instrument. The purified digested pET-Sac linear vector was used in the subsequent ligation step.

The A β _(M1-42) mutant DNA sequences were digested using *SacI* and *NdeI* restriction enzymes. Table 1.S6 details the restriction reaction conditions. Reagents were added in the order they are listed.

Table 1.S6. Double-digestion of the inserts.

Reagents	Amount
DNA sequence encoding mutation	20 μ L of 5 ng/ μ L DNA solution (100.0 ng in total)
10X CutSmart buffer	2.5 μ L
H ₂ O	1.5 μ L
<i>NdeI</i> restriction enzyme	0.5 μ L (0.5 U)
<i>SacI</i> -HF restriction enzyme	0.5 μ L (0.5 U)
Total	25.0 μ L
<hr style="border-top: 1px dashed black;"/>	
Time	1 h
Temperature	37.0 $^{\circ}$ C
Heat inactivation	65.0 $^{\circ}$ C for 20 min

T4 ligation of the A β _(M1-42) mutant DNA sequences and the linear digested pET-Sac vector

The inserts and the vectors were ligated together using T4 ligase. Table 1.S7 details the T4 ligation reaction conditions. Reagents were added in the order they are listed.

Table 1.S7. T4 ligation of the inserts and the vectors.

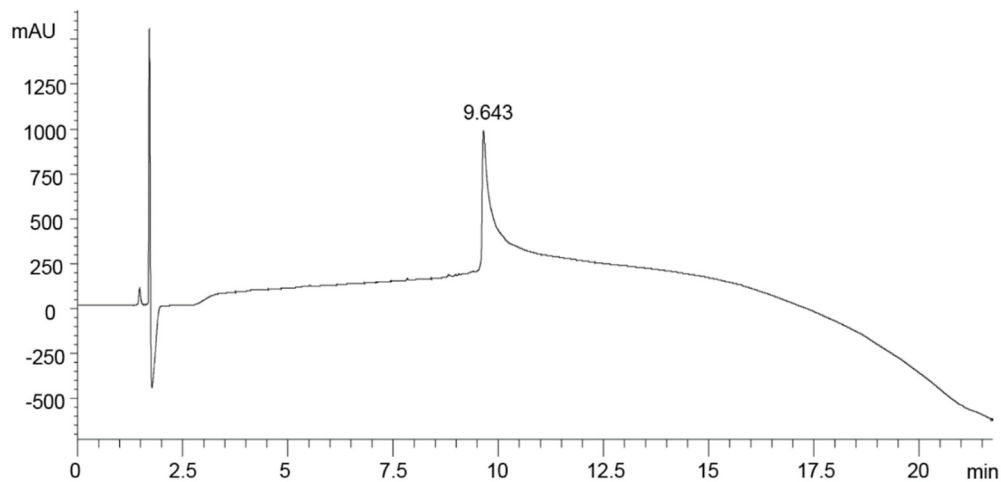
Reagents	Amount
----------	--------

	Insert:Vector = 0:1 (molar ratio) (negative control)	Insert:Vector = 5:1 (molar ratio)
Vector	6.2 μ L of 9.7 ng/ μ L DNA solution (60.0 ng in total)	6.2 μ L of 9.7 ng/ μ L DNA solution (60.0 ng in total)
Insert	---	2.5 μ L of 4.0 ng/ μ L DNA solution (10.0 ng in total)
10X T4 DNA ligase reaction buffer	2.0 μ L	2.0 μ L
T4 DNA ligase	1.0 μ L	1.0 μ L
H ₂ O	10.8 μ L	8.3 μ L
Total	20.0 μ L	20.0 μ L
Time	10 min	
Temperature	22.0 °C (room temperature)	
Heat inactivation	65.0 °C for 10 min	

2 μ L of the ligation reaction mixture was then transformed into TOP10 Ca²⁺-competent *E. coli* using the heat shock method. The cell cultures were spread on LB agar plates containing carbenicillin (50 mg/L). Single colonies were picked to inoculate 5 mL of overnight cultures in LB media with carbenicillin (50 mg/L). The plasmids were extracted from TOP10 cells using Zymo ZR plasmid miniprep kit. The concentration of the plasmids was measured through Thermo Scientific NanoDrop spectrophotometer. The sequences of the A β _(M1-42) mutants were verified by DNA sequencing.

Characterization Data

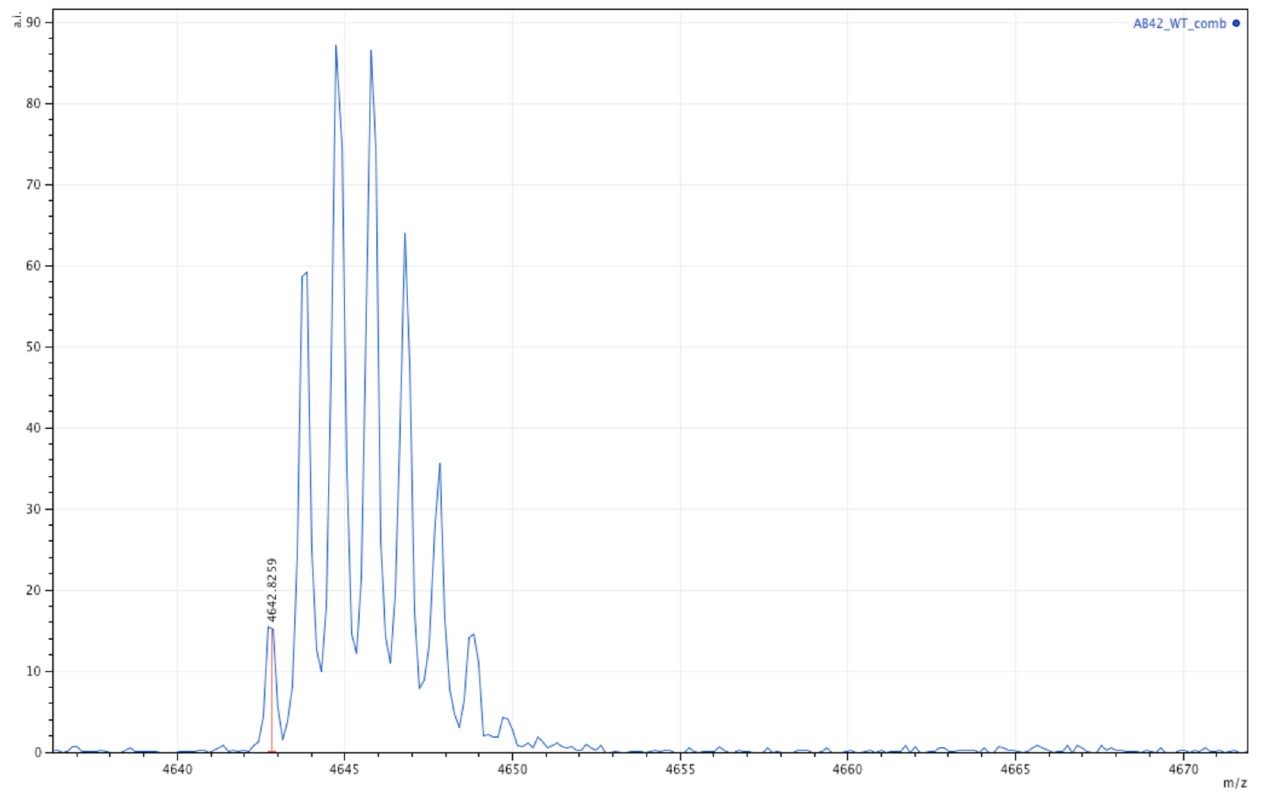
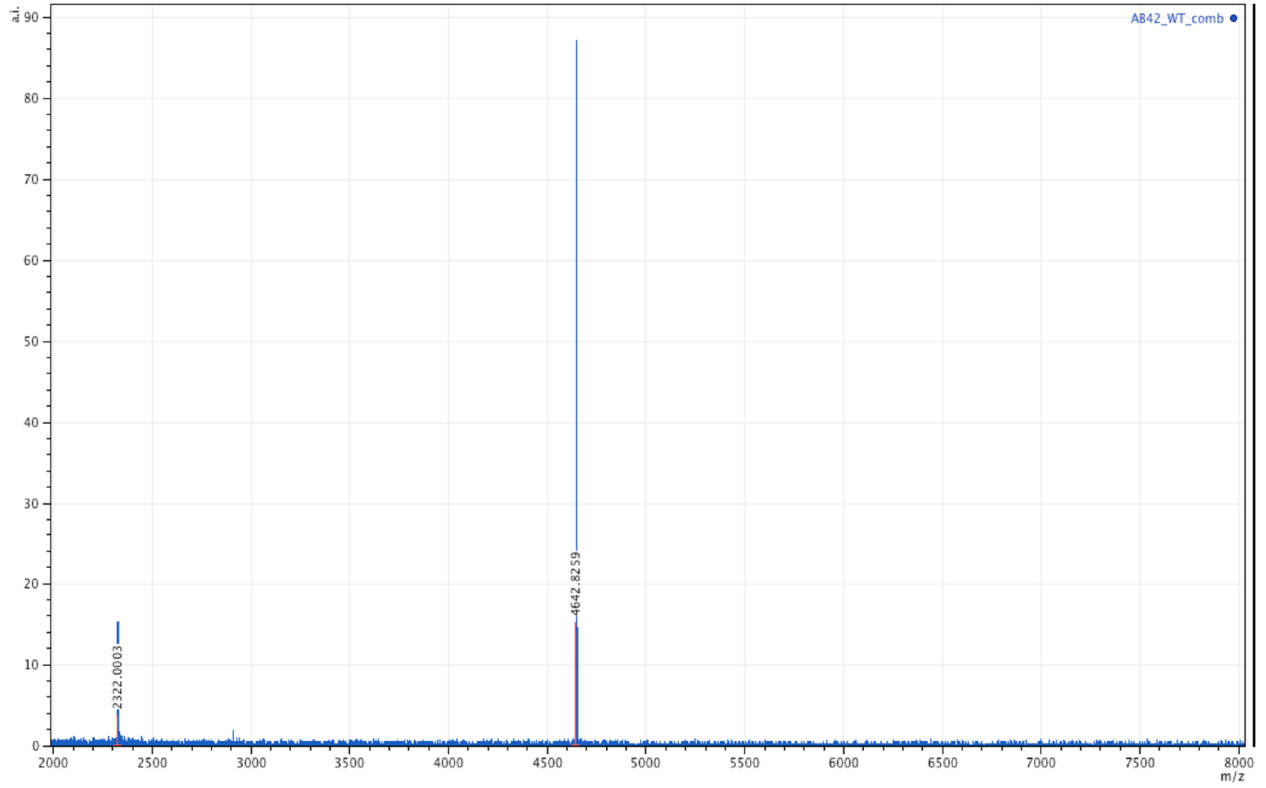
Analytical HPLC trace of $A\beta_{(M1-42)}$. % Purity: >99%



MALDI-MS trace of $A\beta_{(M1-42)}$.

Positive reflector mode; Matrix: 2,5-dihydroxybenzoic acid.

Exact mass calculated for M^+ : 4642.3; Exact mass calculated for $[M+H]^+$: 4643.3; Exact mass calculated for $[M+2H]^{2+}$: 2322.2. Observed $[M+H]^+$: 4642.8; Observed $[M+2H]^{2+}$: 2322.0.



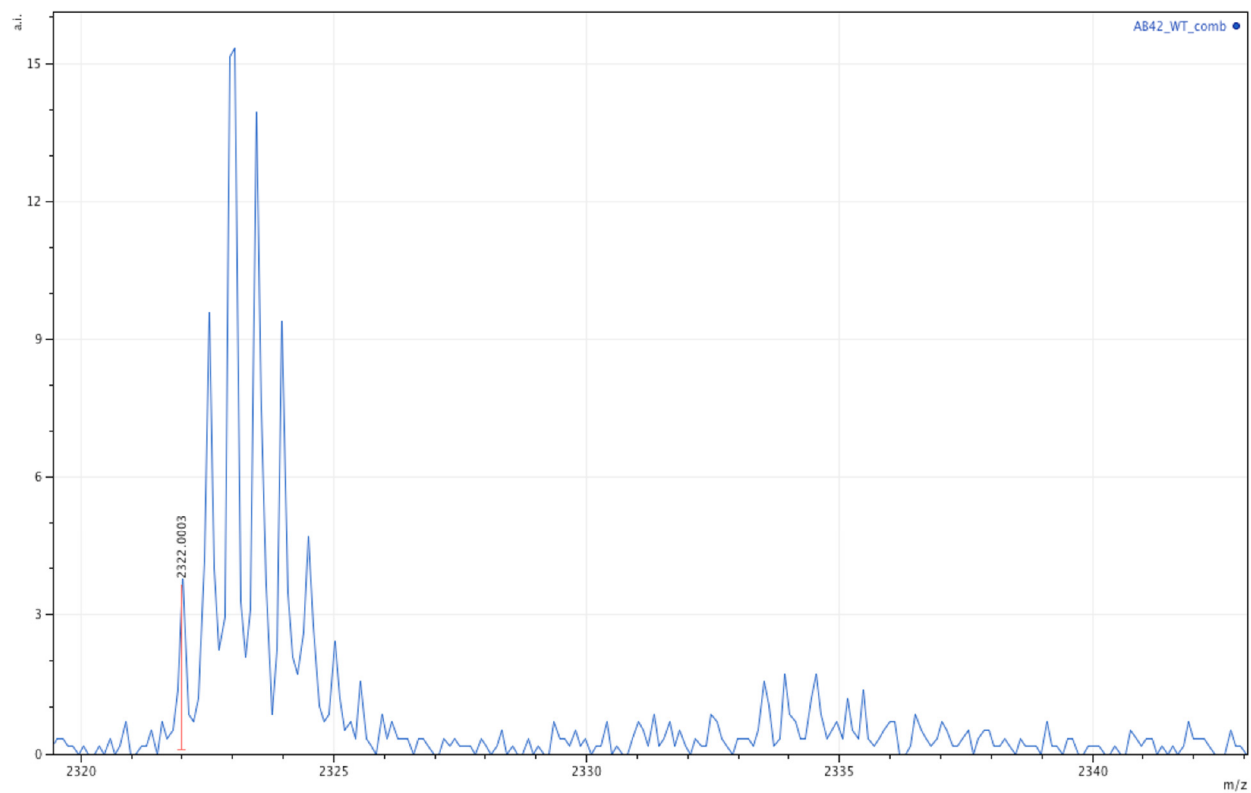
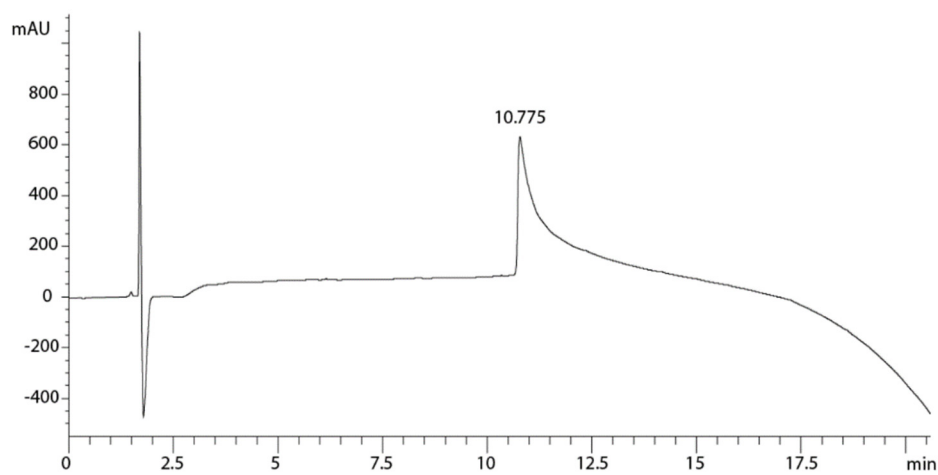


Figure 1.S4. Analytical HPLC and MALDI-MS traces of $A\beta_{(M1-42)}$.

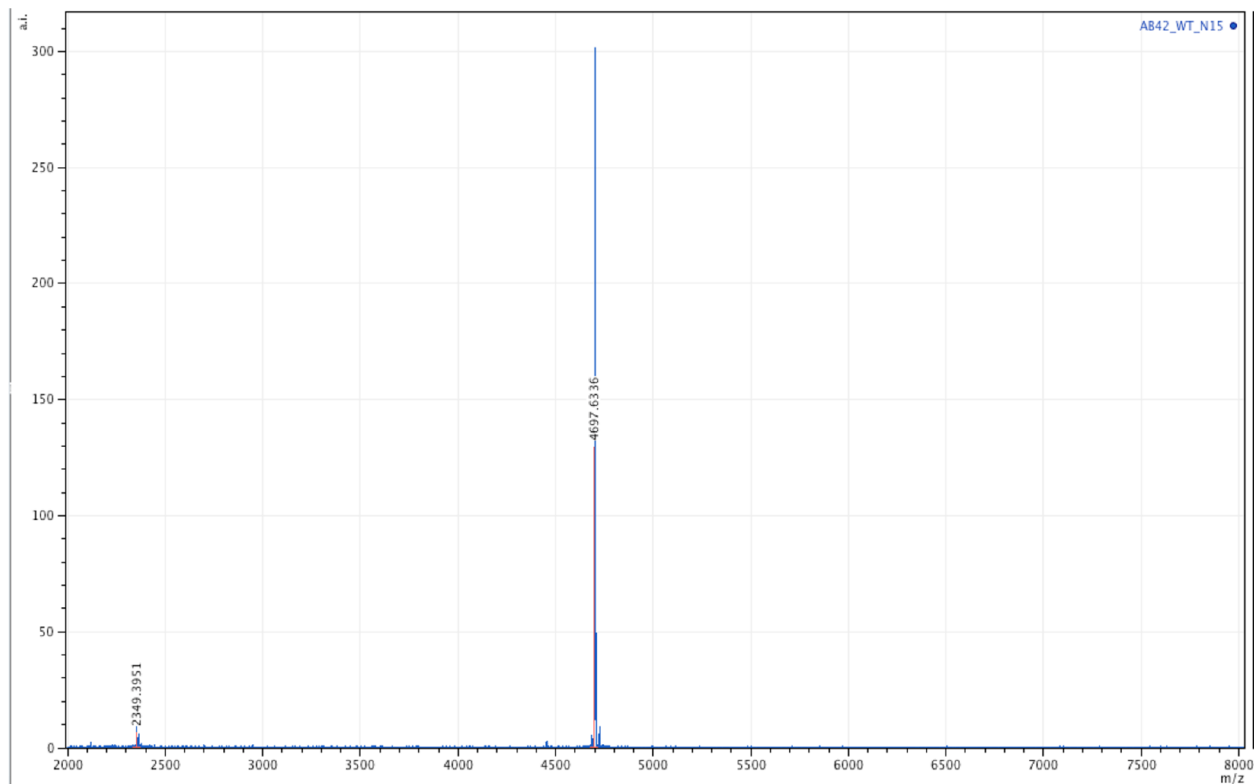
Analytical HPLC trace of ^{15}N -labeled $A\beta_{(M1-42)}$. % Purity: >99%



MALDI-MS trace of ^{15}N -labeled $\text{A}\beta_{(\text{M1-42})}$.

Positive reflector mode. Matrix: 2,5-dihydroxybenzoic acid.

Exact mass calculated for M^+ : 4698.3; Exact mass calculated for $[\text{M}+\text{H}]^+$: 4699.3; Exact mass calculated for $[\text{M}+2\text{H}]^{2+}$: 2350.2. Observed $[\text{M}+\text{H}]^+$: 4697.6; Observed $[\text{M}+2\text{H}]^{2+}$: 2349.4.



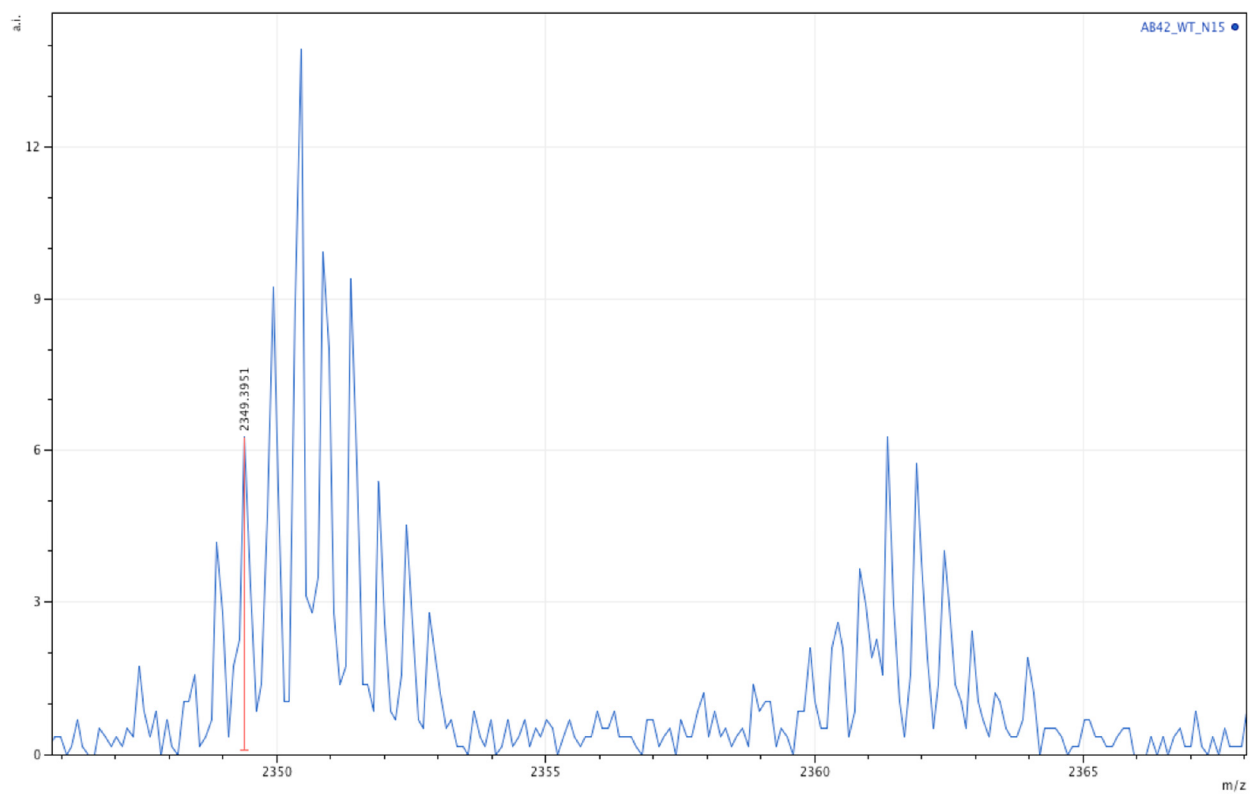
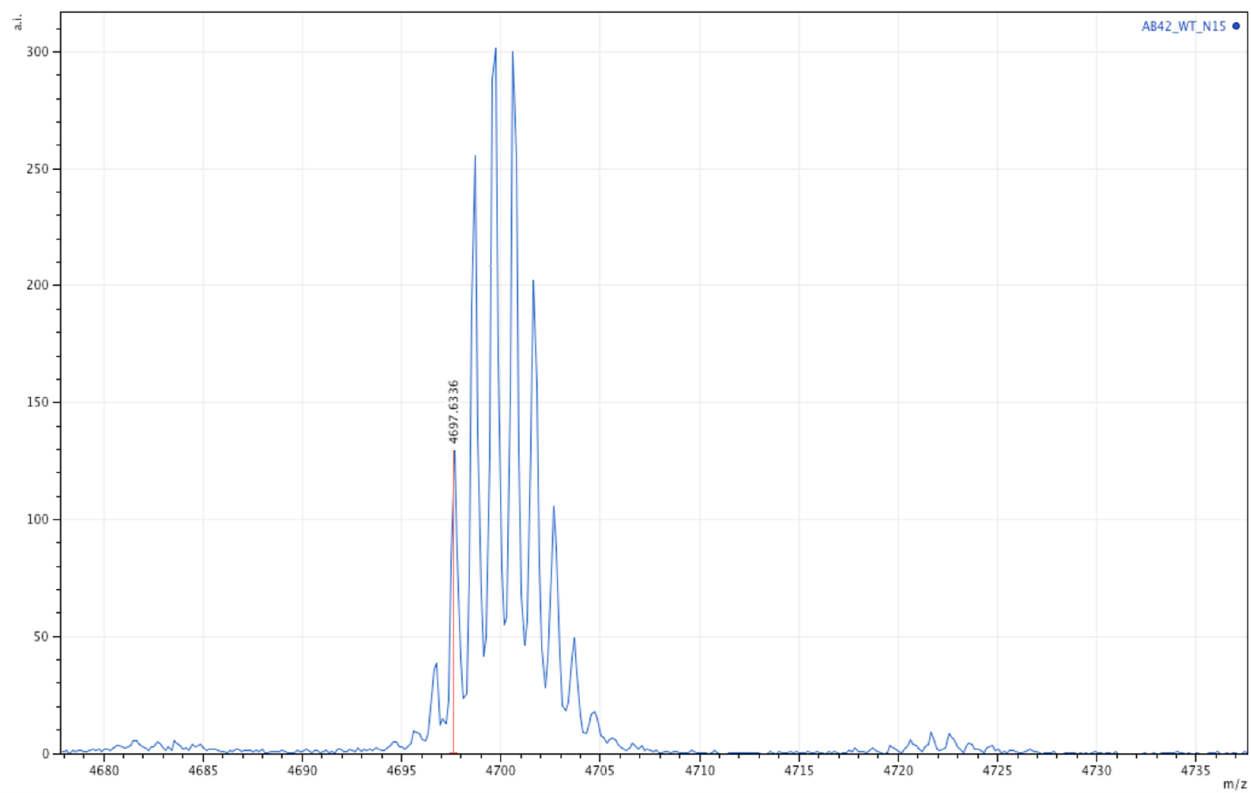
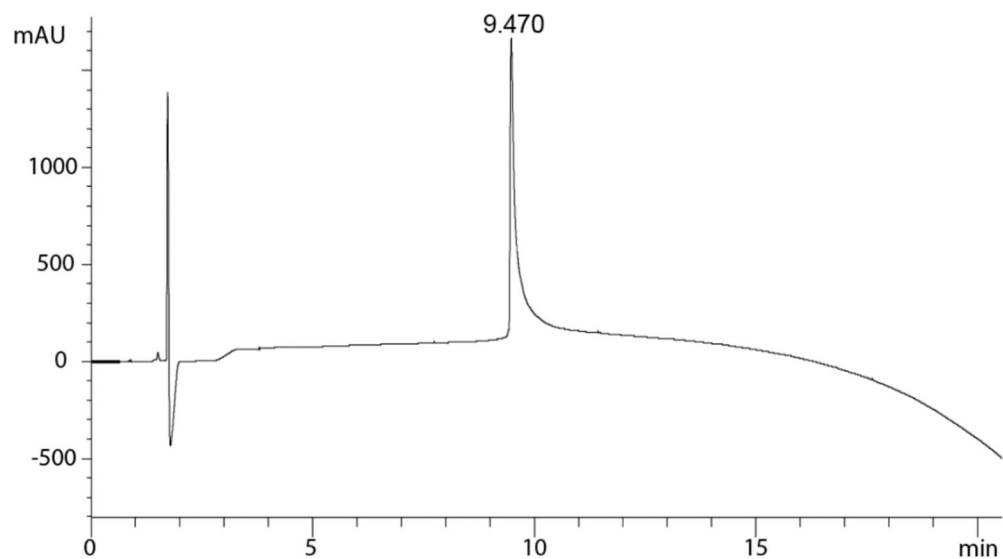


Figure 1.S5. Analytical HPLC and MALDI-MS traces of ¹⁵N-labeled Aβ_(M1-42).

Analytical HPLC trace of $A\beta_{(M1-42/A21G)}$. % purity: >99%



MALDI-MS trace of $A\beta_{(M1-42/A21G)}$.

Positive reflector mode. Matrix: 2,5-dihydroxybenzoic acid.

Exact mass calculated for M^+ : 4628.3; Exact mass calculated for $[M+H]^+$: 4629.3. Observed $[M+H]^+$: 4629.1.

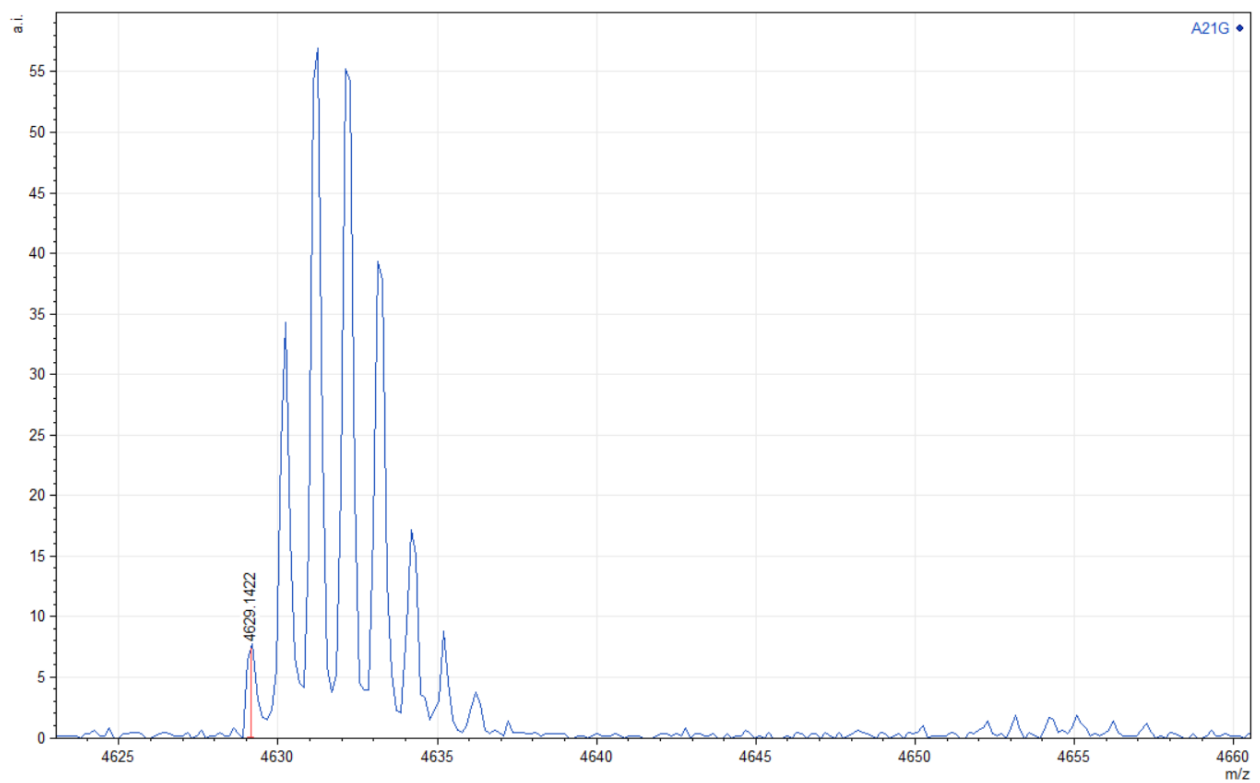
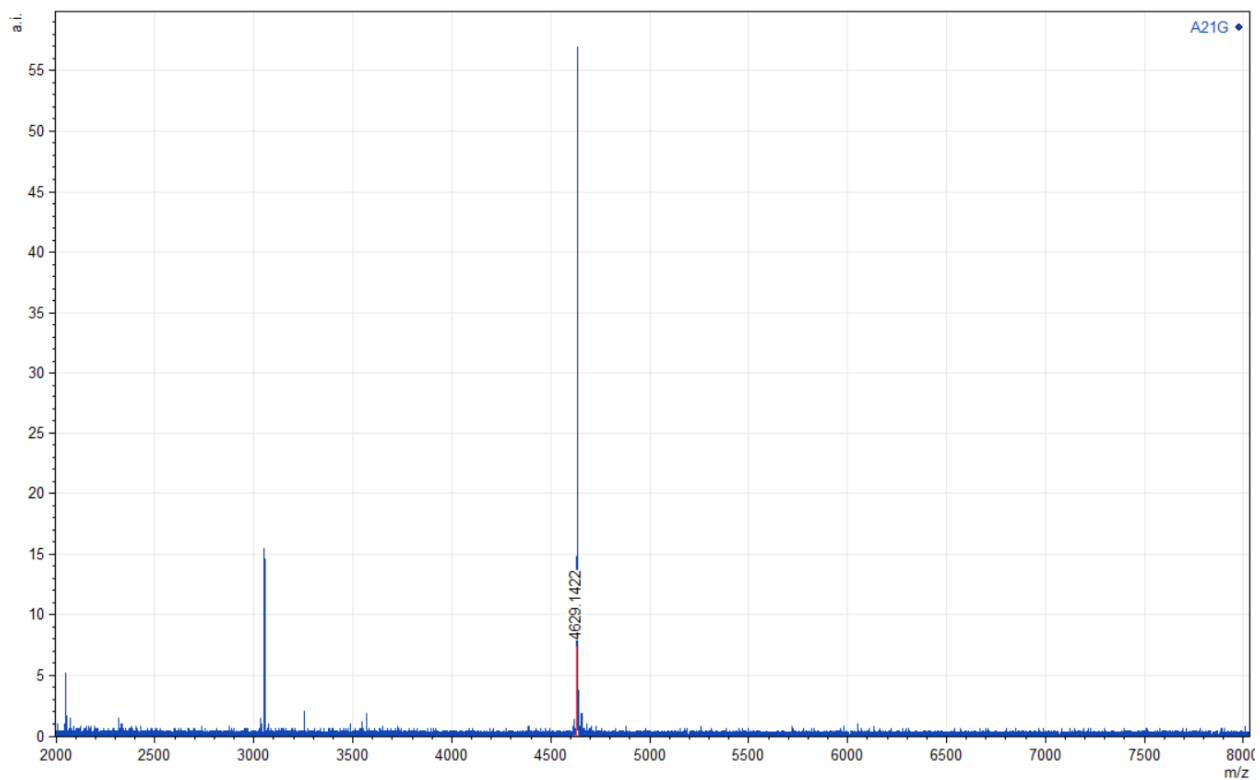
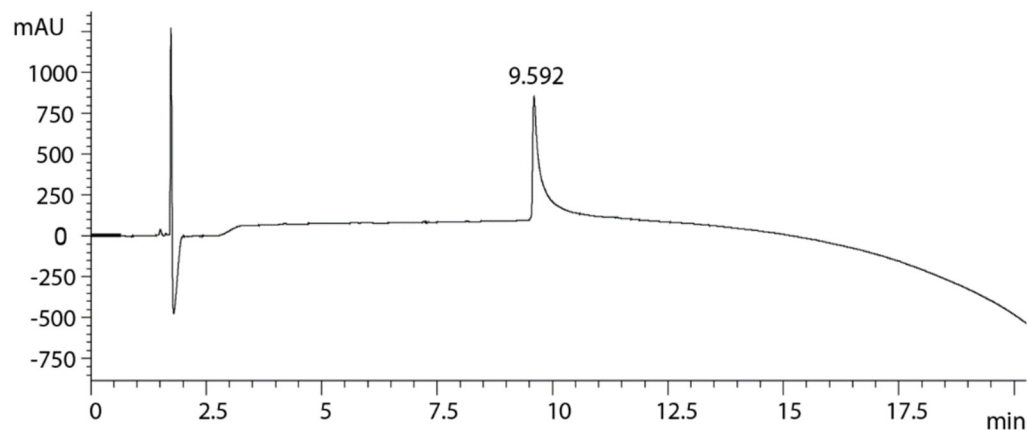


Figure 1.S6. Analytical HPLC and MALDI-MS traces of Aβ_(M1-42/A21G).

Analytical HPLC trace of A β _(M1-42/E22G). % purity: >99%



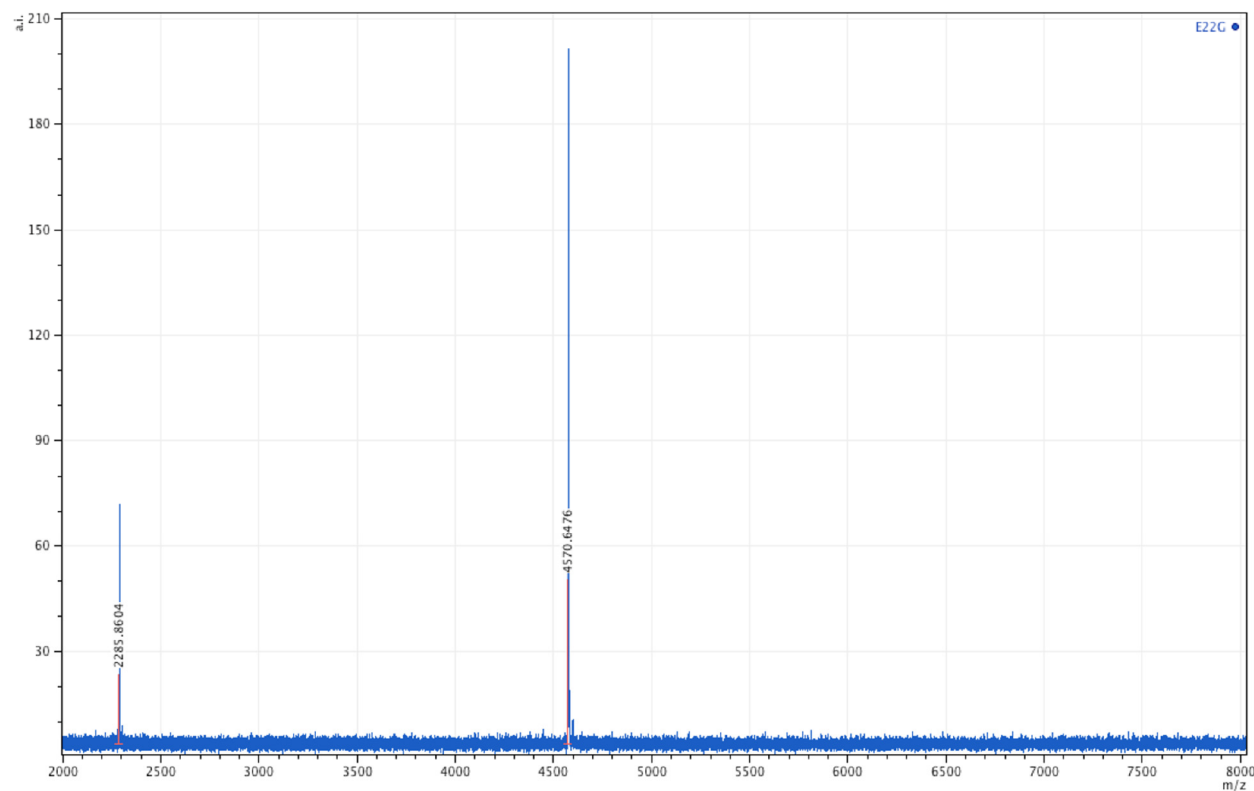
MALDI-MS trace of A β _(M1-42/E22G).

Positive reflector mode.

Matrix: 2,5-dihydroxybenzoic acid.

Exact mass for M⁺: 4570.3; Exact mass calculated for [M+H]⁺: 4571.3; Exact mass calculated for [M+2H]²⁺: 2286.2.

Observed [M+H]⁺: 4570.6; Observed [M+2H]²⁺: 2285.9.



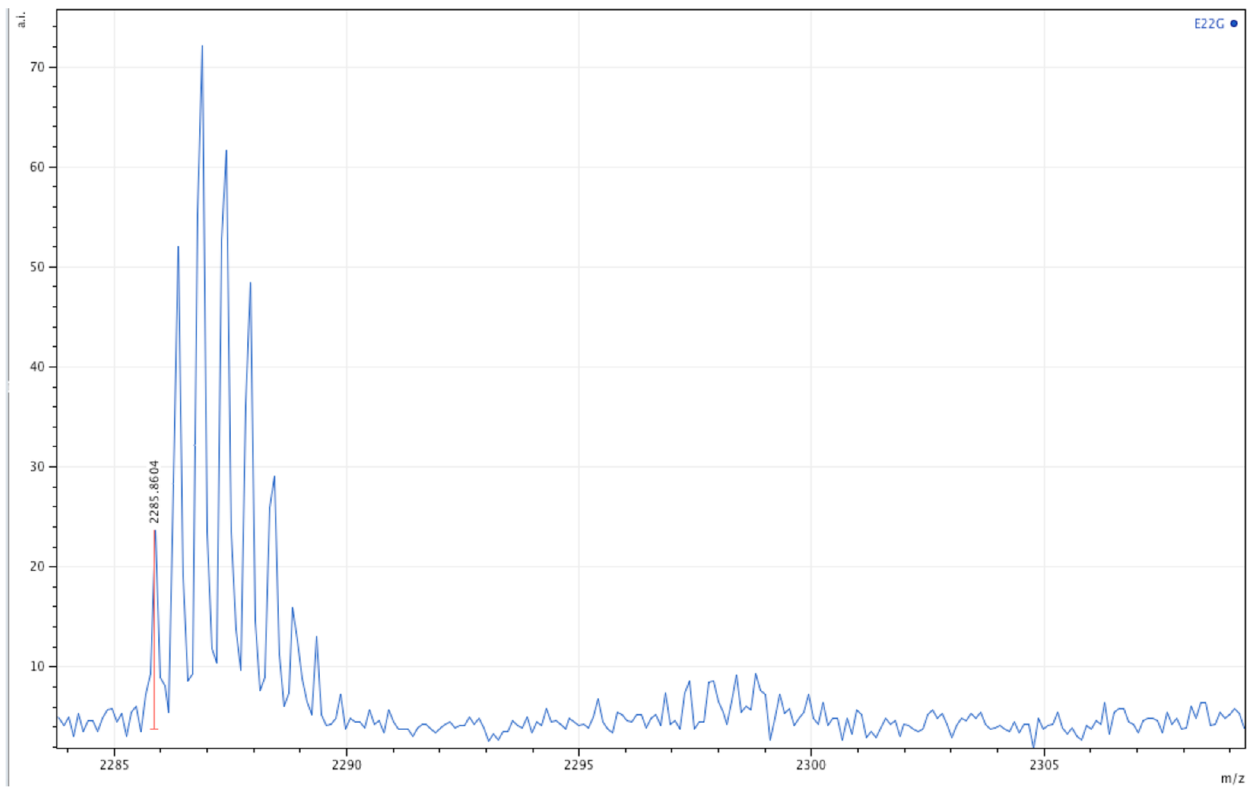
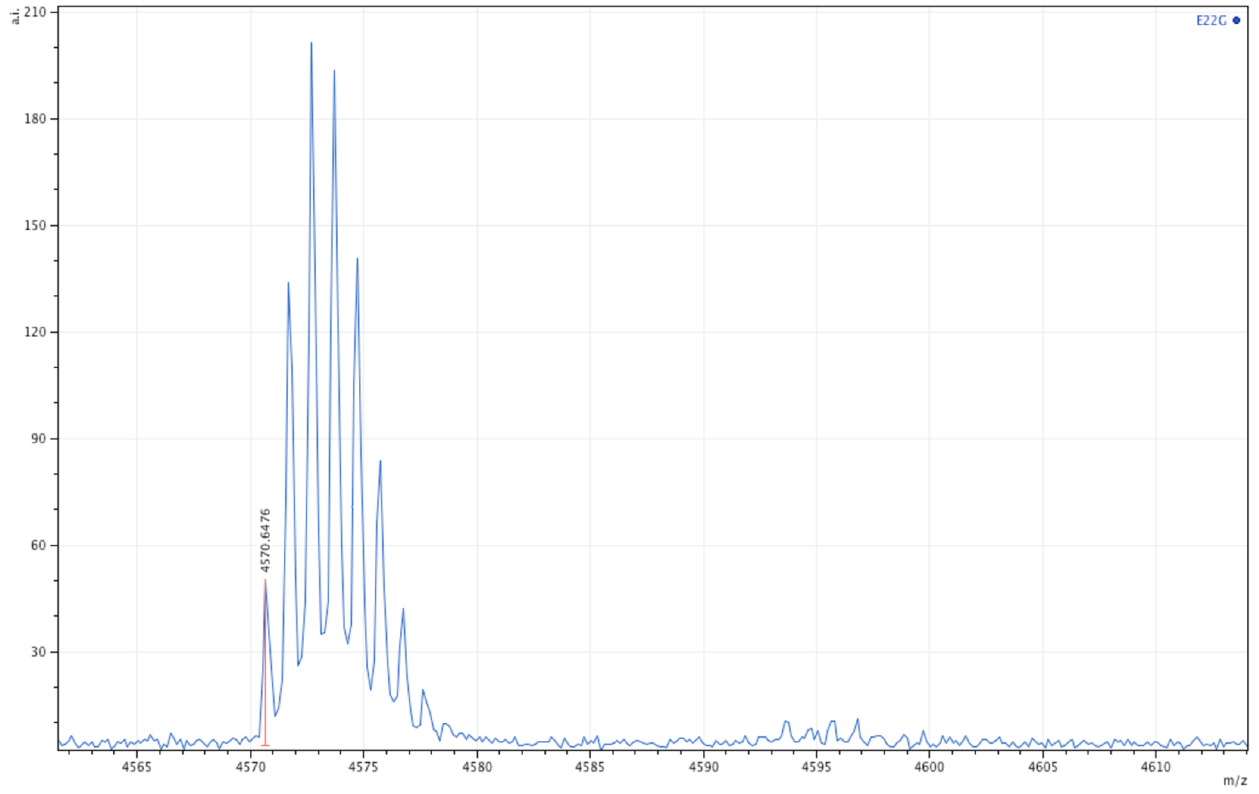
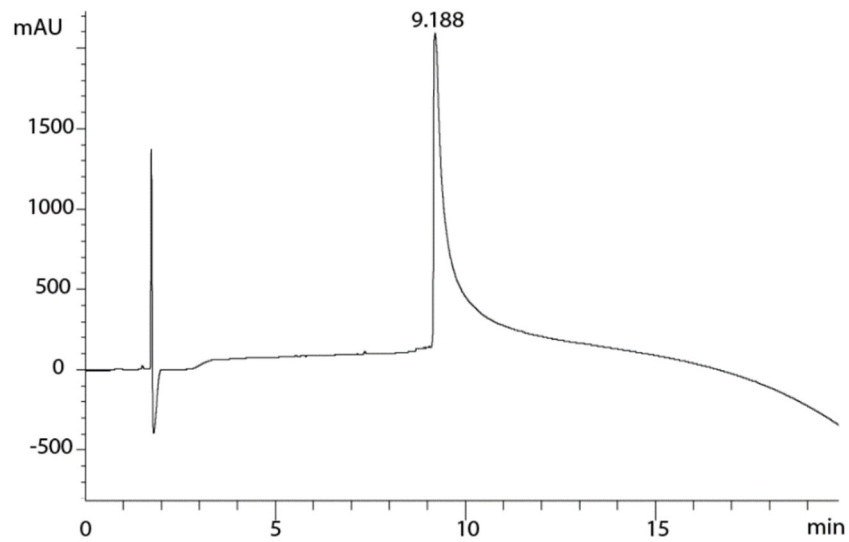


Figure 1.S7. Analytical HPLC and MALDI-MS traces of $A\beta_{(M1-42/E22G)}$.

Analytical HPLC trace of $A\beta_{(M1-42/E22K)}$. % purity: >99%



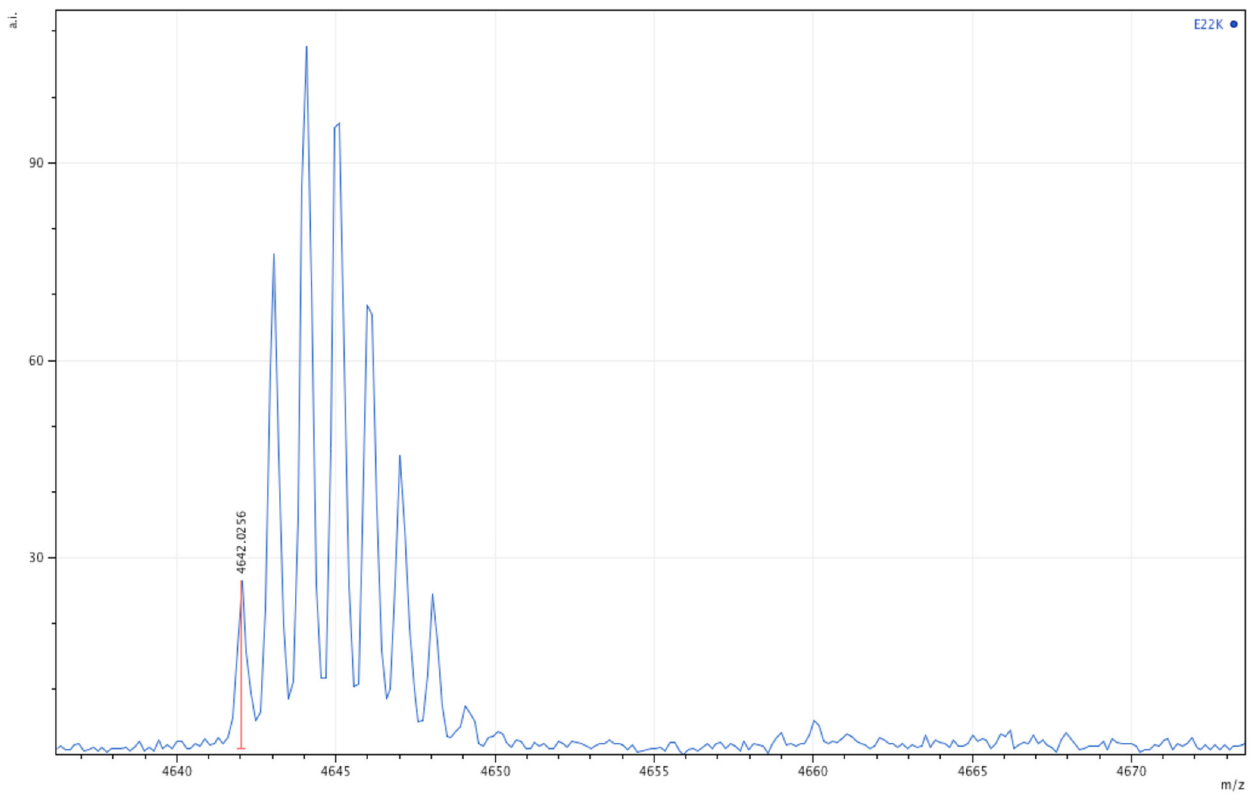
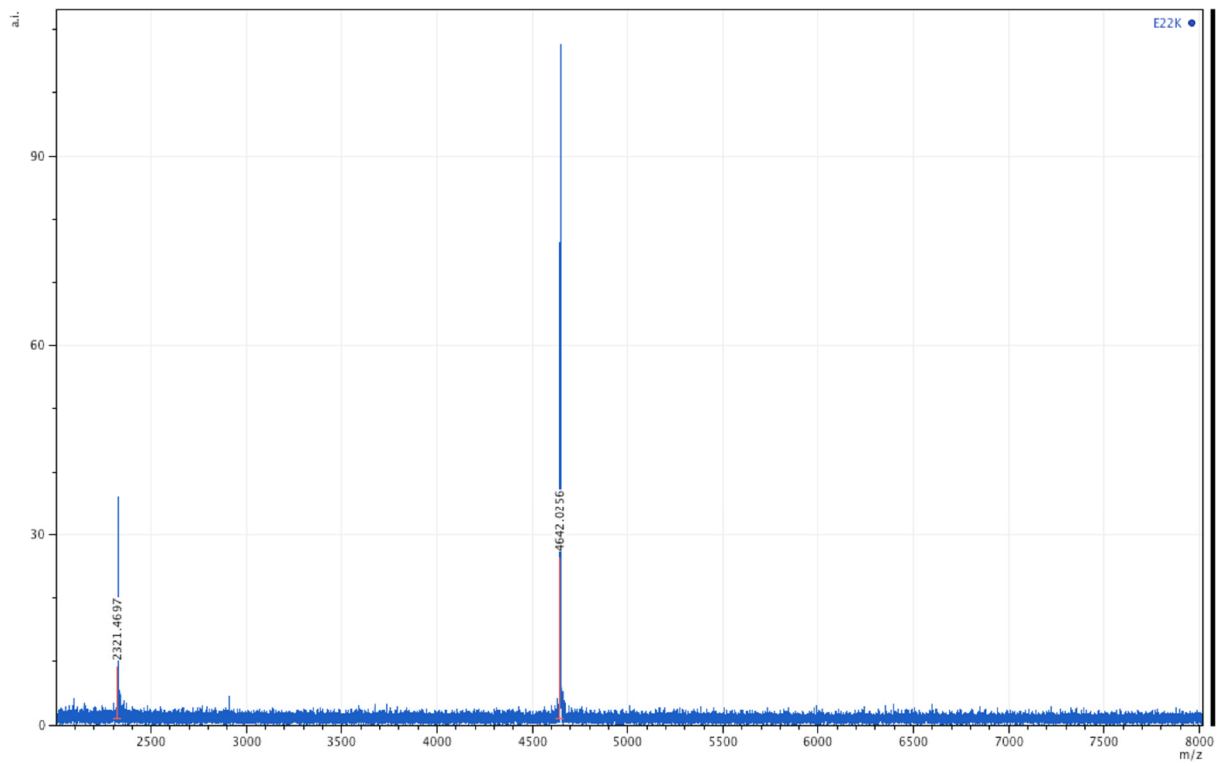
MALDI-MS trace of $A\beta_{(M1-42/E22K)}$.

Positive reflector mode.

Matrix: 2,5-dihydroxybenzoic acid.

Exact mass for M^+ : 4641.3; Exact mass calculated for $[M+H]^+$: 4642.3; Exact mass calculated for $[M+2H]^{2+}$: 2321.7.

Observed $[M+H]^+$: 4642.0; Observed $[M+2H]^{2+}$: 2321.5.



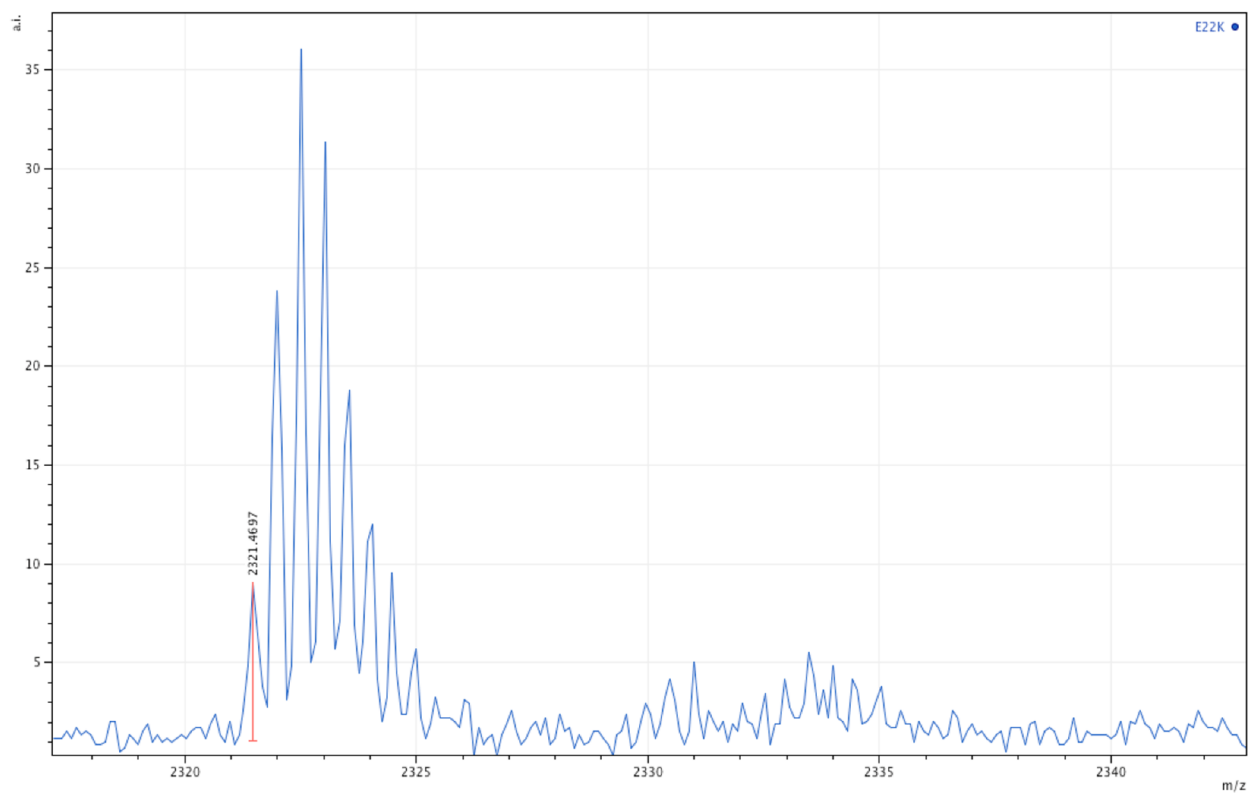
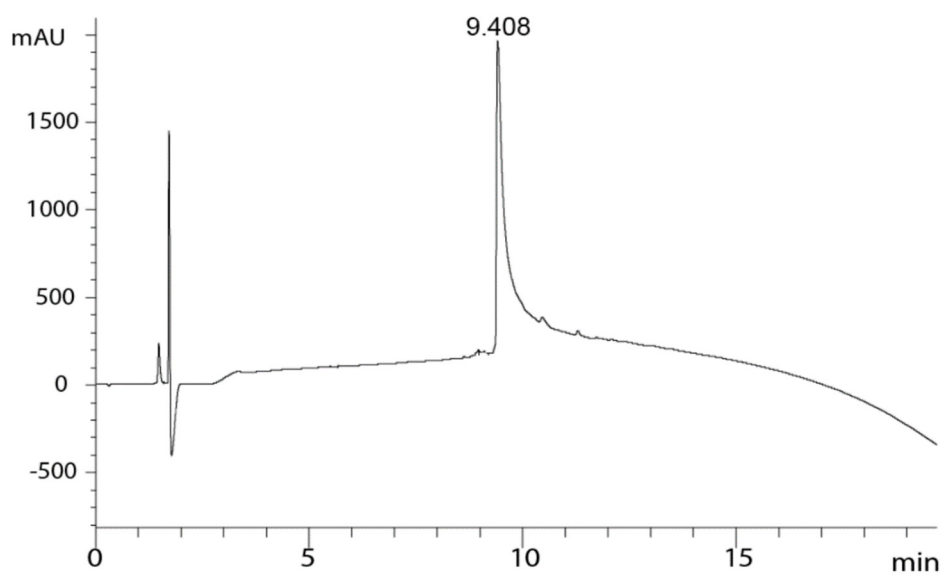


Figure 1.S8. Analytical HPLC and MALDI-MS traces of $A\beta_{(M1-42/E22K)}$.

Analytical HPLC trace of $A\beta_{(M1-42/D23N)}$. % purity: >95%



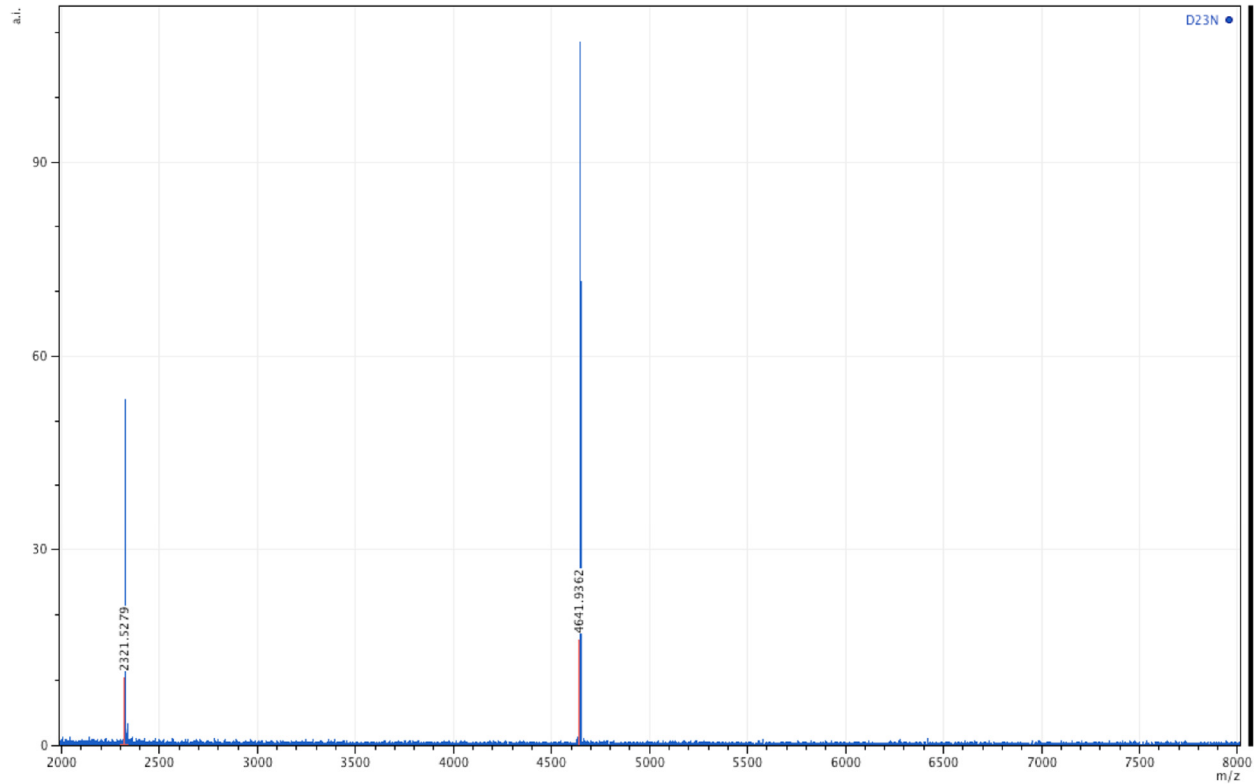
MALDI-MS trace of A β _(M1-42/D23N).

Positive reflector mode.

Matrix: 2,5-dihydroxybenzoic acid.

Exact mass for M⁺: 4641.3; Exact mass calculated for [M+H]⁺: 4642.3; Exact mass calculated for [M+2H]²⁺: 2321.7.

Observed [M+H]⁺: 4641.9; Observed [M+2H]²⁺: 2321.5.



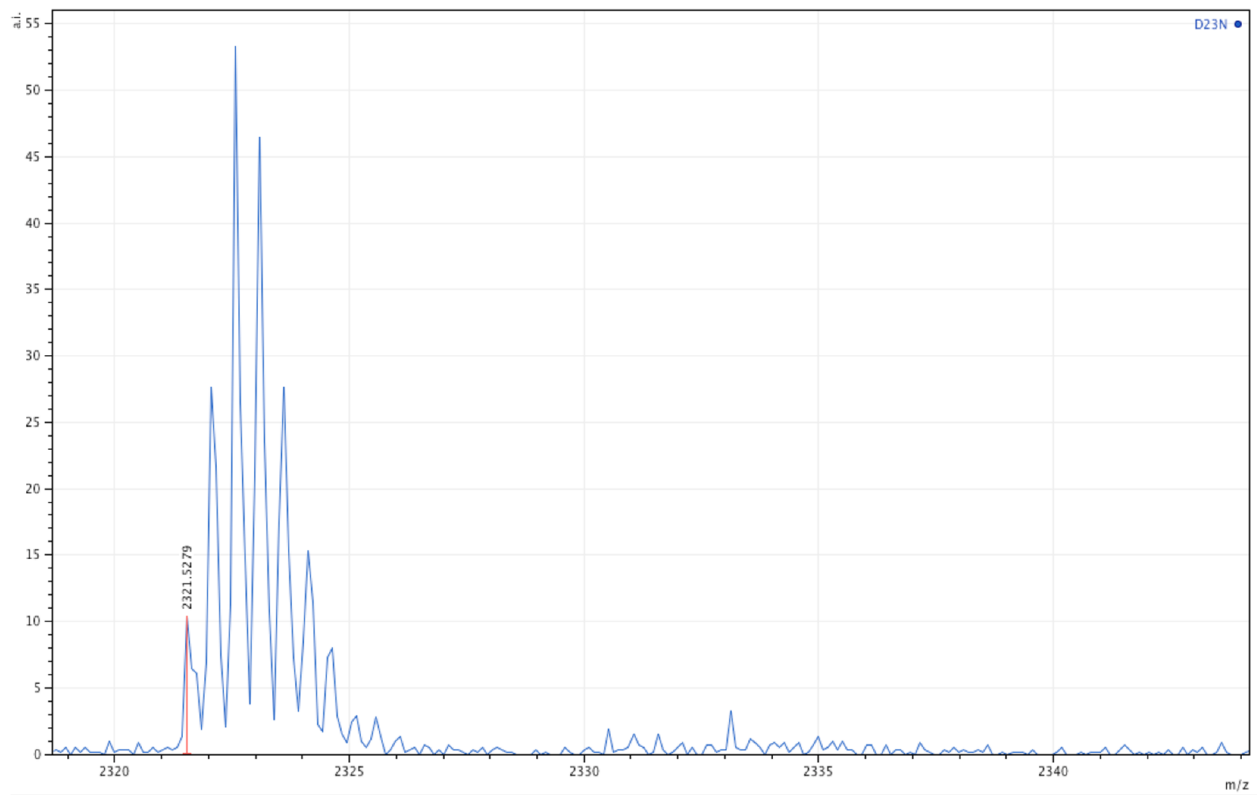
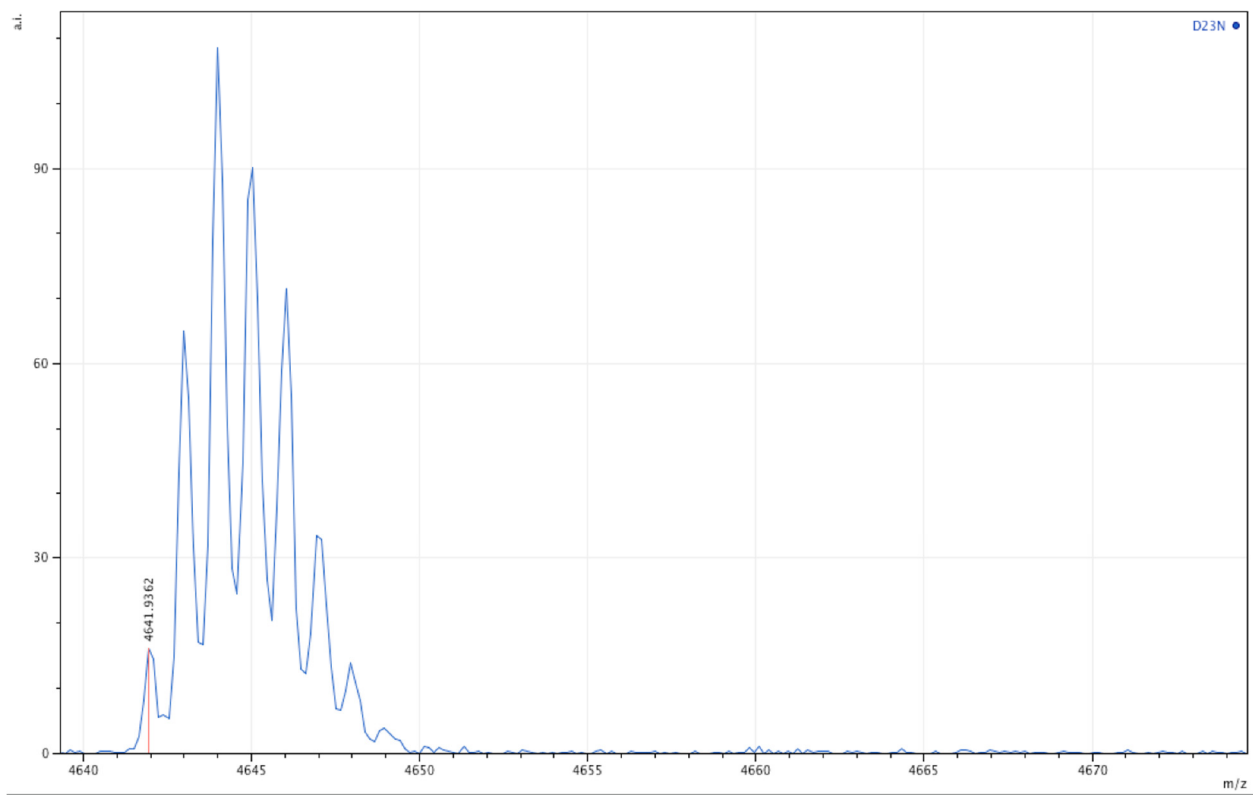


Figure 1.S9. Analytical HPLC and MALDI-MS traces of $A\beta_{(M1-42/D23N)}$

References

1. Walsh, D. M., Thulin, E., Minogue, A. M., Gustavsson, N., Pang, E., Teplow, D. B., and Linse, S. A facile method for expression and purification of the Alzheimer's disease-associated amyloid beta-peptide, *FEBS J.* **2009**, *276*, 1266-1281.
2. Kreutzer, A. G., Yoo, S., Spencer, R. K., and Nowick, J. S. Stabilization, Assembly, and Toxicity of Trimers Derived from Aβ, *J. Am. Chem. Soc.* **2017**, *139*, 966-975.

Chapter 2^a

Expression of N-Terminal Cysteine A β ₄₂ and Conjugation to Generate Fluorescent and Biotinylated A β ₄₂

Introduction

Peptides and proteins bearing an N-terminal cysteine residue are valuable tools in chemical biology research, because the unique reactivity of N-terminal cysteine permits native chemical ligation, conjugation, and other site-specific modifications.¹⁻⁴ Amyloid- β (A β) peptides bearing an N-terminal cysteine offer promise in Alzheimer's disease research through N-terminal labeling with fluorophores or biotin, as well as other N-terminal modifications. N-terminally labeled A β peptides have been widely used to investigate cellular phagocytosis, transport, and clearance of A β through optical fluorescence microscopy, and to screen anti-A β antibodies through enzyme-linked immunosorbent assays (ELISA).⁵⁻²⁹ Site-specific labeling on the N-terminus of A β minimizes perturbation in the structure and function of the peptide, as the central and the C-terminal regions of A β are more involved in fibril and oligomer formation.^{16,27,30} Although some N-terminally

^a This chapter is adapted from Zhang, S.; Guaglianone, G.; Morris, M. A.; Yoo, S.; Howitz, W. J.; Xing, L.; Zheng, J.; Jusuf, H.; Huizar, G.; Lin, J.; Kreutzer, A. G.; Nowick, J. S. *Biochemistry* **2021**, 60, 1191–1200.

labeled derivatives of A β are commercially available, they are expensive (ca. \$1000/mg) and limited to biotin and a few common fluorophores. Ready access to good quantities of pure N-terminally labeled A β can advance Alzheimer's disease research by enabling experiments that would otherwise be hindered by insufficient access to these peptides.

Here we describe an efficient method for recombinant expression and purification of the A β peptide with an N-terminal cysteine, A $\beta_{(C1-42)}$, and the preparation of labeled A $\beta_{(C1-42)}$ peptides. Expressed A β peptides are superior to chemically synthesized A β , because they are free from the amino acid deletions or epimers that form through amino acid racemization during each coupling step.^{31,32} Expressed A β peptides have been found to aggregate more quickly and be more toxic than synthetic A β , and thus are widely used in amyloid research.³³⁻³⁵ Although A β peptides bearing fluorescent and biotin labels can be prepared by chemical synthesis, the expressed A β peptide bioconjugates should also be preferable to those derived from synthetic A β .

Chapter 1 reported an efficient method for expression and purification of N-terminal methionine A β , A $\beta_{(M1-42)}$.³⁶ In chapter 2, we set out to adapt this method to include a cysteine residue for further functionalization by attempting to express A $\beta_{(MC1-42)}$. When we expressed an A $\beta_{(MC1-42)}$ plasmid in *E. coli*, we were surprised to find that the N-terminal methionine is endogenously excised by the *E. coli* methionyl aminopeptidase (MAP), leaving cysteine on the N-terminus and affording A $\beta_{(C1-42)}$ (Figure 2.1).³⁷⁻³⁹ This hitherto unrecognized observation provides a method of preparing the A $\beta_{(C1-42)}$ peptide, without the additional methionine group that originates from the translational start codon.^{30,40} The absence of methionine is significant, because A $\beta_{(C1-42)}$ represents the minimal modification of native A $\beta_{(1-42)}$ that permits further functionalization through robust cysteine-maleimide conjugation. Our method to prepare A $\beta_{(C1-42)}$ is straightforward and does not require any additional treatment with enzymes or reagents after the initial expression

and reverse-phase preparative HPLC purification. This expression method affords ca. 14 mg of $A\beta_{(C1-42)}$ with > 97% purity from one liter of bacterial culture.



Figure 2.1. Sequences of $A\beta_{(1-42)}$, $A\beta_{(MC1-42)}$, and $A\beta_{(C1-42)}$.

The $A\beta_{(C1-42)}$ can be further functionalized to create a variety of derivatives using thiol-maleimide chemistry and readily available maleimide-based labeling reagents.⁴¹ We have developed an optimized labeling protocol to allow $A\beta_{(C1-42)}$ to be labeled with fluorophores or biotin in 15 minutes without $A\beta$ oligomer or fibril formation, and we demonstrate this protocol through the preparation of $A\beta_{(C1-42)}$ labeled with fluorophores (TAMRA and FAM) and biotin. Only two equivalents of the labeling reagents are required to achieve complete labeling, which minimizes the cost of the maleimide reagents. This labeling protocol affords ca. 3 mg of labeled $A\beta$ from one liter of bacterial culture with minimal cost for reagents. HPLC analysis indicates the labeled peptides to be 94–97% pure. We also demonstrate that these labeled $A\beta$ peptides behave similarly to unlabeled $A\beta_{(M1-42)}$ in aggregation and fibrillization assays, which indicates that the labeling of the N-terminus of $A\beta$ does not substantially alter the properties of the $A\beta$. We further demonstrate the application of the fluorophore-labeled $A\beta_{(C1-42)}$ by using fluorescence microscopy to visualize its interactions with mammalian cells and bacteria.

These methods represent a novel and valuable contribution to the $A\beta$ toolbox, because they exploit a hitherto unrecognized cleavage of methionine in expressed $A\beta_{42}$, provide tailored conjugation conditions to enable rapid labeling of this highly aggregation-prone peptide, and allow choice of wide variety of fluorophores and other labels. We anticipate that these methods will

provide researchers with convenient access to useful A β peptides bearing N-terminal labels or a free N-terminal cysteine residue.

Results and Discussion

We expressed A $\beta_{(C1-42)}$ in *E. coli* using a plasmid for A $\beta_{(MC1-42)}$ that we constructed and have subsequently made available through Addgene.⁴² The expressed peptide forms inclusion bodies that are isolated by multiple rounds of washing. The inclusion bodies are then solubilized in urea buffer, and the solubilized A $\beta_{(C1-42)}$ is purified by reverse-phase HPLC. The pure HPLC fractions of A $\beta_{(C1-42)}$ are combined, and the conjugation reactions are performed directly in the combined pure fractions at alkaline pH. The conjugated peptides are purified by another round of HPLC purification. The pure HPLC fractions are then combined and lyophilized. The yields of the labeled peptides are assessed gravimetrically, and the composition and purity of the peptides are assessed by analytical HPLC and matrix-assisted laser desorption ionization mass spectrometry (MALDI-MS). For subsequent biophysical and biological studies, the purified peptide is rendered monomeric by treatment with hexafluoroisopropanol (HFIP). Biophysical experiments show that the labeled A $\beta_{(C1-42)}$ behaves similarly to unlabeled A $\beta_{(M1-42)}$, and fluorescence microscopy studies with mammalian cells and bacteria further demonstrate applications of the labeled A $\beta_{(C1-42)}$.

Expression and Purification of A $\beta_{(C1-42)}$. We prepared a pET-Sac plasmid encoding A $\beta_{(MC1-42)}$ in the same fashion as we had previously described,³⁶ and we deposited the plasmid with Addgene to make it available to others.⁴² We also provide procedures to prepare the plasmid in the *Supporting Information* (Figure 2.S1). To express A $\beta_{(C1-42)}$, we transform the pET-Sac-A $\beta_{(MC1-42)}$ plasmid into BL21(DE3)-pLysS competent *E. coli* and induce expression with

isopropyl β -D-1-thiogalactopyranoside (IPTG) when the cultured *E. coli* reach an optical density (OD₆₀₀) of 0.45. After expression, we lyse the cells, wash the inclusion bodies containing A β _(C1-42) with Tris buffer, and then solubilize the inclusion bodies with 8 M urea. We then filter the solution through a 0.22 μ m hydrophilic polyethersulfone (PES) syringe filter or a 0.22 μ m hydrophilic polyvinylidene fluoride (PVDF) filter (to prevent damaging the HPLC columns) and purify the A β _(C1-42) by preparative reverse-phase HPLC using a C8 column at 80 °C with water and acetonitrile containing 0.1% trifluoroacetic acid (TFA). A typical analytical HPLC trace of the filtered lysate shows four major peaks, with the first peak corresponding to the A β _(C1-42) monomer (Figure 2.S2). The A β _(C1-42) monomer elutes at ca. 34% acetonitrile during the preparative HPLC purification. We then combine the HPLC fractions containing pure A β _(C1-42) monomer, and the combined pure fractions typically show >97% purity, as assessed by analytical HPLC (Figure 2.2A and Figure 2.S7). We measure the concentration of A β _(C1-42) in the combined the HPLC fractions by UV absorbance at 280 nm with an estimated extinction coefficient for tyrosine of 1490 M⁻¹cm⁻¹. On the basis of the spectrophotometrically determined concentration, we typically obtain ca. 14 mg of A β _(C1-42) as the trifluoroacetate salt from one liter of bacterial culture.

MALDI-MS shows that the mass of the peptide is consistent with A β _(C1-42), not A β _(MC1-42) (Figure 2.2B), and tandem mass spectrometry (MS/MS) peptide sequencing confirms that the N-terminus of the peptide begins with cysteine, rather than methionine (Figures 2.S9). The loss of the N-terminal methionine is consistent with a mechanism in which methionyl aminopeptidase (MAP) excises the N-terminal methionine.³⁹⁻⁴¹ The combined pure HPLC fractions of A β _(C1-42) can be directly used for subsequent labeling, or stored at -80 °C for at least three weeks without forming detectable aggregates.

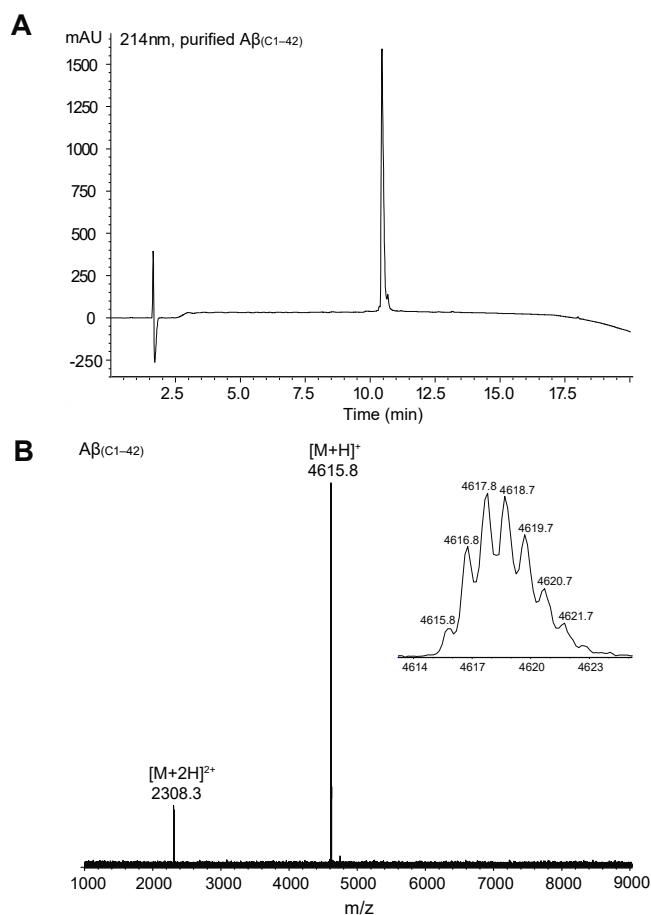


Figure 2.2. Characterization of Aβ_(C1-42). (A) Analytical HPLC trace of purified Aβ_(C1-42). HPLC was performed on a C18 column at 60 °C with elution with 5–67% acetonitrile over 15 minutes. (B) MALDI mass spectrum of Aβ_(C1-42). Mass-to-charge (m/z) labels on peaks correspond to [M+H]⁺ and [M+2H]²⁺.

Labeling of Aβ_(C1-42). Proteins are often labeled with fluorophores or biotin by dissolving the lyophilized protein powder in buffer and adding a reactive derivative of the fluorophore or biotin to the solution of the protein. We found that when we lyophilized the Aβ_(C1-42), it became unsuitable for labeling, because it aggregated during the lyophilization and redissolution process. All of our attempts to label lyophilized Aβ_(C1-42) gave rise to turbid solutions of aggregated Aβ_(C1-42) that were unsuitable for subsequent purification and use. To address this problem, we have developed a protocol to rapidly label the Aβ_(C1-42) in the combined HPLC fractions, where Aβ remains mostly monomeric.

In this protocol, we first we determine the concentration of $A\beta_{(C1-42)}$ in the combined HPLC fractions by UV absorbance at 280 nm. We then calculate the amount of the maleimide-based labeling reagent needed for a 2:1 molar ratio of the reagent to the $A\beta_{(C1-42)}$ peptide. Although typical thiol-maleimide labeling protocols use a 5–20-fold molar excess of the maleimide reagent, we found that a 2-fold molar excess is sufficient to achieve complete labeling of the $A\beta_{(C1-42)}$. Use of only a 2-fold molar excess of the reagent not only minimizes the cost, but also simplifies subsequent purification of the $A\beta_{(C1-42)}$ conjugate. Typical thiol-maleimide labeling protocols suggest treating the cysteine-containing unlabeled peptide with a 10–100-fold molar excess of tris(2-carboxyethyl)phosphine (TCEP) to reduce any disulfide bonds that might have formed. We found that TCEP interferes with the labeling of $A\beta_{(C1-42)}$ and is unnecessary for our $A\beta$ labeling protocol.⁴³

We found that the labeling reaction must be performed in alkaline conditions to proceed rapidly and avoid aggregation of the $A\beta$. The pH of the combined HPLC fractions of $A\beta_{(C1-42)}$ is ca. 2.2 because of the presence of TFA in the mobile phases, which is unfavorable for thiol-maleimide conjugation chemistry. At acidic pH, the thiol-maleimide reaction does not reach completion after overnight incubation, and $A\beta_{(C1-42)}$ aggregates before being completely labeled. Common protein labeling protocols recommend doing the thiol-maleimide conjugation at ca. pH 7.4. $A\beta_{(C1-42)}$ aggregates rapidly at this pH, which is close to its isoelectric point ($pI = 5.6$), where $A\beta_{(C1-42)}$ is not heavily charged and is thus prone to aggregation.⁴⁴ We observed that at pH 7.4, $A\beta$ aggregates in several minutes, which hinders the labeling of $A\beta$. We thus developed a basification protocol to rapidly raise the pH of the acidic HPLC fractions to ca. 9.0. It is essential to bring the pH from ca. 2.2 to ca. 9.0 rapidly to bypass the pI quickly thus prevent $A\beta$ aggregation.⁴⁵ In this protocol, we first titrate a 1 mL portion of the combined HPLC fractions with pH 9.0 sodium borate

buffer until a pH of 9.0 is reached. This portion of the combined HPLC fractions is discarded. We then calculate the quantity of borate buffer needed to basify the remainder of the combined HPLC fractions to pH 9.0 and add it in a single portion. We then add the appropriate amount the maleimide reagent as a solution in DMSO and allow the reaction to proceed for 15 minutes at room temperature to achieve complete labeling of the A β .

Purification, Characterization, and HFIP Treatment of Labeled A β _(C1-42). We purify the labeled A β _(C1-42) by preparative HPLC to remove unreacted maleimide reagent, borate buffer, and oligomers that formed during the labeling reaction. Before HPLC purification, we must filter the reaction mixture to prevent damaging the HPLC column. We have found both hydrophilic polyvinylidene fluoride (PVDF) syringe filters and hydrophilic polyethersulfone (PES) syringe filters are suitable for filtering expressed A β _(M1-42) and A β _(C1-42) before HPLC purification while minimizing peptide loss.³⁶ Nevertheless, we find that *only* PES filters should be used for filtering the labeling reaction mixture, as the use of PVDF filters resulted in substantial loss of fluorophore or biotin labeled A β _(C1-42) peptide. The filtered solution is then subjected to purification by preparative reverse-phase HPLC on a C8 column at 80 °C. The labeled A β _(C1-42) elutes at ca. 34–38% acetonitrile. The pure fractions of labeled A β _(C1-42) peptide are combined.

Using these procedures, we labeled A β with three different maleimide reagents: maleimide-6-carboxyfluorescein (FAM), maleimide-5-tetramethylrhodamine (TAMRA), and maleimide-PEG₂-biotin (Figure 2.3). MALDI-MS corroborated the composition of each labeled A β peptide (Figure 2.4). HPLC analysis indicated the purity of each peptide to be 94.0–96.6% (Figures 2.5, 2.S10, 2.S12, 2.S14). After lyophilizing the combined pure HPLC fractions, we gravimetrically determined the yield of each of the labeled peptides as the trifluoroacetate salt to

be 2.6–3.6 mg per liter of bacterial culture (Table 2.S15). To provide aliquots of monomeric labeled A β for subsequent biophysical and biological studies, we dissolve and incubate the lyophilized powder of labeled A β in HFIP and portion the labeled A β into 0.02 μ mol (ca. 0.1 mg) aliquots. We then lyophilize the aliquots to remove HFIP and store the lyophilized aliquots in a desiccator at -20 °C until further use.

Thiazine Rearrangement of Labeled A β _(C1-42). After we completed the work, Gober et al. recently reported that maleimide conjugates of N-terminal cysteine peptides rearrange to the isomeric thiazines over the course of hours at neutral or basic pH (Figure 2.3A).⁴⁶ To evaluate the occurrence of this rearrangement in the maleimide conjugates of A β _(C1-42) reported in the this chapter, we have performed ultra-performance liquid chromatography–high-energy collision-induced mass spectrometry (UPLC–MS^E) analysis on 5-TAMRA-A β _(C1-42). Upon digestion of 5-TAMRA-A β _(C1-42) with proteinase K at 37 °C at pH 7.2 followed by UPLC–MS^E, we were able to identify a set of three peaks in the UPLC trace associated with 5-TAMRA-A β _(C1-7) (14.4, 16.3, 16.5 minutes) and a set of three peaks in the UPLC trace associated with 5-TAMRA-A β _(C1-5) (15.9, 17.8, and 18.1 minutes) (Figure 2.6). The patterns of three unique peaks associated with each digestion fragment are consistent with the thiazine isomer and the two diastereomers of the maleimide conjugate. Similar patterns of three peaks were reported by Gober et al. for maleimide conjugates of several model tripeptides bearing N-terminal cysteine residues, with the thiazine isomer eluting first and the two diastereomers of the maleimide conjugate eluting subsequently.⁴⁶ The observation of these characteristic sets of three peaks provides strong evidence that 5-TAMRA-A β _(C1-42) has partially rearranged to the thiazine isomer in the course of preparation and isolation. We expect that 6-FAM-A β _(C1-42) and PEG₂-biotin-A β _(C1-42) also partially rearranged to

the thiazine isomers in the course of preparation and isolation. We further expect these $A\beta_{(C1-42)}$ maleimide conjugates to fully rearrange to the corresponding thiazine isomers during the course of common experiments that involve prolonged incubation at neutral pH (Figure 2.3). Because N-terminal substitution does not substantially alter the properties of the $A\beta$, we anticipate that the isomerization of the maleimide conjugates to the isomeric thiazines will not significantly affect the use of the N-terminally labeled $A\beta_{42}$ peptides.

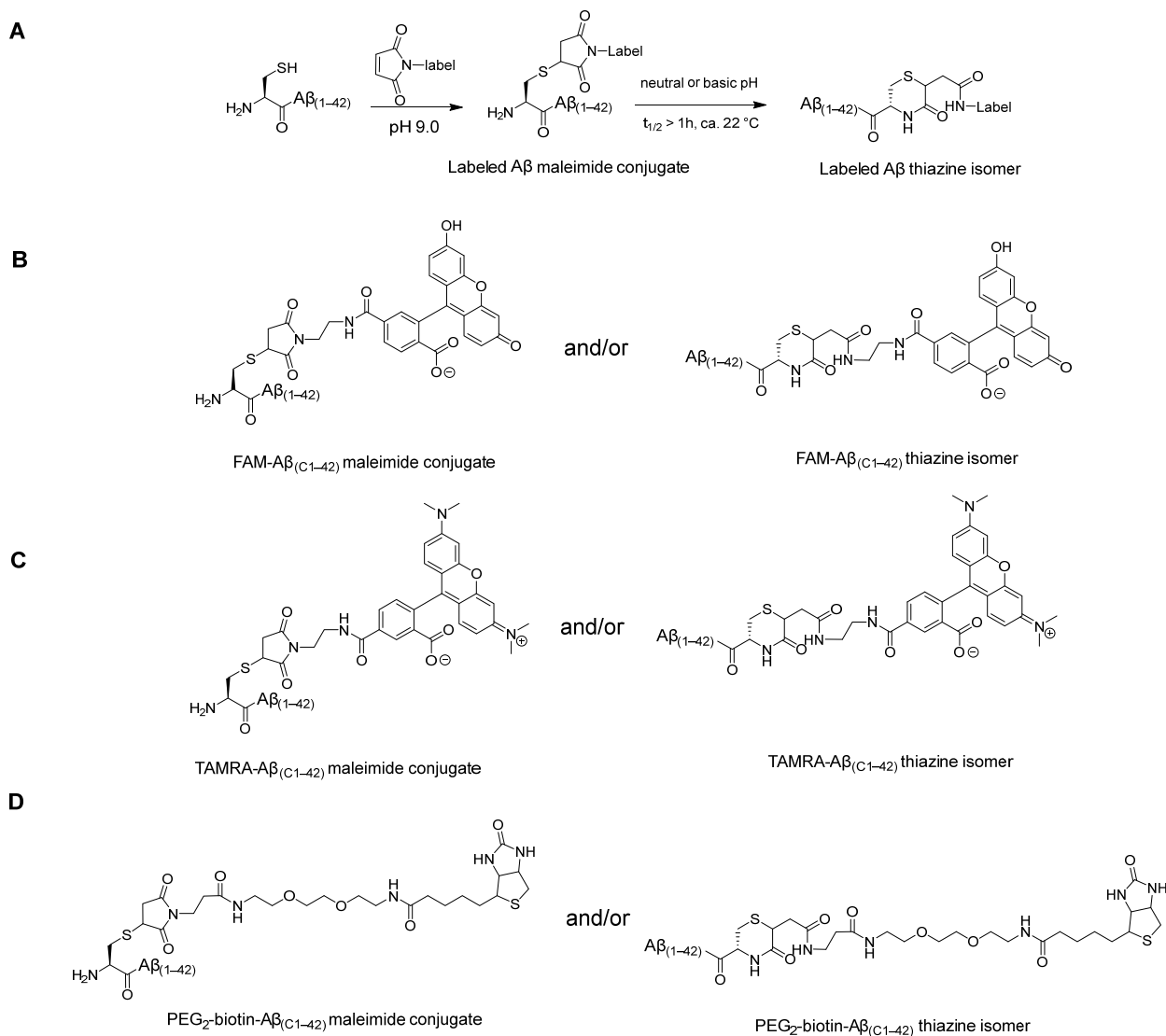


Figure 2.3. Conjugation of $A\beta_{(C1-42)}$ with maleimide reagents (A). Structures of labeled $A\beta$ products: FAM- $A\beta_{(C1-42)}$ (B), TAMRA- $A\beta_{(C1-42)}$ (C), and PEG₂-biotin- $A\beta_{(C1-42)}$ (D).

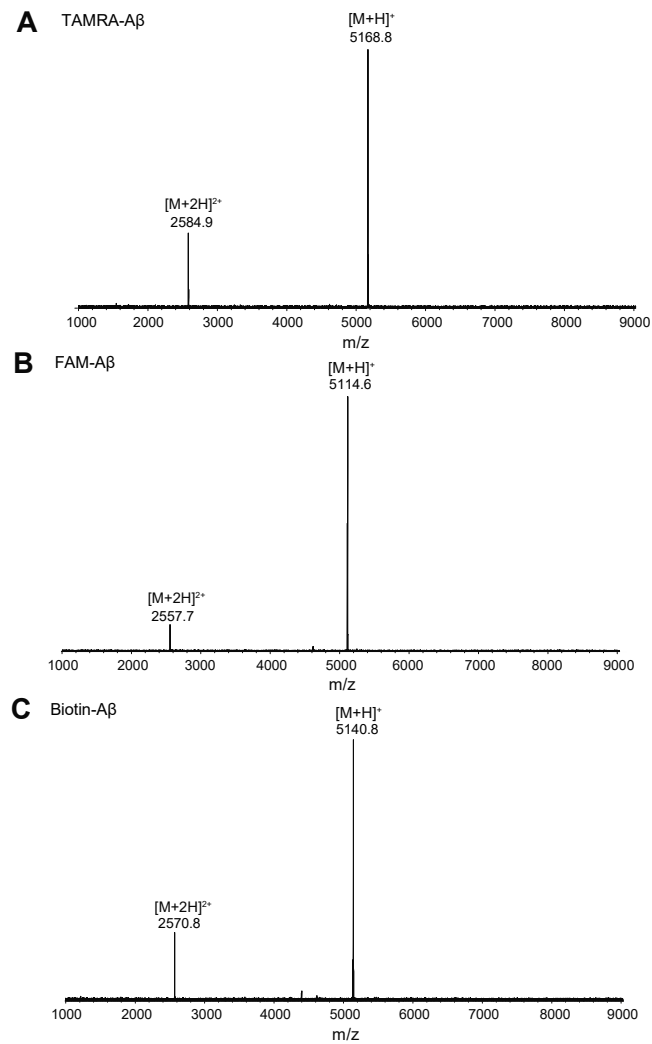


Figure 2.4. MALDI mass spectra of fluorophore and biotin labeled A $\beta_{(C1-42)}$: (A) TAMRA-labeled A β . (B) FAM-labeled A β . (C) Biotin-labeled A β . Mass-to-charge (m/z) labels on peaks correspond to $[M+H]^+$ and $[M+2H]^{2+}$.

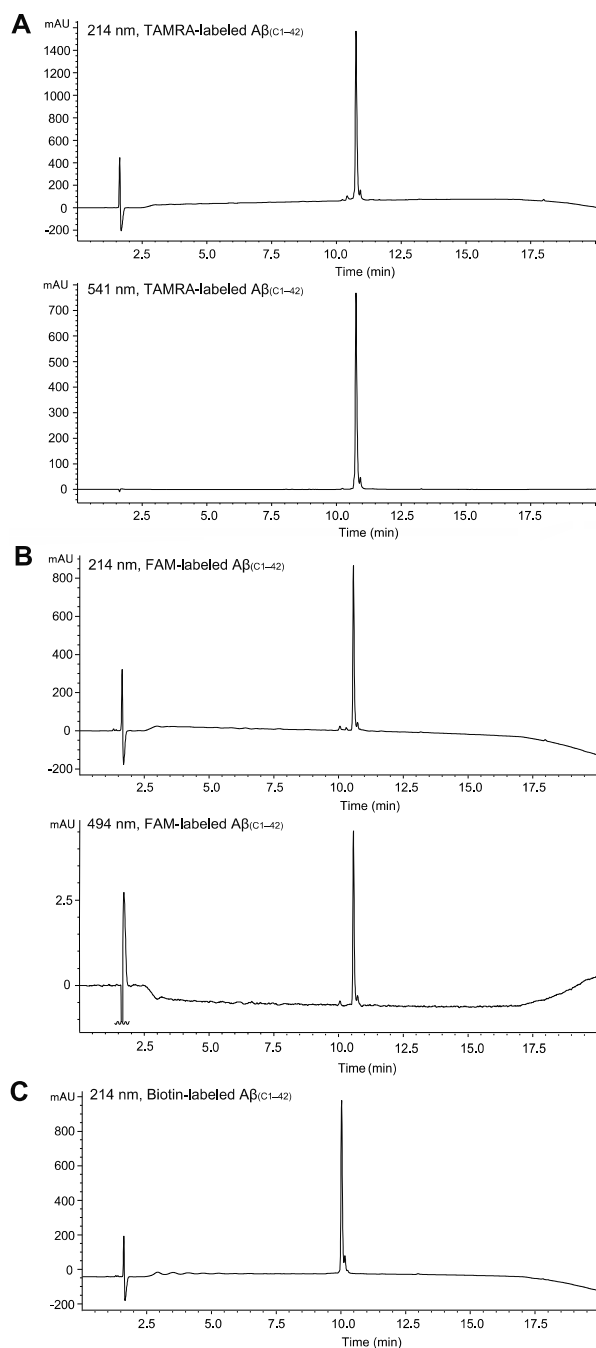


Figure 2.5. Analytical HPLC traces of purified fluorescent and biotin labeled $A\beta_{(C1-42)}$: (A) HPLC trace of TAMRA-labeled $A\beta$ at 214 nm and 541 nm. (B) HPLC trace of FAM-labeled $A\beta$ at 214 nm and 494 nm. (C) HPLC trace of biotin-labeled $A\beta$ at 214 nm. HPLC was performed on a C18 column at 60 °C with elution with 5–67% acetonitrile over 15 minutes. The absorbance of FAM-labeled $A\beta$ at 494 nm is low in the acidic (0.1% TFA) HPLC mobile phase.

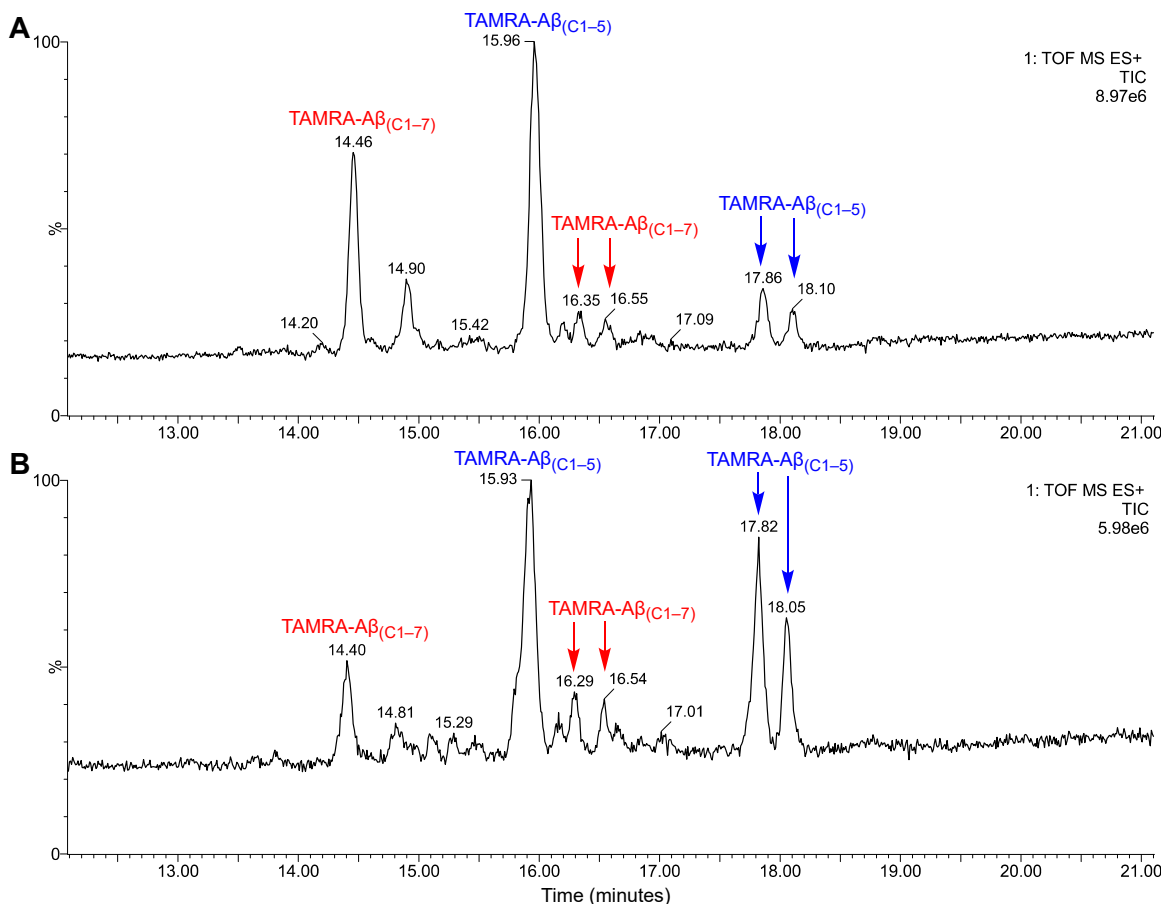


Figure 2.6. UPLC-MS^E total ion current chromatogram of 5-TAMRA-Aβ_(C1-42) digested with proteinase K for either 10 minutes (A) or 60 minutes (B). Peaks were analyzed and assigned by MS^E analysis through identification of b and y ions in the fragmentation mass spectra using Waters BiopharmaLynx software. UPLC was performed on a C4 reverse-phase column with elution with 3–27% acetonitrile containing 0.1% formic acid over 25 minutes.

Oligomerization and Fibrilization Studies of Labeled Aβ_(C1-42). To determine whether N-terminal labeling perturbs the aggregation properties of the Aβ_(C1-42), we compared labeled Aβ to unlabeled Aβ by SDS-PAGE, thioflavin T (ThT) fluorescence assays, fluorescence suppression assays, and transmission electron microscopy (TEM). In these studies we used Aβ_(M1-42), an expressed homologue with properties similar to native Aβ₍₁₋₄₂₎, as an unlabeled Aβ control.³⁶

SDS-PAGE shows that the labeled A β peptides behave similarly to A $\beta_{(M1-42)}$ (Figure 2.7). We ran SDS-PAGE at a range of concentrations to better observe both the monomeric and oligomeric species, and we visualized the peptides by silver staining. We also visualized the FAM- and TAMRA-labeled A β directly by fluorescence imaging. At lower concentrations (e.g., 4 and 8 μ M), the A β shows up exclusively or predominantly as the monomer, which appears as a band between the 4.6 kDa and 10 kDa ladder bands. At higher concentrations (e.g., 125 and 250 μ M), bands associated with trimers and tetramers appear just below and above the 17 kDa ladder band. In spite of the differences among the N-terminal substituents and visualization techniques for the SDS-PAGE gels, all of the gels show remarkably similar patterns of monomers and oligomers among the four peptides.

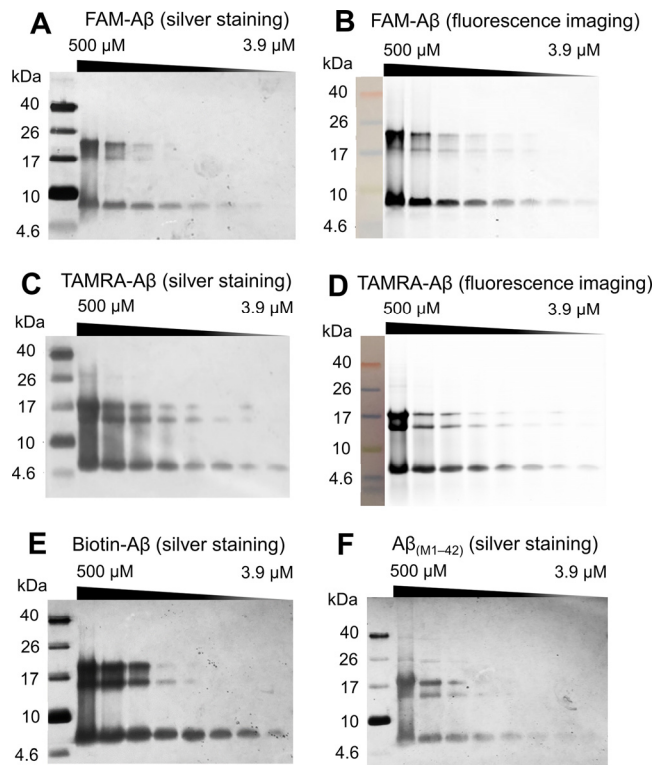


Figure 2.7. SDS-PAGE of labeled A $\beta_{(C1-42)}$ and A $\beta_{(M1-42)}$ at a range of concentrations, visualized by silver staining and fluorescence imaging. (A and B) FAM-labeled A $\beta_{(C1-42)}$ visualized by silver staining and fluorescence imaging. (C and D) TAMRA-labeled A $\beta_{(C1-42)}$ visualized by silver staining and fluorescence imaging. (E and F) Biotin-labeled A $\beta_{(C1-42)}$ and A $\beta_{(M1-42)}$ visualized by silver staining. The contrast of images 6A, 6C, 6E, and 6F have been increased by 40% to enhance the visualization of the silver staining.

ThT fluorescence assays are widely used to study the onset of fibril formation by amyloidogenic peptides. In these assays, A β or a related amyloidogenic peptide is incubated with ThT. After a lag time, the onset of fibril formation is marked by the rapid increase in ThT fluorescence and a subsequent plateau. In a ThT assay, the A $\beta_{(M1-42)}$ exhibited a lag time of ca. 100 minutes, followed by a rapid increase in fluorescence and a plateau, reflecting the formation of fibrils (Figure 2.8A). The biotin-labeled A $\beta_{(C1-42)}$ exhibited a shorter lag time (ca. 20 minutes), followed by a more rapid increase in fluorescence and a plateau (Figure 2.8B). The FAM label absorbs light at wavelengths similar to ThT and does not permit a conventional ThT fluorescence assay to be performed. Aggregation of the FAM- and TAMRA-labeled A β can be observed by a diminution of fluorescence as the labeled A β begins to aggregate, even before the onset of fibril formation.^{27,29} We thus studied the aggregation of these fluorophore-labeled A β peptides through a fluorescence suppression assay. In this assay, the FAM-labeled A $\beta_{(C1-42)}$ exhibited a slight initial diminution in the fluorescence signal, followed by a lag time, and then a rapid drop in fluorescence. The initial diminution in fluorescence may reflect the formation of small oligomers, while the subsequent drop likely reflects the formation of fibrils (Figure 2.8C). In contrast, the TAMRA-labeled A $\beta_{(C1-42)}$ exhibited an immediate substantial drop in fluorescence, suggesting more rapid aggregation and fibril formation (Figure 2.8D). The differences observed between the biotin-labeled A $\beta_{(C1-42)}$ and the A $\beta_{(M1-42)}$, and between the FAM- and TAMRA-labeled A $\beta_{(C1-42)}$, indicate that the choice of label is important in the aggregation of the A β .

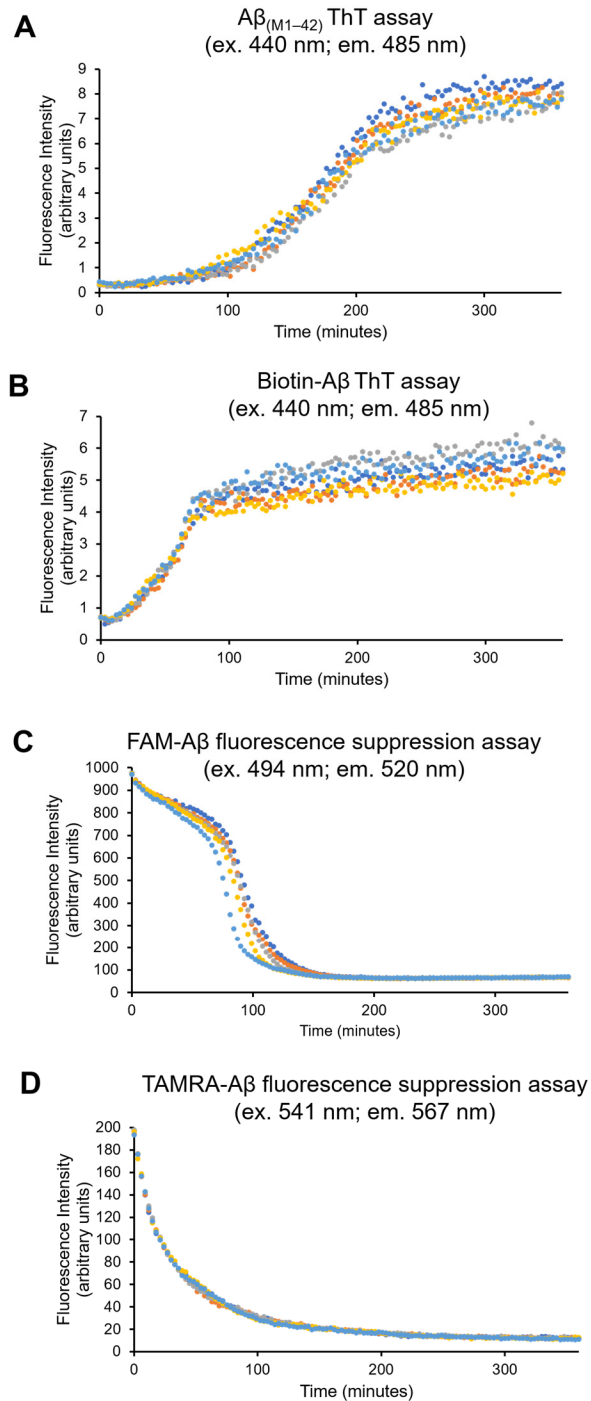


Figure 2.8. ThT fluorescence assays and fluorescence suppression assays of labeled $A\beta_{(C1-42)}$ and $A\beta_{(M1-42)}$. (A and B) ThT fluorescence assays of $A\beta_{(M1-42)}$ and biotin-labeled $A\beta$ (40 μ M peptide, 40 μ M ThT, 37 $^{\circ}$ C, quiescent, 6 hours). (C and D) Fluorescence suppression assays of FAM-labeled $A\beta$ and TAMRA-labeled $A\beta$ (40 μ M peptide, 37 $^{\circ}$ C, quiescent, 6 hours). These assays were performed in five replicates (light blue, dark blue, orange, yellow, and gray).

To directly visualize amyloid fibrils formed by labeled A β , we performed transmission electron microscopy (TEM). TEM studies reveal that A $\beta_{(M1-42)}$, biotin-labeled A $\beta_{(C1-42)}$, FAM-labeled A $\beta_{(C1-42)}$, and TAMRA-labeled A $\beta_{(C1-42)}$ all form fibrils after one day of incubation (Figure 2.9 and Figure 2.S18). The fibrils differ in morphology: A $\beta_{(M1-42)}$ forms wide, twisted, multi-fibrillar assemblies. Biotin-labeled A $\beta_{(C1-42)}$ forms long, thin fibrils. FAM- and TAMRA-labeled A $\beta_{(C1-42)}$ form more heterogenous fibrils. The TEM studies further confirm that the choice of label is important in the aggregation of A β . We performed atomic force microscopy (AFM) to further characterize the fibrils. AFM shows that the fibrils formed by A $\beta_{(M1-42)}$, biotin-labeled A $\beta_{(C1-42)}$, FAM-labeled A $\beta_{(C1-42)}$, and TAMRA-labeled A $\beta_{(C1-42)}$ range in height from ca. 2–5 nm and exhibit some morphological differences (Figure 2.10 and 2.S19). Although there are differences among the rates of fibril formation and the morphologies of the fibrils, the TEM and AFM experiments and the ThT and fluorescence suppression experiments collectively show that all of the labeled A β peptides retain the propensity to form fibrils.

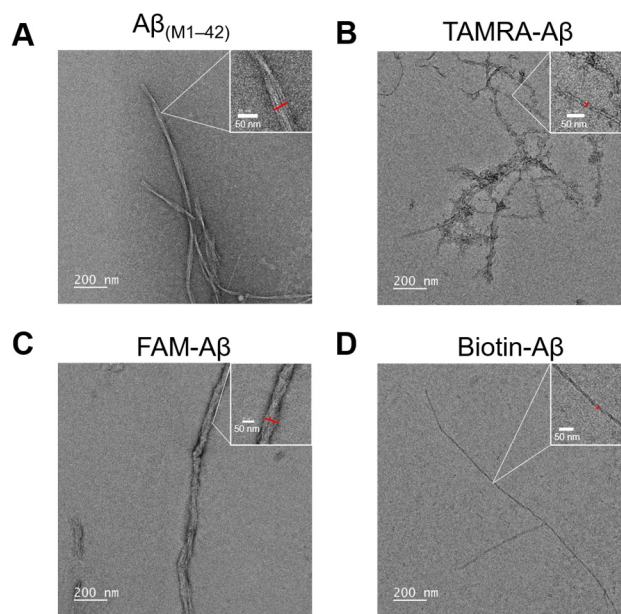


Figure 2.9. Transmission electron micrographs of fibrils formed by A β peptides: (A) A $\beta_{(M1-42)}$, fibril width ca. 36 nm; (B) TAMRA-labeled A β , fibril width ca. 15 nm; (C) FAM-labeled A β , fibril width ca. 56 nm; (D) Biotin-labeled A β , fibril width ca. 12 nm. Fibrils were formed by incubating 40 μ M of each peptide in

PBS buffer (pH 7.4, 37 °C, 1 day, 225 rpm shaking). The red bars indicate the locations where the widths of the fibrils were measured.

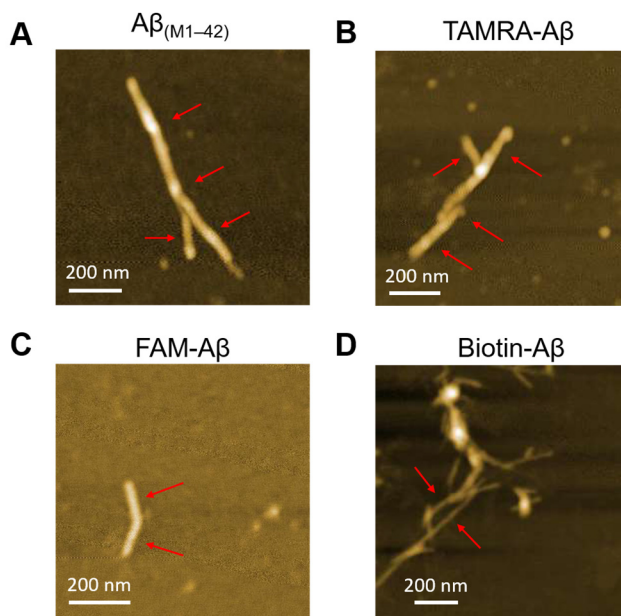


Figure 2.10. Atomic force micrographs of fibrils formed by $A\beta$ peptides: (A) $A\beta_{(M1-42)}$, fibril height ca. 4.5 nm; (B) TAMRA-labeled $A\beta$, fibril height ca. 5.2 nm; (C) FAM-labeled $A\beta$, fibril height ca. 2.3 nm; (D) Biotin-labeled $A\beta$, fibril height ca. 4.1 nm. Fibrils were formed by incubating 40 μ M of each peptide in PBS buffer (pH 7.4, 37 °C, 1 day, 225 rpm shaking). The red arrows indicate the locations where the heights of the fibrils were measured.

Fluorescence Microscopy Studies of Fluorophore-Labeled $A\beta_{(C1-42)}$. To evaluate the applicability of the labeled $A\beta$ in fluorescence microscopy, we visualized the interaction of the FAM- and TAMRA-labeled $A\beta_{(C1-42)}$ with mammalian cells and bacteria. The interaction of $A\beta$ with neuronal cell membranes is thought to be important in neurodegeneration in Alzheimer's disease.^{28,47} When we treated SH-SY5Y neuroblastoma cells with the fluorescent $A\beta$, we observed binding to the cell membranes, internalization of the fluorescent $A\beta$ (Figure 2.11A, 2.11B, and 2.S17). These interactions occurred rapidly (within 3 hours) for the TAMRA- $A\beta$ and more slowly (within 48 hours) for the FAM- $A\beta$. In both cases, we observe small punctate features within the cells, suggesting that internalization occurs through interaction with the cell membranes and the

formation of endosomes. Macrophages have been shown to play an important role in A β clearance.^{48,49} When we treated RAW 264.7 macrophage cells with fluorescent A β , we also observed uptake of the A β , with the uptake of the TAMRA-A β occurring more extensively. The punctate features associated with the internalized peptides are larger, consistent with phagocytosis of the labeled A β by the macrophage (Figure 2.11C, 2.11D, and 2.S17). A β is also thought to have antimicrobial activity and play a role in innate immune response.^{50,51} When we treated *B. subtilis* (Gram-positive) and *E. coli* (Gram-negative) with the fluorescent A β , we observed interaction of what appeared to be aggregated A β with the bacterial cell walls (Figure 2.11E and 2.11F). These results indicate that the fluorescent A β peptides prepared by this method can be used to visualize and monitor interactions between A β and cells, with the TAMRA-A β giving somewhat more rapid and more uniform staining.⁵²

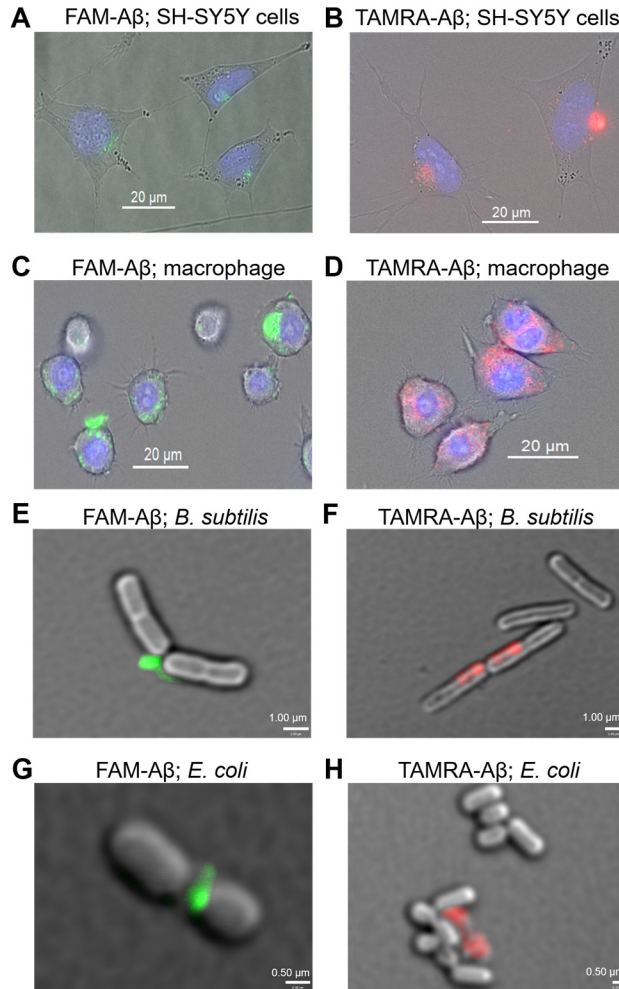


Figure 2.11. Fluorescence micrographs of labeled A β with mammalian cells and bacteria. (A and B) SH-SY5Y neuroblastoma cells treated with FAM- and TAMRA-labeled A β (10 μ M peptides, 37 $^{\circ}$ C, 48 and 3 hours, respectively). The nuclei are shown in blue through Hoechst 33342 staining. (C and D) RAW 264.7 macrophage cells treated with FAM- and TAMRA-labeled A β (10 μ M peptides, 37 $^{\circ}$ C, 4 hours). (E and F) *B. subtilis* treated with FAM- and TAMRA-labeled A β (5 μ M peptides, 37 $^{\circ}$ C, 225 rpm, 225 rpm shaking, 2 hours). (G and H) *E. coli* treated with FAM- and TAMRA-labeled A β (5 μ M peptides, 37 $^{\circ}$ C, 225 rpm, 225 rpm shaking, 2 hours). These micrographs were collected by Gretchen Guaglianone and Dr. Michael Morris.

Conclusions

Our discovery that expression of an A β _(MC1-42) plasmid in *E. coli* leads to endogenous excision of methionine has enabled us to develop methods to express and purify A β _(C1-42) and then label the A β at the N-terminus with fluorophores or biotin through cysteine-maleimide chemistry.

The expression and labeling of A β _(C1-42) provide an efficient and economical route to obtain ca. 14 mg of N-terminal cysteine A β or ca. 3 mg of labeled A β per liter of bacterial culture. Analytical HPLC and MALDI analyses confirm that the A β _(C1-42) and labeled A β are pure and homogeneous. SDS-PAGE, ThT fluorescence assays and related fluorescence suppression assays, and TEM studies establish that N-terminally labeled A β retains aggregation properties similar to unlabeled A β . Fluorescence microscopy shows that the labeled A β can be used to visualize interactions between A β and mammalian or bacterial cells.

Expression offers advantages over solid phase peptide synthesis, because the expressed A β is free of deletion or epimerization impurities. The addition of a single cysteine residue at the N-terminus enables labeling of the expressed A β with complete site specificity using maleimide-based reagents. Although NHS esters are widely used to label lysine residues or the N-terminus of proteins, *site specific* labeling of expressed A β is not possible using NHS-ester based reagents, because multiple labeling sites are present.

The expression, purification, and conjugation methods that we report here should enable other researchers to produce milligram quantities of pure labeled A β in their own laboratories. Ready access to labeled A β peptides will advance amyloid and Alzheimer's disease research by facilitating experiments that might otherwise be hindered by insufficient access to these valuable peptides.⁵³⁻⁶⁵ We anticipate these fluorophore and biotin labeled A β peptides will be especially useful in investigating cellular interactions, transport, and clearance of A β , as well as screening anti-A β antibodies.⁶⁶⁻⁶⁸ Researchers may also apply our methods to label A β with other popular fluorophores, such as Alexa Fluor™ 488 and BODIPY™ FL.^{69,70} The potential to install a variety of fluorophores may enable studies of A β peptide interactions through Förster resonance energy transfer (FRET) studies in which A β has been labeled with FRET donors and acceptors, such as

Cy3 and Cy5. The N-terminal cysteine A β formed through N-terminal methionine excision also promises to be valuable in other applications, such as native chemical ligation or other site-specific modifications. We anticipate that this method of incorporating an N-terminal cysteine residue can be adapted to the expression, purification, and conjugation of other variants of A β , such as familial mutants,³⁶ further enabling a variety of experiments in Alzheimer's disease research.

References

- (1) Ren, H.; Xiao, F.; Zhan, K.; Kim, Y. P.; Xie, H.; Xia, Z.; Rao, J. A Biocompatible Condensation Reaction for the Labeling of Terminal Cysteine Residues on Proteins. *Angew. Chem. Int. Ed.* **2009**, *48*, 9658–9662.
- (2) Wang, P.; Zhang, C. J.; Chen, G.; Na, Z.; Yao, S. Q.; Sun, H. Site-Specific Immobilization of Biomolecules by a Biocompatible Reaction between Terminal Cysteine and 2-Cyanobenzothiazole. *Chem. Commun.* **2013**, *49*, 8644–8646.
- (3) Bandyopadhyay, A.; Cambray, S.; Gao, J. Fast and Selective Labeling of N-Terminal Cysteines at Neutral PH: Via Thiazolidino Boronate Formation. *Chem. Sci.* **2016**, *7*, 4589–4593.
- (4) Rosen, C. B.; Francis, M. B. Targeting the N Terminus for Site-Selective Protein Modification. *Nat. Chem. Biol.* **2017**, *13*, 697–705.
- (5) Parvathy, S.; Rajadas, J.; Ryan, H.; Vaziri, S.; Anderson, L.; Murphy, G. M. A β Peptide Conformation Determines Uptake and Interleukin-1 α Expression by Primary Microglial Cells. *Neurobiol. Aging* **2009**, *30*, 1792–1804.
- (6) Jiang, Q.; Lee, C. Y. D.; Mandrekar, S.; Wilkinson, B.; Cramer, P.; Zelcer, N.; Mann, K.; Lamb, B.; Willson, T. M.; Collins, J. L.; Richardson, J. C.; Smith, J. D.; Comery, T. A.; Riddell,

D.; Holtzman, D. M.; Tontonoz, P.; Landreth, G. E. ApoE Promotes the Proteolytic Degradation of A β . *Neuron* **2008**, *58*, 681–693

(7) Hickman, S. E.; Allison, E. K.; el Khoury, J. Microglial Dysfunction and Defective β -Amyloid Clearance Pathways in Aging Alzheimer's Disease Mice. *J. Neurosci.* **2008**, *28*, 8354–8360.

(8) Giunta, B.; Zhou, Y.; Hou, H.; Rrapo, E.; Fernandez, F.; Tan, J. HIV-1 TAT Inhibits Microglial Phagocytosis of A β Peptide. *Int. J. Clin. Exp. Patho.* **2008**, *1*, 260–275.

(9) Majumdar, A.; Chung, H.; Dolios, G.; Wang, R.; Asamoah, N.; Lobel, P.; Maxfield, F. R. Degradation of Fibrillar Forms of Alzheimer's Amyloid β -Peptide by Macrophages. *Neurobiol. Aging* **2008**, *29*, 707–715.

(10) El Khoury, J.; Toft, M.; Hickman, S. E.; Means, T. K.; Terada, K.; Geula, C.; Luster, A. D. Ccr2 Deficiency Impairs Microglial Accumulation and Accelerates Progression of Alzheimer-like Disease. *Nat. Med.* **2007**, *13*, 432–438.

(11) Chafekar, S. M.; Baas, F.; Scheper, W. Oligomer-Specific A β Toxicity in Cell Models Is Mediated by Selective Uptake. *BBA-Mol. Basis Dis.* **2008**, *1782*, 523–531.

(12) Simakova, O.; Arispe, N. J. The Cell-Selective Neurotoxicity of the Alzheimer's A β Peptide Is Determined by Surface Phosphatidylserine and Cytosolic ATP Levels. Membrane Binding Is Required for A β Toxicity. *J. Neurosci.* **2007**, *27*, 13719–13729.

(13) Saavedra, L.; Mohamed, A.; Ma, V.; Kar, S.; de Chaves, E. P. Internalization of β -Amyloid Peptide by Primary Neurons in the Absence of Apolipoprotein E. *J. Biol. Chem.* **2007**, *282*.

- (14) Clifford, P. M.; Zarrabi, S.; Siu, G.; Kinsler, K. J.; Kosciuk, M. C.; Venkataraman, V.; D'Andrea, M. R.; Dinsmore, S.; Nagele, R. G. A β Peptides Can Enter the Brain through a Defective Blood-Brain Barrier and Bind Selectively to Neurons. *Brain Res.* **2007**, *1142*, 223–236.
- (15) Kuhnke, D.; Jedlitschky, G.; Grube, M.; Krohn, M.; Jucker, M.; Mosyagin, I.; Cascorbi, I.; Walker, L. C.; Kroemer, H. K.; Warzok, R. W.; Vogelgesang, S. MDR1-P-Glycoprotein (ABCB1) Mediates Transport of Alzheimer's Amyloid- β Peptides - Implications for the Mechanisms of A β Clearance at the Blood-Brain Barrier. *Brain Pathol.* **2007**, *17*, 347–353.
- (16) Jungbauer, L. M.; Yu, C.; Laxton, K. J.; LaDu, M. J. Preparation of Fluorescently-Labeled Amyloid-Beta Peptide Assemblies: The Effect of Fluorophore Conjugation on Structure and Function. *J. Mol. Recognit.* **2009**, *22*, 403–413.
- (17) LeVine, H. Biotin-Avidin Interaction-Based Screening Assay for Alzheimer's β -Peptide Oligomer Inhibitors. *Anal. Biochem.* **2006**, *356*, 265–272.
- (18) Dunning, C. J.; McGauran, G.; Willén, K.; Gouras, G. K.; O'Connell, D. J.; Linse, S. Direct High Affinity Interaction between A β 42 and GSK3 α Stimulates Hyperphosphorylation of Tau. A New Molecular Link in Alzheimer's Disease? *ACS Chem. Neurosci.* **2016**, *7*, 161–170.
- (19) Xiang, X.; Werner, G.; Bohrmann, B.; Liesz, A.; Mazaheri, F.; Capell, A.; Feederle, R.; Knuesel, I.; Kleinberger, G.; Haass, C. TREM2 Deficiency Reduces the Efficacy of Immunotherapeutic Amyloid Clearance. *EMBO Mol. Med.* **2016**, *8*, 992–1004.
- (20) Ozawa, D.; Nakamura, T.; Koike, M.; Hirano, K.; Miki, Y.; Beppu, M. Shuttling Protein Nucleolin Is a Microglia Receptor for Amyloid Beta Peptide 1-42. *Biol. Pharm. Bull.* **2013**, *36*, 1587–1593.

- (21) Fleisher-Berkovich, S.; Filipovich-Rimon, T.; Ben-Shmuel, S.; Hülsmann, C.; Kummer, M. P.; Heneka, M. T. Distinct Modulation of Microglial Amyloid β Phagocytosis and Migration by Neuropeptides. *J. Neuroinflamm.* **2010**, *7*, 61
- (22) Domert, J.; Rao, S. B.; Agholme, L.; Brorsson, A. C.; Marcusson, J.; Hallbeck, M.; Nath, S. Spreading of Amyloid- β Peptides via Neuritic Cell-to-Cell Transfer Is Dependent on Insufficient Cellular Clearance. *Neurobiol. Dis.* **2014**, *65*, 82–92.
- (23) Ahn, H. J.; Fraser Glickman, J.; Poon, K. L.; Zamolodchikov, D.; Jno-Charles, O. C.; Norris, E. H.; Strickland, S. A Novel A β -Fibrinogen Interaction Inhibitor Rescues Altered Thrombosis and Cognitive Decline in Alzheimer's Disease Mice. *J. Exp. Med.* **2014**, *211*, 1049–1062.
- (24) Kanekiyo, T.; Ban, T.; Aritake, K.; Huang, Z. L.; Qu, W. M.; Okazaki, I.; Mohri, I.; Murayama, S.; Ozono, K.; Taniike, M.; Goto, Y.; Urade, Y. Lipocalin-Type Prostaglandin D Synthase/ β -Trace Is a Major Amyloid β -Chaperone in Human Cerebrospinal Fluid. *Proc. Natl. Acad. Sci. U. S. A.* **2007**, *104*, 6412–6417.
- (25) Arriagada, C.; Bustamante, M.; Atwater, I.; Rojas, E.; Caviedes, R.; Caviedes, P. Apoptosis Is Directly Related to Intracellular Amyloid Accumulation in a Cell Line Derived from the Cerebral Cortex of a Trisomy 16 Mouse, an Animal Model of Down Syndrome. *Neurosci. Lett.* **2010**, *470*, 81–85.
- (26) Abraham, J. D.; Promé, S.; Salvétat, N.; Rubrecht, L.; Cobo, S.; du Paty, E.; Galéa, P.; Mathieu-Dupas, E.; Ranaldi, S.; Caillava, C.; Crémer, G. A.; Rieunier, F.; Robert, P.; Molina, F.; Laune, D.; Checler, F.; Fareh, J. Cerebrospinal A β 11-x and 17-x Levels as Indicators of Mild

Cognitive Impairment and Patients' Stratification in Alzheimer's Disease. *Transl. Psychiat.* **2013**, *3*, e281.

(27) Dutta, S.; Finn, T. S.; Kuhn, A. J.; Abrams, B.; Raskatov, J. A. Chirality Dependence of Amyloid β Cellular Uptake and a New Mechanistic Perspective. *ChemBioChem* **2019**, *20*, 1023–1026.

(28) Foley, A. R.; Roseman, G. P.; Chan, K.; Smart, A.; Finn, T. S.; Yang, K.; Scott Lokey, R.; Millhauser, G. L.; Raskatov, J. A. Evidence for Aggregation-Independent, PrPC-Mediated A β Cellular Internalization. *Proc. Natl. Acad. Sci. U. S. A.* **2020**, *117*, 28625–28631.

(29) Garai, K.; Frieden, C. Quantitative Analysis of the Time Course of A β Oligomerization and Subsequent Growth Steps Using Tetramethylrhodamine-Labeled A β . *Proc. Natl. Acad. Sci. U. S. A.* **2013**, *110*, 3321–3326.

(30) Nasir, I.; Linse, S.; Cabaleiro-Lago, C. Fluorescent Filter-Trap Assay for Amyloid Fibril Formation Kinetics in Complex Solutions. *ACS Chem. Neurosci.* **2015**, *6*, 1436–1444

(31) Pedersen, S. L.; Tofteng, A. P.; Malik, L.; Jensen, K. J. Microwave Heating in Solid-Phase Peptide Synthesis. *Chem. Soc. Rev.* **2012**, *41*, 1826–1844.

(32) D'Hondt, M.; Bracke, N.; Taevernier, L.; Gevaert, B.; Verbeke, F.; Wynendaele, E.; de Spiegeleer, B. Related Impurities in Peptide Medicines. *J. Pharmaceut. Biomed.* **2014**, *101*, 2–30.

(33) Finder, V. H.; Vodopivec, I.; Nitsch, R. M.; Glockshuber, R. The Recombinant Amyloid- β Peptide A β 1-42 Aggregates Faster and Is More Neurotoxic than Synthetic A β 1-42. *J. Mol. Biol.* **2010**, *396*, 9–18.

(34) Sahoo, B. R.; Bekier, M. E.; Liu, Z.; Kocman, V.; Stoddard, A. K.; Anantharamaiah, G. M.; Nowick, J.; Fierke, C. A.; Wang, Y.; Ramamoorthy, A. Structural Interaction of

Apolipoprotein A-I Mimetic Peptide with Amyloid- β Generates Toxic Hetero-Oligomers. *J. Mol. Biol.* **2020**, *432*, 1020–1034.

(35) Sahoo, B. R.; Genjo, T.; Nakayama, T. W.; Stoddard, A. K.; Ando, T.; Yasuhara, K.; Fierke, C. A.; Ramamoorthy, A. A Cationic Polymethacrylate-Copolymer Acts as an Agonist for β -Amyloid and an Antagonist for Amylin Fibrillation. *Chem. Sci.* **2019**, *10*, 3976–3986.

(36) Yoo, S.; Zhang, S.; Kreutzer, A. G.; Nowick, J. S. An Efficient Method for the Expression and Purification of A β (M1-42). *Biochemistry* **2018**, *57*, 3861–3866.

(37) Hirel, P. H.; Schmitter, J. M.; Dessen, P.; Fayat, G.; Blanquet, S. Extent of N-Terminal Methionine Excision from Escherichia Coli Proteins Is Governed by the Side-Chain Length of the Penultimate Amino Acid. *Proc. Natl. Acad. Sci. U. S. A.* **1989**, *86*, 8247–8251.

(38) Blanquet and co-workers reported (reference 37) that the degree of N-terminal methionine excision depends on the size of the amino acid after the N-terminal methionine when proteins are expressed in *E. coli*, with N-terminal methionine excision occurring most extensively when a small amino acid follows the N-terminal methionine.

(39) Giglione, C.; Boularot, A.; Meinnel, T. Protein N-Terminal Methionine Excision. *Cell. Mol. Life Sci.* **2004**, *61*, 1455–1474.

(40) Stephens, A. D.; Lu, M.; Fernandez-Villegas, A.; Kaminski Schierle, G. S. Fast Purification of Recombinant Monomeric Amyloid- β from *E. coli* and Amyloid- β -MCherry Aggregates from Mammalian Cells. *ACS Chem. Neurosci.* **2020**, *11*, 3204–3213.

(41) Ochtrop, P.; Hackenberger, C. P. R. Recent Advances of Thiol-Selective Bioconjugation Reactions. *Curr. Opin. Chem. Biol.* **2020**, *58*, 28–36.

(42) Addgene, pET-Sac-Abeta(MC1-42), Plasmid #127151.

<https://www.addgene.org/127151/>.

(43) Tyagarajan, K.; Pretzer, E.; Wiktorowicz, J. E. Thiol-Reactive Dyes for Fluorescence Labeling of Proteomic Samples. *Electrophoresis* **2003**, *24*, 2348–2358.

(44) We calculated the isoelectric point (pI) of A β _(C1-42) using Protein Calculator (v3.4): <http://protcalc.sourceforge.net/>.

(45) Fezoui, Y.; Hartley, D. M.; Harper, J. D.; Khurana, R.; Walsh, D. M.; Condrón, M. M.; Selkoe, D. J.; Lansbury, J.; Fink, A. L.; Teplow, D. B. An Improved Method of Preparing the Amyloid β -Protein for Fibrillogenesis and Neurotoxicity Experiments. *Amyloid* **2000**, *7*, 166–178.

(46) Gober, I. N.; Riemen, A. J.; Villain, M. Sequence Sensitivity and PH Dependence of Maleimide Conjugated N-Terminal Cysteine Peptides to Thiazine Rearrangement. *J. Pept. Sci.* **2021**, *27*, e3323.

(47) Sepulveda, F. J.; Parodi, J.; Peoples, R. W.; Opazo, C.; Aguayo, L. G. Synaptotoxicity of Alzheimer Beta Amyloid Can Be Explained by Its Membrane Perforating Property. *PLoS One* **2010**, *5*, e11820.

(48) Li, S.; Hayden, E. Y.; Garcia, V. J.; Fuchs, D. T.; Sheyn, J.; Daley, D. A.; Rentsendorj, A.; Torbati, T.; Black, K. L.; Rutishauser, U.; Teplow, D. B.; Koronyo, Y.; Koronyo-Hamaoui, M. Activated Bone Marrow-Derived Macrophages Eradicate Alzheimer's-Related A β ₄₂ Oligomers and Protect Synapses. *Front. Immunol.* **2020**, *11*, 49.

(49) Lai, A. Y.; McLaurin, J. Clearance of Amyloid- β Peptides by Microglia and Macrophages: The Issue of What, When and Where. *Future Neurology.* **2012**, *7*, 165–176.

(50) Frost, G. R.; Jonas, L. A.; Li, Y. M. Friend, Foe or Both? Immune Activity in Alzheimer's Disease. *Front. Aging Neurosci.* **2019**, *11*, 337.

- (51) Pastore, A.; Raimondi, F.; Rajendran, L.; Temussi, P. A. Why Does the A β Peptide of Alzheimer Share Structural Similarity with Antimicrobial Peptides? *Commun. Biol.* **2020**, *3*, 135.
- (52) Hughes, L. D.; Rawle, R. J.; Boxer, S. G. Choose Your Label Wisely: Water-Soluble Fluorophores Often Interact with Lipid Bilayers. *PLoS One* **2014**, *9*, e87649.
- (53) Szczepankiewicz, O.; Linse, B.; Meisl, G.; Thulin, E.; Frohm, B.; Sala Frigerio, C.; Colvin, M. T.; Jacavone, A. C.; Griffin, R. G.; Knowles, T.; Walsh, D. M.; Linse, S. N-Terminal Extensions Retard A β 42 Fibril Formation but Allow Cross-Seeding and Coaggregation with A β 42. *J. Am. Chem. Soc.* **2015**, *137*, 14673–14685.
- (54) Nespovitaya, N.; Gath, J.; Barylyuk, K.; Seuring, C.; Meier, B. H.; Riek, R. Dynamic Assembly and Disassembly of Functional β -Endorphin Amyloid Fibrils. *J. Am. Chem. Soc.* **2016**, *138*, 846–856.
- (55) Yeung, P. S. W.; Axelsen, P. H. The Crowded Environment of a Reverse Micelle Induces the Formation of β -Strand Seed Structures for Nucleating Amyloid Fibril Formation. *J. Am. Chem. Soc.* **2012**, *134*, 6061–6063.
- (56) Derrick, J. S.; Kerr, R. A.; Nam, Y.; Oh, S. B.; Lee, H. J.; Earnest, K. G.; Suh, N.; Peck, K. L.; Ozbil, M.; Korshavn, K. J.; Ramamoorthy, A.; Prabhakar, R.; Merino, E. J.; Shearer, J.; Lee, J. Y.; Ruotolo, B. T.; Lim, M. H. A Redox-Active, Compact Molecule for Cross-Linking Amyloidogenic Peptides into Nontoxic, Off-Pathway Aggregates: In Vitro and in Vivo Efficacy and Molecular Mechanisms. *J. Am. Chem. Soc.* **2015**, *137*, 14785–14797.
- (57) Yoo, B. K.; Xiao, Y.; McElheny, D.; Ishii, Y. E22G Pathogenic Mutation of β -Amyloid (A β) Enhances Misfolding of A β 40 by Unexpected Prion-like Cross Talk between A β 42 and A β 40. *J. Am. Chem. Soc.* **2018**, *140*, 2781–2784.

- (58) Hatai, J.; Motiei, L.; Margulies, D. Analyzing Amyloid Beta Aggregates with a Combinatorial Fluorescent Molecular Sensor. *J. Am. Chem. Soc.* **2017**, *139*, 2136–2139.
- (59) Potapov, A.; Yau, W. M.; Ghirlando, R.; Thurber, K. R.; Tycko, R. Successive Stages of Amyloid- β Self-Assembly Characterized by Solid-State Nuclear Magnetic Resonance with Dynamic Nuclear Polarization. *J. Am. Chem. Soc.* **2015**, *137*, 8294–8307.
- (60) Economou, N. J.; Giammona, M. J.; Do, T. D.; Zheng, X.; Teplow, D. B.; Buratto, S. K.; Bowers, M. T. Amyloid β -Protein Assembly and Alzheimer's Disease: Dodecamers of A β 42, but Not of A β 40, Seed Fibril Formation. *J. Am. Chem. Soc.* **2016**, *138*, 1772–1775.
- (61) Ma, M.; Liu, Z.; Gao, N.; Pi, Z.; Du, X.; Ren, J.; Qu, X. Self-Protecting Biomimetic Nanozyme for Selective and Synergistic Clearance of Peripheral Amyloid- β in an Alzheimer's Disease Model. *J. Am. Chem. Soc.* **2020**, *142*, 21702–21711.
- (62) Narayan, P.; Ganzinger, K. A.; McColl, J.; Weimann, L.; Meehan, S.; Qamar, S.; Carver, J. A.; Wilson, M. R.; St. George-Hyslop, P.; Dobson, C. M.; Klenerman, D. Single Molecule Characterization of the Interactions between Amyloid- β Peptides and the Membranes of Hippocampal Cells. *J. Am. Chem. Soc.* **2013**, *135*, 1491–1498.
- (63) Ivanova, M. I.; Lin, Y.; Lee, Y. H.; Zheng, J.; Ramamoorthy, A. Biophysical Processes Underlying Cross-Seeding in Amyloid Aggregation and Implications in Amyloid Pathology. *Biophys. Chem.* **2021**, *269*, 106507.
- (64) Meleleo, D.; Sblano, C.; Storelli, M. M.; Mallamaci, R. Evidence of Cadmium and Mercury Involvement in the A β 42 Aggregation Process. *Biophys. Chem.* **2020**, *266*, 106453.

- (65) Saranya, V.; Mary, P. V.; Vijayakumar, S.; Shankar, R. The Hazardous Effects of the Environmental Toxic Gases on Amyloid Beta-Peptide Aggregation: A Theoretical Perspective. *Biophys. Chem.* **2020**, *263*, 106394.
- (66) Venegas, C.; Kumar, S.; Franklin, B. S.; Dierkes, T.; Brinkschulte, R.; Tejera, D.; Vieira-Saecker, A.; Schwartz, S.; Santarelli, F.; Kummer, M. P.; Griep, A.; Gelpi, E.; Beilharz, M.; Riedel, D.; Golenbock, D. T.; Geyer, M.; Walter, J.; Latz, E.; Heneka, M. T. Microglia-Derived ASC Specks Crossseed Amyloid- β in Alzheimer's Disease. *Nature* **2017**, *552*, 355–361.
- (67) Ohnishi, T.; Yanazawa, M.; Sasahara, T.; Kitamura, Y.; Hiroaki, H.; Fukazawa, Y.; Kii, I.; Nishiyama, T.; Kakita, A.; Takeda, H.; Takeuchi, A.; Arai, Y.; Ito, A.; Komura, H.; Hirao, H.; Satomura, K.; Inoue, M.; Muramatsu, S. I.; Matsui, K.; Tada, M.; Sato, M.; Saijo, E.; Shigemitsu, Y.; Sakai, S.; Umetsu, Y.; Goda, N.; Takino, N.; Takahashi, H.; Hagiwara, M.; Sawasaki, T.; Iwasaki, G.; Nakamura, Y.; Nabeshima, Y. I.; Teplow, D. B.; Hoshi, M.; Südhof, T. C. Na, K-ATPase A3 Is a Death Target of Alzheimer Patient Amyloid- β Assembly. *Proc. Natl. Acad. Sci. U. S. A.* **2015**, *112*, E4465–E4474.
- (68) Heckmann, B. L.; Teubner, B. J. W.; Tummers, B.; Boada-Romero, E.; Harris, L.; Yang, M.; Guy, C. S.; Zakharenko, S. S.; Green, D. R. LC3-Associated Endocytosis Facilitates β -Amyloid Clearance and Mitigates Neurodegeneration in Murine Alzheimer's Disease. *Cell* **2019**, *178*, 536–551.
- (69) Narayan, P.; Ganzinger, K. A.; McColl, J.; Weimann, L.; Meehan, S.; Qamar, S.; Carver, J. A.; Wilson, M. R.; St. George-Hyslop, P.; Dobson, C. M.; Klenerman, D. Single Molecule Characterization of the Interactions between Amyloid- β Peptides and the Membranes of Hippocampal Cells. *J. Am. Chem. Soc.* **2013**, *135*, 1491–1498.

(70) Iliff, J. J.; Wang, M.; Liao, Y.; Plogg, B. A.; Peng, W.; Gundersen, G. A.; Benveniste, H.; Vates, G. E.; Deane, R.; Goldman, S. A.; Nagelhus, E. A.; Nedergaard, M. A Paravascular Pathway Facilitates CSF Flow through the Brain Parenchyma and the Clearance of Interstitial Solutes, Including Amyloid β . *Sci. Transl. Med.* **2012**, *4*, 147ra111.

Supporting Information

Table of Contents

Materials and Methods¹	84
General Information	
884	
Chemicals and Supplies	84
Instrumentation	85
Molecular Cloning	87
Isolation of pET-Sac-A $\beta_{(M1-42)}$ Plasmid	87
Restriction Enzyme Digestion of pET-Sac-A $\beta_{(M1-42)}$ Plasmid	87
Table 2.S1. Restriction enzyme digestion of the pET- Sac A $\beta_{(M1-42)}$ plasmid	88
Table 2.S2. rSAP treatment of the vector backbones	88
Design of the DNA Sequence for A $\beta_{(MCI-42)}$	89
Figure 2.S1. Design of the DNA sequence for A $\beta_{(MCI-42)}$	89
Restriction Enzyme Digestion of A $\beta_{(MCI-42)}$ DNA Fragment	89
Table 2.S3. Restriction enzyme digestion of the A $\beta_{(MCI-42)}$ DNA fragment	90
T4 Ligation of the A $\beta_{(MCI-42)}$ DNA Fragment and the pET-Sac Vector	91
Table 2.S4. T4 ligation of the insert and the vector	91
A $\beta_{(MCI-42)}$ Recombinant Plasmid Preparation	91
Representative Schedule for the Expression, Purification, and Labeling of A$\beta_{(C1-42)}$	92
Table 2.S5. Representative schedule for the expression, purification, and labeling of A $\beta_{(C1-42)}$	92
Bacterial expression of A$\beta_{(C1-42)}$	92
Transformation of A $\beta_{(MCI-42)}$ Plasmid	92
Expression of A $\beta_{(C1-42)}$	93

Purification of the Aβ_(C1-42) Peptide	93
Cell Lysis	93
Sample Filtering and Analytical HPLC	94
Figure 2.S2. Representative HPLC trace of filtered, unpurified A β _(C1-42)	95
Preparative HPLC Purification of A β _(C1-42)	95
Table 2.S6. HPLC solvent gradient for the purification of A β _(C1-42)	96
Column Maintenance	96
Table 2.S7. Prep-HPLC column cleaning protocol	96
Characterization of Purified A β _(C1-42)	96
Storage of the Combined Pure HPLC Fractions of A β _(C1-42)	97
Labeling of Aβ_(C1-42)	98
Stoichiometry Calculation	98
Table 2.S8. Reagent table for labeling A β _(C1-42) with maleimide-5-TAMRA	99
Sodium Borate Buffer Preparation	99
Table 2.S9. Recipe of making 750 mM sodium borate buffer (pH 9.0)	99
Titration	99
Table 2.S10. Titration of a 1.0 mL portion of the combined HPLC fractions of A β _(C1-42)	100
Basification	100
Table 2.S11. Basification of the remainder of the combined HPLC fractions of A β _(C1-42)	101
Figure 2.S3. Representative HPLC trace of basified combined pure fractions of A β _(C1-42)	101
Labeling	101
Purification of Labeled Aβ_(C1-42)	102
Sample Filtering and Analytical HPLC	102
Figure 2.S4. Representative analytical HPLC trace of filtered, unpurified TAMRA-labeled A β _(C1-42)	103

Figure 2.S5. Representative analytical HPLC traces of filtered, unpurified FAM-labeled A β _(C1-42) .	104
Figure 2.S6. Representative analytical HPLC trace of filtered, unpurified PEG ₂ -biotin-labeled A β _(C1-42)	105
Table 2.S12. Analytical HPLC retention time	105
Preparative HPLC Purification of Labeled A β _(C1-42)	105
Table 2.S13. HPLC solvent gradient for the purification of labeled-A β _(C1-42)	106
Characterization of Purified labeled A β _(C1-42)	106
Table 2.S14. Typical purities of labeled-A β _(C1-42) peptides	107
Storage of the Purified Labeled A β _(C1-42)	107
Yields of Labeled A β _(C1-42) Peptides	107
Table 2.S15. Typical yields of labeled-A β _(C1-42) peptides	108
HFIP Treatment of Labeled Aβ_(C1-42) Peptides	108
Table 2.S16. Volumes of HFIP peptide solution per aliquot	109
Mass Spectrometry	109
SDS-PAGE, Silver staining, and Fluorescence Imaging	109
Sample Preparation and SDS-PAGE	109
Silver Staining	110
Fluorescence Imaging	111
Thioflavin T (ThT) Assay	111
ThT Solution Preparation	111
Peptide Working Solution Preparation	111
ThT Fluorescence Assay Setup	111
Fluorescence Suppression Assay	112
Peptide Working Solution Preparation	112
Fluorescence Suppression Assay Setup	112

Transmission Electron Microscopy (TEM)	113
Sample Preparation	113
TEM Imaging	113
Atomic Force Microscopy (AFM)	113
Sample Preparation	113
AFM Imaging	113
Fluorescence Microscopy	114
SH-SY5Y Cell Preparation, Treatment, and Imaging	114
RAW 264.7 Cell Preparation, Treatment, and Imaging	115
Bacteria Culturing, Treatment, and Imaging	116
Characterization Data and Additional Figures	118
Analytical HPLC Trace, MALDI Mass Spectrum, and MS/MS Spectrum of Aβ_(C1-42)	118
Figure 2.S7. Representative analytical HPLC trace of A β _(C1-42)	118
Figure 2.S8. Representative MALDI mass spectrum of A β _(C1-42)	119
Figure 2.S9. Representative MS/MS spectrum of A β _(C1-42)	120
Analytical HPLC Trace and MALDI Mass Spectrum of 5-TAMRA-Aβ_(C1-42)	121
Figure 2.S10. Representative analytical HPLC trace of 5-TAMRA-A β _(C1-42)	121
Figure 2.S11. Representative MALDI mass spectrum of 5-TAMRA-A β _(C1-42)	122
Analytical HPLC Trace and MALDI Mass Spectrum of 6-FAM-Aβ_(C1-42)	123
Figure 2.S12. Representative analytical HPLC trace of 6-FAM-A β _(C1-42)	123
Figure 2.S13. Representative MALDI mass spectrum of 6-FAM-A β _(C1-42)	124
Analytical HPLC Trace and MALDI Mass Spectrum of PEG₂-Biotin-Aβ_(C1-42)	125
Figure 2.S14. Representative analytical HPLC trace of PEG ₂ -biotin-A β _(C1-42)	125
Figure 2.S15. Representative MALDI mass spectrum of PEG ₂ -biotin-A β _(C1-42)	126

Figure 2.S16. ThT fluorescence assays and fluorescence suppression assays of labeled A β _(C1-42) and A β _(M1-42)	127
Figure 2.S17. Fluorescence micrographs of labeled A β with mammalian cells (low magnification views)	128
Figure 2.S18. Transmission electron micrographs of the fibrils formed by A β peptides	129
Figure 2.S19. Atomic force micrographs of the fibrils formed by A β peptides	130
References and Notes	131

Materials and Methods¹

General Information

Chemicals and Supplies. All chemicals were used as received unless otherwise noted. Deionized water (18 M Ω) was obtained from a Thermo Fisher Scientific Barnstead Genpure Pro water purification system. The pET-Sac-A β _(M1-42) plasmid was a gift from Dominic Walsh (Addgene plasmid # 71875). DNA sequences that encode A β _(M1-42) was purchased in 500 ng quantities from Genewiz. *NdeI* and *SacI* restriction enzymes, CutSmart buffer, and shrimp alkaline phosphatase (rSAP) were purchased from New England Biolabs (NEB). TOP10 Ca²⁺-competent *E. coli* and BL21 DE3 PLYS Star Ca²⁺-competent *E. coli*, T4 ligase, and ethidium bromide were purchased from Thermo Fisher Scientific. Zymo ZR plasmid miniprep kit was purchased from Zymo Research. Zymoclean Gel DNA Recovery Kit was purchased from Zymo Research. Fisher BioReagents LB Broth was purchased from Thermo Fisher Scientific. Carbenicillin was purchased from Gold Biotechnology and added to culture media as a 1000X stock solution (50.0 mg/mL) in water. Chloramphenicol was purchased from RPI Research Products and added to culture media as a 1000X stock solution (34.0 mg/mL) in EtOH. Isopropyl β -D-1-thiogalactopyranoside (IPTG) was purchased from Gold Biotechnology and added to the culture media as a 1000X stock solution

(23.8 mg/mL) in water. Maleimide-6-carboxyfluorescein (FAM) and maleimide-5-tetramethylrhodamine (TAMRA) were purchased from Lumiprobe and maleimide-PEG₂-biotin was purchased from Thermo Fisher Scientific. DMSO was purchased from Thermo Fisher Scientific. Urea and sodium borate were purchased from Thermo Fisher Scientific. Boric acid was purchased from Sigma-Aldrich. Tris hydrochloride was purchased from Avantor. Ethylenediaminetetraacetic acid (EDTA) was purchased from Sigma-Aldrich. Trifluoroacetic acid (TFA), and HPLC grade acetonitrile (ACN) were purchased from Thermo Fisher Scientific. 1,1,1,3,3,3-Hexafluoro-2-propanol (HFIP) was purchased from Oakwood Chemical. Thioflavin T (ThT) was purchased from Sigma-Aldrich. Spectra multicolor low range protein ladder and 6X SDS-PAGE loading buffer were purchased from Thermo Fisher Scientific. Sodium carbonate ($\geq 99.5\%$) was purchased from Sigma-Aldrich.^a Ammonium persulfate, formaldehyde, and silver nitrate were purchased from Thermo Fisher Scientific. N,N,N',N'-tetramethylethylenediamine (TEMEDA) was purchased from Alfa Aesar. Sodium thiosulfate was purchased from Avantor. Corning® 96-well half area black/clear flat bottom polystyrene nonbinding surface (NBS) microplates (product number: 3881) were purchased from Corning Incorporated.^b 0.22 μm Hydrophilic polyethersulfone (PES) syringe filters were purchased from Genesee Scientific (catalog number: 25-244). 0.20 μm Nylon syringe filters were purchased from Thermo Fisher Scientific (catalog number: 09-719-006). DMEM:F12 media were purchased from Thermo Fisher Scientific. Molecular biology grade agarose was purchased from Thermo Fisher Scientific. Difco Mueller Hinton broth was purchased from Becton Dickinson and Company.

^a Use of high-purity sodium carbonate is crucial for successful silver staining.

^b Microplates with a non-binding surface give reproducible ThT assay results.

Instrumentation. The concentrations of the DNA and peptide samples were measured using a Thermo Fisher Scientific NanoDrop One spectrophotometer. *E. coli* were incubated in a Thermo Fisher Scientific MaxQ Shaker 6000. *E. coli* were pelleted by centrifugation using Beckman Coulter Avanti J-E centrifuge with JA-10 and JA-18 rotors. *E. coli* were lysed using a QSonica Q500 ultrasonic homogenizer. Analytical reverse-phase HPLC was performed on an Agilent 1260 Infinity II instrument equipped with a Phenomenex bioZen Peptide XB-C18 LC column (4.6 x 150 mm, 2.6 μm particle size). Preparative reverse-phase HPLC was performed on a Rainin Dynamax instrument SD-200 equipped an Agilent ZORBAX 300SB-C8 semi-preparative column (9.4 x 250 mm, 5.0 μm particle size) with a ZORBAX 300SB-C3 preparative guard column (9.4 x 15 mm, 7.0 μm particle size). During preparative HPLC purification, the C8 column and the guard column were heated to 80 °C in a Sterlite plastic bin equipped with a Wancle Sous Vide immersion circulator. HPLC grade acetonitrile and deionized water (18 M Ω), each containing 0.1% trifluoroacetic acid (TFA), were used for analytical and preparative reverse-phase HPLC. MALDI-TOF mass spectrometry and tandem mass spectrometry (MS/MS) peptide sequencing were performed using an AB SCIEX TOF/TOF 5800 System. Rotary evaporation was conducted using a Büchi Rotavapor. Lyophilization was conducted using a Labconco FreeZone Freeze Dry System. Sonication of the peptide DMSO stock was performed using a SharperTek ultrasonic cleaner. pH of the solutions was measures using a Thermo Fisher Scientific AB150 Benchtop pH Meter and a Fisherbrand™ accumet™ pH probe. Fluorescence suppression assays and ThT fluorescence assays were performed using a Thermo Fisher Scientific Varioskan Lux microplate reader. The absorbance of the ThT solution and peptide solutions were measured using a Thermo Fisher Scientific Multiskan Go microplate spectrophotometer. SDS-PAGE gels were visualized using a ChemiDoc Touch Imaging System. Mammalian cell fluorescence microscopy was

performed using a Keyence BZ-X810 fluorescence microscope. Mammalian cell fluorescence microscopy was performed using a Zeiss LSM 780 confocal fluorescence microscope. TEM images were obtained using a JEOL JEM-2100F-cryo-TEM instrument.

Molecular Cloning

This section describes the preparation of the pET-Sac-A β _(MC1-42) plasmid. We have now deposited the pET-Sac-A β _(MC1-42) plasmid with Addgene to make it available to others.²

Isolation of pET-Sac-A β _(M1-42) Plasmid. The pET-Sac-A β _(M1-42) plasmid was purchased as a bacterial stab from Addgene (Addgene plasmid #71875)³, which was made available as a gift from D. Walsh.⁴ The bacterial stab was immediately streaked onto a LB agar-plate containing carbenicillin (50 mg/L). Colonies grew in < 24 h. Single colonies were picked and used to inoculate 5 mL of LB broth containing carbenicillin (50 mg/L). The cultures were shaken at 225 rpm overnight at 37 °C. To isolate the pET-Sac-A β _(M1-42) plasmids, minipreps were performed using a Zymo ZR plasmid miniprep kit. The concentration of the plasmids was measured using a Thermo Scientific Nanodrop instrument.

Restriction Enzyme Digestion of pET-Sac-A β _(M1-42) Plasmid. The pET-Sac-A β _(M1-42) plasmid was digested using *SacI* and *NdeI* restriction enzymes to remove the A β _(M1-42) sequence and prepare vector backbones for the subsequent generation of A β _(MC1-42) recombinant plasmid. Table 2.S1 details the restriction reaction conditions. Reagents were added in the order they are listed.

Table 2.S1. Restriction enzyme digestion of the pET- Sac A β _(M1-42) plasmid

Reagents	Amount
pET-Sac A β _(M1-42)	20 μ L of 50 ng/ μ L plasmid solution (1.0 μ g in total)
10X CutSmart buffer	5.0 μ L
H ₂ O	23.0 μ L
<i>NdeI</i> restriction enzyme	1.0 μ L (1 U)
<i>SacI</i> -HF restriction enzyme	1.0 μ L (1 U)
Total	50.0 μ L
Time	1.0 h
Temperature	37.0 °C

Next, to prevent vector backbone self-ligation, the digested plasmid was treated with shrimp alkaline phosphatase (rSAP). Table 2.S2 details the rSAP reaction conditions.

Table 2.S2. rSAP treatment of the vector backbones

Reagents	Amount
Restriction enzyme digestion mixture	50.0 μ L
rSAP	1.0 μ L (1U)
Total	51.0 μ L
Time	0.5 h
Temperature	37.0 °C
Heat inactivation	65.0 °C for 20 min

After the rSAP reaction and heat inactivation were complete, the reaction mixture was mixed with DNA loading buffer and loaded onto a 1% agarose gel containing ethidium bromide (5 μ L per 100 mL gel). The agarose gel was run at 100 V for ca. 30 min. A UV box was used to visualize the digested pET-Sac vector (ca.4500 bp), which was excised from the gel using a razor blade. The digested pET-Sac vector was purified from the agarose gel using a Zymoclean Gel DNA Recovery Kit. The concentration of the vector after purification was measured using a

Thermo Scientific Nanodrop instrument. The purified digested pET-Sac linear vector was used in the subsequent ligation step.

Design of the DNA Sequence for A β _(MC1-42). DNA fragment for A β _(MC1-42) was ordered from Genewiz. Figure 2.S1 shows the design of the DNA sequence for A β _(MC1-42).

■ 3' and 5' overhangs ■ *NdeI* restriction site/start codon

■ stop codons ■ *SacI* restriction site

GAT ATA CAT ATG TGC GAC GCT GAA TTC CGT CAC GAC TCT GGT TAC GAA GTT
CAC CAC CAG AAG CTG GTG TTC TTC GCT GAA GAC GTG GGT TCT AAC AAG GGT
GCT ATC ATC GGT CTG ATG GTT GGT GGC GTT GTG ATC GCT TAA TAG GAG CTC
GAT CCG

Figure 2.S1. Design of the DNA sequence for A β _(MC1-42).

Restriction Enzyme Digestion of A β _(MC1-42) DNA Fragment. The A β _(MC1-42) DNA fragment was digested using *SacI* and *NdeI* restriction enzymes to generate the insert DNA. Table 2.S3 details the restriction reaction conditions. Reagents were added in the order they are listed.

Table 2.S3. Restriction enzyme digestion of the A β _(MC1-42) DNA fragment

Reagents	Amount
DNA sequence encoding mutation	20 μ L of 5 ng/ μ L DNA solution (100.0 ng in total)
10X CutSmart buffer	2.5 μ L
H ₂ O	1.5 μ L
<i>NdeI</i> restriction enzyme	0.5 μ L (0.5 U)
<i>SacI</i> -HF restriction enzyme	0.5 μ L (0.5 U)
Total	25.0 μ L
Time	1.0 h
Temperature	37.0 $^{\circ}$ C
Heat inactivation	65.0 $^{\circ}$ C for 20 min

T4 Ligation of the A β _(MC1-42) DNA Fragment and the pET-Sac Vector. The A β _(MC1-42) DNA fragment (insert) and the backbone vector were ligated together using T4 ligase. Table 2.S4 details the T4 ligation reaction conditions. Reagents were added in the order they are listed.

Table 2.S4. T4 ligation of the insert and the vector

Reagents	Amount	
	Insert:Vector = 0:1 (molar ratio) (negative control)	Insert:Vector = 5:1 (molar ratio)
Vector	6.2 μ L of 9.7 ng/ μ L DNA solution (60.0 ng in total)	6.2 μ L of 9.7 ng/ μ L DNA solution (60.0 ng in total)
Insert	---	2.5 μ L of 4.0 ng/ μ L DNA solution (10.0 ng in total)
10X T4 DNA ligase reaction buffer	2.0 μ L	2.0 μ L
T4 DNA ligase	1.0 μ L	1.0 μ L
H ₂ O	10.8 μ L	8.3 μ L
Total	20.0 μ L	20.0 μ L
Ligation time	10 min	
Temp	22.0 °C (room temperature)	
Heat inactivation	65.0 °C for 10 min	

A β _(MC1-42) Recombinant Plasmid Preparation. 2 μ L of the ligation reaction mixture was then transformed into TOP10 Ca²⁺-competent *E. coli* using the heat shock method. The cell cultures were spread on LB agar plates containing carbenicillin (50 mg/L). Single colonies were picked to inoculate 5 mL of overnight cultures in LB media with carbenicillin (50 mg/L). The plasmid was extracted from TOP10 cells using Zymo ZR plasmid miniprep kit. The concentration of the plasmid was measured through Thermo Scientific NanoDrop spectrophotometer. The DNA sequence of the A β _(MC1-42) recombinant plasmid was verified by DNA sequencing. The A β _(MC1-42) recombinant plasmid was deposited to Addgene.²

Representative Schedule for the Expression, Purification, and Labeling of A β _(C1-42)

Table 2.S5. Representative schedule for the expression, purification, and labeling of A β _(C1-42)

Day	Time	Steps
Day 1	Evening	Starter culture
Day 2	Morning	Daytime culture
	Afternoon	IPTG induced expression of A β _(C1-42)
	Evening	Cell pelleting
Day 3	Morning	Cell lysis and urea extraction to obtain peptide solution
	Afternoon	Prep-HPLC purification of the 1 st batch of peptide solution
	Evening	Prep-HPLC purification of the 2 nd batch of peptide solution
A total of ca. 14.0 mg ^a of pure A β _(C1-42) is obtained (in two batches of combined HPLC fractions)		
Day 4	Morning	Labeling of the 1 st batch of A β _(C1-42) ; prep-HPLC purification
	Afternoon	Labeling of the 2 nd batch of A β _(C1-42) ; prep-HPLC purification
Day 4–5	Overnight	Lyophilization of purified labeled A β _(C1-42)
A total of ca. 3.0 mg ^b of pure labeled A β _(C1-42) is obtained		
Day 5	Afternoon	HFIP treatment of pure labeled A β _(C1-42) ; lyophilization

Bacterial expression of A β _(C1-42)

Transformation of A β _(MC1-42) Plasmid. All liquid cultures were performed in culture media (LB broth containing 50 mg/L carbenicillin and 34 mg/L chloramphenicol). A β _(MC1-42) plasmid was transformed into BL21 DE3 PLYS Star Ca²⁺-competent *E. coli* through heat shock method. The cell cultures were spread on LB agar plates containing carbenicillin (50 mg/L) and

^a The yield of A β _(C1-42) was determined spectrophotometrically.

^b The yield of labeled A β _(C1-42) was determined gravimetrically.

chloramphenicol (34 mg/L). Single colonies were picked to inoculate 5 mL of culture media for overnight culture (ca. 14 h). A glycerol stock of BL21 DE3 PLysS Star Ca²⁺-competent *E. coli* bearing the plasmid was made. The glycerol stock was stored at -80 °C and was used in all subsequent expression procedures.

Expression of A β _(C1-42). For a typical expression procedure, a starter culture was made by inoculating culture media with an aliquot of the glycerol stock. The next day, all 5 mL of the overnight culture were used to inoculate 1 L of culture media. After inoculation, the culture was shaken at 225 rpm at 37 °C (for ca. 3 hours and 50 minutes) until the cell density reached an OD₆₀₀ of ca. 0.45. Protein expression was then induced by the addition of isopropyl β -D-1-thiogalactopyranoside (IPTG) to a final concentration of 0.1 mM, and the cells were shaken at 225 rpm at 37 °C for 4 more hours with IPTG. The cells were then harvested by centrifugation at 4000 rpm using a JA-10 rotor (2800 x g) at 4 °C for 25 minutes, and the cell pellets were then stored at -80 °C.

Purification of the A β _(C1-42) Peptide

Cell Lysis. To lyse the cells, the cell pellet was resuspended in 20 mL of buffer A (10 mM Tris/HCl, 1 mM EDTA, pH 8.0) and sonicated for 2 minutes on ice (50% duty cycle) until the lysate appeared homogenous. The lysate was then centrifuged for 25 minutes at 16000 rpm using a JA-18 rotor (38000 x g) at 4 °C. The supernatant was removed, and the pellet was resuspended in buffer A, sonicated and centrifuged as described above. The sonication and centrifugation steps were repeated two additional times. After the third supernatant was removed, the remaining pellet (inclusion bodies) was resuspended in 15 mL of freshly prepared buffer B (8 M urea, 10 mM

Tris/HCl, 1 mM EDTA, pH 8.0), and was sonicated as described above, until the peptide solution became clear.

Sample Filtering and Analytical HPLC. The peptide solution (ca. 15 mL) was then diluted with 10 mL of buffer A and filtered through a 0.22 μm hydrophilic PES syringe filter from Genesee Scientific (catalog number: 25-244) or a 0.22 μm hydrophilic PVDF syringe filter from Thermo Fisher Scientific (catalog number: 09-719-006).^a Successful expression of the $\text{A}\beta_{(\text{C1-42})}$ peptide was confirmed by analytical reverse-phase HPLC as follows: A 20- μL sample of the above solution was injected onto an Agilent 1260 Infinity II instrument equipped with a Phenomenex bioZen Peptide XB-C18 LC column (4.6 x 150 mm, 2.6 μm particle size). HPLC grade acetonitrile (ACN) and 18 M Ω deionized water, each containing 0.1% trifluoroacetic acid, were used as the mobile phase. The sample was eluted at 1.0 mL/min with a 5–67% acetonitrile gradient over 15 minutes, at 60 °C. The absorbance was taken at 214 nm. A typical analytical HPLC trace of the successfully expressed $\text{A}\beta_{(\text{C1-42})}$ shows four major peaks, with the first peak (ca. 10.4 min) corresponding to the $\text{A}\beta_{(\text{C1-42})}$ monomer (Figure 2.S2).

^a Use of appropriate filter materials is essential for minimizing loss of peptide by adsorption during filtration.

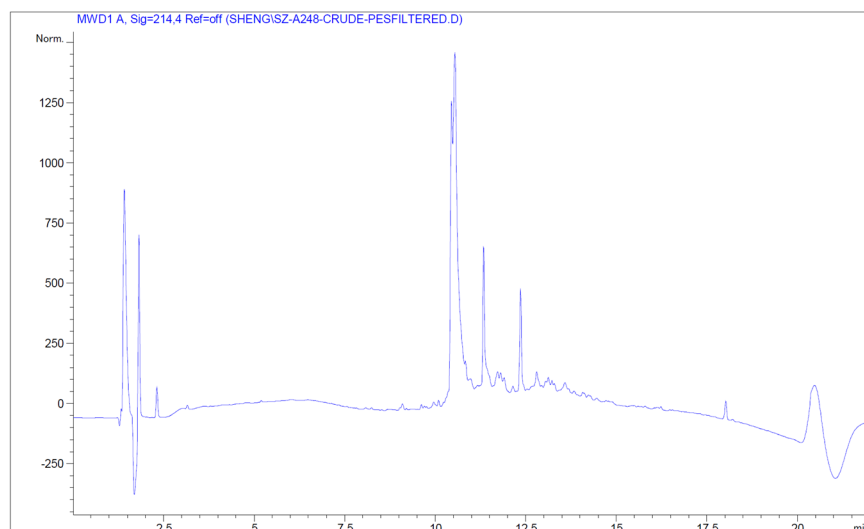


Figure 2.S2. Representative HPLC trace of filtered, unpurified $A\beta_{(C1-42)}$. HPLC was performed on a C18 column at 60 °C with elution with 5–67% acetonitrile over 15 minutes, and absorbance was monitored at 214 nm.

Preparative HPLC Purification of $A\beta_{(C1-42)}$. The filtered peptide solution was then purified by preparative reverse-phase HPLC equipped with an Agilent ZORBAX 300SB-C8 semi-preparative column (9.4 x 250 mm) with a ZORBAX 300SB-C3 preparative guard column (9.4 x 15 mm). The C8 column and the guard column were heated to 80 °C in water bath using a Sterlite plastic bin equipped with a Wancle Sous Vide immersion circulator.^a HPLC grade acetonitrile (ACN) and 18 M Ω deionized water, each containing 0.1% trifluoroacetic acid, were used as the mobile phase at a flow-rate of 5 mL/min. The filtered peptide solution (ca. 24 mL) was split into two ca. 12 mL batches and purified in two separate runs, with three injections in each run.^b In each run, the peptide was loaded onto the column while flowing 20% ACN through the column. The $A\beta_{(C1-42)}$ peptide was then eluted using the following solvent gradient (Table 2.S6). The

^a Any water heater large enough to submerge a HPLC column should be sufficient.

^b It may be possible to purify the peptide in a single batch if a larger diameter column is used (e.g., 21.4 x 250 mm).

absorbance was taken at 214 nm. Fractions containing the monomeric A β _(C1-42) generally eluted from 33% to 35% ACN.

Table 2.S6. HPLC solvent gradient for the purification of A β _(C1-42)

% H ₂ O	% ACN	Elapsed Time
80	20	0 min
80	20	15 min
40	65	60 min
5	95	61 min
5	95	80 min

Column Maintenance. After the peptide was collected, the column was washed by injecting 5 mL of filtered buffer B (8 M urea, 10 mM Tris/HCl, 1 mM EDTA, pH 8.0) while flushing at 95% ACN for 15 minutes. This cleaning procedure ensures elution of the peptide that is retained in the column and avoids problems of cross-contamination between runs. If an increase in column back-pressure is seen after several purifications, back-flushing the semi-preparative HPLC column using the following cleaning protocol will solve the problem (Table 2.S7).

Table 2.S7. Prep-HPLC column cleaning protocol

Solvent	Flow rate	Washing Time
100% ACN	5 mL/min	10 min
100% isopropanol	2 mL/min	15 min
100% hexanes	2 mL/min	20 min
100% isopropanol	2 mL/min	15 min
100% ACN	5 mL/min	10 min

Characterization of Purified A β _(C1-42). The purity of each fraction was assessed using analytical reverse-phase HPLC. A 20- μ L sample was injected onto the analytical HPLC. The

sample was eluted at 1.0 mL/min with a 5–67% acetonitrile gradient over 15 min, at 60 °C. The absorbance was taken at 214 nm. Pure fractions were combined and the purity of the combined fractions were checked using analytical HPLC. The purity of A β _(C1-42) was determined to be 97.7% by integration of the analytical HPLC trace at 214 nm (Figure 2.S7). The yield of A β _(C1-42) was determined to be ca. 14.0 mg per liter of bacterial culture, on the basis of the spectrophotometrically determined concentration of A β _(C1-42) in the combined pure HPLC fractions of each batch and the total volume of the two batches of the combined pure HPLC fractions. The details of spectrophotometric determination of the concentration of A β _(C1-42) in the combined pure HPLC fractions can be found in the “Labeling of A β _(C1-42)” section of the Supporting Information. The composition of the combined peptides was assessed by matrix-assisted laser desorption ionization mass spectrometry (MALDI-MS) and tandem mass spectrometry (MS/MS) (Figure 2.S8 and 2.S9). The details of running MALDI-MS and MS/MS can be found in the “Mass Spectrometry” section of the Supporting Information.

Storage of the Combined Pure HPLC Fractions of A β _(C1-42). The combined pure HPLC fractions of A β _(C1-42) can be directly used for subsequent labeling, or stored at -80 °C for at least three weeks without forming detectable aggregates. It is recommended to combine and freeze (at -80 °C or with dry ice) the purified fractions within 5 hours after purification to avoid oxidation of methionine.

Labeling of A β _(C1-42)

The labeling was performed for the first batch of combined pure HPLC fractions of A β _(C1-42), and then repeated for the second batch of A β _(C1-42). A representative protocol to label one batch of combined pure HPLC fractions of A β _(C1-42) is provided below.^a

Stoichiometry Calculation. The combined pure HPLC fractions of A β _(C1-42) was removed from the freezer or dry ice and allowed to thaw (ca. 20 min). The concentration of A β _(C1-42) in the combined HPLC fractions was determined by UV absorbance at 280 nm using an estimated extinction coefficient (ϵ) for tyrosine of 1490 M⁻¹cm⁻¹. A 35% ACN solution (acetonitrile 35%, water 64.9% and trifluoroacetic acid 0.1%) was used as blank solution for the UV absorbance measurement.^b The amount of the maleimide-based labeling reagent needed was then calculated based on a 2:1 molar ratio of the reagent to the A β _(C1-42) peptide. A typical reagent table for labeling A β _(C1-42) with maleimide-5-tetramethylrhodamine (TAMRA) is provided here (Table 2.S8). Labeling of A β _(C1-42) with maleimide-6-carboxyfluorescein (FAM) or maleimide-PEG₂-biotin was performed in a similar manner.

^a It may be possible to label and purify the peptide in a single batch if a larger diameter column is used (e.g., 21.4 x 250 mm).

^b The typical volume of the combined pure HPLC fractions from purifying a 12-mL batch of peptide solution is ca. 10 mL. The typical UV absorbance of the combined pure HPLC fractions at 280 nm is ca. 0.2 and the typical peptide concentration in the combined pure HPLC fractions is ca. 140 μ M.

Table 2.S8. Reagent table for labeling A $\beta_{(C1-42)}$ with maleimide-5-TAMRA

Reagent	Combined HPLC fractions of A $\beta_{(C1-42)}$	Maleimide-5-TAMRA
Concentration	141.9 μ M	---
volume	8.0 mL	---
Mass	---	1.26 mg dissolved in 126 μ L DMSO
Molecular weight	---	552.6 g/mol
Moles	1.14 μ mol	2.28 μ mol
Molar equivalent	1.0	2.0

Sodium Borate Buffer Preparation. A 750 mM sodium borate buffer solution (pH 9.0) was made by dissolving 1.54 g of sodium borate decahydrate (Na₂B₄O₇•10H₂O) and 0.25 g of boric acid (H₃BO₃) in 22 mL of deionized water (18 M Ω), followed by adding more deionized water (18 M Ω) until the total volume was 27 mL (Table 2.S9). The final pH of the 750 mM sodium borate buffer solution made through this recipe is typically 9.0. It is not necessary to further adjust the pH using acid or base.

Table 2.S9. Recipe of making 750 mM sodium borate buffer (pH 9.0)

Reagent	Molecular weight	Mass/Volume
Sodium borate decahydrate (Na ₂ B ₄ O ₇ •10H ₂ O)	381.43 g/mol	1.54 g
Boric acid (H ₃ BO ₃)	61.84 g/mol	0.25 g
Deionized water (18 M Ω)	---	Add 22 mL to dissolve Na ₂ B ₄ O ₇ •10H ₂ O and H ₃ BO ₃ , then fill up to a total volume of 27 mL

Titration. A 1.0 mL portion of the combined HPLC fractions of A $\beta_{(C1-42)}$ was then set aside on ice and titrated with the 750 mM sodium borate buffer in increments of 20 μ L without stirring or shaking. The pH of the solution was checked with a pH meter after the addition of each aliquot.

After a pH of 9.0 was reached, one additional 20 μL increment of sodium borate buffer was added. The titration results were recorded in a table and the titrated 1.0 mL portion of the combined HPLC fractions of $\text{A}\beta_{(\text{C1-42})}$ was discarded. A typical titration table is provided below (Table 2.S10).

Table 2.S10. Titration of a 1.0 mL portion of the combined HPLC fractions of $\text{A}\beta_{(\text{C1-42})}$

Total volume of 750 mM sodium borate buffer (pH 9.0) added	pH
0	2.3
20 μL	2.4
40 μL	6.0
60 μL	8.3
80 μL	8.8
100 μL	8.9
120 μL	9.0
140 μL	9.1

Basification. The volume of sodium borate buffer needed to basify the remainder of the combined HPLC fractions to pH 9.0 was calculated from the total volume of the sodium borate buffer used to titrate the 1.0 mL portion of the combined HPLC fractions of $\text{A}\beta_{(\text{C1-42})}$. The appropriate volume of the sodium borate buffer was added in a single portion to the remainder of the combined HPLC fractions on ice without stirring or shaking (Table 2.S11). The pH of the basified solution was checked with a pH meter. The basified solution was also checked with analytical HPLC to make sure $\text{A}\beta_{(\text{C1-42})}$ stayed in mostly monomeric form after basification (Figure 2.S3).^a

^a If the basification process is not properly performed, a substantial (> 20%) oligomer peak will appear after the monomer peak (at ca. 11.1 and 10.3 min, respectively). The labeling will still work, but the yield of labeled $\text{A}\beta$ will be compromised.

Table 2.S11. Basification of the remainder of the combined HPLC fractions of A β _(C1-42)

Total volume of 750 mM sodium borate buffer (pH 9.0) added	pH
0	2.4
1120 μ L	8.9

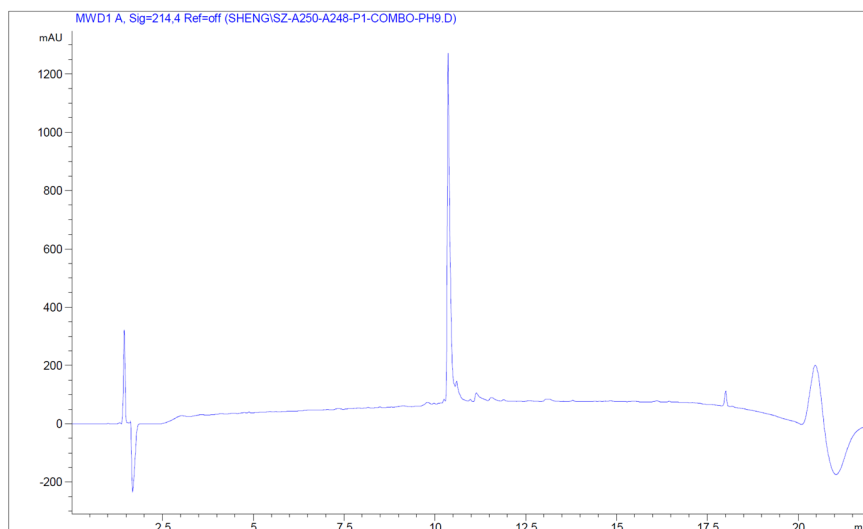


Figure 2.S3. Representative HPLC trace of basified combined pure fractions of A β _(C1-42). HPLC was performed on a C18 column at 60 °C with elution with 5–67% acetonitrile over 15 minutes, and absorbance was monitored at 214 nm.

Labeling. After basification, the remainder of the combined HPLC fractions of A β _(C1-42) was removed from the ice bath. The calculated amount the maleimide reagent (Table 2.S8) was dissolved in DMSO to give a 10 mg/mL stock solution. The maleimide reagent stock solution was slowly added to the remainder of the combined HPLC fractions of A β _(C1-42) with gentle swirling. The reaction mixture^a was then allowed to stand without stirring or shaking at room temperature

^a The composition of the reaction mixture: ca. 30.6% v/v acetonitrile, 0.1% v/v trifluoroacetic acid, 1.4% v/v DMSO, 67.9% v/v water, 92 mM sodium borate/boric acid, 250 μ M maleimide reagent, and 125 μ M A β _(C1-42).

for 15 minutes. If maleimide-5-TAMRA or maleimide-6-FAM was used as the labeling reagent, the reaction mixture was also protected from light.

Purification of Labeled A β _(C1-42)

Sample Filtering and Analytical HPLC. After the reaction had proceeded for 15 minutes, the reaction mixture was filtered through a 0.22 μ m hydrophilic PES syringe filter from Genesee Scientific (catalog number: 25-244). A PVDF syringe filter should not be used to filter the reaction mixture as it will lead to a substantial loss of labeled peptide in the reaction mixture. Successful labeling of the A β _(C1-42) peptide was confirmed by analytical reverse-phase HPLC as follows: A 20- μ L sample of the above solution was injected onto an Agilent 1260 Infinity II instrument equipped with a Phenomenex bioZen Peptide XB-C18 LC column (4.6 x 150 mm, 2.6 μ m particle size). HPLC grade acetonitrile (ACN) and 18 M Ω deionized water, each containing 0.1% trifluoroacetic acid, were used as the mobile phase. The sample was eluted at 1.0 mL/min with a 5–67% acetonitrile gradient over 15 minutes at 60 °C. If maleimide-5-TAMRA was used as the labeling reagent, the absorbance was taken at 214 nm and 541 nm. If maleimide-6-FAM was used as the labeling reagent, the absorbance was taken at 214 nm and 494 nm. If maleimide-PEG₂-biotin was used as the labeling reagent, the absorbance was taken at 214 nm. A typical analytical HPLC trace of the successfully labeled A β _(C1-42) shows a sharp peak corresponds to monomeric labeled A β _(C1-42) at ca. 10.2 minutes, with a slight retention time change compare to the unlabeled A β _(C1-42) (Figure 2.S4, 2.S5, and 2.S6) (Table 2.S12).

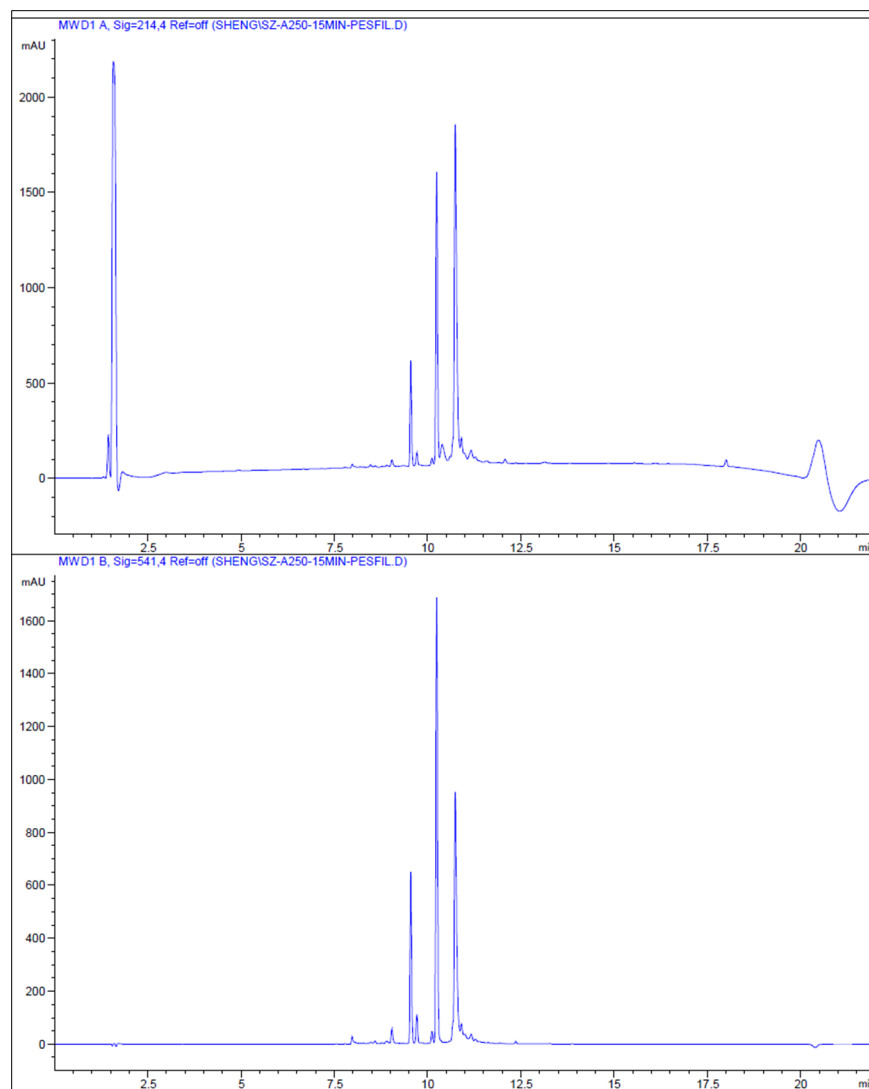


Figure 2.S4. Representative analytical HPLC trace of filtered, unpurified TAMRA-labeled $A\beta_{(C1-42)}$. HPLC was performed on a C18 column at 60 °C with elution with 5–67% acetonitrile over 15 minutes, and absorbance was monitored at 214 nm (top) and 541 nm (bottom).

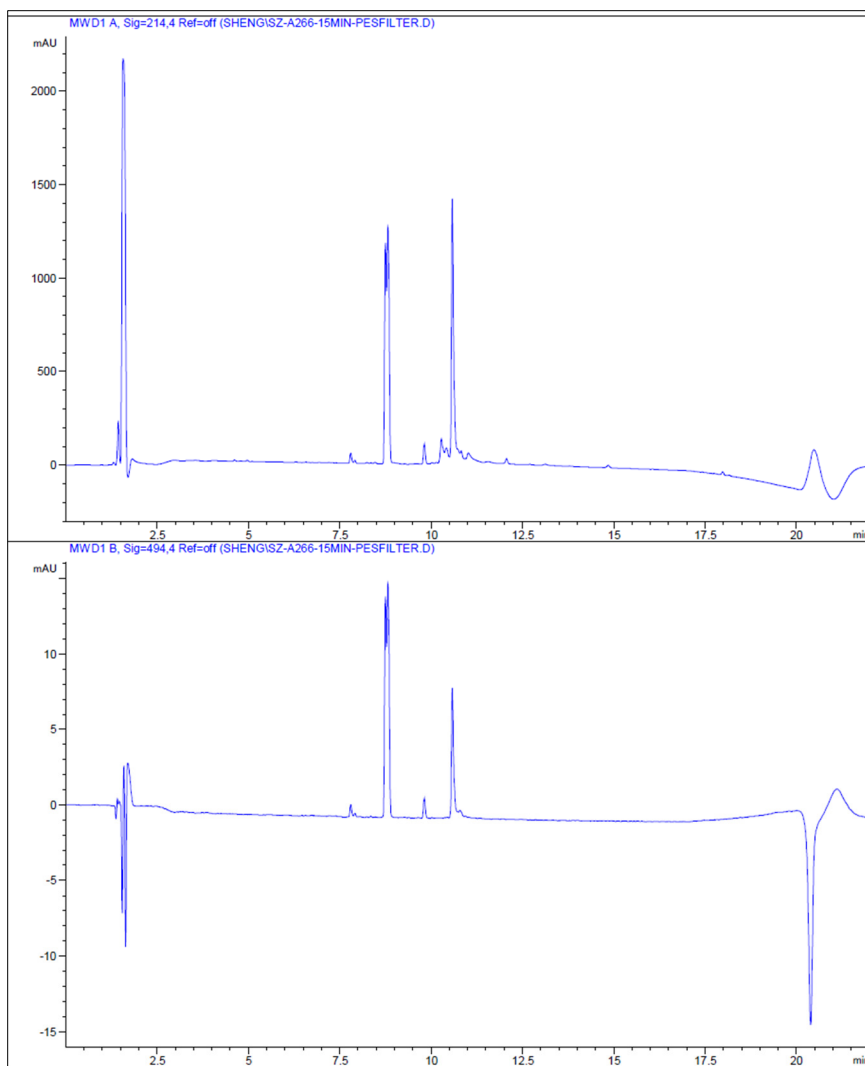


Figure 2.S5. Representative analytical HPLC traces of filtered, unpurified FAM-labeled $A\beta_{(C1-42)}$. HPLC was performed on a C18 column at 60 °C with elution with 5–67% acetonitrile over 15 minutes, and absorbance was monitored at 214 nm (top) and 494 nm (bottom).

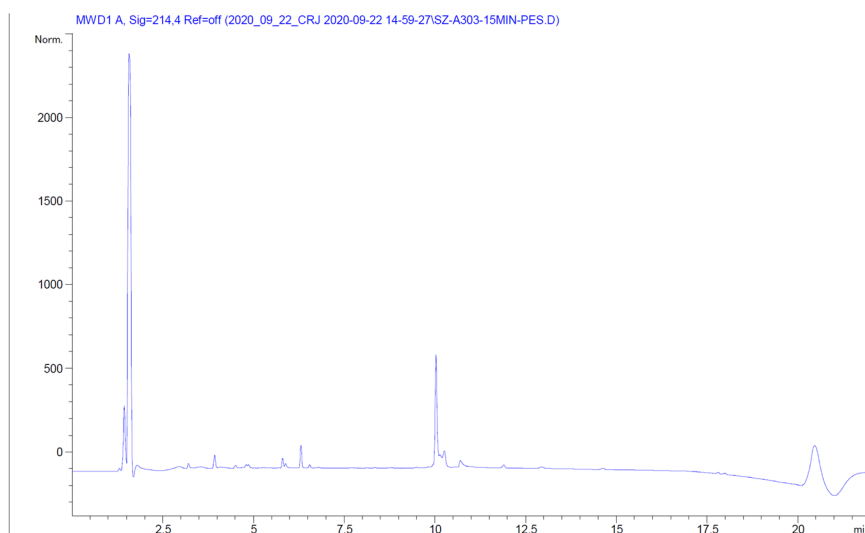


Figure 2.S6. Representative analytical HPLC trace of filtered, unpurified biotin-labeled $A\beta_{(C1-42)}$. The absorbance was taken at 214 nm. HPLC was performed on a C18 column at 60 °C with elution with 5–67% acetonitrile over 15 minutes, and absorbance was monitored at 214 nm.

Table 2.S12. Analytical HPLC retention time

Peptide	Analytical HPLC retention time
Unlabeled $A\beta_{(C1-42)}$	10.4 min
TAMRA- $A\beta_{(C1-42)}$	10.7 min
FAM- $A\beta_{(C1-42)}$	10.6 min
Biotin- $A\beta_{(C1-42)}$	10.0 min

Preparative HPLC Purification of Labeled $A\beta_{(C1-42)}$. The reaction mixture was then purified by preparative reverse-phase HPLC equipped with an Agilent ZORBAX 300SB-C8 semi-preparative column (9.4 x 250 mm) with a ZORBAX 300SB-C3 preparative guard column (9.4 x 15 mm).^a The C8 column and the guard column were heated to 80 °C in water bath using a Sterlite

^a It may be possible to label and purify the peptide in a single batch if a larger diameter column is used (e.g., 21.4 x 250 mm).

plastic bin equipped with a Wancle Sous Vide immersion circulator.^a HPLC grade acetonitrile (ACN) and 18 M Ω deionized water, each containing 0.1% trifluoroacetic acid, were used as the mobile phase at a flow rate of 5 mL/min. The filtered reaction mixture was loaded with two 4-mL injections onto the column while flowing 20% ACN through the column. The labeled-A $\beta_{(C1-42)}$ peptide was then purified using the following solvent gradient (Table 2.S13). The absorbance was taken at 214 nm. Fractions containing the monomeric labeled-A $\beta_{(C1-42)}$ generally eluted from 34% to 38% ACN.^b

Table 2.S13. HPLC solvent gradient for the purification of labeled-A $\beta_{(C1-42)}$

% H ₂ O	% ACN	Elapsed Time
80	20	0 min
80	20	15 min
40	65	60 min
5	95	61 min
5	95	80 min

Characterization of Purified labeled A $\beta_{(C1-42)}$. The purity of each fraction was assessed using analytical reverse-phase HPLC. A 20- μ L sample was injected onto the analytical HPLC. The sample was eluted at 1.0 mL/min with a 5–67% acetonitrile gradient over 15 min, at 60 °C. If maleimide-5-TAMRA was used as the labeling reagent, the absorbance was taken at 214 nm and 541 nm. If maleimide-6-FAM was used as the labeling reagent, the absorbance was taken at 214 nm and 494 nm. If maleimide-PEG₂-biotin was used as the labeling reagent, the absorbance was taken at 214 nm. Pure fractions were combined and the purity of the combined fractions were

^a Any water heater large enough to submerge a HPLC column should be sufficient.

^b An increase in column back-pressure is rare after purifying the reaction mixture. If column maintenance is needed, please refer to the “Column Maintenance” procedures from the “Purification of the A $\beta_{(C1-42)}$ Peptide” section.

checked using analytical HPLC. The purities of labeled $A\beta_{(C1-42)}$ were determined by integration of the analytical HPLC trace at 214 nm (Figure 2.S10, 2.S12, and 2.S14) (Table 2.S14). The composition of the combined peptides was assessed by matrix-assisted laser desorption ionization mass spectrometry (MALDI-MS) (Figure 2.S11, 2.S13, and 2.S15). The details of running MALDI-MS can be found in the “Mass Spectrometry” section of the Supporting Information.

Table 2.S14. Typical purities of labeled- $A\beta_{(C1-42)}$ peptides

Labeled- $A\beta_{(C1-42)}$ peptides	Purity
TAMRA- $A\beta_{(C1-42)}$	94.7%
FAM- $A\beta_{(C1-42)}$	94.0%
Biotin- $A\beta_{(C1-42)}$	96.6%

Storage of the Purified Labeled $A\beta_{(C1-42)}$. The combined pure HPLC fractions of labeled- $A\beta_{(C1-42)}$ were concentrated by rotary evaporation to remove ACN,^a and then frozen with dry ice. It is recommended to combine and freeze the purified fractions within 5 hours after purification to avoid oxidation of methionine. The frozen sample was then lyophilized. For TAMRA- and FAM-labeled $A\beta_{(C1-42)}$, the sample should be protected from light during lyophilization process.

Yields of Labeled $A\beta_{(C1-42)}$ Peptides. After the lyophilization was completed, the lyophilized labeled $A\beta$ from two batches of purifications are combined, and the yields of the labeled peptides were assessed gravimetrically. Table 2.S15 shows the typical yields of labeled- $A\beta_{(C1-42)}$ peptides per liter of bacterial culture.

^a The water bath for the rotary evaporator should not be heated.

Table 2.S15. Typical yields of labeled-A $\beta_{(C1-42)}$ peptides

Labeled-A $\beta_{(C1-42)}$ peptides	Yield (per liter of bacterial culture)
TAMRA-A $\beta_{(C1-42)}$	3.6 mg
FAM-A $\beta_{(C1-42)}$	2.6 mg
Biotin-A $\beta_{(C1-42)}$	3.0 mg

HFIP Treatment of Labeled A $\beta_{(C1-42)}$ Peptides

The lyophilized labeled A $\beta_{(C1-42)}$ peptides were then treated with HFIP to provide aliquots of monomeric A β for subsequent biophysical and biological studies. Briefly, the lyophilized peptide was dissolved in HFIP to give a clear solution with 0.25 mg/mL concentration of peptide. The peptide solution was allowed to stand without stirring or shaking at room temperature for 3 hours. The solution was then placed on ice for an additional 30 minutes. For TAMRA-labeled A $\beta_{(C1-42)}$ and FAM-labeled A $\beta_{(C1-42)}$, the samples were protected from light. The A $\beta_{(M1-42)}$ peptide, which was prepared as a control, was treated in a similar fashion.^a

The chilled peptide solution was then aliquoted into microcentrifuge tubes using a single-channel pipette.^b We typically aliquot 0.02 μ mol of peptide (ca. 0.1 mg) per tube, as shown in Table 2.S16. The tubes were then frozen in dry ice and lyophilized to remove HFIP. The lyophilized aliquots were stored in a desiccator at -20 °C until needed for further use. For TAMRA-labeled A $\beta_{(C1-42)}$ and FAM-labeled A $\beta_{(C1-42)}$, the samples were protected from light.

^a A $\beta_{(M1-42)}$ is an expressed homologue with properties similar to native A $\beta_{(1-42)}$, which was used as an unlabeled A β control for subsequent biophysical and biological studies. A $\beta_{(M1-42)}$ was expressed, purified, and lyophilized following the protocol we published previously.¹

^b It is important to chill the HFIP solution to minimize evaporation and allow dispensing with a single-channel pipette. Alternatively, a positive displacement pipette may be used.

Table 2.S16. Volumes of HFIP peptide solution per aliquot

Peptide	Moles of peptide per tube ^a	Molecular weight ^a	Mass of peptide per tube	HFIP peptide solution concentration	Volume of HFIP peptide solution per tube
TAMRA-A $\beta_{(C1-42)}$	0.02 μ mol	5170 g/mol	0.103 mg	0.25 mg/mL	412 μ L
FAM-A $\beta_{(C1-42)}$		5116 g/mol	0.102 mg		408 μ L
Biotin-A $\beta_{(C1-42)}$		5143 g/mol	0.103 mg		412 μ L
A $\beta_{(M1-42)}$		4645 g/mol	0.093 mg		372 μ L

^a Molecular weight calculated for the free peptide. If trifluoroacetate counterions are present from HPLC purification, then the effective molecular weight of the peptide will be higher (by ca. 10-15%, depending on the number of trifluoroacetate counterions per peptide), and the number of μ mol of peptide per tube will be slightly lower (by ca. 10-15%, depending on the number of trifluoroacetate counterions per peptide).

Mass Spectrometry

Matrix-assisted laser desorption ionization mass spectrometry (MALDI-MS) and tandem mass spectrometry (MS/MS) were performed using an AB SCIEX TOF/TOF 5800 System. 0.5 μ L of 2,5-dihydroxybenzoic acid (DHB) was dispensed onto a MALDI sample support, followed by the addition of 0.5 μ L peptide sample. The mixture was allowed to air-dry. MALDI analyses were performed in positive reflector mode, collecting data with a molecular weight range of 1000–9000 Da. MS/MS analysis of the A $\beta_{(C1-42)}$ peptide was performed using CID fragmentation of the precursor mass 4617 ± 2 Da. The B&Y fragment ion was calculated with fragment ion calculators.

SDS-PAGE, Silver staining, and Fluorescence Imaging

Sample Preparation and SDS-PAGE. A 0.02 μ mol aliquot of labeled A $\beta_{(C1-42)}$ or A $\beta_{(M1-42)}$ was dissolved in 20.0 μ L of DMSO first, then diluted with 13.3 μ L of 10 mM sodium phosphate buffer (pH 7.4) to give a 600 μ M peptide stock solution. 15.0 μ L of the 600 μ M peptide stock solution was serially diluted with 15.0 μ L of 10 mM sodium phosphate buffer (pH 7.4) to create 15.0

μL of peptide stock solutions with concentrations of 300 μM to 4.7 μM . The peptide stock solutions were then immediately diluted with 3.0 μL of 6X SDS-PAGE loading buffer to give 18.0 μL of peptide working solutions with concentrations from 500 μM to 3.9 μM . All 18.0 μL of each working solution was loaded on a 4% stacking polyacrylamide gel with a 16% running polyacrylamide gel. The gels were run at a constant 90 volts at room temperature for ca. 3 hours. For FAM-labeled $\text{A}\beta_{(\text{C1-42})}$ and TAMRA-labeled $\text{A}\beta_{(\text{C1-42})}$, the gels were protected from light.

Silver Staining. Silver staining method was used to visualize the SDS-PAGE gels for labeled $\text{A}\beta_{(\text{C1-42})}$ and $\text{A}\beta_{(\text{M1-42})}$. Briefly, the gel was first rocked in fixing solution (50% (v/v) methanol and 5% (v/v) acetic acid in deionized water) for 20 minutes. Next, the fixing solution was discarded and the gel was rocked in 50% (v/v) aqueous methanol for 10 minutes. Next, the 50% methanol was discarded and the gel was rocked in deionized water for 10 minutes. Next, the water was discarded and the gel was rocked in 0.02% (w/v) sodium thiosulfate in deionized water for 1 minutes. The sodium thiosulfate was discarded and the gel was rinsed twice with deionized water for 1 minute (2X). After the last rinse, the gel was submerged in chilled 0.1% (w/v) silver nitrate in deionized water and rocked at 4 °C for 20 minutes. Next, the silver nitrate solution was discarded and the gel was rinsed with deionized water for 15 seconds (2X). To develop the gel, the gel was incubated in developing solution (2% (w/v) sodium carbonate,^a 0.04% (w/v) formaldehyde until the desired intensity of staining was reached (ca. 1–3 min). When the desired intensity of staining was reached, the development was stopped by discarding the developing solution and submerging the gel in 5% aqueous acetic acid.

^a Use of high-purity ($\geq 99.5\%$) sodium carbonate is crucial for successful silver staining.

Fluorescence Imaging. Fluorescence imaging was also used to visualize the SDS-PAGE gels for TAMRA-labeled A β _(C1-42) and FAM-labeled A β _(C1-42). Before silver staining, the gels for TAMRA-labeled A β _(C1-42) and FAM-labeled A β _(C1-42) were imaged using a ChemiDoc Touch Imaging System. The gel for TAMRA-labeled A β _(C1-42) was imaged with Krypton channel (excitation at ca. 530 nm, exposure time: 0.2 seconds). The gel for FAM-labeled A β _(C1-42) was imaged with Fluorescein channel (excitation at ca. 490 nm, exposure time: 0.2 seconds).

Thioflavin T (ThT) Assay

ThT Solution Preparation. The ThT solution was freshly prepared and placed on ice before use. Briefly, a solution of ca. 40 μ M ThT was prepared in a 1x PBS buffer (pH 7.4). The concentration of ThT in the solution was determined by UV absorbance at 412 nm using an estimated extinction coefficient (ϵ) of 36000 M⁻¹cm⁻¹ and adjusted to 41.7 μ M. The solution was filtered through a 0.22 μ m nylon syringe filter. The ThT solution was stored on ice and protected from light.

Peptide Working Solution Preparation. A 0.02 μ mol aliquot of biotin-labeled A β _(C1-42) or A β _(M1-42) was dissolved in 20 μ L of DMSO first and sonicated for 30 s in a water bath, then diluted with 480 μ L of ThT solution to give a working solution with final peptide concentration of 40 μ M and ThT concentration of 40 μ M. The peptide working solution was stored on ice and protected from light.

ThT Fluorescence Assay Setup. ThT fluorescence assays were conducted in Corning® 96-well half area black/clear flat bottom polystyrene nonbinding surface (NBS) microplates (product number: 3881). A 100- μ L aliquot of the working solution was immediately transferred to each of

five wells of 96-well plate, and the plate was kept at room temperature. ThT solution was transferred to each of five wells of 96-well plate as negative control. The 96-well plate was sealed with adhesive plate sealer. The 96-well plate was immediately inserted into a Thermo Fisher Scientific Varioskan Lux microplate reader. The plate was incubated at 37 °C with or without shaking (240 rpm, low shaking force) and the ThT fluorescence was monitored (440 nm excitation, 485 nm emission, 5 nm bandwidth) over 6 hours using the bottom-read mode.

Fluorescence Suppression Assay

Peptide Working Solution Preparation. A 0.02 μmol aliquot of TAMRA-labeled $\text{A}\beta_{(\text{C1-42})}$ or FAM-labeled $\text{A}\beta_{(\text{C1-42})}$ was dissolved in 20 μL of DMSO first and sonicated for 30 s in a water bath, then diluted with 480 μL of 1X PBS (pH 7.4) to give a working solution with final peptide concentration of 40 μM . The peptide working solution was stored on ice and protected from light.

Fluorescence Suppression Assay Setup. Fluorescence suppression assays were conducted in Corning® 96-well half area black/clear flat bottom polystyrene nonbinding surface (NBS) microplates (product number: 3881). A 100- μL aliquot of the working solution was immediately transferred to each of five wells of 96-well plate, and the plate was kept at room temperature. 1X PBS buffer was transferred to each of five wells of 96-well plate as negative control. The 96-well plate was sealed with adhesive plate sealer. The 96-well plate was immediately inserted into a Thermo Fisher Scientific Varioskan Lux microplate reader incubated at 37°C with or without shaking (240 rpm, low shaking force). The fluorescence was monitored with 541 nm excitation, 567 nm emission, 5 nm bandwidth for TAMRA-labeled $\text{A}\beta_{(\text{C1-42})}$ and with 494 nm excitation, 520 nm emission, 5 nm bandwidth for FAM-labeled $\text{A}\beta_{(\text{C1-42})}$ over 6 hours using the bottom-read mode.

Transmission Electron Microscopy (TEM)

Sample Preparation. A 0.02 μmol aliquot of labeled $\text{A}\beta_{(\text{C1-42})}$ or $\text{A}\beta_{(\text{M1-42})}$ was dissolved in 20 μL of DMSO first, then diluted with 480 μL of 1X PBS buffer (pH 7.4) to give a 40 μM peptide solution. The peptide solutions were then incubated at 37 $^{\circ}\text{C}$ for 24 hours, while shaking at 225 rpm.

TEM Imaging. TEM images of $\text{A}\beta$ peptides were taken with a JEM-2100F transmission electron microscope (JEOL, Peabody, MA, USA) at 200 kV with an electron dose of ca. 15 e^-/A^2 . The sample was cooled at liquid nitrogen temperature through the cryostage. The images were recorded on a Gatan OneView CCD (Gatan, Pleasanton, CA, USA), at magnification of 30000x with a pixel size of 3.7 Angstrom at specimen space. The contrast and brightness of the images were adjusted as appropriate.

Atomic Force Microscopy (AFM)

Sample Preparation. A 0.02 μmol aliquot of labeled $\text{A}\beta_{(\text{C1-42})}$ or $\text{A}\beta_{(\text{M1-42})}$ was dissolved in 20 μL of DMSO first, then diluted with 480 μL of 1X PBS buffer (pH 7.4) to give a 40 μM peptide solution. The peptide solutions were then incubated at 37 $^{\circ}\text{C}$ for 21 hours, while shaking at 225 rpm.

AFM Imaging. A drop of the peptide sample solution (3 μL) was deposited on freshly cleaved mica mounted on glass slides. After 5 minutes, the mica was gently rinsed once or twice with 50 μL aliquots of deionized water (18 $\text{M}\Omega$) to remove salts. Excess liquid was blotted off by

Whatman filter papers and the mica was left air-dry for an additional 5 minutes, and the samples were imaged immediately after the mica is dry. All AFM images of A β peptides were taken under ambient condition with an Anton Paar Tosca 400 AFM instrument. Scanning parameters were as follows: tapping mode, setpoint at 285.6 kHz which is 5% below cantilever resonance frequency, scan rate at 1.0 Hz.

Fluorescence Microscopy

SH-SY5Y Cell Preparation, Treatment, and Imaging. SH-SY5Y cells were plated in an Ibidi μ -Slide 8 Well Chamber Slide at 20,000 cells per well. Cells were incubated in 500 μ L of a 1:1 mixture of DMEM:F12 media supplemented with 10% fetal bovine serum, 100 U/mL penicillin, and 100 μ g/mL streptomycin at 37 °C in a 5% CO₂ atmosphere and allowed to adhere to the bottom of the slide for 24 hours. Working solutions of FAM-A β and TAMRA-A β were prepared immediately prior to cell treatment by adding 10 μ L of 20 mM NaOH to one aliquot of 0.02 μ mol lyophilized FAM-A β or TAMRA-A β . The resulting solution was diluted with 190 μ L of media bringing this solution to a peptide concentration of 100 μ M. An 80 μ L aliquot of the 100 μ M stock solution was added to 720 μ L of warmed media for a final peptide concentration of 10 μ M. After 24 hours, the media was removed from the wells and replaced with 200 μ L of 1 μ g/mL Hoechst in phenol red free 1:1 DMEM:F12 media. After 30 minutes, the Hoechst-containing media was removed and replaced with 200 μ L of 10 μ M FAM-A β or TAMRA-A β . Control wells were treated with media containing no peptide. The slide was incubated in the microscope chamber for 0–48 hours and imaged for the duration using a Keyence BZ-X810 fluorescence microscope. Images were collected with a 60x oil immersion objective lens. Fluorescence micrographs of treated cells were recorded using the GFP filter cube [excitation wavelength = 470/40 nm (450–

490 nm) and emission wavelength = 525/50 nm (500–550 nm)] for FAM-A β , and the TexasRed filter cube [excitation wavelength = 560/40 nm (540–580 nm) and emission wavelength = 630/75 nm (592.5–667.5 nm)] for TAMRA-A β . The image brightness of the FAM and TAMRA channels was adjusted using BZ-X810 Analyzer software.

RAW 264.7 Cell Preparation, Treatment, and Imaging. RAW 264.7 cells were plated in an Ibidi μ -Slide 8 Well Chamber Slide at 25,000 cells per well. Cells were incubated in 500 μ L of DMEM media supplemented with 10% fetal bovine serum at 37 °C in a 5% CO₂ atmosphere and allowed to adhere to the bottom of the slide for 24 hours. Working solutions of FAM-A β and TAMRA-A β were prepared immediately prior to cell treatment by adding 10 μ L of 20 mM NaOH to one aliquot of 0.02 μ mol lyophilized FAM-A β or TAMRA-A β . This solution was diluted with 190 μ L of media for a peptide concentration of 100 μ M. An 80 μ L aliquot of the 100 μ M stock solution was added to 720 μ L of warmed media for a final peptide concentration of 10 μ M. After 24 hours, the media was removed from the wells and replaced with 200 μ L of 1 μ g/mL Hoechst in phenol red free 1:1 DMEM:F12 media. After 30 minutes, the Hoechst-containing media was removed and replaced with 200 μ L of 10 μ M FAM-A β or TAMRA-A β . Control wells were treated with media containing no peptide. The slide was incubated for 4 hours and imaged using a Keyence BZ-X810 fluorescence microscope. Images were collected with a 60x oil immersion objective lens. Fluorescence micrographs of treated cells were recorded using the GFP filter cube [excitation wavelength = 470/40 nm (450–490 nm) and emission wavelength = 525/50 nm (500–550 nm)] for FAM-A β , and the TexasRed filter cube [excitation wavelength = 560/40 nm (540–580 nm) and emission wavelength = 630/75 nm (592.5–667.5 nm)] for TAMRA-A β . The image brightness of the FAM and TAMRA channels was adjusted using BZ-X800 Analyzer software.

*Bacteria Culturing, Treatment, and Imaging.*⁵ *B. subtilis* (ATCC 6051) and *E. coli* (ATCC 10798) were allowed to grow overnight (ca. 16 h) in Mueller-Hinton broth in a shaking incubator at 225 rpm and 37 °C. The following morning, the cultures were diluted 1:100 in the appropriate broth and were allowed to grow exponentially in a shaking incubator at 225 rpm and 37 °C. Once an OD₆₀₀ of ca. 0.3 was achieved, 500 µL of bacteria was transferred to a sterile Eppendorf tube and the bacteria were centrifuged at 4000 rpm (1300 x G) for 5 min.

1 mg/mL DMSO stock solutions of FAM- and TAMRA-labeled Aβ were prepared by dissolving a 0.02 µmol aliquot of the lyophilized peptide (ca. 0.1 mg) in 100 µL of sterile DMSO in an autoclaved Eppendorf tube. Solutions of labeled Aβ were protected from excessive exposure to light in the imaging experiments by use of an unlit biosafety cabinet and minimizing exposure to room lights.

A 2% stock solution of agarose was prepared by adding 1.0 g of agarose into 50 mL of sodium phosphate buffer, autoclaving, and allowing the solution to cool until it completely solidified. While the bacteria were growing in the shaking incubator, fresh 2% agarose beds were prepared to immobilize bacteria for fluorescence microscopy studies as follow: On a laboratory bench equipped with an alcohol burner (to help maintain sterility), microscope slides were gently warmed on a hot plate. While the slides were gently warming, the solidified 2% agarose solution was heated in a microwave oven until it became a homogenous liquid. Once the microscope slides were warm to the touch, a 75-µL aliquot of the molten 2% agarose solution was applied to each microscope slide, and a No. 1.5 coverslip was immediately applied gently to the drop of agarose. The assembly was allowed to set for at least 45 minutes before use.

While the bacteria were being centrifuged, 25 µg/mL solutions of FAM- and TAMRA-labeled Aβ were freshly prepared and then used immediately to stain the bacteria. The 25 µg/mL

solutions were prepared by diluting 15 μL of each 1 mg/mL DMSO stock solution with 585 μL of sterile PBS. The diluted solutions were subsequently vortexed for 30 seconds and then used immediately to stain the bacteria.

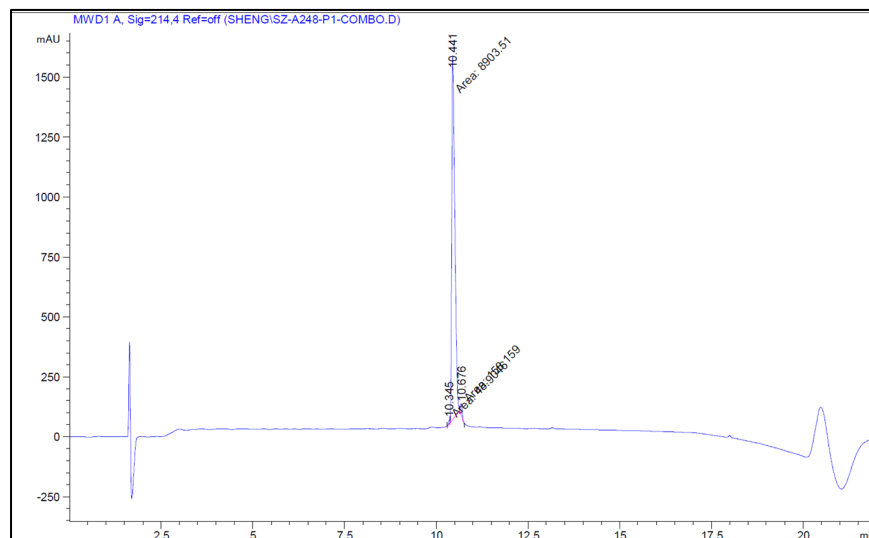
After centrifuging the bacteria (see above), the supernatant was removed, the pellet was resuspended in 500 μL of 25 $\mu\text{g}/\text{mL}$ of the probe solution, and the bacteria were incubated in a shaking incubator at 225 rpm, 37 °C for 2 h. The bacteria were centrifuged at 4000 rpm (1300 x G) for 5 min, and the supernatant was removed. The pellet was resuspended in 500 μL of sterile PBS, the suspension was centrifuged at 4000 rpm (1300 x G) for 5 min, and the supernatant was removed. This washing process was repeated two additional times. After the last wash, the cells were resuspended in 200–500 μL of sterile PBS.^a On a sterile bench, the coverslip of each agarose bed was removed, and a 5- μL aliquot of the stained bacteria was applied to the coverslip. The coverslip was then sandwiched on top of the agarose bed.

The stained bacteria were immediately imaged on a Zeiss LSM 780 confocal fluorescence microscope. Images were collected with a 63x oil immersion objective lens, with additional optical zoom used as needed to provide detailed images. Fluorescence micrographs of bacteria treated with FAM-labeled A β were recorded with excitation at 488 nm and emission between 490–544 nm. Fluorescence micrographs of bacteria treated with TAMRA-labeled A β were recorded with excitation at 561 nm and emission between 568–639 nm. The image brightness of the FAM and TAMRA channels were adjusted linearly using Volocity 6.3 (Quorum Technologies), and a medium filter in the Volocity software was used to reduce noise in all channels.

^a The volume of phosphate buffer was selected based on the size of the pellet remaining after the washing steps.

Characterization Data and Additional Figures

Analytical HPLC Trace, MALDI Mass Spectrum, and MS/MS Spectrum of A β _(C1-42)



Signal 1: MWD1 A, Sig=214,4 Ref=off

Peak #	RetTime [min]	Type	Width [min]	Area [mAU*s]	Height [mAU]	Area %
1	10.345	MM	0.0500	48.90459	16.30959	0.5368
2	10.441	MM	0.0972	8903.51074	1526.55994	97.7272
3	10.676	MM	0.0565	158.15851	46.64415	1.7360
Totals :				9110.57384	1589.51367	

Figure 2.S7. Representative analytical HPLC trace of A β _(C1-42). HPLC was performed on a C18 column at 60 °C with elution with 5–67% acetonitrile over 15 minutes, and absorbance was monitored at 214 nm. Purity: = 97.7%.

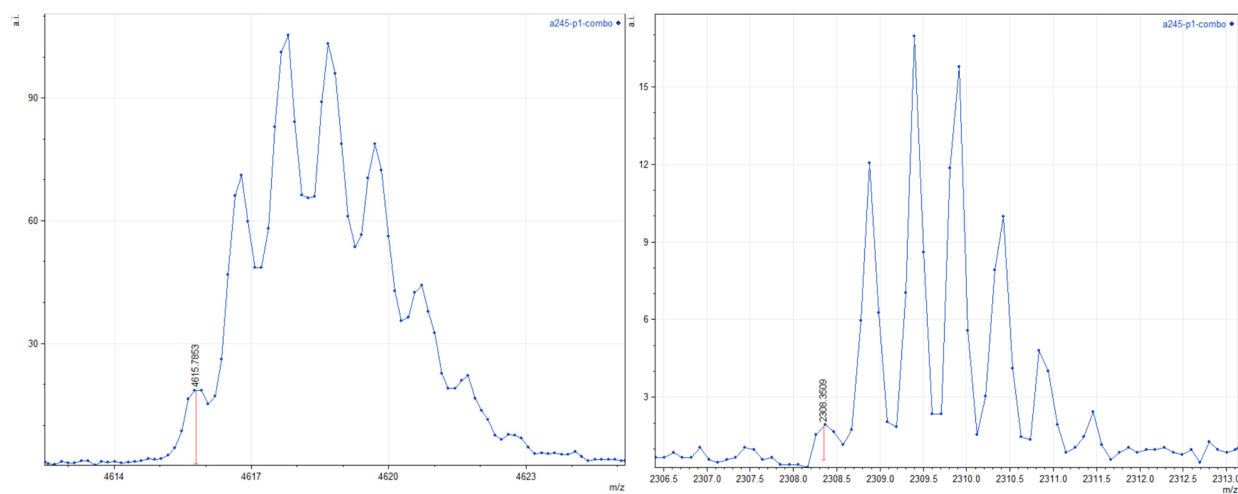
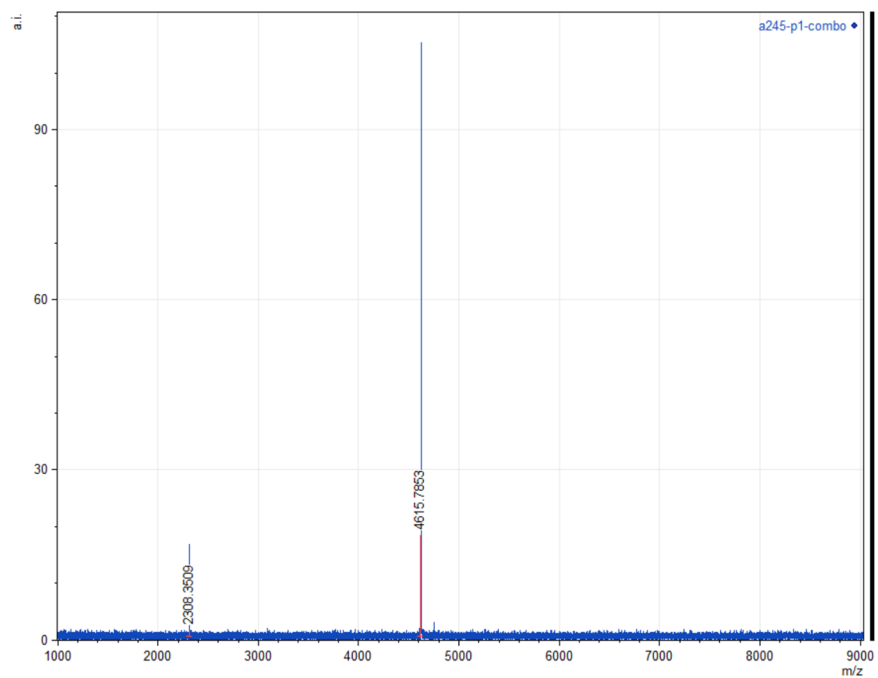
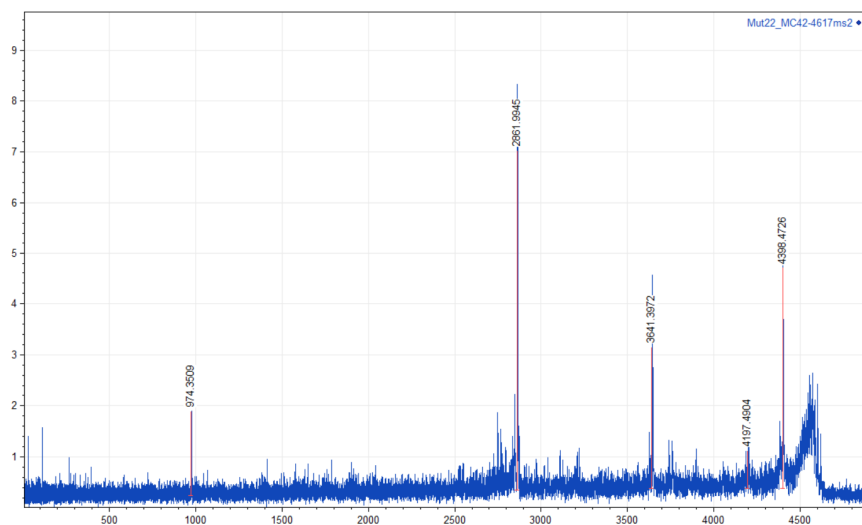


Figure 2.S8. Representative MALDI mass spectrum of $A\beta_{(C1-42)}$. Positive reflector mode; Matrix: 2,5-dihydroxybenzoic acid. Exact mass calculated for M^+ : 4614.3; Exact mass calculated for $[M+H]^+$: 4615.3; Exact mass calculated for $[M+2H]^{2+}$: 2308.1. Observed $[M+H]^+$: 4615.8; Observed $[M+2H]^{2+}$: 2308.4.



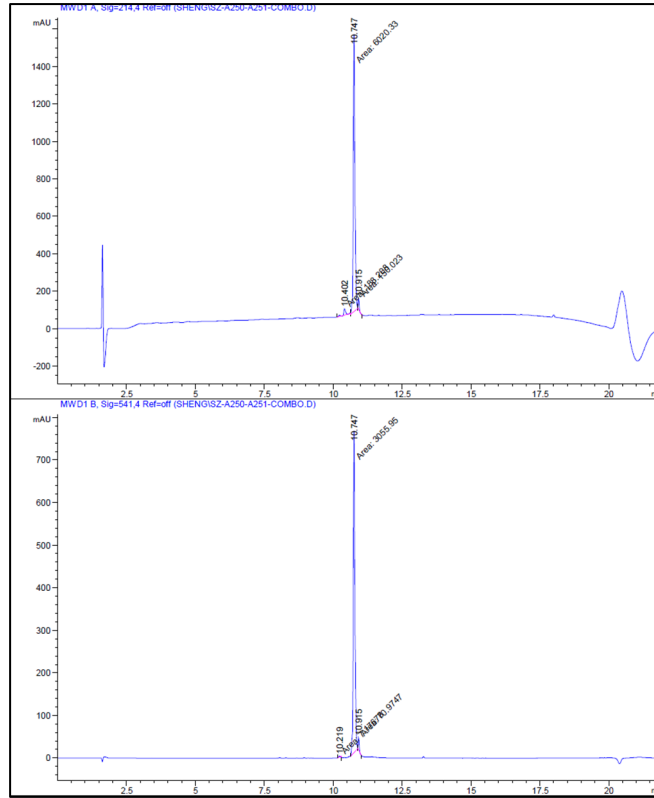
Sequence: CDAEFRHDSGYEVHHQKLVFFAEDVGSNKGAIIGLMVGGVVIA, pl: 5.31109

Fragment Ion Table, monoisotopic masses

Seq	#	B	Y	# (+1)
C	1	104.01651	4615.28610	43
D	2	219.04345	4512.27691	42
A	3	290.08056	4397.24937	41
E	4	419.12316	4326.21286	40
F	5	566.19157	4197.17027	39
R	6	722.29268	4050.10185	38
H	7	859.35159	3894.00074	37
D	8	974.3509	3756.94183	36
S	9	1061.41056	3641.3872	35
G	10	1118.43203	3554.88286	34
Y	11	1281.49535	3497.86139	33
E	12	1410.53795	3334.79807	32
V	13	1509.60636	3205.75547	31
H	14	1646.66527	3106.68706	30
H	15	1783.72418	2969.62815	29
Q	16	1911.78276	2832.56924	28
K	17	2039.87772	2704.51066	27
L	18	2152.96179	2576.41570	26
V	19	2252.03020	2463.33163	25
F	20	2399.09861	2364.26322	24
F	21	2546.16703	2217.19481	23
A	22	2617.20414	2070.12639	22
E	23	2746.24673	1999.08928	21
D	24	2861.27368	1870.04669	20
V	25	2960.34209	1755.01974	19
G	26	3017.36355	1655.95133	18
S	27	3104.39558	1598.92987	17
N	28	3218.43851	1511.89784	16
K	29	3346.53347	1397.85491	15
G	30	3403.55494	1269.75995	14
A	31	3474.59205	1212.73848	13
I	32	3587.67611	1141.70137	12
I	33	3700.76018	1028.61731	11
G	34	3757.78164	915.53324	10
L	35	3870.86570	858.51178	9
M	36	4001.90619	745.42772	8
V	37	4100.97460	614.38723	7
G	38	4157.99607	515.31882	6
G	39	4215.01753	458.29735	5
V	40	4314.08594	401.27589	4
V	41	4413.15436	302.20748	3
I	42	4526.23842	203.13906	2
A	43	4597.27554	90.05500	1

Figure 2.S9. Representative MS/MS spectrum of $\alpha\beta_{(C1-42)}$. MS/MS analysis was performed using CID fragmentation of the precursor mass 4617 ± 2 Da. The B&Y fragment ion was calculated with fragment ion calculators. The peptide sequence was determined to be CDAEFRHDSGYEVHHQKLVFFAEDVGSNKGAIIGLMVGGVVIA.

Analytical HPLC Trace and MALDI Mass Spectrum of 5-TAMRA-A β (C1-42)



```
Signal 1: MWD1 A, Sig=214,4 Ref=off
```

Peak #	RetTime [min]	Type	Width [min]	Area [mAU*s]	Height [mAU]	Area %
1	10.402	MM	0.0923	188.20799	33.99847	2.9599
2	10.747	MM	0.0674	6020.33154	1488.95044	94.6807
3	10.915	MM	0.0440	150.02261	56.76593	2.3594
Totals :				6358.56215	1579.71484	


```
Signal 2: MWD1 B, Sig=541,4 Ref=off
```

Peak #	RetTime [min]	Type	Width [min]	Area [mAU*s]	Height [mAU]	Area %
1	10.219	MM	0.0480	7.17678	2.49154	0.2290
2	10.747	MM	0.0670	3055.95190	759.94574	97.5064
3	10.915	MM	0.0416	70.97472	28.44521	2.2646
Totals :				3134.10341	790.88250	

Figure 2.S10. Representative analytical HPLC trace of 5-TAMRA-A β (C1-42). HPLC was performed on a C18 column at 60 °C with elution with 5–67% acetonitrile over 15 minutes, and absorbance was monitored at 214 nm (top) and 541 nm (bottom). Purity: = 94.7%.

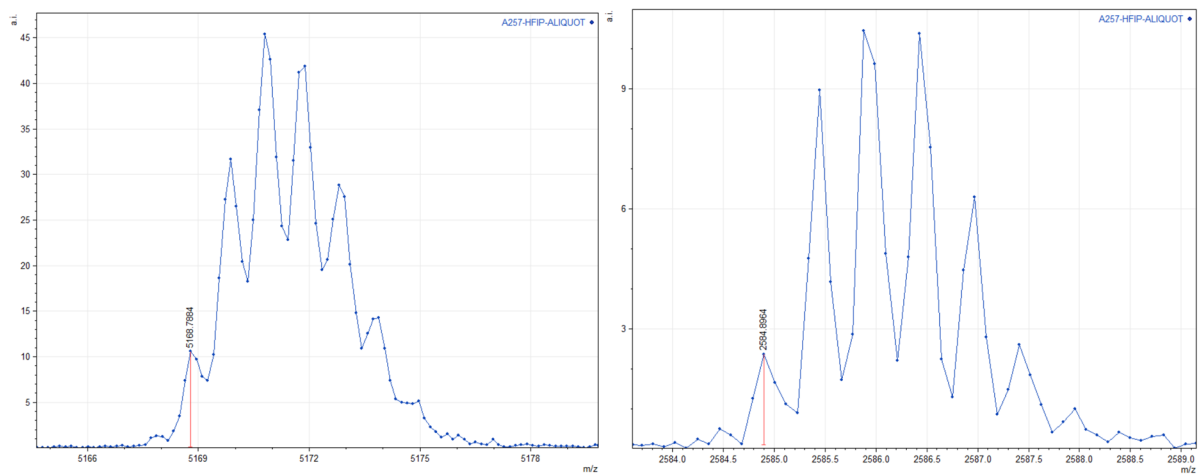
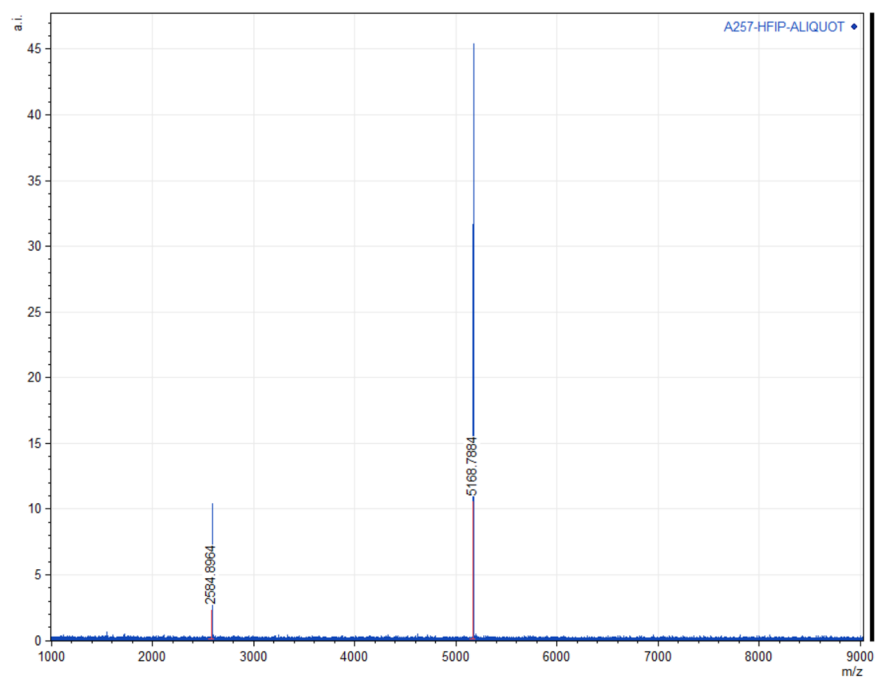
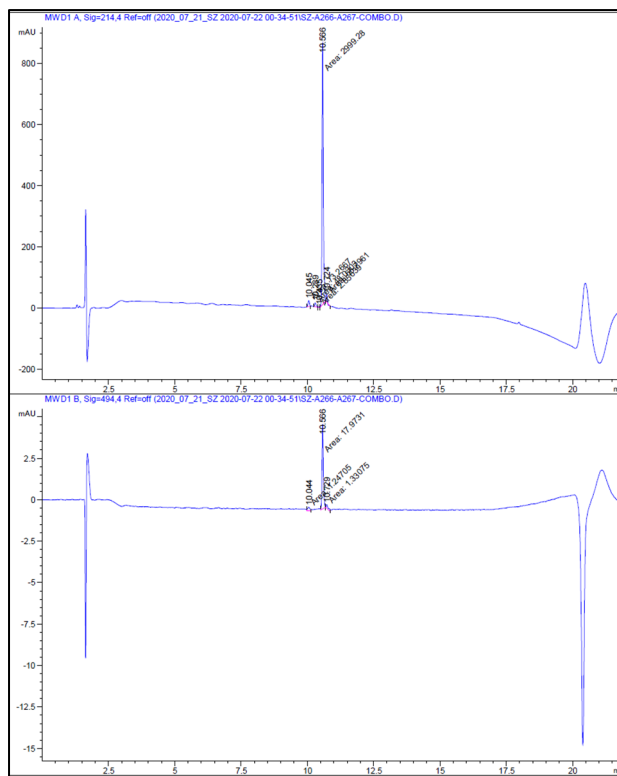


Figure 2.S11. Representative MALDI mass spectrum of 5-TAMRA-A β (C1-42). Positive reflector mode; Matrix: 2,5-dihydroxybenzoic acid. Exact mass calculated for M^+ : 5166.5; Exact mass calculated for $[M+H]^+$: 5167.5; Exact mass calculated for $[M+2H]^{2+}$: 2584.2. Observed $[M+H]^+$: 5168.8; Observed $[M+2H]^{2+}$: 2584.9.

Analytical HPLC Trace and MALDI Mass Spectrum of 6-FAM-A β (C1-42)



Signal 1: MWD1 A, Sig=214,4 Ref=off						
Peak #	RetTime [min]	Type	Width [min]	Area [mAU*s]	Height [mAU]	Area %
1	10.045	MM	0.0628	73.26669	19.44060	2.2973
2	10.289	MM	0.0602	48.03032	13.30617	1.5060
3	10.435	MM	0.0371	2.85639	1.28238	0.0896
4	10.566	MM	0.0577	2999.27979	866.74207	94.0440
5	10.724	MM	0.0422	65.79608	25.96672	2.0631
Totals :				3189.22927	926.73793	
Signal 2: MWD1 B, Sig=494,4 Ref=off						
Peak #	RetTime [min]	Type	Width [min]	Area [mAU*s]	Height [mAU]	Area %
1	10.044	MM	0.1043	1.24705	1.99304e-1	6.0681
2	10.566	MM	0.0582	17.97314	5.15007	87.4565
3	10.729	MM	0.1004	1.33075	2.20823e-1	6.4754
Totals :				20.55094	5.57020	

Figure 2.S12. Representative analytical HPLC trace of 6-FAM-A β (C1-42). HPLC was performed on a C18 column at 60 °C with elution with 5–67% acetonitrile over 15 minutes, and absorbance was monitored at 214 nm (top) and 494 nm (bottom). Purity: = 94.0%.

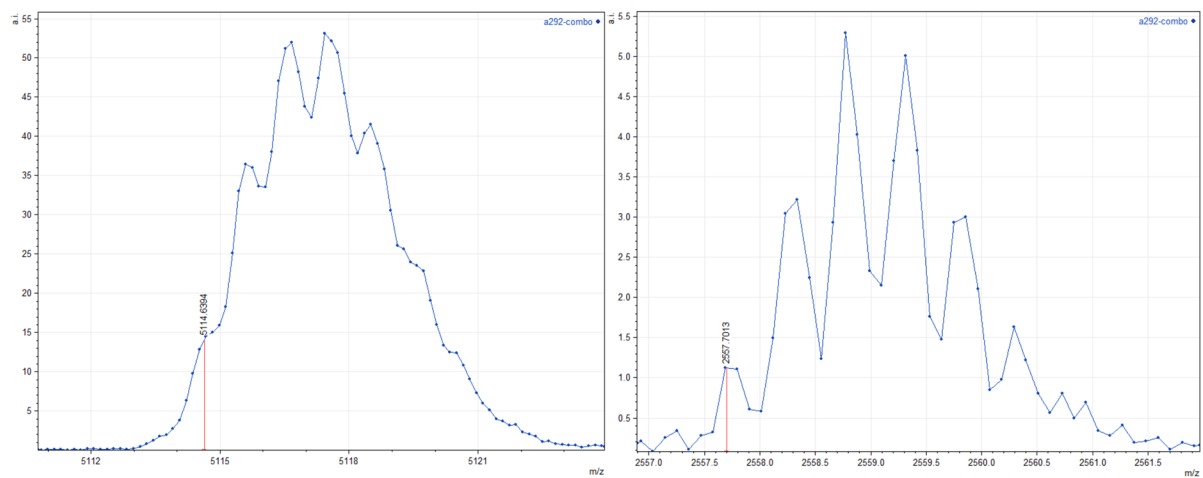
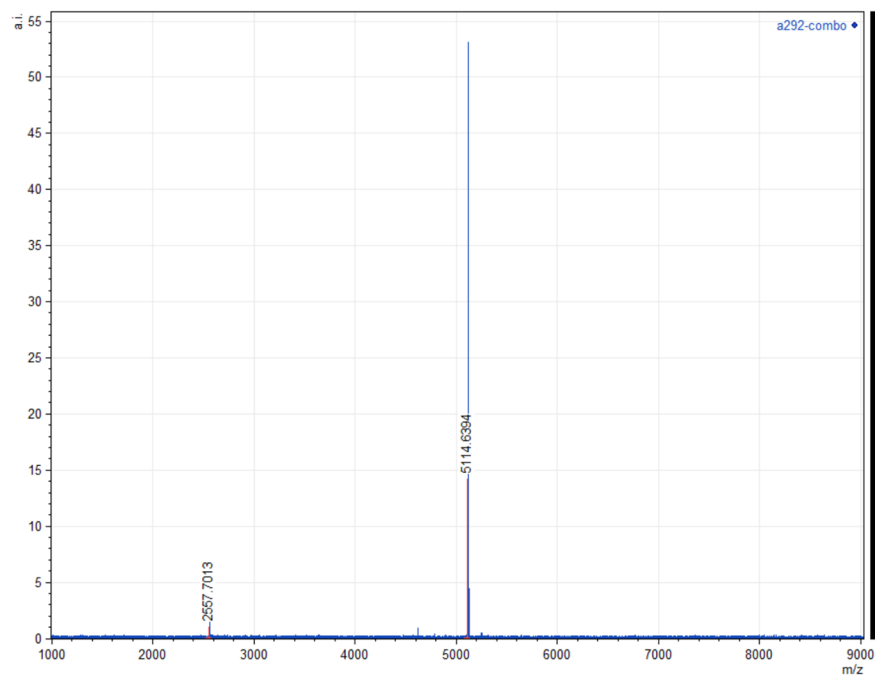
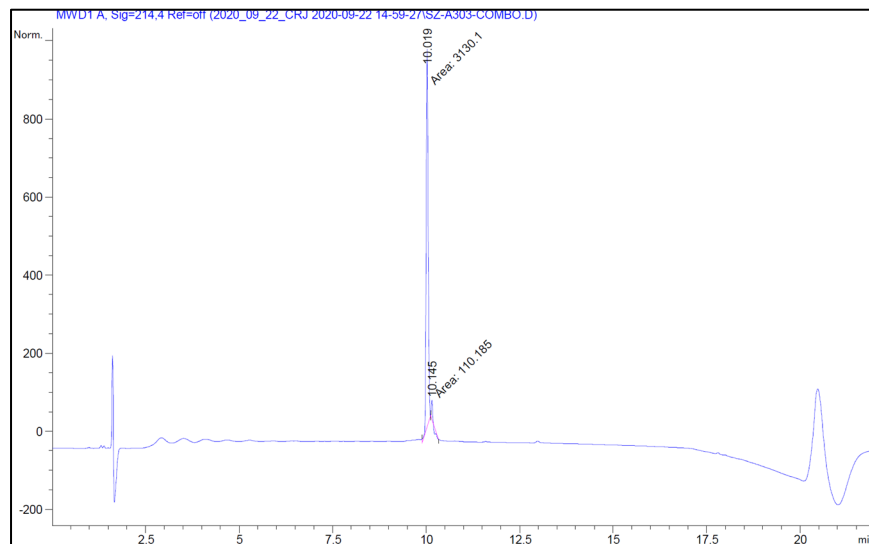


Figure 2.S13. Representative MALDI mass spectrum of 6-FAM-Aβ_(C1-42). Positive reflector mode; Matrix: 2,5-dihydroxybenzoic acid. Exact mass calculated for M⁺: 5112.4; Exact mass calculated for [M+H]⁺: 5113.4; Exact mass calculated for [M+2H]²⁺: 2557.2. Observed [M+H]⁺: 5114.6; Observed [M+2H]²⁺: 2557.7.

Analytical HPLC Trace and MALDI Mass Spectrum of PEG₂-Biotin-A β _(C1-42)



Signal 1: MWD1 A, Sig=214,4 Ref=off

Peak #	RetTime [min]	Type	Width [min]	Area [mAU*s]	Height [mAU]	Area %
1	10.019	MM	0.0595	3130.10132	876.57098	96.5995
2	10.145	MM	0.0403	110.18530	45.62219	3.4005
Totals :				3240.28662	922.19318	

Figure 2.S14. Representative analytical HPLC trace of PEG₂-biotin-A β _(C1-42). HPLC was performed on a C18 column at 60 °C with elution with 5–67% acetonitrile over 15 minutes, and absorbance was monitored at 214 nm. Purity: = 96.6%.

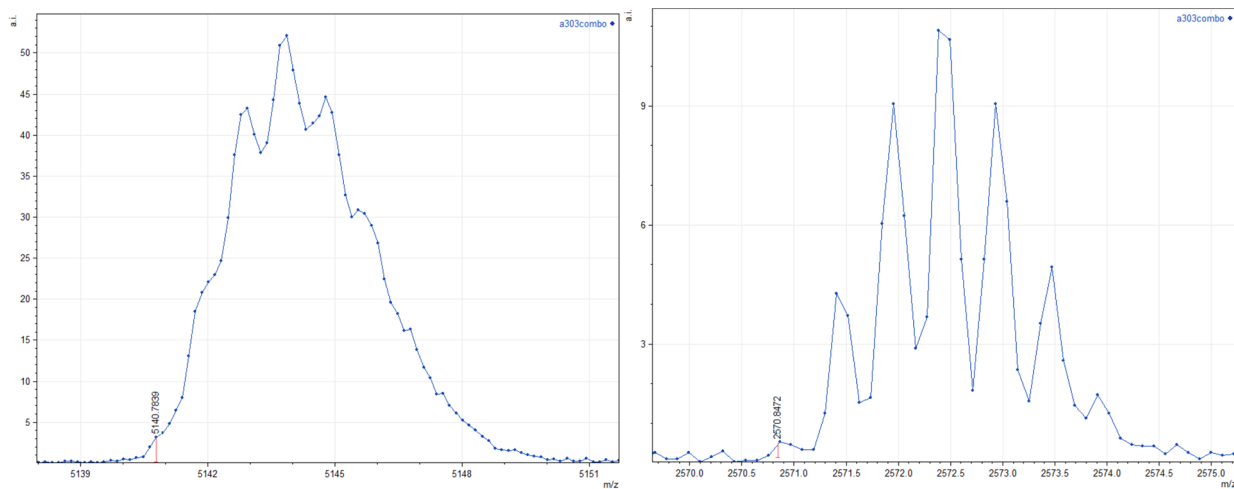
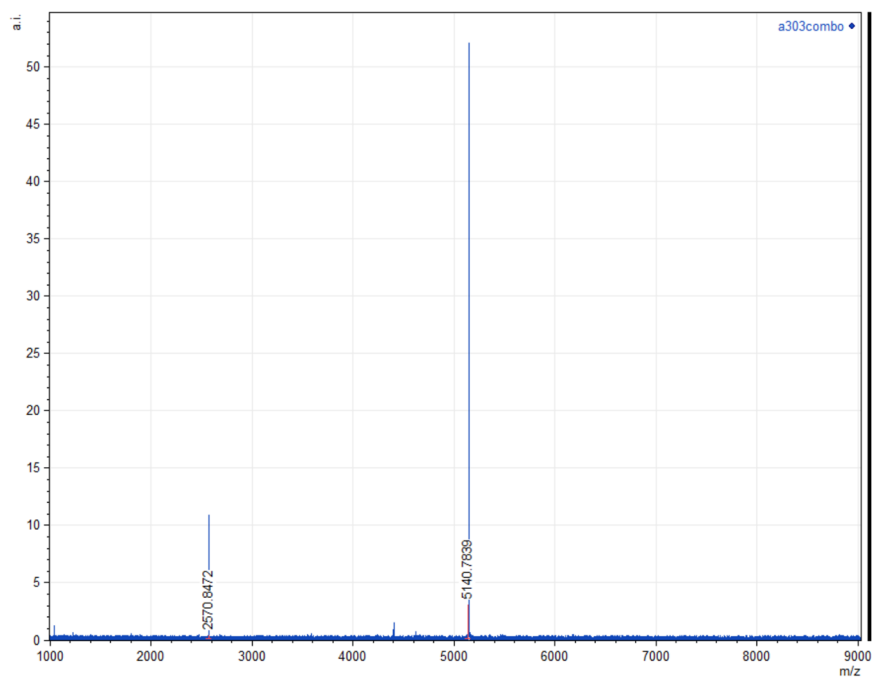


Figure 2.S15. Representative MALDI mass spectrum of PEG₂-biotin-A β (C1-42). Positive reflector mode; Matrix: 2,5-dihydroxybenzoic acid. Exact mass calculated for M⁺: 5139.5; Exact mass calculated for [M+H]⁺: 5140.5; Exact mass calculated for [M+2H]²⁺: 2570.8. Observed [M+H]⁺: 5140.8; Observed [M+2H]²⁺: 2570.8.

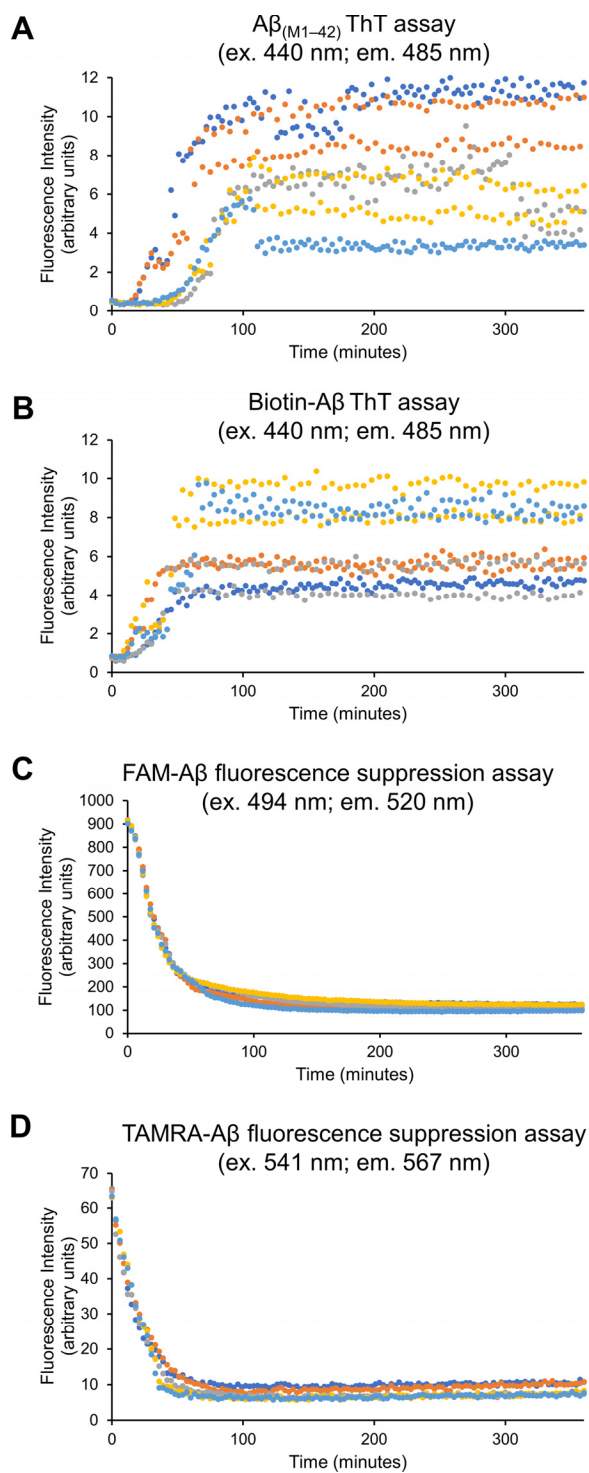


Figure 2.S16. ThT fluorescence assays and fluorescence suppression assays of labeled $A\beta_{(C1-42)}$ and $A\beta_{(M1-42)}$. (A and B) ThT fluorescence assays of $A\beta_{(M1-42)}$ and biotin-labeled $A\beta$ (40 μ M peptide, 40 μ M ThT, 37 $^{\circ}$ C, 240 rpm shaking, 6 hours). (C and D) Fluorescence suppression assays of FAM-labeled $A\beta$ and TAMRA-labeled $A\beta$ (40 μ M peptide, 37 $^{\circ}$ C, 240 rpm shaking, 6 hours). These assays were performed in five replicates (light blue, dark blue, orange, yellow, and gray).

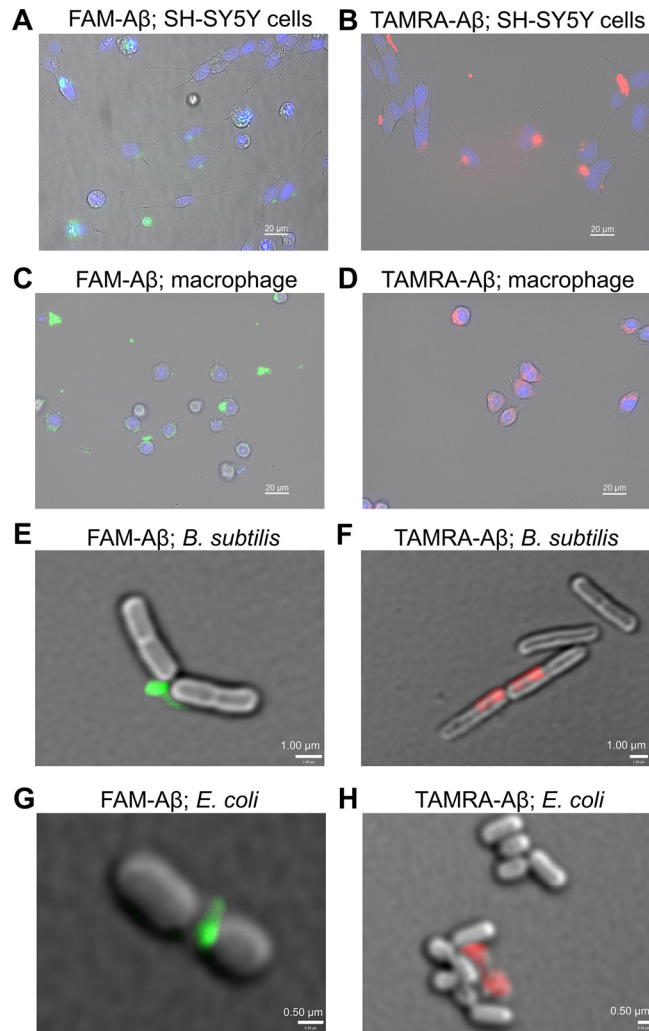


Figure 2.S17. Fluorescence micrographs of labeled A β with mammalian cells (low magnification views). (A and B) SH-SY5Y neuroblastoma cells treated with FAM- and TAMRA-labeled A β (10 μ M peptides, 37 $^{\circ}$ C, 48 and 3 hours, respectively). Nuclei are shown in blue through DAPI staining. (C and D) RAW 264.7 macrophage cells treated with FAM- and TAMRA-labeled A β (10 μ M peptides, 37 $^{\circ}$ C, 4 hours).

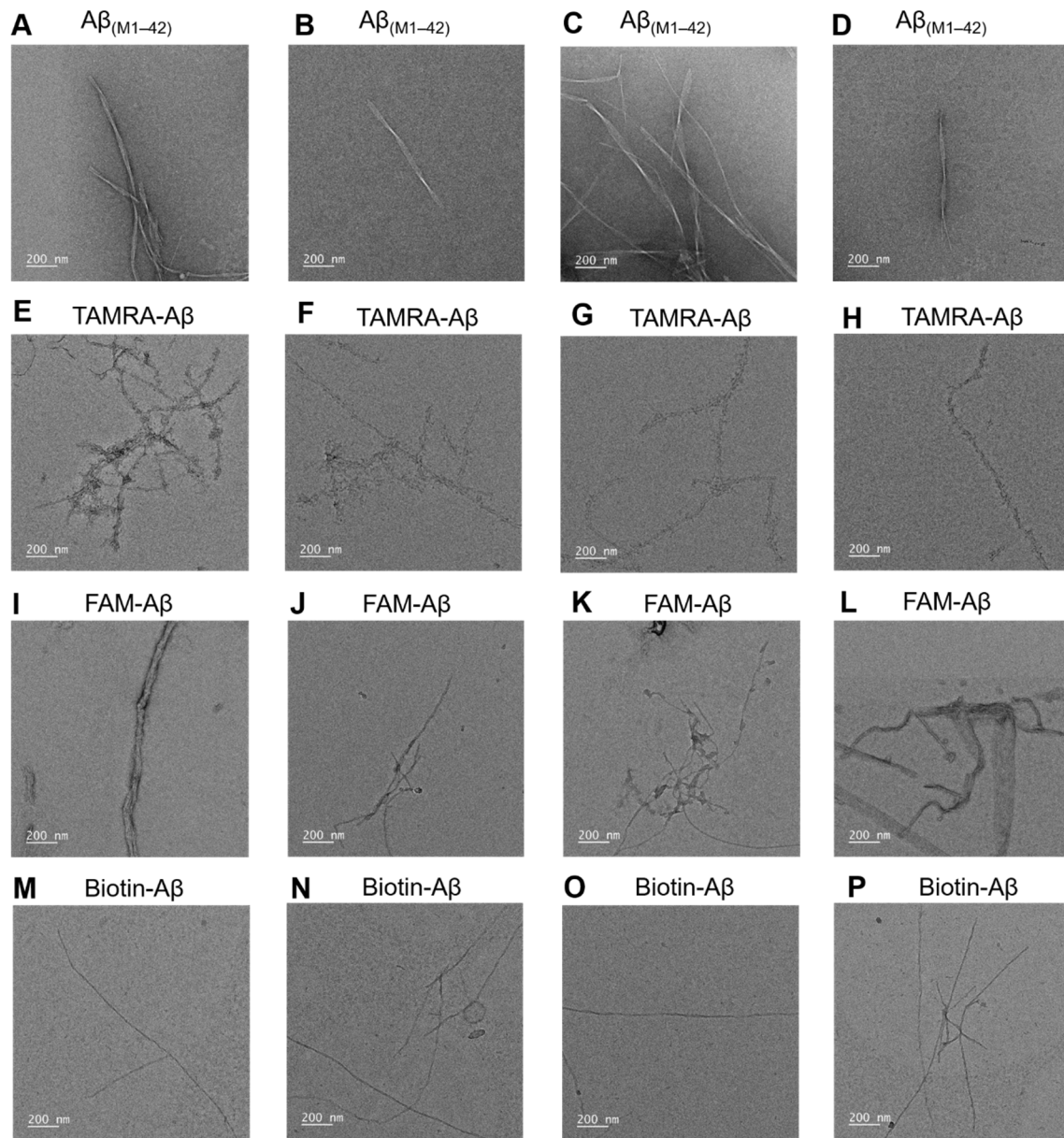


Figure 2.S18. Transmission electron micrographs of the fibrils formed by A β peptides: (A–D) A β _(M1–42); (E–H) TAMRA-labeled A β ; (I–L) FAM-labeled A β ; (M–P) Biotin-labeled A β . Fibrils were formed by incubating 40 μ M of each peptide in PBS buffer (pH 7.4, 37 $^{\circ}$ C, 1 day, 225 rpm shaking).

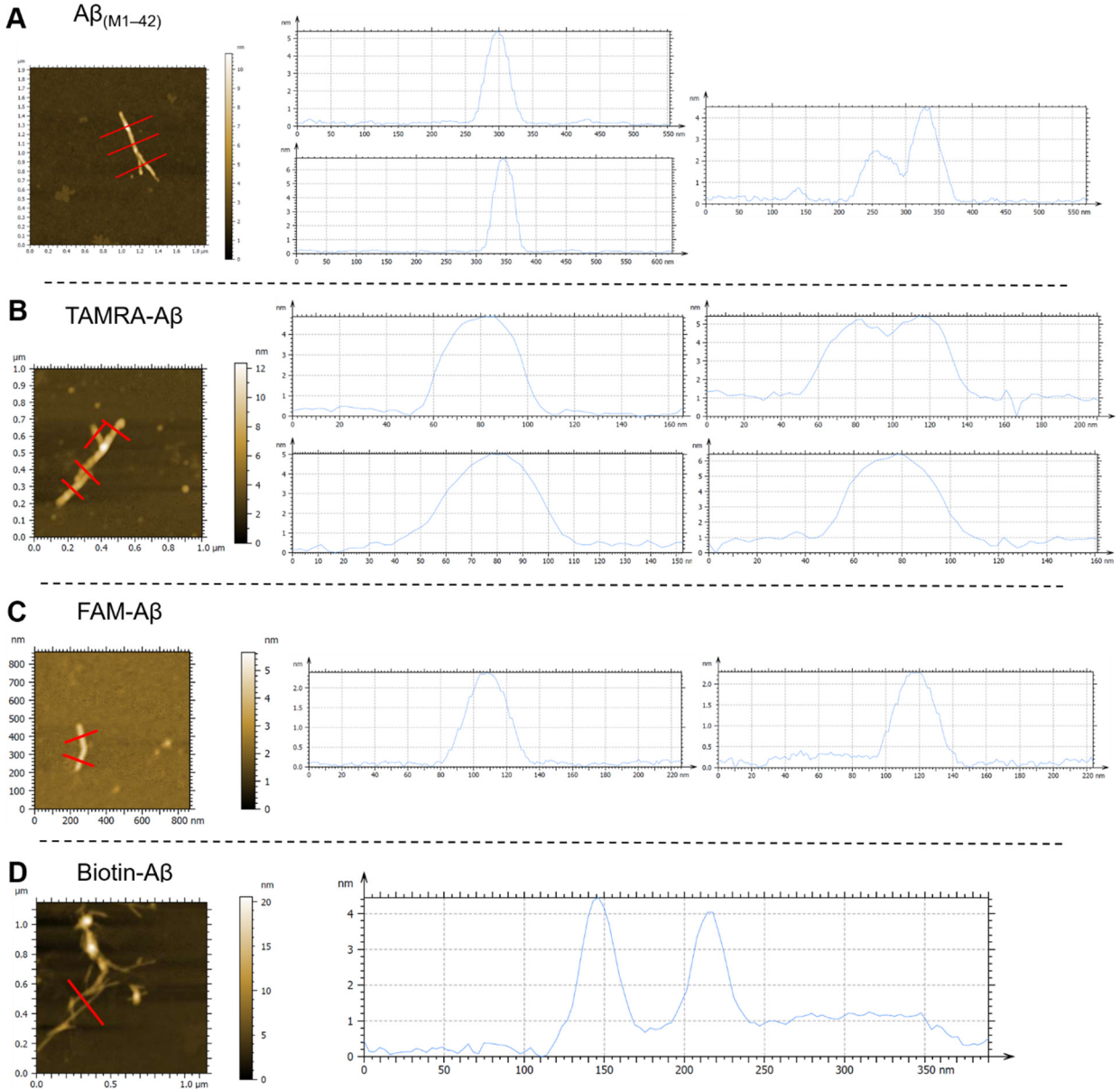


Figure 2.S19. Atomic force micrographs of the fibrils formed by A β peptides: (A) A $\beta_{(M1-42)}$ AFM image and fibril height measurement data, fibril height ca. 4.5 nm; (B) TAMRA-labeled A β AFM image and fibril height measurement data, fibril height ca. 5.2 nm; (C) FAM-labeled A β AFM image and fibril height measurement data, fibril height ca. 2.3 nm; (D) Biotin-labeled A β AFM image and fibril height measurement data, fibril height ca. 4.1 nm. Fibrils were formed by incubating 40 μ M of each peptide in PBS buffer (pH 7.4, 37 $^{\circ}$ C, 1 day, 225 rpm shaking). The red bars indicate the locations where the heights of the fibrils were measured.

References and Notes

1. The molecular cloning, protein expression, protein purification, and SDS-PAGE procedures in this section are adapted from and in some cases taken verbatim from Yoo, S.; Zhang, S.; Kreutzer, A. G.; Nowick, J. S. An Efficient Method for the Expression and Purification of A β (M1-42). *Biochemistry* **2018**, *57*, 3861–3866.
2. Addgene, pET-Sac-Abeta(MC1-42), Plasmid #127151. <https://www.addgene.org/127151/>.
3. Addgene, pET-Sac-Abeta(M1-42), Plasmid #71875. <https://www.addgene.org/71875/>.
4. Walsh, D. M.; Thulin, E.; Minogue, A. M.; Gustavsson, N.; Pang, E.; Teplow, D. B.; Linse, S., A facile method for expression and purification of the Alzheimer's disease-associated amyloid beta-peptide. *FEBS J.* **2009**, *276*, 1266-81.
5. Bacteria imaging protocol was adapted from: Morris, M. A.; Malek, M.; Hashemian, M. H.; Nguyen, B. T.; Manuse, S.; Lewis, K.; Nowick, J. S. A Fluorescent Teixobactin Analogue. *ACS Chem. Biol.* **2020**, *15*, 1222–1231.

Chapter 3

Preparation and Studies of a Disulfide-Stapled A β that Forms Dimers but Does Not Form Fibrils

Introduction

Although A β fibrils are the most commonly found species in Alzheimer's disease (AD) brains, A β oligomers are the key contributors to the neurodegeneration observed in AD.¹⁻⁶ Small oligomers of A β have been shown to be far more neurotoxic than the large oligomers.⁷⁻⁹ The A β dimer has been proposed to be the basic building block of many larger A β oligomers and is thought to be one of the most neurotoxic and pathologically relevant species in AD.¹⁰⁻¹⁸ A β dimers are challenging to characterize and study, because A β oligomers are heterogenous and metastable. The oligomers vary in size and can rapidly aggregate into more stable fibrils.¹⁹⁻²⁷ A plentiful source of homogenous and stable A β dimer would be valuable to the research in the pathogenesis of A β dimers in AD.

Biogenic A β oligomers isolated from AD brains are arguably most biologically relevant, but the dimers and other oligomers are only present in minute concentrations and are thus difficult to study.^{7,12-15,28} For this reason, researchers have developed artificial covalent A β dimers by crosslinking A β monomers through several types of intermolecular crosslinkers, including isopeptide bond,²⁸⁻³⁰ dityrosine bond,^{28,29,31-33} disulfide bond,^{16,18,32,34-36} homocysteine-disulfide

bond,³⁶ alkyl linker,³⁶⁻³⁹ 4-hydroxynonenal induced crosslinking,⁴⁰ and photoinduced crosslinking of unmodified proteins (PICUP).^{23,24,41-43} These covalent A β dimers generally aggregate further with time into a heterogenous mixture of larger oligomers, globulomers, protofibrils, or fibrils (Figure 3.1).

Non-covalent A β dimers may be more biologically relevant than covalent dimers because they mimic native A β dimers that are formed through non-covalent interactions.^{5,31,44-46} Previous approaches to generate non-covalent oligomers have relied upon stabilizing intramolecular linkages, including intramolecular disulfide bonds and oximes, to facilitate non-covalent A β oligomer formation.⁴⁷⁻⁵³ The intramolecular linkages were designed to enforce a β -hairpin conformation, and thus promote A β oligomer formation and arrest A β in the oligomeric state. These modified A β peptides bearing intramolecular linkages formed various sizes of oligomers upon incubation in solution (Figure 3.1).

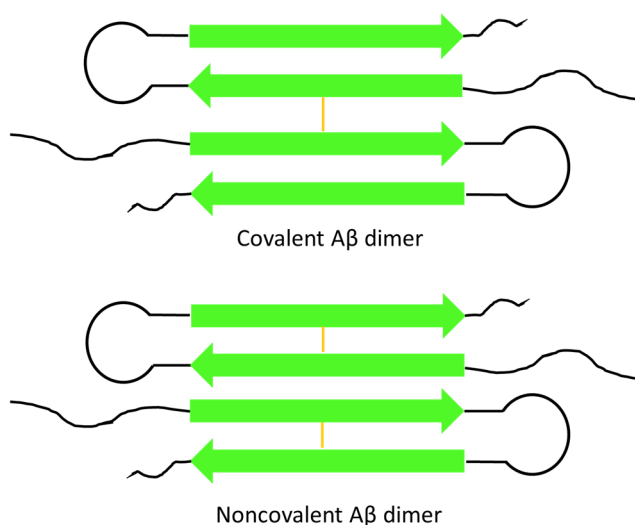


Figure 3.1. Cartoons of covalent A β dimer generated by intermolecular disulfide bridges and non-covalent A β dimer generated by intramolecular disulfide bridges.

Although the A β oligomers formed by A β peptides bearing intermolecular or intramolecular linkages are often heterogenous, those artificial oligomers have proved useful in amyloid and Alzheimer's disease research. These artificial oligomers have been used as chemical models to study A β peptide's neurotoxicity,^{16,35–37,47,48,51} aggregation kinetics and pathways,^{23,24,28–32,34,38,40,48,52} effects on behavioral deficits and neuroplasticity,¹⁸ antibody-binding activities,^{39,53} and structural information.⁴⁹ Although these efforts have provided useful chemical model systems, most of the oligomers produced are heterogenous. There are, to our knowledge, none that form stable homogeneous dimers.

Our laboratory has recently developed conditions that permit the efficient expression and purification of A β ₄₂ peptides and mutants thereof. In the current study we set out to explore the effect of introduction of disulfide linkages into A β ₄₂ peptides, by preparing and studying a variety of mutant A β ₄₂ peptides containing two cysteine residues. Here, we report the discovery of A β _{C18C33}, a mutant A β ₄₂ peptide containing a disulfide bond that forms stable homogeneous dimers.

Results

Design of Disulfide-Stapled A β Peptides. In previous studies, our laboratory has observed that homologous β -hairpin peptide containing different residue pairings form different types of oligomeric assemblies.⁵⁴ Inspired by earlier studies of A β peptides containing disulfide linkages,^{47–49,53} we expressed and purified five mutant A β ₄₂ peptides containing pairs of cysteine residues at positions 21 and 30, 18 and 33, 21 and 32, 24 and 29, and 21 and 31, respectively (Figure 3.2). The first of which corresponds to a peptide reported to form a mixtures of dimers and trimers in

SDS-PAGE and hexamers in the solid state.^{48,49} In each peptide, we replaced one residue from the hydrophobic central region of A β and one from the hydrophobic C-terminal region, with the goal of inducing β -hairpin formation with different residue pairings.

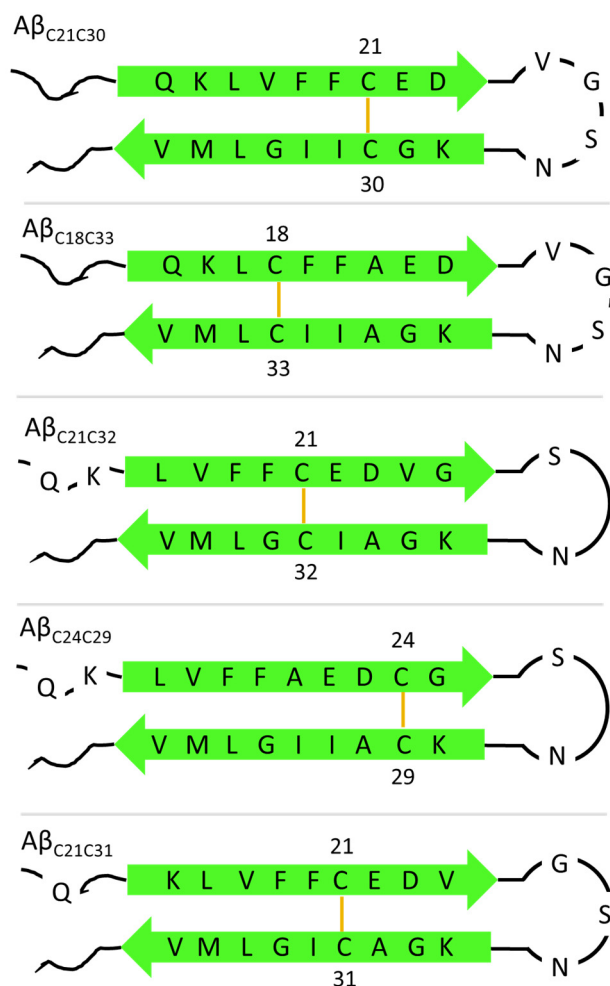


Figure 3.2. Cartoons of mutant A β peptides that are constrained in β -hairpin conformation by intermolecular disulfide bridges.

Preparation of Disulfide-Stapled A β Peptides. We prepared the recombinant plasmid encoding mutant A β peptides bearing double cysteine mutations through molecular cloning (Figure 3.S1 and 3.S2). We then transformed the recombinant plasmid into *E. coli* and express mutant A β peptides through isopropyl β -D-1-thiogalactopyranoside (IPTG) induction. After

expression, we lysed the cells and solubilize the inclusion bodies using urea to obtain cell lysate containing mutant A β peptides. We then added dimethyl sulfoxide (DMSO) to the cell lysate to oxidize the cysteines and form the intramolecular disulfide bridge in mutant A β peptides. Finally, we purified the disulfide-stapled A β peptides by preparative reverse-phase HPLC using a C8 column at 80 °C with water and acetonitrile containing 0.1% trifluoroacetic acid (TFA). Each of the peptides contains an N-terminal methionine residue, which is associated with the start codon for the expression. For comparison, we also prepared A $\beta_{(M1-42)}$, which is a homologue of full-length A β_{42} with properties similar to native A β_{42} .^{55,56}

SDS-PAGE Studies: Discovery of the A β_{C18C33} Dimer. To evaluate the propensities of these disulfide-stapled A β peptides to form oligomers, we performed sodium dodecyl sulfate–polyacrylamide gel electrophoresis (SDS-PAGE) and used silver staining to visualize the species formed by each of the peptides we prepared (Figure 3.3A). In the SDS-PAGE, A $\beta_{(M1-42)}$ runs with main band just above the 5 kDa ladder band, at ca. 6 kDa, that corresponds to the monomer, as well as a pair of weaker bands at ca. 13 and 15 kDa, which are generally attributed to trimer and tetramer.^{57,58} The previously reported A β_{C21C30} peptide gives a pair of bands, with similar appearance but slightly lower in position. These bands have previously been attributed to dimer and trimer.⁴⁸ The A β_{C21C32} and A β_{C21C31} peptides give bands just above the 5 kDa ladder band, at ca. 6 kDa, and thus form monomers. The A β_{C24C29} peptide gives a pattern of monomer, trimer, and tetramer bands similar in position and appearance to those of A $\beta_{(M1-42)}$. The A β_{C18C33} peptide stands out among the mutant peptides, giving an intense band midway between the 10 and 15 kDa ladder bands, at ca. 12 kDa, which corresponds to the dimer.

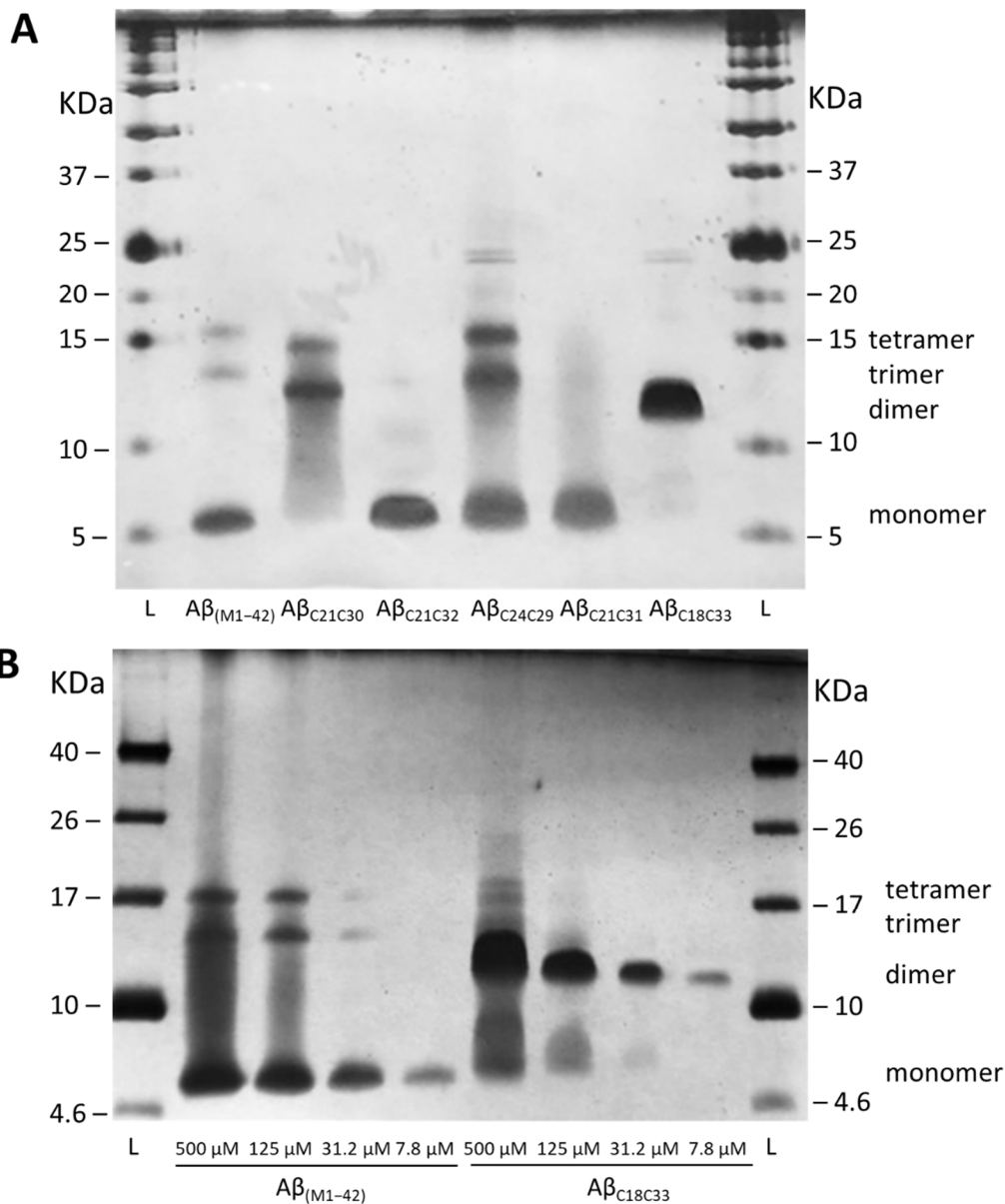


Figure 3.3. SDS-PAGE studies of the oligomerization propensities of the disulfide-stapled A β peptides. (A) oligomerization patterns of disulfide-stapled A β peptides at 80 μ M concentration. (B) Comparison of the oligomerization pattern of A $\beta_{(M1-42)}$ and A β_{C18C33} peptides at various concentrations.

To further explore the dimerization of the A β_{C18C33} peptide, we ran SDS-PAGE at concentrations ranging from 7.8 to 500 μ M (Figure 3.3B). At each concentration, the dimer band predominates, with small bands corresponding to monomer and higher-order oligomers at higher

concentrations. In contrast, $A\beta_{(M1-42)}$ shows a predominance of the monomer at all concentrations, with the trimer and tetramer bands appearing at higher concentrations.

To investigate the effect of the disulfide bond of $A\beta_{C18C33}$ upon dimer formation, we reduced the disulfide bond of $A\beta_{C18C33}$ using tris(2-carboxyethyl)phosphine hydrochloride (TCEP) and studied the oligomerization of the reduced $A\beta_{C18C33}$ peptide by SDS-PAGE (Figure 3.4). The reduced $A\beta_{C18C33}$ peptide shows distinct bands corresponding to monomer, dimer, trimer, and tetramer, at lower concentrations, as well as an additional band corresponding to the pentamer at higher concentrations. These results demonstrate that the disulfide bond is essential for non-covalent dimer formation and establish that the cysteine mutations alone do not induce the formation of a well-defined dimer.

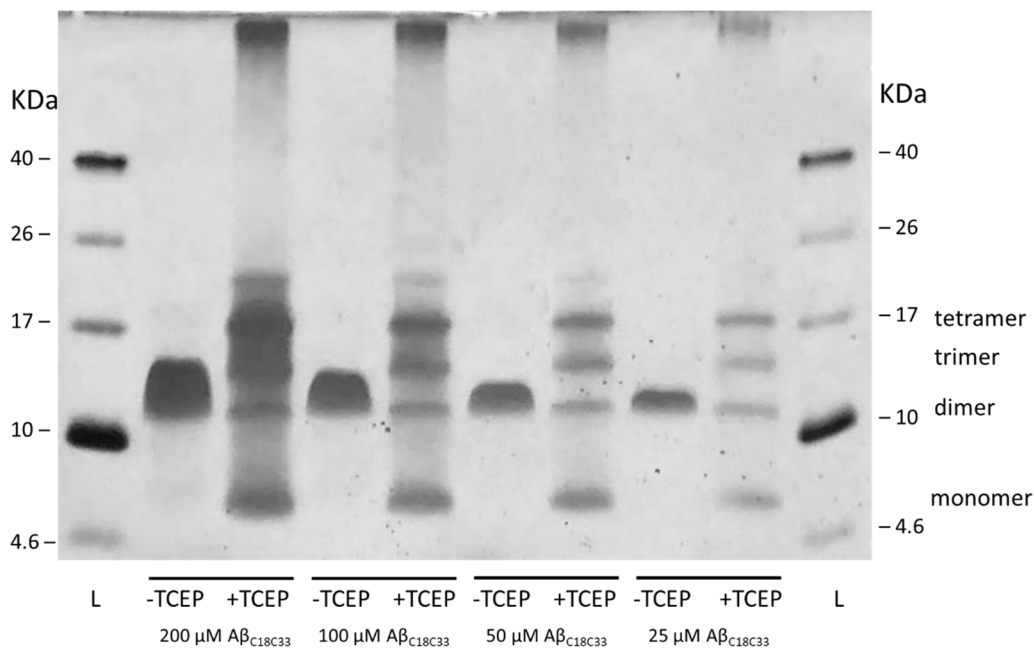


Figure 3.4. SDS-PAGE studies of $A\beta_{C18C33}$ before and after TCEP reduction at various concentrations.

MS Studies of A β _{C18C33}. To further corroborate the formation of non-covalent dimers and to exclude the possibility of covalent dimer formation through a pair of intermolecular disulfide bonds, we performed mass spectrometry. Matrix-assisted laser desorption/ionization mass spectrometry shows exclusively the A β _{C18C33} monomer (Figure 3.S12). This observation is significant, because it establishes that the dimer observed for A β _{C18C33} in SDS-PAGE is non-covalent, rather than a covalent dimer formation through a pair of intermolecular disulfide bonds or a catenane. The A β _{C18C33} peptide also shows monomer in the ESI mass spectrum in SEC-MS, eluting with ammonium formate and acetonitrile at pH 10 (Figure 3.5A). Addition of the non-ionic detergent dodecyl maltoside (DDM) to the SEC eluant gives a new peak in the total ion current chromatogram associated with the dimer (Figure 3.5B). Analysis of this peak reveals 5+ and 6+ ions associated with the dimer (Figure 3.5C and 3.5D). The observation of non-covalent dimers in SEC-MS experiments with DDM provide further evidence that A β _{C18C33} forms well-defined dimers in the presence of detergent.

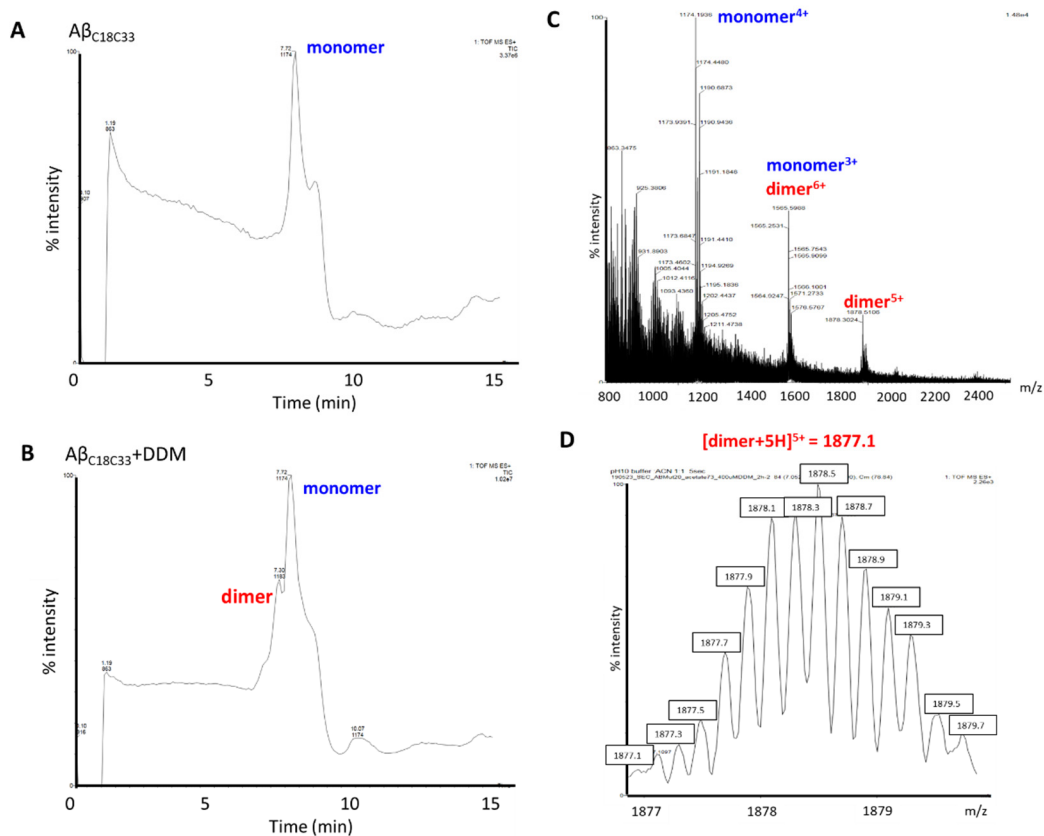


Figure 3.5. SEC-MS studies of $A\beta_{C18C33}$ peptide. (A) SEC chromatogram showing $A\beta_{C18C33}$ monomers. (B) SEC chromatogram showing the formation of $A\beta_{C18C33}$ dimers after coincubation with DDM. (C) Mass spectrum of the SEC peak corresponding to $A\beta_{C18C33}$ dimers and monomers. (D) A representative mass peak corresponds to $5+$ ion associated with $A\beta_{C18C33}$ dimers.

To further characterize the non-covalent $A\beta_{C18C33}$ dimers, we performed native ion mobility–mass spectrometry (IM-MS). In this technique, the sample is directly injected into the mass spectrometer, and species are separated in the gas phase on the basis of mobility. A solution of $25 \mu\text{M}$ $A\beta_{C18C33}$ and $300 \mu\text{M}$ DDM in 200 mM ammonium acetate buffer pH 7.4 directly injected into the instrument gave an ion mobility chromatogram with two main peaks at 7.8 and 11.1 ms, corresponding to the dimer and monomer (Figure 3.6). Analysis of the isotope patterns and m/z ratios confirmed that the peaks correspond to the dimer and monomer. The SEC-MS and

IM-MS results agree with SDS-PAGE results that A β _{C18C33} forms well-defined dimers in the presence of detergent micelles.

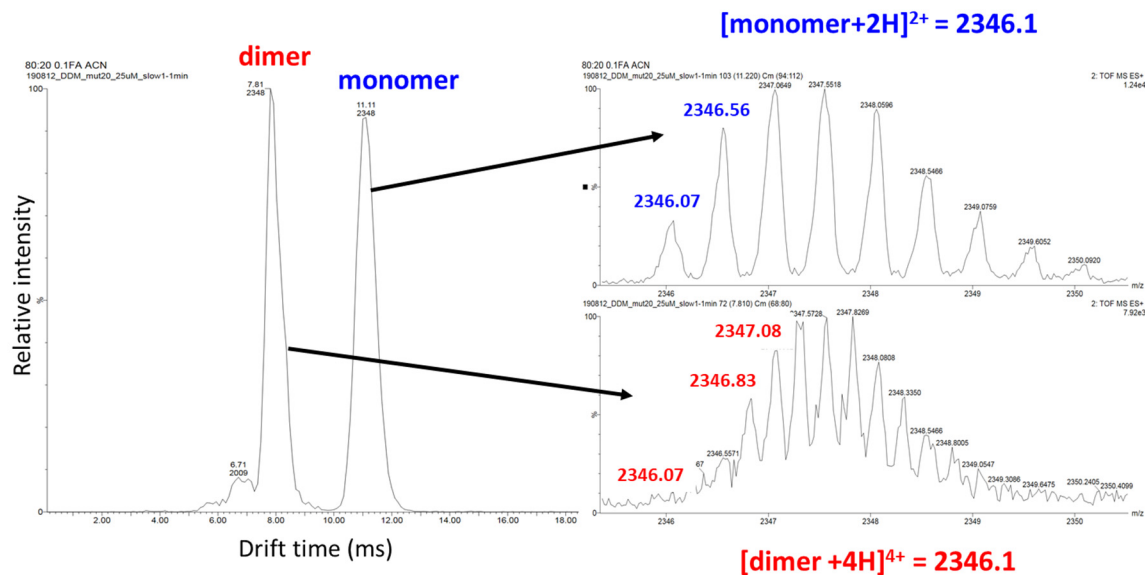


Figure 3.6. IM-MS studies of A β _{C18C33} peptide.

CD Studies of A β _{C18C33}. To explore the structure of dimers formed by A β _{C18C33}, we turned to circular dichroism (CD) spectroscopy. In the absence of SDS, a 30 μ M solution of A β _{C18C33} in 10 mM sodium phosphate buffer at pH 7.4 exhibits a broad negative band below 230 nm, with a shallow minimum at 203 nm (Figure 3.7A). With 20 mM SDS, the CD spectrum shows a well-defined minimum at 212 nm and maximum at 191 nm (Figure 3.7A). These data indicate that the A β _{C18C33} peptide adopts β -sheet structure in the presence of SDS, but that random coil structure predominates in the absence of SDS. The spectrum in the presence of SDS differs dramatically from that of A β _(M1-42), which exhibits minima at 207 and 222 nm and a maximum at 190 nm in SDS and thus adopts α -helical structure (Figure 3.7B). These results bring into sharp perspective the effect of the disulfide staple upon the conformation of A β _{C18C33}, preventing α -helix formation and enforcing β -sheet formation under conditions most relevant to SDS-PAGE.

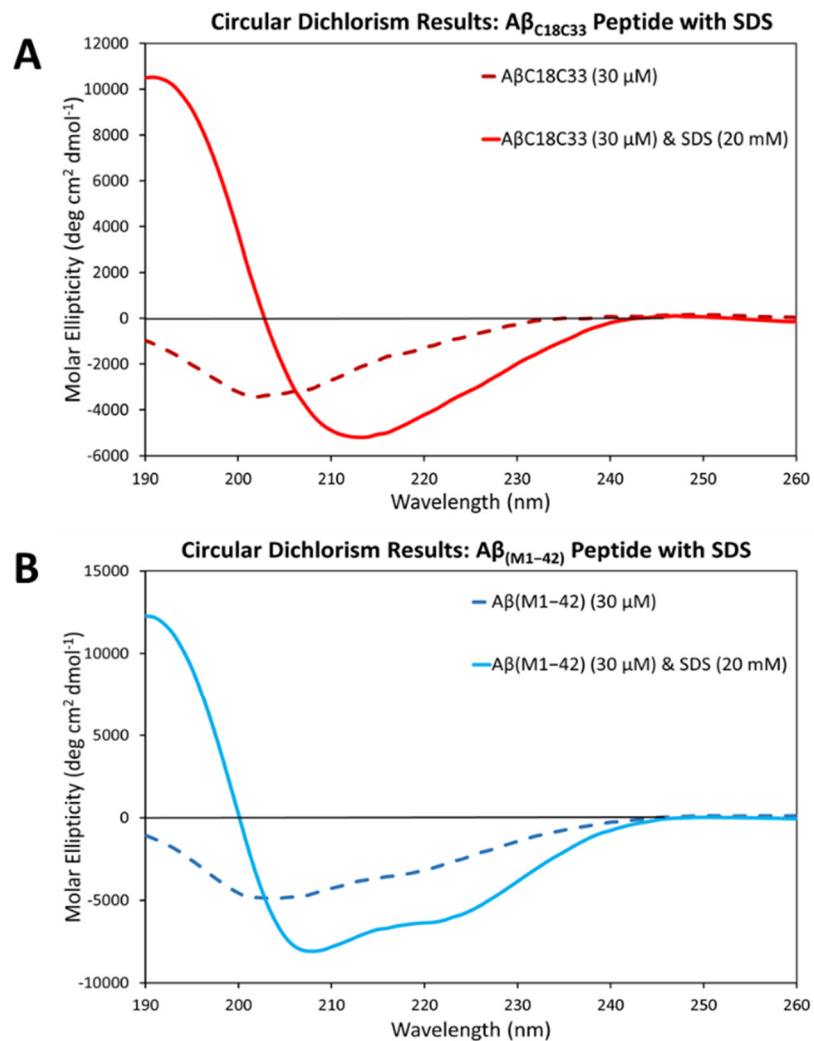


Figure 3.7. CD spectra of $A\beta_{C18C33}$ (A) and $A\beta_{(M1-42)}$ (B) in the absence or in the presence of SDS.

To gain further insight into the structure of $A\beta_{C18C33}$ dimers under conditions relevant to the SEC-MS and IM-MS experiments described above, we collected CD spectra of $A\beta_{C18C33}$ and $A\beta_{(M1-42)}$ with various concentrations of DDM. The CD spectra of $A\beta_{C18C33}$ with DDM at concentrations well above the critical micelle concentration (CMC, 0.17 mM), resemble the spectrum of $A\beta_{C18C33}$ with 20 mM SDS (CMC 8 mM), exhibiting a well-defined minimum at 214 nm and maximum at ca. 190 nm (Figure 3.8A). The CD spectrum of $A\beta_{(M1-42)}$ with DDM shows

a broader minimum, centered at 215 nm, and a weaker maximum at ca.190 nm (Figure 3.8B). Analysis of the $A\beta_{C18C33}$ spectra using secondary structure analysis server BeStSel^{59,60} shows the formation of ca. 50% antiparallel β -sheet structure as the concentration of DDM is raised above the CMC (Figure 3.8C). In contrast, the $A\beta_{(M1-42)}$ spectra shows only ca. 20% antiparallel β -sheet structure under these conditions (Figure 3.8C). These results further support a model in which the disulfide staple enforces a β -hairpin conformation in $A\beta_{C18C33}$ in the membrane-like environments provided by detergents.^{48,61}

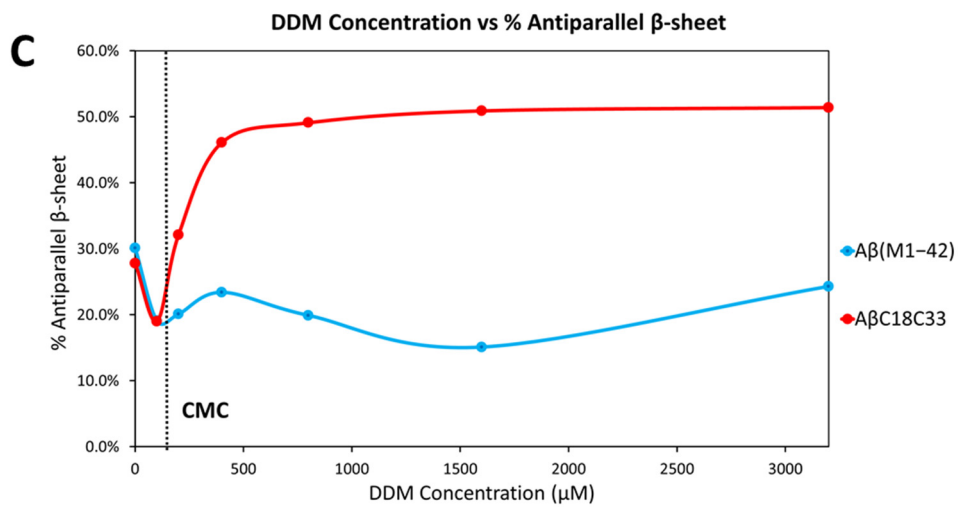
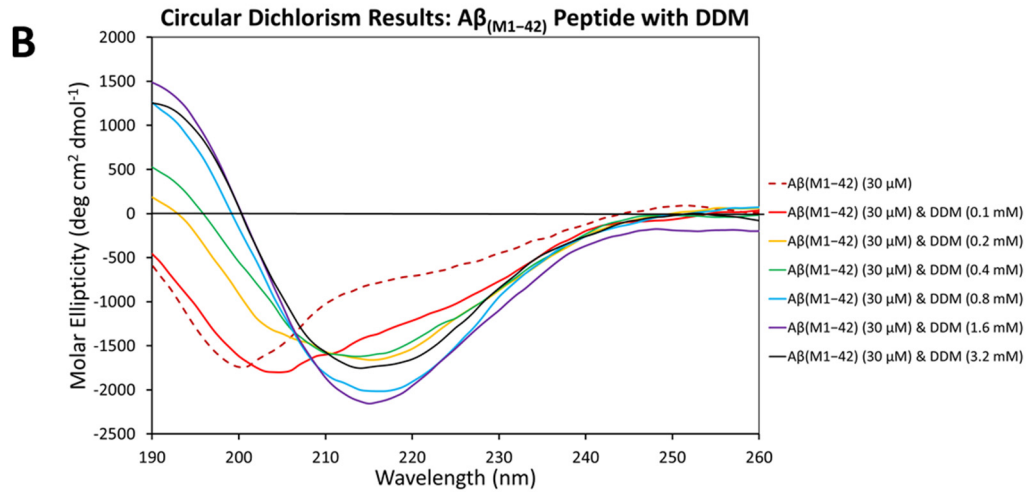
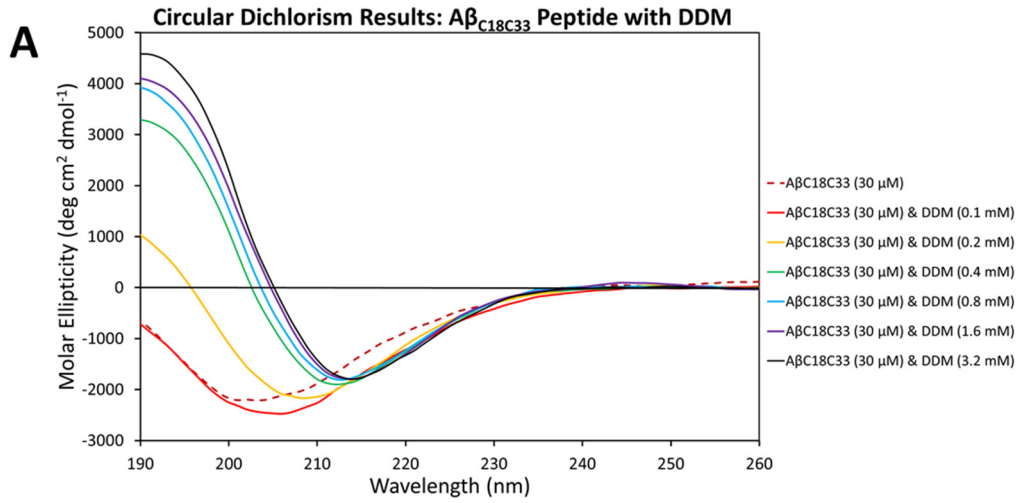


Figure 3.8. CD spectra of $A\beta_{C18C33}$ and $A\beta_{(M1-42)}$ in the presence of DDM. (A) CD spectra of $A\beta_{C18C33}$ in the presence of various concentrations of DDM. (B) CD spectra of $A\beta_{(M1-42)}$ in the presence of various concentrations of DDM. (C) Percent composition of antiparallel β -sheet structure of $A\beta_{C18C33}$ and $A\beta_{(M1-42)}$ peptides in the presence of various concentrations of DDM. The CD spectra were analyzed using secondary structure analysis server BeStSel. The critical micelle concentration (CMC) of DDM (ca. 0.15 mM) was marked with a dashed line.

ThT, TEM, AUC, and DLS Studies of $A\beta_{C18C33}$. To determine the effect of the disulfide staple upon fibril formation, we performed thioflavin T (ThT) fluorescence assays. Solutions of $A\beta_{C18C33}$ and $A\beta_{(M1-42)}$ were incubated in PBS buffer at pH 7.4 in the presence of ThT at 37 °C. Under these conditions, $A\beta_{(M1-42)}$ showed a characteristic lag time followed by a rapid onset of fluorescence at ca. 30 minutes (Figure 3.9B). In contrast, $A\beta_{C18C33}$ showed no appreciable increase in fluorescence over 24 hours (Figure 3.9A). To rule out the possibility that the $A\beta_{C18C33}$ peptide is resistant to fibrilization because of the point mutations rather than the intramolecular disulfide bridge, we performed a ThT assay using an $A\beta_{C18C33}$ analogue peptide bearing double alanine mutations, $A\beta_{A18A33}$. Under comparable conditions, the $A\beta_{A18A33}$ peptide showed a lag time of ca. 4.5 hr, followed by a rapid onset of fluorescence (Figure 3.9C). These observations demonstrate that the disulfide bond prevents fibril formation. The longer lag time associated with the $A\beta_{A18A33}$ mutant likely reflect the effect of valine-to-alanine mutation at position 18 of the critical $^{17}LVFFA^{21}$ amyloidogenic region of $A\beta$.

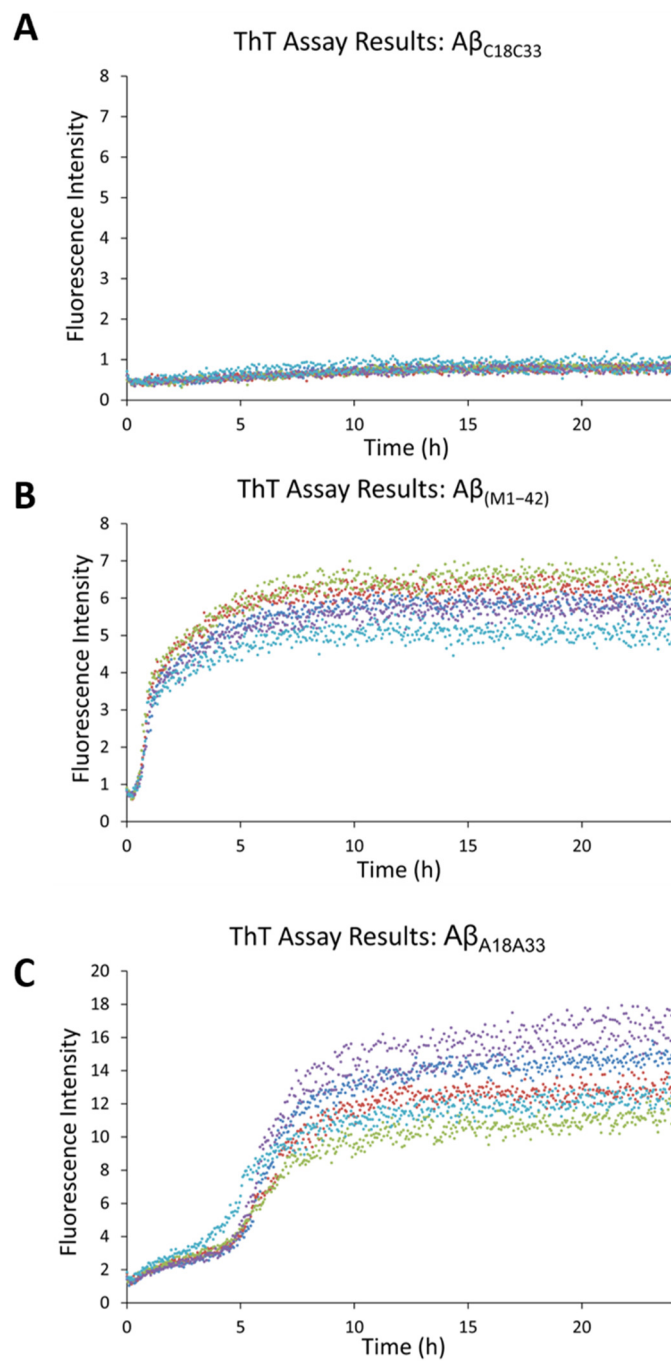


Figure 3.9. ThT fluorescence assays of (A) $A\beta_{C18C33}$, (B) $A\beta_{(M1-42)}$, and (C) $A\beta_{A18A33}$. Assays were performed with 40 μ M $A\beta$ and 40 μ M ThT in PBS buffer at 37 $^{\circ}$ C without shaking (quiescent conditions). Fluorescence was monitored with 440 nm excitation and 485 nm emission. The ThT assays were performed in five technical replicates (purple, dark blue, red, light blue, and green).

We performed transmission electron microscopy (TEM) to corroborate that $A\beta_{C18C33}$ does not fibrilize. Incubation of $A\beta_{C18C33}$ at 37 °C for 24 hours in PBS buffer, followed by imaging by TEM, showed no fibrils (Figure 3.10A). In contrast, $A\beta_{(M1-42)}$ showed long fibrils, characteristic of $A\beta$ (Figure 3.10B). $A\beta_{A18A33}$ also showed fibrils, albeit shorter than the characteristic $A\beta_{(M1-42)}$ fibrils (Figure 3.10C). Upon treatment with TCEP to reduce the disulfide bond and incubation in PBS buffer, $A\beta_{C18C33}$ showed fibrils (Figure 3.10D). Collectively, these results confirm that the intramolecular disulfide bond is critical to arresting the $A\beta_{C18C33}$ peptide in the oligomeric state.

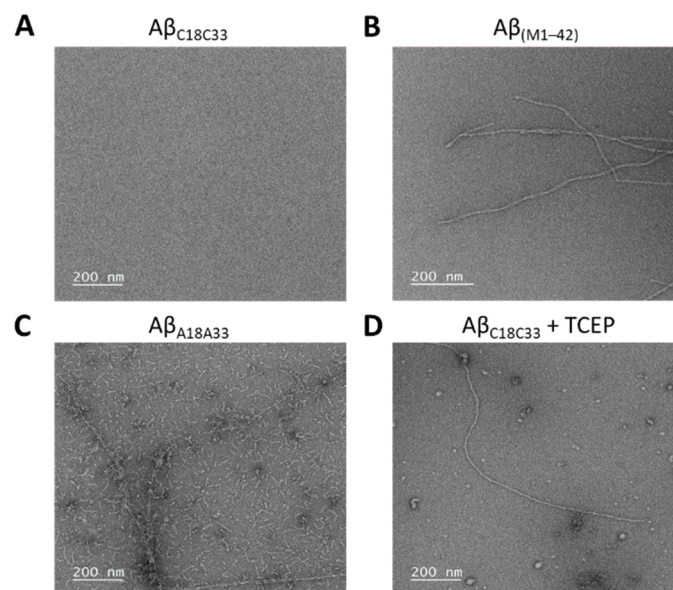


Figure 3.10. Transmission electron micrographs of $A\beta$ peptides: (A) $A\beta_{C18C33}$, (B) $A\beta_{(M1-42)}$, (C) $A\beta_{A18A33}$, and (D) $A\beta_{C18C33}$ with TCEP. Solution of the $A\beta$ peptides were incubated in PBS buffer for 24 hours at 37 °C and then imaged by TEM with uranyl acetate staining.

To further evaluate the $A\beta_{C18C33}$ peptide in aqueous solutions, we performed analytical ultracentrifugation (AUC) and dynamic light scattering (DLS) experiments. Sedimentation velocity AUC experiments in 10 mM sodium phosphate buffer with 25 mM NaCl at pH 7.4 on samples of

$A\beta_{C18C33}$ at 5–160 μM show distinct species with sedimentation coefficients of 0.54 and 1.01, which correspond to the monomer and the dimer (Figure 3.S13). Larger aggregates that settled rapidly were also observed to pellet in these 60,000 rpm experiments and constituted 52–76% of the sample. In DLS experiments, a freshly prepared solution of $A\beta_{C18C33}$ (30 μM in 10 mM sodium phosphate buffer at pH 7.4) shows a peak centered at 24.4 nm (Figure 3.11). Upon incubation for 24 hours at 37 $^{\circ}\text{C}$, the peak shifted to 32.7 nm. These results show that $A\beta_{C18C33}$ forms large stable oligomeric assemblies in aqueous solution in the absence of detergent, and are consistent with the pelleting observed in the AUC experiments. Monomer and dimer, which are observed in the AUC experiments, are likely in equilibrium with these assemblies, but are too small to be observed by DLS. In contrast, a freshly prepared solution of $A\beta_{(M1-42)}$ shows a peak centered at 58.8 nm, which shifts to 955 nm upon incubation for 24 hours (Figure 3.11). These observations are consistent with the fibril formation observed in the ThT and TEM experiments.

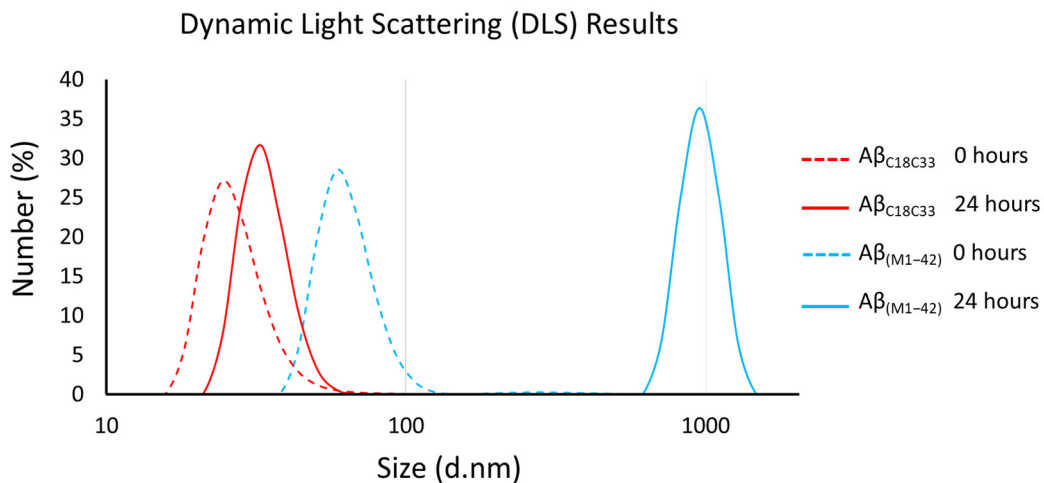


Figure 3.11. Dynamic light scattering experiments of $A\beta_{C18C33}$ and $A\beta_{(M1-42)}$. DLS experiments were performed on 30 μM solutions of the $A\beta$ peptides in 10 mM sodium phosphate buffer at pH 7.4. DLS data were recorded for freshly prepared solutions and then after the solutions were incubated for 24 hours at 37 $^{\circ}\text{C}$.

Conclusion and Discussion

A β _{C18C33}, a double mutant of the expressed peptide A β _(M1-42) containing a disulfide staple, forms stable dimers in the presence of anionic and non-ionic detergents. The dimers exhibit a high degree of β -sheet character and can readily be observed by SDS-PAGE and mass spectrometry. In aqueous buffer, the A β _{C18C33} peptide does not aggregate to form fibrils, but instead forms stable solutions of large oligomers as well as detectable monomer and dimer. The A β _{C18C33} is readily prepared by expression in *E. coli* and can be purified by preparative reverse-phase HPLC.

We anticipate that A β _{C18C33} will be a valuable tool in biological and biophysical experiments, by providing ready access to stable, homogenous, non-covalent A β dimers. Oligomers of native A β peptides (A β ₁₋₄₀, A β ₁₋₄₂, A β _(M1-42), etc.) are heterogeneous and prone to further aggregation to form fibrils. Oligomeric preparations of these peptides can thus be problematic to use in biological and biophysical studies. The A β _{C18C33} peptide provides an attractive alternative to these preparations, because of the stability and homogeneity of the dimers that it forms in membrane-like environments.

References

- (1) Narayan, P.; Ganzinger, K. A.; McColl, J.; Weimann, L.; Meehan, S.; Qamar, S.; Carver, J. A.; Wilson, M. R.; St. George-Hyslop, P.; Dobson, C. M.; Klenerman, D. Single Molecule Characterization of the Interactions between Amyloid- β Peptides and the Membranes of Hippocampal Cells. *J. Am. Chem. Soc.* **2013**, *135*, 1491–1498.
- (2) Evangelisti, E.; Cascella, R.; Becatti, M.; Marrazza, G.; Dobson, C. M.; Chiti, F.; Stefani, M.; Cecchi, C. Binding Affinity of Amyloid Oligomers to Cellular Membranes Is a Generic

- Indicator of Cellular Dysfunction in Protein Misfolding Diseases. *Sci. Rep.* **2016**, *6*: 32721.
- (3) Haass, C.; Selkoe, D. J. Soluble Protein Oligomers in Neurodegeneration: Lessons from the Alzheimer's Amyloid β -Peptide. *Nat. Rev. Mol. Cell Biol.* **2007**, *8*, 101–112.
 - (4) Ferreira, S. T.; Lourenco, M. V.; Oliveira, M. M.; De Felice, F. G. Soluble Amyloid- β Oligomers as Synaptotoxins Leading to Cognitive Impairment in Alzheimer's Disease. *Front. Cell. Neurosci.* **2015**, *9*, 191.
 - (5) Benilova, I.; Karran, E.; De Strooper, B. The Toxic A β Oligomer and Alzheimer's Disease: An Emperor in Need of Clothes. *Nat. Neurosci.* **2012**, *15*, 349–357.
 - (6) Selkoe, D. J.; Hardy, J. The Amyloid Hypothesis of Alzheimer's Disease at 25 Years. *EMBO Mol. Med.* **2016**, *8*, 595–608.
 - (7) Yang, T.; Li, S.; Xu, H.; Walsh, D. M.; Selkoe, D. J. Large Soluble Oligomers of Amyloid β -Protein from Alzheimer Brain Are Far Less Neuroactive than the Smaller Oligomers to Which They Dissociate. *J. Neurosci.* **2017**, *37*, 152–163.
 - (8) Cizas, P.; Budvytyte, R.; Morkuniene, R.; Moldovan, R.; Broccio, M.; Lösche, M.; Niaura, G.; Valincius, G.; Borutaite, V. Size-Dependent Neurotoxicity of β -Amyloid Oligomers. *Arch. Biochem. Biophys.* **2010**, *496*, 84–92.
 - (9) Ono, K.; Condrón, M. M.; Teplov, D. B. Structure-Neurotoxicity Relationships of Amyloid β -Protein Oligomers. *Proc. Natl. Acad. Sci. U. S. A.* **2009**, *106*, 14745–14750.
 - (10) Man, V. H.; Nguyen, P. H.; Derreumaux, P. High-Resolution Structures of the Amyloid- β 1-42 Dimers from the Comparison of Four Atomistic Force Fields. *J. Phys. Chem. B* **2017**, *121*, 5977–5987.

- (11) Vázquez De La Torre, A.; Gay, M.; Vilapriñó-Pascual, S.; Mazzucato, R.; Serra-Batiste, M.; Vilaseca, M.; Carulla, N. Direct Evidence of the Presence of Cross-Linked A β Dimers in the Brains of Alzheimer's Disease Patients. *Anal. Chem.* **2018**, *90*, 4552–4560.
- (12) Brinkmalm, G.; Hong, W.; Wang, Z.; Liu, W.; O'Malley, T. T.; Sun, X.; Frosch, M. P.; Selkoe, D. J.; Portelius, E.; Zetterberg, H.; Blennow, K.; Walsh, D. M. Identification of Neurotoxic Cross-Linked Amyloid- β Dimers in the Alzheimer's Brain. *Brain* **2019**, *142*, 1441–1457.
- (13) Jin, M.; Shepardson, N.; Yang, T.; Chen, G.; Walsh, D.; Selkoe, D. J. Soluble Amyloid β -Protein Dimers Isolated from Alzheimer Cortex Directly Induce Tau Hyperphosphorylation and Neuritic Degeneration. *Proc. Natl. Acad. Sci. U. S. A.* **2011**, *108*, 5819–5824.
- (14) Klyubin, I.; Betts, V.; Welzel, A. T.; Blennow, K.; Zetterberg, H.; Wallin, A.; Lemere, C. A.; Cullen, W. K.; Peng, Y.; Wisniewski, T.; Selkoe, D. J.; Anwyl, R.; Walsh, D. M.; Rowan, M. J. Amyloid β Protein Dimer-Containing Human CSF Disrupts Synaptic Plasticity: Prevention by Systemic Passive Immunization. *J. Neurosci.* **2008**, *28*, 4231–4237.
- (15) Shankar, G. M.; Li, S.; Mehta, T. H.; Garcia-Munoz, A.; Shepardson, N. E.; Smith, I.; Brett, F. M.; Farrell, M. A.; Rowan, M. J.; Lemere, C. A.; Regan, C. M.; Walsh, D. M.; Sabatini, B. L.; Selkoe, D. J. Amyloid- β Protein Dimers Isolated Directly from Alzheimer's Brains Impair Synaptic Plasticity and Memory. *Nat. Med.* **2008**, *14*, 837–842.
- (16) O'Nuallain, B.; Freir, D. B.; Nicoll, A. J.; Risse, E.; Ferguson, N.; Herron, C. E.; Collinge, J.; Walsh, D. M. Amyloid β -Protein Dimers Rapidly Form Stable Synaptotoxic Protofibrils. *J. Neurosci.* **2010**, *30*, 14411–14419.

- (17) Abdel-Hafiz, L.; Müller-Schiffmann, A.; Korth, C.; Fazari, B.; Chao, O. Y.; Nikolaus, S.; Schäble, S.; Herring, A.; Keyvani, K.; Lamounier-Zepter, V.; Huston, J. P.; de Souza Silva, M. A. A β Dimers Induce Behavioral and Neurochemical Deficits of Relevance to Early Alzheimer's Disease. *Neurobiol. Aging* **2018**, *69*, 1–9.
- (18) Müller-Schiffmann, A.; Herring, A.; Abdel-Hafiz, L.; Chepkova, A. N.; Schäble, S.; Wedel, D.; Horn, A. H. C.; Sticht, H.; De Souza Silva, M. A.; Gottmann, K.; Sergeeva, O. A.; Huston, J. P.; Keyvani, K.; Korth, C. Amyloid- β Dimers in the Absence of Plaque Pathology Impair Learning and Synaptic Plasticity. *Brain* **2016**, *139*, 509–525.
- (19) Hirel, P. H.; Schmitter, J. M.; Dessen, P.; Fayat, G.; Blanquet, S. Extent of N-Terminal Methionine Excision from Escherichia Coli Proteins Is Governed by the Side-Chain Length of the Penultimate Amino Acid. *Proc. Natl. Acad. Sci. U. S. A.* **1989**, *86*, 8247–8251.
- (20) Salveson, P. J.; Spencer, R. K.; Kreuzer, A. G.; Nowick, J. S. X-Ray Crystallographic Structure of a Compact Dodecamer from a Peptide Derived from A β 16-36. *Org. Lett.* **2017**, *19*, 3462–3465.
- (21) Cline, E. N.; Bicca, M. A.; Viola, K. L.; Klein, W. L. The Amyloid- β Oligomer Hypothesis: Beginning of the Third Decade. *J. Alzheimers. Dis.* **2018**, *64*, S567–S610.
- (22) Orte, A.; Birkett, N. R.; Clarke, R. W.; Devlin, G. L.; Dobson, C. M.; Klenerman, D. Direct Characterization of Amyloidogenic Oligomers by Single-Molecule Fluorescence. *Proc. Natl. Acad. Sci. U. S. A.* **2008**, *105*, 14424–14429.
- (23) Marina, G. B.; Kirkitadze, D.; Lomakin, A.; Vollers, S. S.; Benedek, G. B.; Teplow, D. B. Amyloid β -Protein (A β) Assembly: A β 40 and A β 42 Oligomerize through Distinct Pathways. *Proc. Natl. Acad. Sci. U. S. A.* **2003**, *100*, 330–335.

- (24) Bitan, G.; Lomakin, A.; Teplow, D. B. Amyloid β -Protein Oligomerization: Prenucleation Interactions Revealed by Photo-Induced Cross-Linking of Unmodified Proteins. *J. Biol. Chem.* **2001**, *276*, 35176–35184.
- (25) Chen, G. F.; Xu, T. H.; Yan, Y.; Zhou, Y. R.; Jiang, Y.; Melcher, K.; Xu, H. E. Amyloid Beta: Structure, Biology and Structure-Based Therapeutic Development. *Acta Pharmacol. Sin.* **2017**, *38*, 1205–1235.
- (26) Knowles, T. P. J.; Vendruscolo, M.; Dobson, C. M. The Amyloid State and Its Association with Protein Misfolding Diseases. *Nat. Rev. Mol. Cell Biol* **2014**, *15*, 384–396.
- (27) Makin, O. S.; Atkins, E.; Sikorski, P.; Johansson, J.; Serpell, L. C. Molecular Basis for Amyloid Fibril Formation and Stability. *Proc. Natl. Acad. Sci. U. S. A.* **2005**, *102*, 315–320.
- (28) O'Malley, T. T.; Walsh, D. M. Lessons from the Study of Covalent Dimers of the Alzheimer's Disease-Associate Amyloid β -Protein. *Biochem. Physiol. Open Access* **2018**, *7*, 229.
- (29) O'Malley, T. T.; Witbold, W. M.; Linse, S.; Walsh, D. M. The Aggregation Paths and Products of A β 42 Dimers Are Distinct from Those of the A β 42 Monomer. *Biochemistry* **2016**, *55*, 6150–6161.
- (30) Hartley, D. M.; Zhao, C.; Speier, A. C.; Woodard, G. A.; Li, S.; Li, Z.; Walz, T. Transglutaminase Induces Protofibril-like Amyloid β -Protein Assemblies That Are Protease-Resistant and Inhibit Long-Term Potentiation. *J. Biol. Chem.* **2008**, *283*, 16790–16800.
- (31) Sitkiewicz, E.; Ołędzki, J.; Poznański, J.; Dadlez, M. Di-Tyrosine Cross-Link Decreases the

- Collisional Cross-Section of A β Peptide Dimers and Trimers in the Gas Phase: An Ion Mobility Study. *PLoS One* **2014**, *9*, e100200.
- (32) O'Malley, T. T.; Oktaviani, N. A.; Zhang, D.; Lomakin, A.; O'Nuallain, B.; Linse, S.; Benedek, G. B.; Rowan, M. J.; Mulder, F. A. A.; Walsh, D. M. A β Dimers Differ from Monomers in Structural Propensity, Aggregation Paths and Population of Synaptotoxic Assemblies. *Biochem. J.* **2014**, *461*, 413–426.
- (33) Atwood, C. S.; Perry, G.; Zeng, H.; Kato, Y.; Jones, W. D.; Ling, K. Q.; Huang, X.; Moir, R. D.; Wang, D.; Sayre, L. M.; Smith, M. A.; Chen, S. G.; Bush, A. I. Copper Mediates Dityrosine Cross-Linking of Alzheimer's Amyloid- β . *Biochemistry* **2004**, *43*, 560–568.
- (34) Yamaguchi, T.; Yagi, H.; Goto, Y.; Matsuzaki, K.; Hoshino, M. A Disulfide-Linked Amyloid- β Peptide Dimer Forms a Protofibril-like Oligomer through a Distinct Pathway from Amyloid Fibril Formation. *Biochemistry* **2010**, *49*, 7100–7107.
- (35) Müller-Schiffmann, A.; Andreyeva, A.; Horn, A. H. C.; Gottmann, K.; Korth, C.; Sticht, H. Molecular Engineering of a Secreted, Highly Homogeneous, and Neurotoxic A β Dimer. *ACS Chem. Neurosci.* **2011**, *2*, 242–248.
- (36) Murakami, K.; Kato, H.; Hanaki, M.; Monobe, Y.; Akagi, K. I.; Kawase, T.; Hirose, K.; Irie, K. Synthetic and Biochemical Studies on the Effect of Persulfidation on Disulfide Dimer Models of Amyloid SS42 at Position 35 in Alzheimer's Etiology. *RSC Adv.* **2020**, *10*, 19506–19512.
- (37) Murakami, K.; Suzuki, T.; Hanaki, M.; Monobe, Y.; Akagi, K. I.; Irie, K. Synthesis and Characterization of the Amyloid B40 Dimer Model with a Linker at Position 30 Adjacent to the Intermolecular β -Sheet Region. *Biochem. Biophys. Res. Commun.* **2015**, *466*, 463–

467.

- (38) Kok, W. M.; Scanlon, D. B.; Karas, J. A.; Miles, L. A.; Tew, D. J.; Parker, M. W.; Barnham, K. J.; Hutton, C. A. Solid-Phase Synthesis of Homodimeric Peptides: Preparation of Covalently-Linked Dimers of Amyloid β Peptide. *Chem. Commun.* **2009**, *41*, 6228–6230.
- (39) Murakami, K.; Tokuda, M.; Suzuki, T.; Irie, Y.; Hanaki, M.; Izuo, N.; Monobe, Y.; Akagi, K. I.; Ishii, R.; Tatebe, H.; Tokuda, T.; Maeda, M.; Kume, T.; Shimizu, T.; Irie, K. Monoclonal Antibody with Conformational Specificity for a Toxic Conformer of Amyloid B42 and Its Application toward the Alzheimer's Disease Diagnosis. *Sci. Rep.* **2016**, *6*: 29038.
- (40) Siegel, S. J.; Bieschke, J.; Powers, E. T.; Kelly, J. W. The Oxidative Stress Metabolite 4-Hydroxynonenal Promotes Alzheimer Protofibril Formation. *Biochemistry* **2007**, *46*, 1503–1510.
- (41) Hayden, E. Y.; Conovaloff, J. L.; Mason, A.; Bitan, G.; Teplow, D. B. Preparation of Pure Populations of Amyloid β -Protein Oligomers of Defined Size. In *Methods. Mol. Biol.* **2018**; *1779*, 3–12.
- (42) Rosensweig, C.; Ono, K.; Murakami, K.; Lowenstein, D. K.; Bitan, G.; Teplow, D. B. Preparation of Stable Amyloid β -Protein Oligomers of Defined Assembly Order. *Methods Mol. Biol.* **2012**, *849*, 23–31.
- (43) Hayden, E. Y.; Conovaloff, J. L.; Mason, A.; Bitan, G.; Teplow, D. B. Preparation of Pure Populations of Covalently Stabilized Amyloid β -Protein Oligomers of Specific Sizes. *Anal. Biochem.* **2017**, *518*, 78–85.

- (44) Nag, S.; Sarkar, B.; Bandyopadhyay, A.; Sahoo, B.; Sreenivasan, V. K. A.; Kombrabail, M.; Muralidharan, C.; Maiti, S. Nature of the Amyloid- β Monomer and the Monomer-Oligomer Equilibrium. *J. Biol. Chem.* **2011**, *286*, 13827–13833.
- (45) Soreghan, B.; Kosmoski, J.; Glabe, C. Surfactant Properties of Alzheimer's A β Peptides and the Mechanism of Amyloid Aggregation. *J. Biol. Chem.* **1994**, *269*, 28551–28554.
- (46) Dear, A. J.; Michaels, T. C. T.; Meisl, G.; Klenerman, D.; Wu, S.; Perrett, S.; Linse, S.; Dobson, C. M.; Knowles, T. P. J. Kinetic Diversity of Amyloid Oligomers. *Proc. Natl. Acad. Sci. U. S. A.* **2020**, *117*, 12087–12094.
- (47) Dubnovitsky, A.; Sandberg, A.; Rahman, M. M.; Benilova, I.; Lendel, C.; Härd, T. Amyloid- β Protofibrils: Size, Morphology and Synaptotoxicity of an Engineered Mimic. *PLoS One* **2013**, *8*, e66101.
- (48) Sandberg, A.; Luheshi, L. M.; Söllvander, S.; De Barros, T. P.; Macao, B.; Knowles, T. P. J.; Biverstål, H.; Lendel, C.; Ekholm-Petterson, F.; Dubnovitsky, A.; Lannfelt, L.; Dobson, C. M.; Härd, T. Stabilization of Neurotoxic Alzheimer Amyloid- β Oligomers by Protein Engineering. *Proc. Natl. Acad. Sci. U. S. A.* **2010**, *107*, 15595–15600.
- (49) Lendel, C.; Bjerring, M.; Dubnovitsky, A.; Kelly, R. T.; Filippov, A.; Antzutkin, O. N.; Nielsen, N. C.; Härd, T. A Hexameric Peptide Barrel as Building Block of Amyloid- β Protofibrils. *Angew. Chemie - Int. Ed.* **2014**, *53*, 12756–12760.
- (50) Hoyer, W.; Grönwall, C.; Jonsson, A.; Ståhl, S.; Härd, T. Stabilization of a β -Hairpin in Monomeric Alzheimer's Amyloid- β Peptide Inhibits Amyloid Formation. *Proc. Natl. Acad. Sci. U. S. A.* **2008**, *105*, 5099–5104.

- (51) Matsushima, Y.; Yanagita, R. C.; Irie, K. Control of the Toxic Conformation of Amyloid B42 by Intramolecular Disulfide Bond Formation. *Chem. Commun.* **2020**, *56*, 4118–4121.
- (52) Yamamoto, M.; Shinoda, K.; Ni, J.; Sasaki, D.; Kanai, M.; Sohma, Y. A Chemically Engineered, Stable Oligomer Mimic of Amyloid B42 Containing an Oxime Switch for Fibril Formation. *Org. Biomol. Chem.* **2018**, *16*, 6537–6542.
- (53) Yu, L.; Edalji, R.; Harlan, J. E.; Holzman, T. F.; Lopez, A. P.; Labkovsky, B.; Hillen, H.; Barghorn, S.; Ebert, U.; Richardson, P. L.; Miesbauer, L.; Solomon, L.; Bartley, D.; Walter, K.; Johnson, R. W.; Hajduk, P. J.; Olejniczak, E. T. Structural Characterization of a Soluble Amyloid β -Peptide Oligomer. *Biochemistry* **2009**, *48*, 1870–1877.
- (54) Salveson, P. J.; Spencer, R. K.; Kreutzer, A. G.; Nowick, J. S. X-Ray Crystallographic Structure of a Compact Dodecamer from a Peptide Derived from A β 16-36. *Org. Lett.* **2017**, *19*, 3462–3465.
- (55) Yoo, S.; Zhang, S.; Kreutzer, A. G.; Nowick, J. S. An Efficient Method for the Expression and Purification of A β (M1-42). *Biochemistry* **2018**, *57*, 3861–3866.
- (56) Silvers, R.; Colvin, M. T.; Frederick, K. K.; Jacavone, A. C.; Lindquist, S.; Linse, S.; Griffin, R. G. Aggregation and Fibril Structure of A β M01-42 and A β 1-42. *Biochemistry* **2017**, *56*, 4850–4859.
- (57) Kreutzer, A. G.; Samdin, T. D.; Guaglianone, G.; Spencer, R. K.; Nowick, J. S. X-Ray Crystallography Reveals Parallel and Antiparallel β -Sheet Dimers of a β -Hairpin Derived from A β 16-36 that Assemble to Form Different Tetramers. *ACS Chem. Neurosci.* **2020**, *11*, 2340–2347.

- (58) Pujol-Pina, R.; Vilaprinnyó-Pascual, S.; Mazzucato, R.; Arcella, A.; Vilaseca, M.; Orozco, M.; Carulla, N. SDS-PAGE Analysis of A β Oligomers Is Disserving Research into Alzheimer's Disease: Appealing for ESI-IM-MS. *Sci. Rep.* **2015**, *5*: 14809.
- (59) Micsonai, A.; Wien, F.; Kernya, L.; Lee, Y. H.; Goto, Y.; Réfrégiers, M.; Kardos, J. Accurate Secondary Structure Prediction and Fold Recognition for Circular Dichroism Spectroscopy. *Proc. Natl. Acad. Sci. U. S. A.* **2015**, *112*, E3095–E3103.
- (60) Micsonai, A.; Wien, F.; Bulyáki, É.; Kun, J.; Moussong, É.; Lee, Y. H.; Goto, Y.; Réfrégiers, M.; Kardos, J. BeStSel: A Web Server for Accurate Protein Secondary Structure Prediction and Fold Recognition from the Circular Dichroism Spectra. *Nucleic Acids Res.* **2018**, *46*, W315–W322.
- (61) Cerf, E.; Sarroukh, R.; Tamamizu-Kato, S.; Breydo, L.; Derclayes, S.; Dufrênes, Y. F.; Narayanaswami, V.; Goormaghtigh, E.; Ruyschaert, J. M.; Raussens, V. Antiparallel β -Sheet: A Signature Structure of the Oligomeric Amyloid β -Peptide. *Biochem. J.* **2009**, *421*, 415–423.

Supporting Information

Table of Contents

General information on materials and methods	160
Isolation of pET-Sac-A β _(M1-42) plasmid	162
Molecular cloning	162
Figure 3.S1. Design of the DNA sequences for A β _(M1-42) mutants	163
Figure 3.S2. Molecular cloning strategy for constructing recombinant plasmids of A β _(M1-42) mutants	164
Table 3.S1. Double-digestion of the pET-Sac-A β _(M1-42) plasmids	164
Table 3.S2. SAP treatment of the vectors	165
Table 3.S3. Double-digestion of the inserts	166
Table 3.S4. T4 ligation of the inserts and the vectors	166
Bacterial expression of A β _(M1-42) mutant peptides	167
Cell lysis, inclusion body preparation, and disulfide bond formation by DMSO	168
Purification of A β _(M1-42) mutant peptides	169
NaOH treatment and peptide concentration determination	170
SDS-PAGE	170
Thioflavin T (ThT) fibrillization assay	171
Dynamic light scattering (DLS)	172
Circular dichroism (CD)	173
Mass spectrometry	173
Transmission electron microscopy (TEM)	174

Characterization Data and Additional Figures

Figure 3.S3. An analytical HPLC trace of A β _{C21C30} peptide	175
Figure 3.S4. An analytical HPLC trace of A β _{C21C32} peptide	176
Figure 3.S5. An analytical HPLC trace of A β _{C24C29} peptide	177
Figure 3.S6. An analytical HPLC trace of A β _{C21C31} peptide	178
Figure 3.S7. An analytical HPLC trace of A β _{C18C33} peptide	179
Figure 3.S8. MALDI-TOF mass spectra of A β _{C21C30} peptide	180
Figure 3.S9. MALDI-TOF mass spectra of A β _{C21C32} peptide	181
Figure 3.S10. MALDI-TOF mass spectra of A β _{C24C29} peptide	182
Figure 3.S11. MALDI-TOF mass spectra of A β _{C21C31} peptide	183
Figure 3.S12. MALDI-TOF mass spectra of A β _{C18C33} peptide	184
Figure 3.S13. Analytical ultracentrifugation studies of A β _{C18C33} peptide	185

General information on materials and methods

All chemicals were used as received unless otherwise noted. Deionized water (18 M Ω) was obtained from a Thermo Scientific Barnstead Genpure Pro water purification system. The pET-Sac-A β _(M1-42) plasmid was a gift from Dominic Walsh (Addgene plasmid # 71875).² DNA sequences that encode A β _{C21C30}, A β _{C21C32}, A β _{C24C29}, A β _{C21C31}, and A β _{C18C33} were purchased in 500 ng quantities from Genewiz. *NdeI* and *SacI* restriction enzymes, CutSmart buffer, and shrimp alkaline phosphatase (rSAP) were purchased from New England Biolabs (NEB). TOP10 Ca²⁺-competent *E. coli* and BL21 DE3 PLYsS Star Ca²⁺-competent *E. coli*, T4 ligase, and ethidium bromide were purchased from Thermo Fisher Scientific. Zymo ZR plasmid miniprep kit and

Zymoclean Gel DNA recovery kit was purchased from Zymo Research. Carbenicillin and chloramphenicol were purchased from RPI Research Products. The carbenicillin was added to culture media as a 1000X stock solution (50 mg/mL) in water. The chloramphenicol was added to culture media as a 1000X stock solution (34 mg/mL) in EtOH. Dimethyl sulfoxide (DMSO) was purchased from Thermo Fisher Scientific and stored in a desiccator. 3-(4,5-Dimethylthiazol-2-yl)-2,5-Diphenyltetrazolium Bromide (MTT) reagent were purchased from Thermo Fisher Scientific.

The concentration of the DNA sequences was measured using a Thermo Scientific NanoDrop spectrophotometer. *E. coli* were incubated in a Thermo Scientific MaxQ Shaker 6000. *E. coli* were lysed using a QSonica Q500 ultrasonic homogenizer. Analytical reverse-phase HPLC was performed on an Agilent 1200 instrument equipped with a Phenomenex Aeris PEPTIDE 2.6u XB-C18 column with a Phenomenex SecurityGuard ULTRA cartridges guard column for C18 column. Preparative reverse-phase HPLC was performed on a Rainin Dynamax instrument SD-200 equipped an Agilent ZORBAX 300SB-C8 semi-preparative column (9.4 x 250 mm) with a ZORBAX 300SB-C3 preparative guard column (9.4 x 15 mm). During purifications, the C8 column and the guard column were heated to 80 °C in a Sterlite plastic bin equipped with a Kitchen Gizmo Sous Vide immersion circulator. HPLC grade acetonitrile and deionized water (18 MΩ), each containing 0.1% trifluoroacetic acid (TFA), were used for analytical and preparative reverse-phase HPLC. MALDI-TOF mass spectrometry was performed using an AB SCIEX TOF/TOF 5800 system. SEC mass spectrometry and ion mobility mass spectrometry were performed using Waters Synapt G2 HD system. The dynamic light scattering (DLS) experiments were performed in disposable cuvettes using the Malvern Zetasizer μ V instrument.







Isolation of pET-Sac-A β _(M1-42) plasmid

We received the pET-Sac-A β _(M1-42) plasmid from Addgene as bacterial stabs and immediately streaked the bacteria onto LB agar plates containing carbenicillin (50 mg/L). Colonies grew in less than 24h. Single colonies were picked and used to inoculate 5 mL of LB broth containing carbenicillin (50 mg/L). The cultures were shaken at 225 rpm overnight at 37°C. To isolate the pET-Sac-A β _(M1-42) plasmid, minipreps were performed using a Zymo ZR plasmid miniprep kit. The concentration of the plasmids was measured using a Thermo Scientific Nanodrop instrument.







Molecular cloning

DNA sequences encoding mutant peptides

DNA sequences encoding mutant peptides were ordered from Genewiz. Figure 3.S1 shows the design of these DNA sequences.

 3' and 5' overhangs  *NdeI* restriction site/start codon  stop codons
 *SacI* restriction site  codon for cysteine  codon for alanine

A β _(MCI-42): 5'- GAT ATA  CAT ATG GAC GCT GAA TTC CGT CAC GAC TCT GGT TAC
GAA GTT CAC CAC CAG AAG CTG GTG TTC TTC GCT GAA GAC GTG GGT TCT AAC
AAG GGT GCT ATC ATC GGT CTG ATG GTT GGT GGC GTT GTG ATC GCT  TAA TAG
 GAG CTC  GAT CCG-3'

A β _{C21C30}: 5'- GAT ATA  CAT ATG GAC GCT GAA TTC CGT CAC GAC TCT GGT TAC
GAA GTT CAC CAC CAG AAG CTG GTG TTC TTC  TGC GAA GAC GTG GGT TCT AAC
AAG GGT  TGC ATC ATC GGT CTG ATG GTT GGT GGC GTT GTG ATC GCT  TAA TAG
 GAG CTC  GAT CCG-3'

A β _{C21C32}: 5'-GAT ATA CAT ATG GAC GCT GAA TTC CGT CAC GAC TCT GGT TAC
GAA GTT CAC CAC CAG AAG CTG GTG TTC TTC TGC GAA GAC GTG GGT TCT AAC
AAG GGT GCT ATC TGC GGT CTG ATG GTT GGT GGC GTT GTG ATC GCT TAA TAG
GAG CTC GAT CCG-3'

A β _{C24C29}: 5'-GAT ATA CAT ATG GAC GCT GAA TTC CGT CAC GAC TCT GGT TAC
GAA GTT CAC CAC CAG AAG CTG GTG TTC TTC GCT GAA GAC TGC GGT TCT AAC
AAG TGC GCT ATC ATC GGT CTG ATG GTT GGT GGC GTT GTG ATC GCT TAA TAG
GAG CTC GAT CCG-3'

A β _{C21C31}: 5'-GAT ATA CAT ATG GAC GCT GAA TTC CGT CAC GAC TCT GGT TAC
GAA GTT CAC CAC CAG AAG CTG GTG TTC TTC TGC GAA GAC GTG GGT TCT AAC
AAG GGT GCT TGC ATC GGT CTG ATG GTT GGT GGC GTT GTG ATC GCT TAA TAG
GAG CTC GAT CCG-3'

A β _{C18C33}: 5'-GAT ATA CAT ATG GAC GCT GAA TTC CGT CAC GAC TCT GGT TAC
GAA GTT CAC CAC CAG AAG CTG TGC TTC TTC GCT GAA GAC GTG GGT TCT AAC
AAG GGT GCT ATC ATC TGC CTG ATG GTT GGT GGC GTT GTG ATC GCT TAA TAG
GAG CTC GAT CCG -3'

A β _{A18A33}: 5'-GAT ATA CAT ATG GAC GCT GAA TTC CGT CAC GAC TCT GGT TAC
GAA GTT CAC CAC CAG AAG CTG GCT TTC TTC GCT GAA GAC GTG GGT TCT AAC
AAG GGT GCT ATC ATC GCT CTG ATG GTT GGT GGC GTT GTG ATC GCT TAA TAG
GAG CTC GAT CCG -3'

Figure 3.S1. Design of the DNA sequences for A β _(MCI-42) mutants.

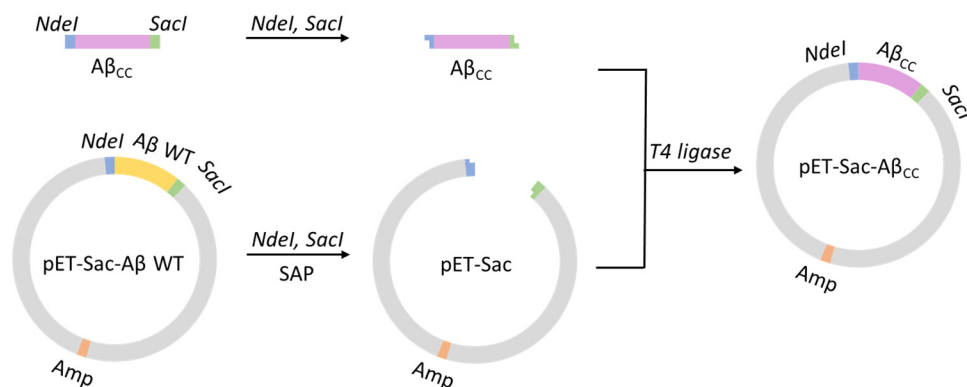


Figure 3.S2. Molecular cloning strategy for constructing recombinant plasmids of $A\beta_{(MC1-42)}$ mutants.

Restriction enzyme digestion of pET-Sac-A $\beta_{(M1-42)}$ plasmid

The pET-Sac-A $\beta_{(M1-42)}$ plasmid was digested using *SacI* and *NdeI* restriction enzymes. Table 3.S1 details the restriction reaction conditions. Reagents were added in the order they are listed.

Table 3.S1. Double-digestion of the pET- Sac A $\beta_{(M1-42)}$ plasmid.

Reagents	Amount
pET-Sac A $\beta_{(M1-42)}$	20 μ L of 50 ng/ μ L plasmid solution (1.0 μ g in total)
10X CutSmart buffer	5.0 μ L
H ₂ O	23.0 μ L
<i>NdeI</i> restriction enzyme	1.0 μ L (1 U)
<i>SacI</i> -HF restriction enzyme	1.0 μ L (1 U)
Total	50.0 μ L
Time	1.0 h
Temperature	37.0 $^{\circ}$ C

Next, to prevent backbone self-ligation, the digested plasmid was treated with shrimp alkaline phosphatase (rSAP). Table 3.S2 details the rSAP reaction conditions.

Table 3.S2. SAP treatment of the vectors.

Reagents	Amount
Double-digestion mixture	50.0 μ L
rSAP	1.0 μ L (1U)
Total	51.0 μ L
Time	0.5 h
Temperature	37.0 $^{\circ}$ C
Heat inactivation	65.0 $^{\circ}$ C for 20 min

After the rSAP reaction and heat inactivation were complete, the reaction mixture was mixed with DNA loading buffer and loaded onto a 1% agarose gel containing ethidium bromide (5 μ L per 100 mL gel). The agarose gel was run at 100 V for ~30 min. A UV box was used to visualize the digested pET-Sac vector (~4500 bp), which was excised from the gel using a razor blade. The digested pET-Sac vector was purified from the agarose gel using a Zymoclean gel DNA recovery kit. The concentration of the vector after purification was measured using a Thermo Scientific Nanodrop instrument. The purified digested pET-Sac linear vector was used in the subsequent ligation step.

The A β _(MCI-42) mutant DNA sequences were digested using *SacI* and *NdeI* restriction enzymes. Table 3.S3 details the restriction reaction conditions. Reagents were added in the order they are listed.

Table 3.S3. Double-digestion of the inserts.

Reagents	Amount
DNA sequence encoding mutation	20 μL of 5 ng/ μL DNA solution (100.0 ng in total)
10X CutSmart buffer	2.5 μL
H ₂ O	1.5 μL
<i>NdeI</i> restriction enzyme	0.5 μL (0.5 U)
<i>SacI</i> -HF restriction enzyme	0.5 μL (0.5 U)
Total	25.0 μL
Time	1.0 h
Temperature	37.0 °C
Heat inactivation	65.0 °C for 20 min

T4 ligation of the $A\beta_{(MCI-42)}$ mutant DNA sequence and the linear digested pET-Sac vector

The inserts and the vectors were ligated together using T4 ligase. Table 3.S4 details the T4 ligation reaction conditions. Reagents were added in the order they are listed.

Table 3.S4. T4 ligation of the inserts and the vectors.

Reagents	Amount	
	Insert:Vector = 0:1 (molar ratio) (negative control)	Insert:Vector = 5:1 (molar ratio)
Vector	9.1 μL of 6.6 ng/ μL DNA solution (60.0 ng in total)	9.1 μL of 6.6 ng/ μL DNA solution (60.0 ng in total)
Insert	---	2.5 μL of 4.0 ng/ μL DNA solution (10.0 ng in total)
10X T4 DNA ligase reaction buffer	2.0 μL	2.0 μL
T4 DNA ligase	1.0 μL	1.0 μL
H ₂ O	7.9 μL	5.4 μL

Total	20.0 μ L	20.0 μ L
Ligation time	10 min	
Temp	22.0 $^{\circ}$ C (room temperature)	
Heat inactivation	65.0 $^{\circ}$ C for 10 min	

2 μ L of the ligation reaction mixture was then transformed into TOP10 Ca²⁺-competent *E. coli* using the heat shock method. The cell cultures were spread on LB agar plates containing carbenicillin (50 mg/L). Single colonies were picked to inoculate 5 mL of overnight cultures in LB media with carbenicillin (50 mg/L). The plasmids were extracted from TOP10 cells using Zymo ZR plasmid miniprep kit. The concentration of the plasmids was measured through Thermo Scientific NanoDrop spectrophotometer. The DNA sequences of the recombinant A β _(MCI-42) plasmid was verified by DNA sequencing.

Bacterial expression of A β _(M1-42) mutant peptides

Transformation and expression of A β _(M1-42) mutant peptides

All liquid cultures were performed in culture media (LB broth containing 50 mg/L carbenicillin and 34 mg/L chloramphenicol). A β _(MCI-42) mutant plasmid was transformed into BL21 DE3 PLYS Star Ca²⁺-competent *E. coli* through heat shock method. The cell cultures were spread on LB agar plates containing carbenicillin (50 mg/L) and chloramphenicol (34 mg/L). Single colonies were picked to inoculate 5 mL of culture media for overnight culture. [A glycerol stock of BL21 DE3 PLYS Star Ca²⁺-competent *E. coli* bearing the plasmids was made, and the future expressions were started by inoculating culture media with an aliquot of the glycerol stock.]

The next day, all 5 mL of the overnight culture were used to inoculate 1 L of culture media. After inoculation, the culture was shaken at 225 rpm at 37 °C until the cell density reached an OD₆₀₀ of approximately 0.45. Protein expression was then induced by the addition of isopropyl β-D-1-thiogalactopyranoside (IPTG) to a final concentration of 0.1 mM, and the cells were shaken at 225 rpm at 37 °C for 4 h with IPTG. The cells were then harvested by centrifugation at 4000 rpm using a JA-10 rotor (2800 x g) at 4 °C for 25 min, and the cell pellets were then stored at -80°C.

Cell lysis, inclusion body preparation, and disulfide bond formation by DMSO

To lyse the cells, the cell pellet was resuspended in 20 mL of buffer A (10 mM Tris/HCl, 1 mM EDTA, pH 8.0) and sonicated for 2 min on ice (50% duty cycle) until the lysate appeared homogenous. The lysate was then centrifuged for 25 min at 16000 rpm using a JA-18 rotor (38000 x g) at 4°C. The supernatant was removed, and the pellet was resuspended in buffer A, sonicated and centrifuged as described above. The sonication and centrifugation steps were repeated three times. After the last round of sonication and centrifugation, the supernatant was removed, the remaining pellet was resuspended in 15 mL of freshly prepared buffer B (8 M urea, 10 mM Tris/HCl, 1 mM EDTA, pH 8.0), and was sonicated as described above, until the solution became clear. The solution was diluted with 10 mL of buffer A, and 5 mL of DMSO was added to the solution. The resulting mixture (30 mL) was incubated on a shaker at room temperature for 2-6 days.

Purification of A β _(M1-42) mutant peptides

The reaction mixture was titrated with 1M NaOH to a pH of ~10.5, and was filtered through a Fisher Brand 0.22 μ m non-sterile hydrophilic PVDF syringe filter (Catalog No. 09-719-00). After filtering, the solution was titrated with 1M HCl to pH ca. 8.0. Successful expression of the A β _(M1-42) mutant peptide was confirmed by analytical reverse-phase HPLC as follows: A 20- μ L sample of the above solution was injected onto an Agilent 1200 instrument equipped with a Phenomenex Aeris PEPTIDE 2.6u XB-C18 column with a Phenomenex SecurityGuard ULTRA cartridges guard column for C18 column. HPLC grade acetonitrile (ACN) and 18 M Ω deionized water, each containing 0.1% trifluoroacetic acid, were used as the mobile phase. The sample was eluted at 1.0 mL/min with a 5–100% acetonitrile gradient over 20 min at 35 °C.

A β _(M1-42) mutant peptides were then purified by preparative reverse-phase HPLC equipped with an Agilent ZORBAX 300SB-C8 semi-preparative column (9.4 x 250 mm) with a ZORBAX 300SB-C3 preparative guard column (9.4 x 15 mm). The C8 column and the guard column were heated to 80 °C in a water bath. HPLC grade acetonitrile (ACN) and 18 M Ω deionized water, each containing 0.1% trifluoroacetic acid, were used as the mobile phase at a flow-rate of 5 mL/min. The peptide solution was split into two ca. 15 mL batches and purified in two separate runs, with four injections in each run. In each run, the peptide was loaded onto the column by flowing 20% ACN for 15 min and then eluted with a gradient of 20–40% ACN over 20 min. Fractions containing the monomer generally eluted from 34% to 38% ACN. After the peptide was collected, the column was washed by flushing with 100% isopropanol for 15 minutes. This cleaning procedure ensures elution of the peptide that is retained in the column and avoids problems of cross-contamination between runs.

The purity of each fraction was assessed using analytical reverse-phase HPLC. A 20- μ L sample was injected onto the analytical HPLC. The sample was eluted at 1.0 mL/min with a 5–100% acetonitrile gradient over 20 min, at 35 °C. Pure fractions were combined and the purity of the combined fractions were checked using analytical HPLC. The combined fractions were concentrated by rotary evaporation to remove ACN, and then frozen with dry ice, liquid nitrogen, or a -80 °C freezer. [It is recommended to combine and freeze the purified fractions within 5 hours after purification to avoid oxidation of methionine.] The frozen sample was then lyophilized to give a fine white powder.

NaOH treatment and peptide concentration determination

The lyophilized peptide was then dissolved in 2 mM NaOH to achieve a concentration of ~0.5 mg/mL. The pH was adjusted by addition of 0.1 M NaOH to give a solution of pH ~10.5. The sample was sonicated in a water ultrasonic bath at room temperature for 1 min or until the solution became clear. The concentration of the peptide was determined by absorbance at 280 nm using the extinction coefficient (ϵ) for tyrosine of 1490 $\text{M}^{-1}\text{cm}^{-1}$ ($c = A/1490$). The peptide solution was then aliquoted into 0.020 μ mol aliquots in 0.5 mL microcentrifuge tubes. The aliquots were lyophilized and then stored in a desiccator at -20 °C for future use.

SDS-PAGE

The concentrations of the peptide working solutions vary for different SDS-PAGE assays. Here we provide a general procedure for the SDS-PAGE assays we conducted in this chapter. For the sample preparation, a 0.02 μ mol aliquot of peptide was dissolved in 208.4 μ L of deionized

water to give a 96 μM peptide stock solution. A 20 μL aliquot of the 96 μM peptide stock solution and 4 μL of 6X SDS-PAGE loading buffer (100 mM Tris buffer at pH 6.8, 20% (v/v) glycerol, and 4% w/v SDS) was then combined to give a 24 μL of peptide working solution with a concentration of 80 μM . A 10 μL aliquot of the working solution was run on a 16% polyacrylamide gel with a 4% stacking polyacrylamide gel. The gels were run at a constant 90 volts at room temperature.

Staining with silver nitrate was used to visualize peptides in the SDS-PAGE gel. Briefly, the gel was first rocked in fixing solution (50% (v/v) methanol and 5% (v/v) acetic acid in deionized water) for 20 min. Next, the fixing solution was discarded and the gel was rocked in 50% (v/v) aqueous methanol for 10 min. Next, the 50% methanol was discarded and the gel was rocked in deionized water for 10 min. Next, the water was discarded and the gel was rocked in 0.02% (w/v) sodium thiosulfate in deionized water for 1 min. The sodium thiosulfate was discarded and the gel was rinsed twice with deionized water for 1 min (2X). After the last rinse, the gel was submerged in chilled 0.1% (w/v) silver nitrate in deionized water and rocked at 4 $^{\circ}\text{C}$ for 20 min. Next, the silver nitrate solution was discarded and the gel was rinsed with deionized water for 1 min (2X). To develop the gel, the gel was incubated in developing solution (2% (w/v) sodium carbonate, 0.04% (w/v) formaldehyde until the desired intensity of staining was reached (~1–3 min). When the desired intensity of staining was reached, the development was stopped by discarding the developing solution and submerging the gel in 5% aqueous acetic acid.

Thioflavin T (ThT) fibrillization assay

ThT Solution Preparation. The ThT solution was freshly prepared and placed on ice before

use. Briefly, a solution of ca. 40 μM ThT was prepared in a 1x PBS buffer (pH 7.4). The concentration of ThT in the solution was determined by UV absorbance at 412 nm using an estimated extinction coefficient (ϵ) of $36000 \text{ M}^{-1}\text{cm}^{-1}$ and adjusted to 41.7 μM . The solution was filtered through a 0.22 μm nylon syringe filter. The ThT solution was stored on ice and protected from light.

Peptide Working Solution Preparation. A 0.02 μmol aliquot of A β peptide was dissolved in 500 μL of ThT solution to give a working solution with final peptide concentration of 40 μM and ThT concentration of 40 μM . The peptide working solution was stored on ice and protected from light.

ThT Fluorescence Assay Setup. ThT fluorescence assays were conducted in Corning® 96-well half area black/clear flat bottom polystyrene nonbinding surface (NBS) microplates (product number: 3881). A 100- μL aliquot of the working solution was immediately transferred to each of five wells of 96-well plate, and the plate was kept at room temperature. ThT solution was transferred to each of five wells of 96-well plate as negative control. The 96-well plate was sealed with adhesive plate sealer. The 96-well plate was immediately inserted into a Thermo Fisher Scientific Varioskan Lux microplate reader. The plate was incubated at 37 °C without shaking and the ThT fluorescence was monitored (440 nm excitation, 485 nm emission, 5 nm bandwidth) over 24 hours using the bottom-read mode.

Dynamic light scattering (DLS)

A 30 μM solution of A β peptide was freshly prepared in 10 mM sodium phosphate buffer (pH 7.4) , or incubated in the buffer at 37 °C for 24 hours with 225 rpm shaking. The dynamic

light scattering (DLS) experiments were performed in disposable cuvettes using the Malvern Zetasizer μ V instrument at 25 °C. Scattering data were collected as an average of 10 scans for each measurement.

Circular dichroism (CD)

A 30 μ M solution of A β peptide was freshly prepared in 10 mM sodium phosphate buffer with or without detergent (pH 7.4). CD spectra were acquired on a Jasco J-810 circular dichroism spectropolarimeter at room temperature. The instrumental parameters to record the CD spectra were: 260 nm to 190 nm measurement range, 1 nm data pitch, 2 nm band width, standard sensitivity, 50 nm/min of scanning speed. The data were averaged over 3 accumulations with 21-point smoothing. The CD spectra were analyzed using secondary structure analysis server BeStSel.

Mass spectrometry

Matrix-assisted laser desorption/ionization mass spectrometry (MALDI-MS) was performed using an AB SCIEX TOF/TOF 5800 System. 0.5 μ L of sinapinic acid (SA) or 2,5-dihydroxybenzoic acid (DHB) was dispensed onto a MALDI sample support, followed by the addition of 0.5 μ L peptide sample. The mixture was allowed to air-dry. All analyses were performed in positive reflector mode, collecting data with a molecular weight range of 1500–8000 Da or 1800–10000 Da.

Size exclusion chromatography-mass spectrometry (SEC-MS) was performed using a Waters Synapt G2 system. A β peptide was dissolved in 10 mM ammonium acetate buffer with or

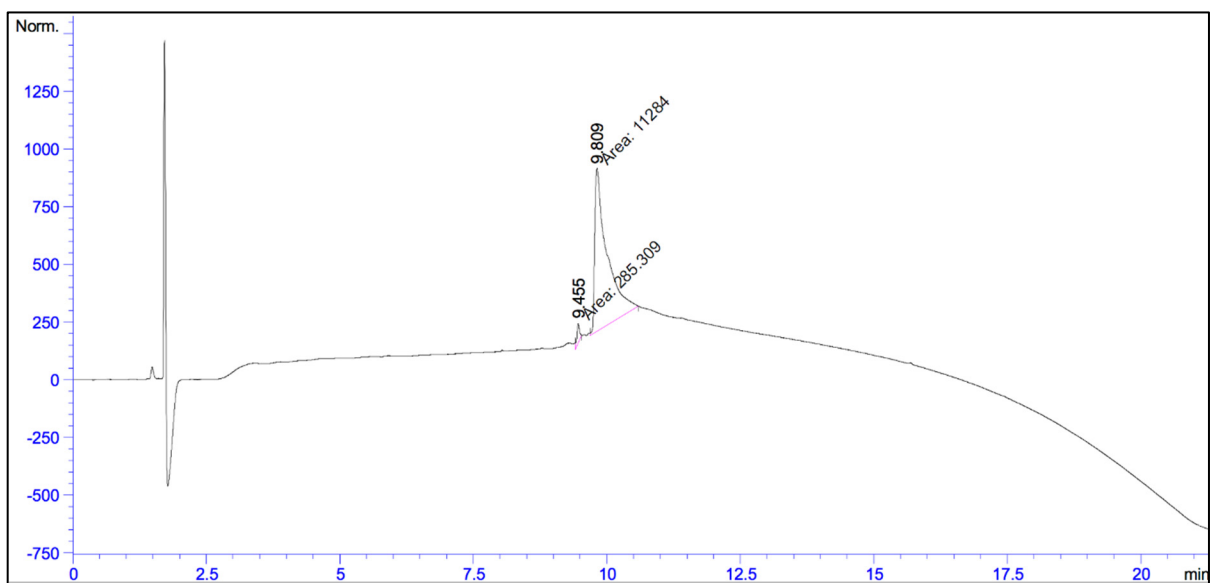
without 0.4 mM n-Dodecyl β -D-maltoside (DDM) (pH 7.3) to a final peptide concentration of 0.25 mg/mL and incubated at 37 °C for 2 hours. 2 μ g of A β peptide was injected on the SEC column and the SEC was run in 1:1 ammonium formate: acetonitrile running buffer (pH 10.0).

Ion mobility mass spectrometry (IM-MS) was performed using a Waters Synapt G2 system. A β peptide was dissolved in 200 mM ammonium acetate buffer containing 0.3 mM DDM (pH 7.4) to a final concentration of 25 μ M. 40 μ L of the 25 μ M peptide solution was then immediately injected on the IM-MS system.

Transmission electron microscopy (TEM)

TEM images of A β peptide were taken with a JEM-2100F transmission electron microscope (JEOL, Peabody, MA, USA) at 200 kV with an electron dose of approximately 15 e⁻/Å². The microscope was equipped with Gatan K2 Summit direct electron detector (Gatan, Pleasanton, CA, USA) at 15,000x or 25,000x magnification. The sample was cooled at liquid nitrogen temperature through the cryostage. Contrast and brightness of the images were adjusted as appropriate.

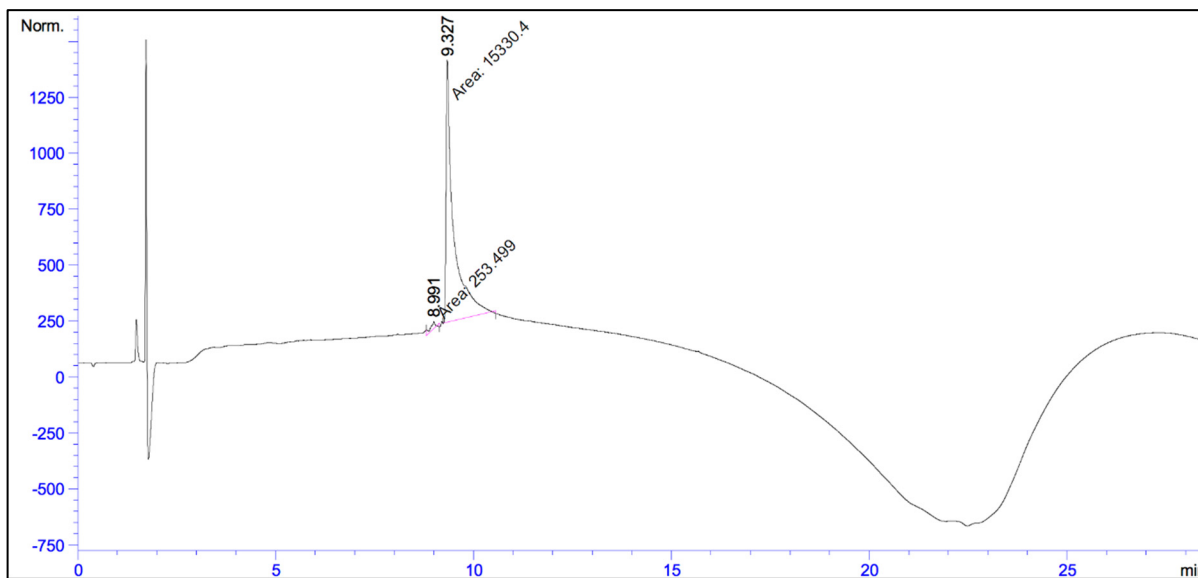
Characterization Data and Additional Figures



Signal 1: VWD1 A, Wavelength=214 nm

Peak #	RetTime [min]	Type	Width [min]	Area mAU *s	Height [mAU]	Area %
1	9.455	MM	0.0544	285.30859	87.47525	2.4661
2	9.809	MM	0.2659	1.12840e4	707.17889	97.5339
Totals :				1.15693e4	794.65414	

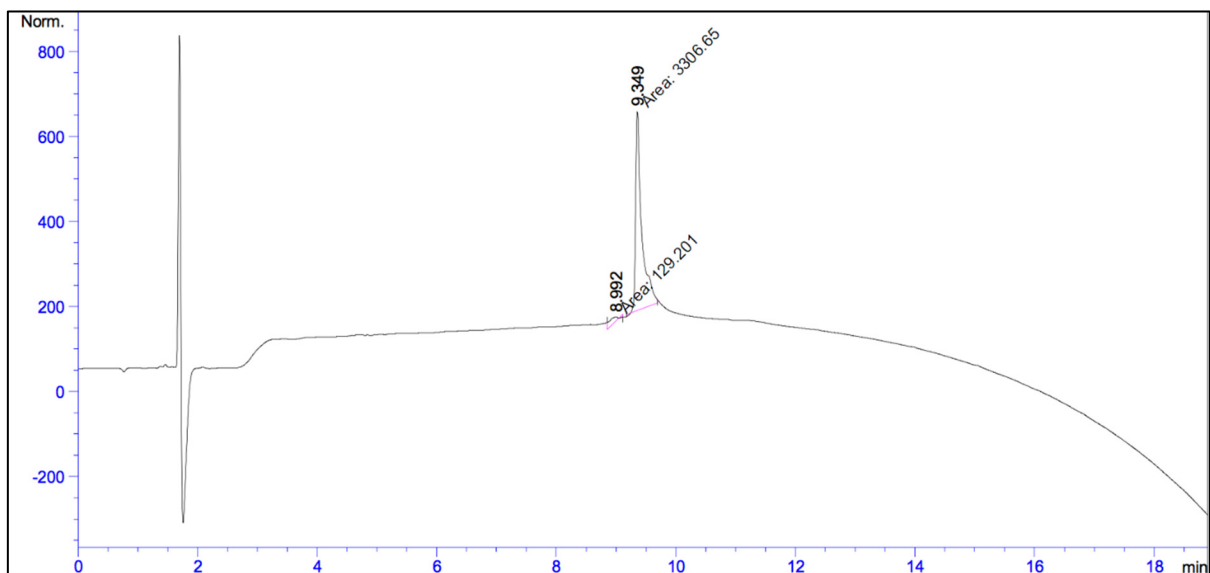
Figure 3.S3. An analytical HPLC trace of A β _{C21C30} peptide. Temperature: 35.0 °C. Sample purity: 97.5 %.



Signal 1: VWD1 A, Wavelength=214 nm

Peak #	RetTime [min]	Type	Width [min]	Area mAU *s	Height [mAU]	Area %
1	8.991	MM	0.1461	253.49934	28.90966	1.6267
2	9.327	MM	0.2182	1.53304e4	1171.01709	98.3733
Totals :				1.55839e4	1199.92675	

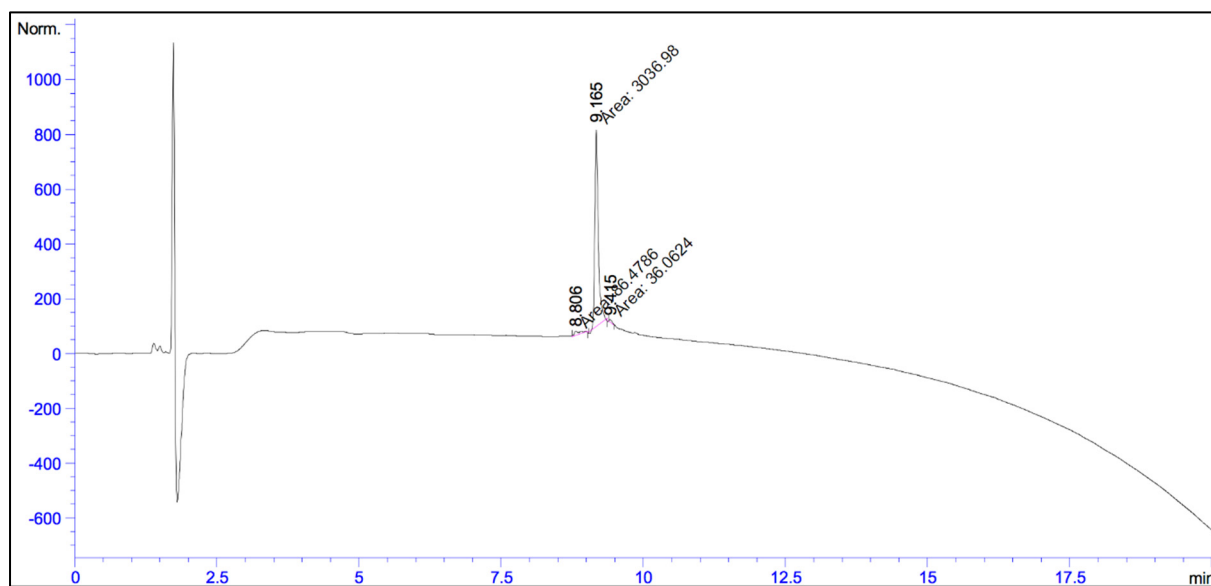
Figure 3.S4. An analytical HPLC trace of A β _{C21C32} peptide. Temperature: 35.0 °C. Sample purity: 98.3 %.



Signal 1: VWD1 A, Wavelength=214 nm

Peak #	RetTime [min]	Type	Width [min]	Area mAU *s	Height [mAU]	Area %
1	8.992	MM	0.1710	129.20132	9.55200	3.7604
2	9.349	MM	0.1173	3306.64746	469.76645	96.2396
Totals :				3435.84879	479.31845	

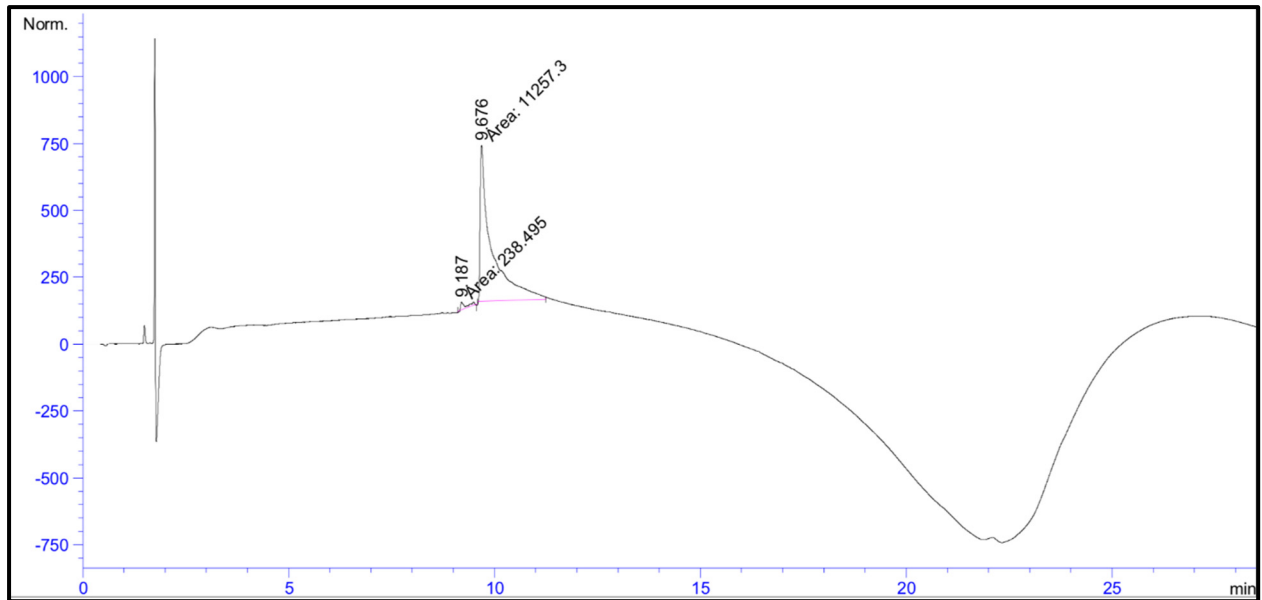
Figure 3.S5. An analytical HPLC trace of A β _{C24C29} peptide. Temperature: 55.0 °C. Sample purity: 96.2 %.



Signal 1: VWD1 A, Wavelength=214 nm

Peak #	RetTime [min]	Type	Width [min]	Area mAU *s	Height [mAU]	Area %
1	8.806	MM	0.0954	86.47856	15.11022	2.7371
2	9.165	MM	0.0694	3036.98242	728.98315	96.1215
3	9.415	MM	0.0585	36.06243	10.27097	1.1414
Totals :				3159.52341	754.36435	

Figure 3.S6. An analytical HPLC trace of A β _{C21C31} peptide. Temperature: 55.0 °C. Sample purity: 96.1 %.



Signal 1: VWD1 A, Wavelength=214 nm

Peak #	RetTime [min]	Type	Width [min]	Area mAU *s	Height [mAU]	Area %
1	9.187	MM	0.1343	238.49503	29.60134	2.0746
2	9.676	MM	0.3206	1.12573e4	585.14197	97.9254
Totals :				1.14958e4	614.74330	

Figure 3.S7. An analytical HPLC trace of A β _{C18C33} peptide. Temperature: 35.0 °C. Sample purity: 97.9 %.

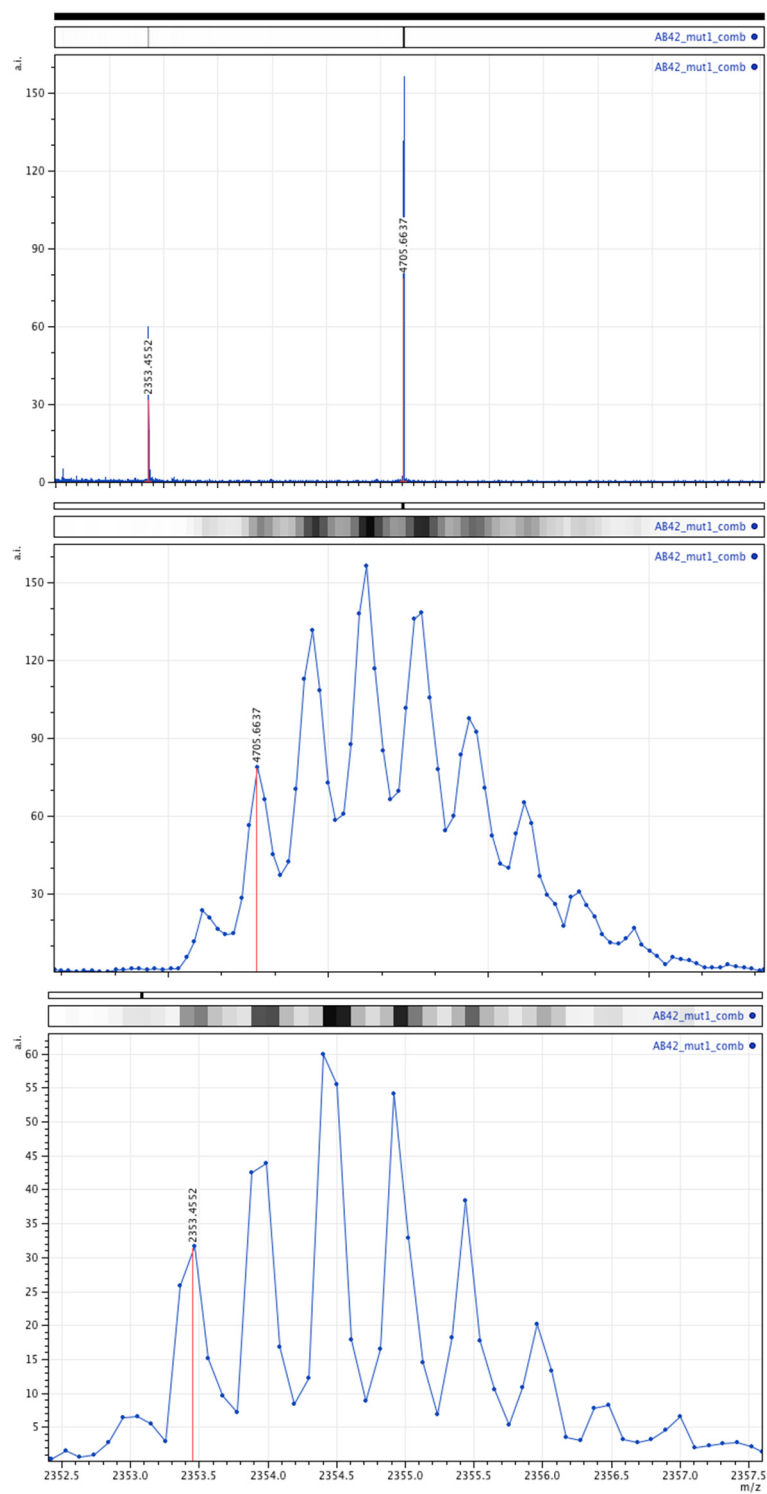


Figure 3.S8. MALDI-TOF mass spectra of Aβ_{C21C30} peptide. Positive reflector mode. Matrix: 2,5-dihydroxybenzoic acid. Exact mass: 4704.2; Observed [M+H]⁺: 4705.6637; Observed [M+2H]²⁺: 2353.4552.

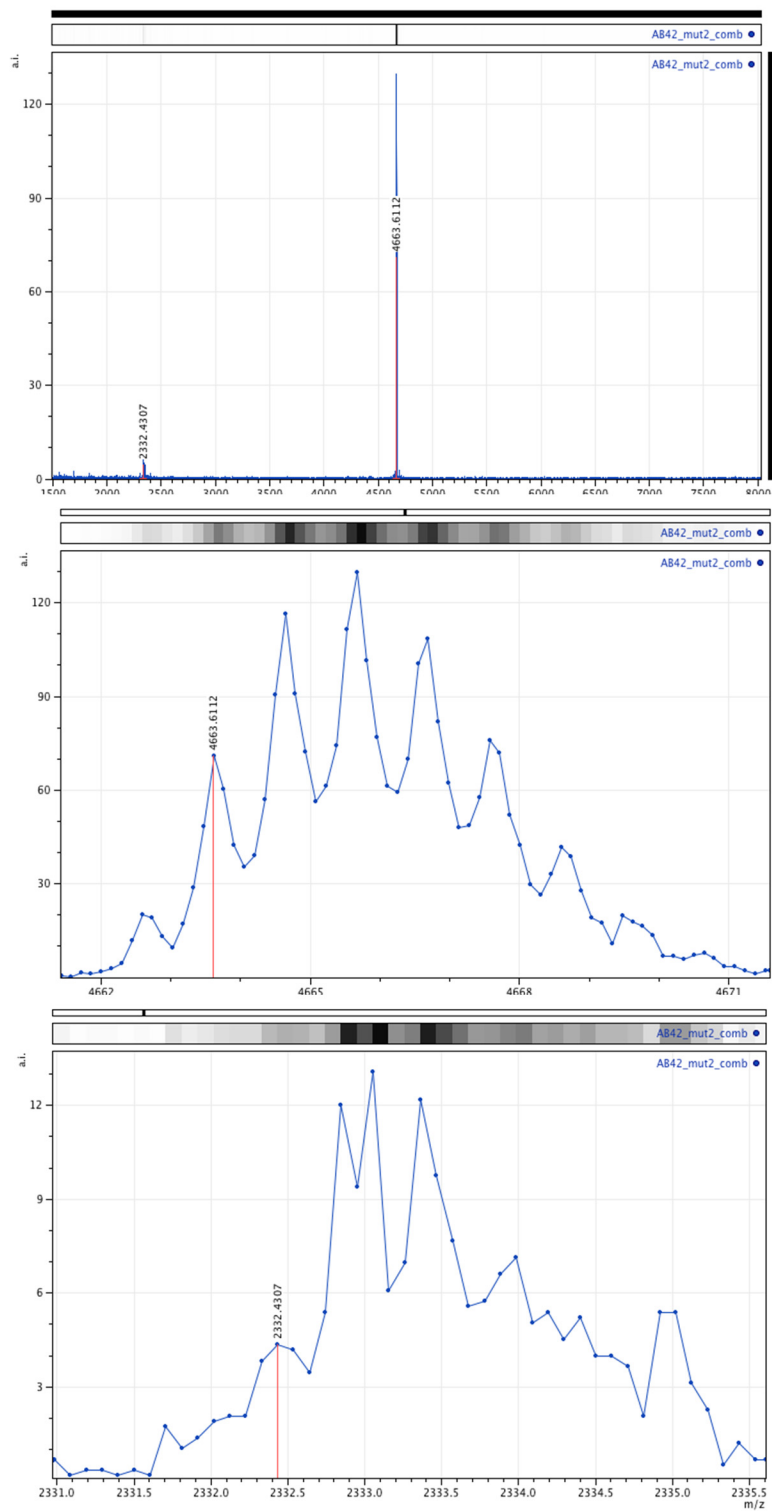


Figure 3.S9. MALDI-TOF mass spectra of Aβ_{C21C32} peptide. Positive reflector mode.

Matrix: 2,5-dihydroxybenzoic acid. Exact mass: 4662.2; Observed [M+H]⁺: 4663.6112; Observed [M+2H]²⁺: 2332.4307.

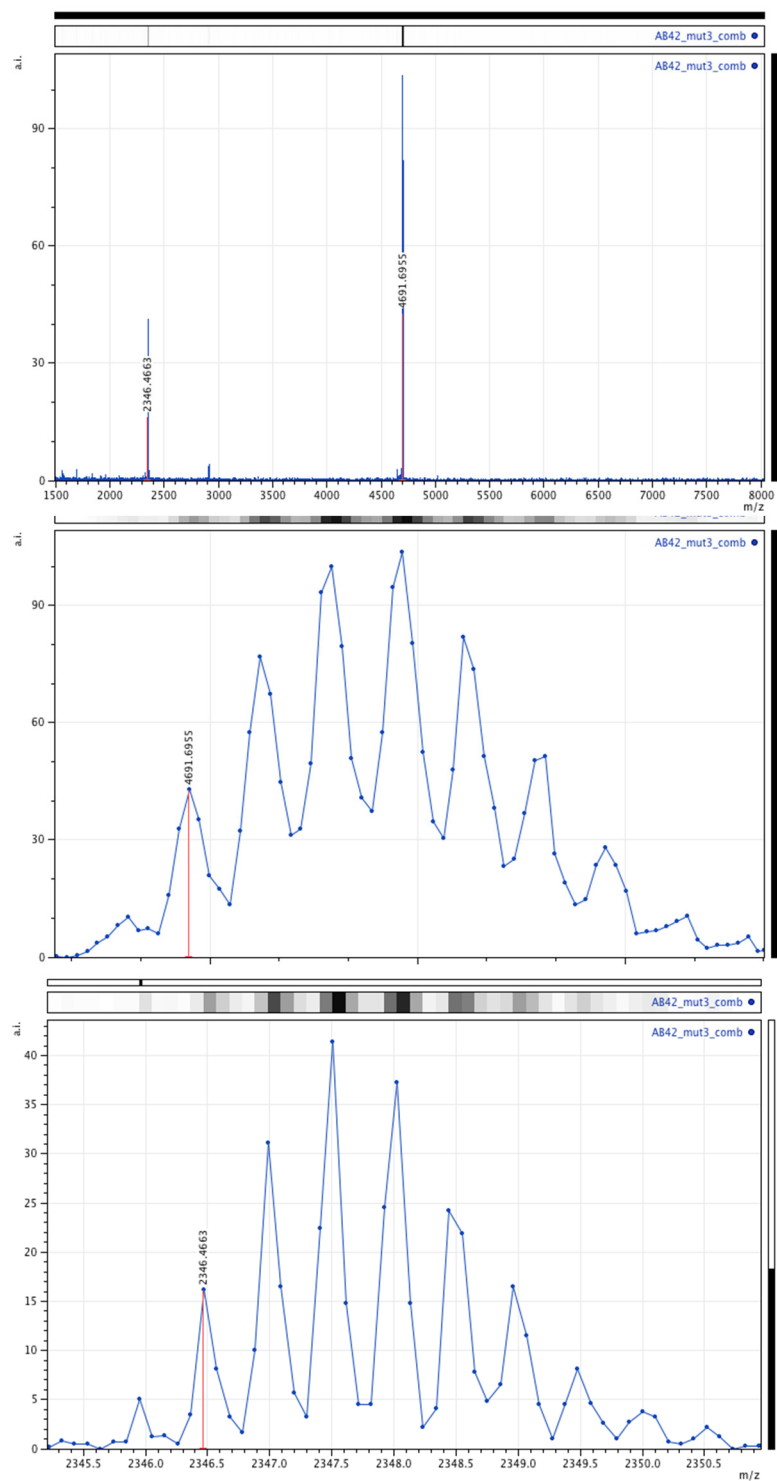


Figure 3.S10. MALDI-TOF mass spectra of Aβ_{C24C29} peptide. Positive reflector mode. Matrix: 2,5-dihydroxybenzoic acid. Exact mass: 4690.2; Observed [M+H]⁺: 4691.6955; Observed [M+2H]²⁺: 2346.4663.

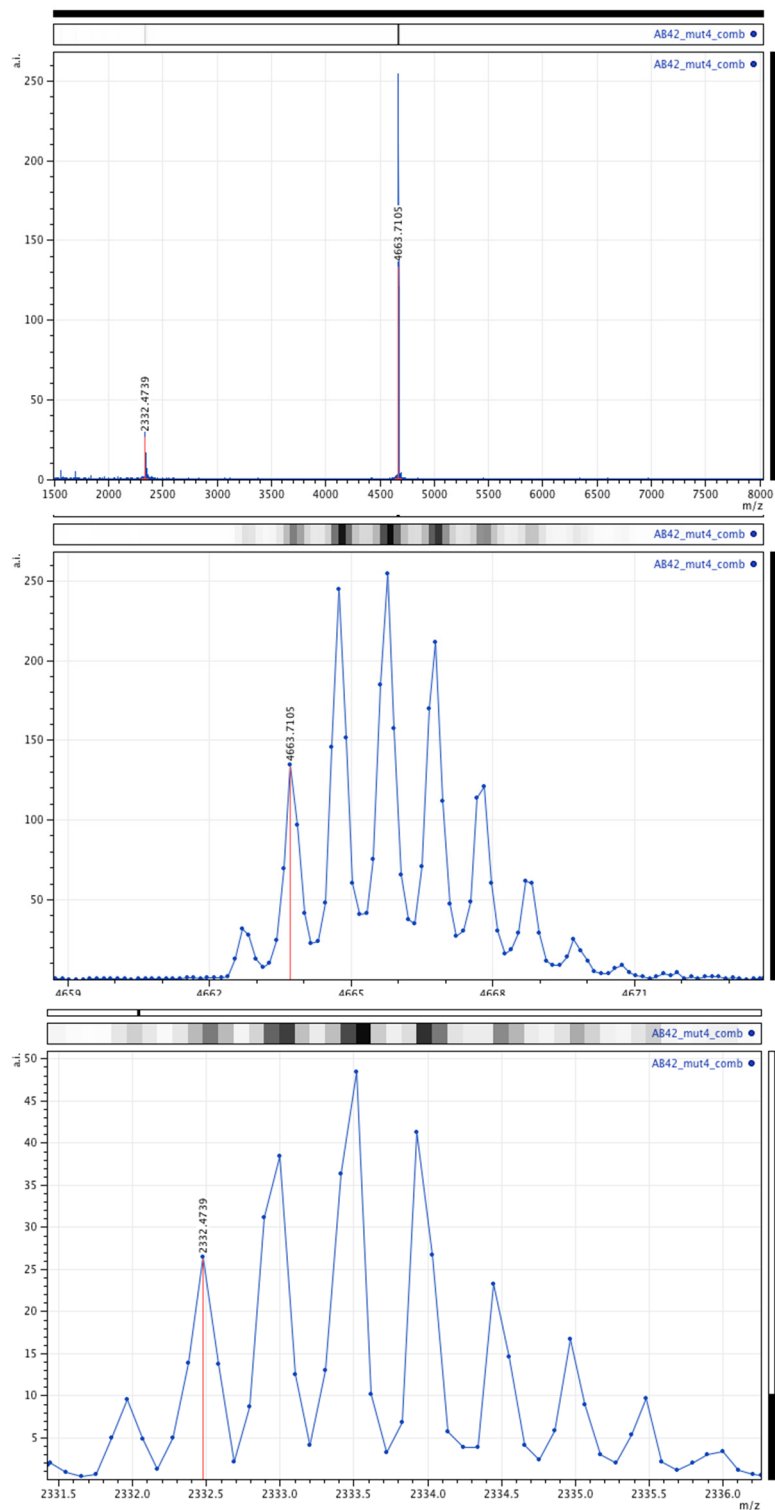


Figure 3.S11. MALDI-TOF mass spectra of Aβ_{C21C31} peptide. Positive reflector mode.

Matrix: 2,5-dihydroxybenzoic acid. Exact mass: 4662.2; Observed [M+H]⁺: 4663.7105; Observed [M+2H]²⁺: 2332.4739.

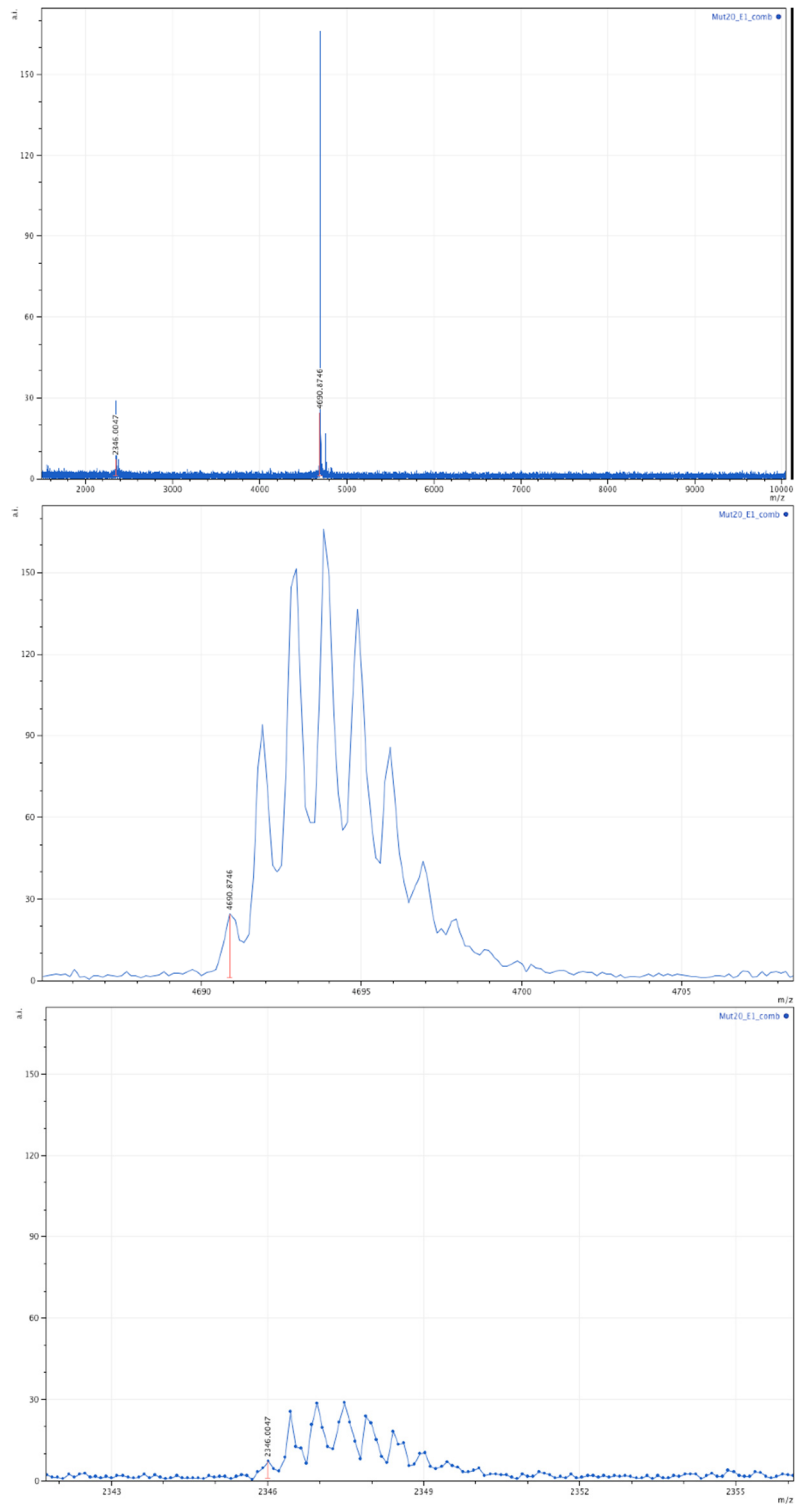


Figure 3.S12. MALDI-TOF mass spectra of A β _{C18C33} peptide. Positive reflector mode.

Matrix: 2,5-dihydroxybenzoic acid. Exact mass: 4690.2; Observed [M+H]⁺: 4690.8746; Observed [M+2H]²⁺: 2346.0047.

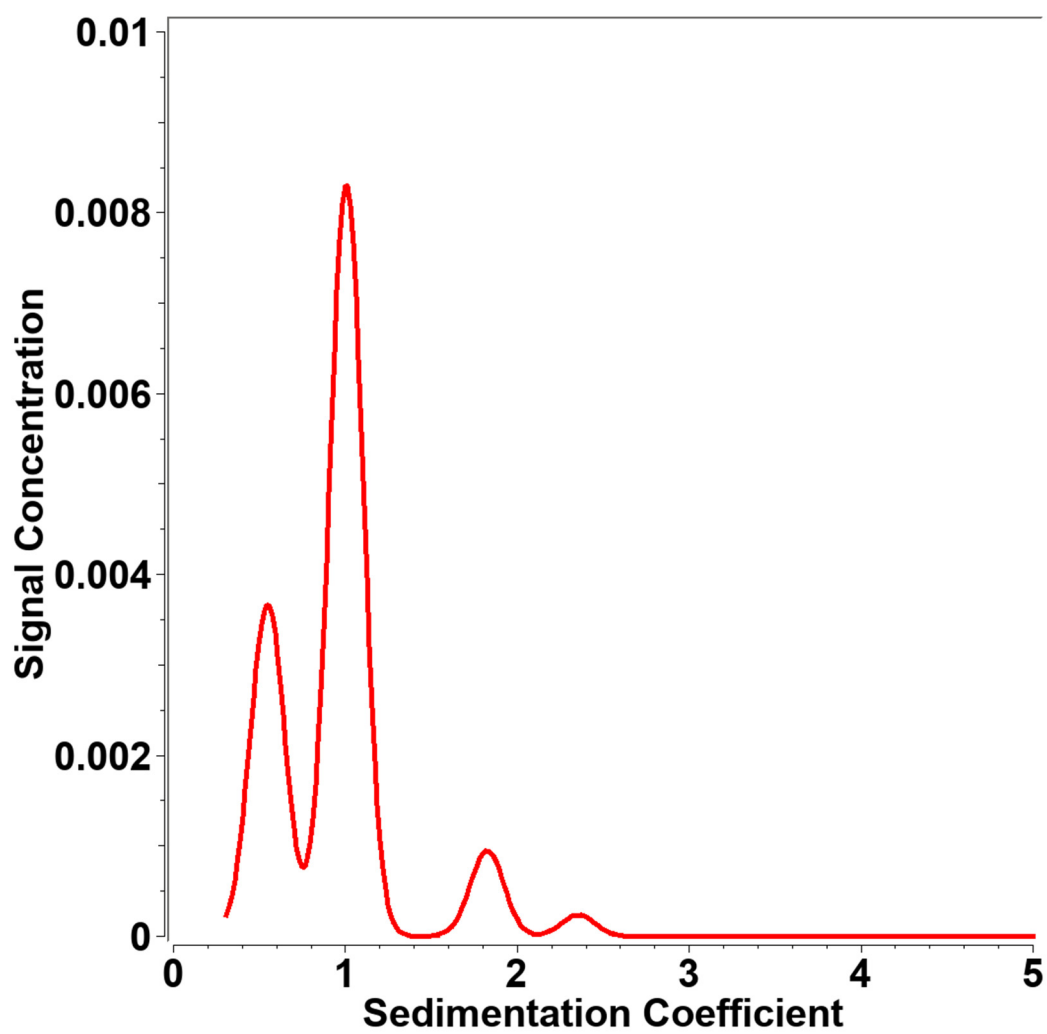


Figure 3.S13. Analytical ultracentrifugation studies of Aβ_{C18C33} peptide. The studies were performed by collaborator Dr. Borries Demeler.

Chapter 4^a

Structure-Based Drug Design of an Inhibitor of the SARS-CoV-2 Main Protease

Introduction

SARS-CoV-2 is a highly infectious virus that causes COVID-19, a serious respiratory infection that has caused over 178 million infections and over 3.8 million deaths worldwide as of June 2021.¹ SARS-CoV-2 causes infected cells to express a main protease (M^{pro} or 3CL protease) that is responsible for site-specifically cleaving the polyprotein, which is translated from viral mRNA within human cells. The proteolytic activity of M^{pro} is essential for the virus to generate the individual proteins that are necessary for replication and infection. The essential role of M^{pro}, as well as the success of HIV protease inhibitors in the treatment of HIV/AIDS, make M^{pro} an attractive therapeutic target to treat COVID-19.²⁻⁷

Proteases are enzymes that cleave polypeptide chains, hydrolyzing an amide bond within the polypeptide chain. Once the polypeptide is bound within the active site of the protease, the

^a This chapter is adapted from Zhang, S.; Krumberger, M.‡; Morris, M. A.‡; Parrocha, C. M. T.; Kreutzer, A. G.; Nowick, J. S. *Eur. J. Med. Chem.* **2021**, *218*, 11390.

scissile amide bond is hydrolyzed to generate a carboxylic acid and amine (Figure 4.1A). The binding pockets of a protease are referred to as subsites, denoted by “S”. Typically, each subsite interacts with a specific side chain of the polypeptide substrate, denoted by “P”. The position at which the polypeptide substrate is cleaved determines the assignment of prime or no-prime notation. Prime notation refers to the C-terminal side and no-prime notation refers to the *N*-terminal side of the polypeptide and corresponding pockets (Figure 4.1B).

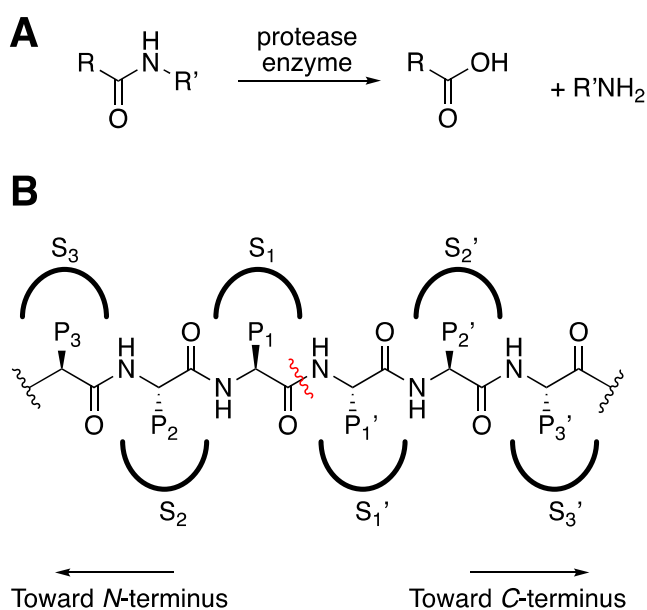


Figure 4.1. A: Amide bond hydrolysis by a protease enzyme. B: Binding of a protease to a polypeptide substrate. The side chains of the protein (P1, P2, P3, etc. and P1', P2', P3', etc.) fit into pockets of the enzyme (S1, S2, S3, etc. and S1', S2', S3', etc.). The scissile bond is designated with a wavy red line. This figure was prepared by Dr. Michael Morris.

SARS-CoV-2 M^{pro} is a member of the class of enzymes called cysteine proteases. These proteases usually contain a catalytic dyad of cysteine and histidine residues in the active site, which catalyze the cleavage of polypeptides, as shown below. The histidine deprotonates the cysteine thiol to give a nucleophilic thiolate, which adds to the amide carbonyl of the substrate to form a tetrahedral intermediate. The tetrahedral intermediate then breaks down to give a thiol ester and

an amine. The electrophilic thiol ester is then hydrolyzed by water to give a carboxylic acid, thus completing the cleavage of the polypeptide substrate and regenerating the active enzyme (Figure 4.2).

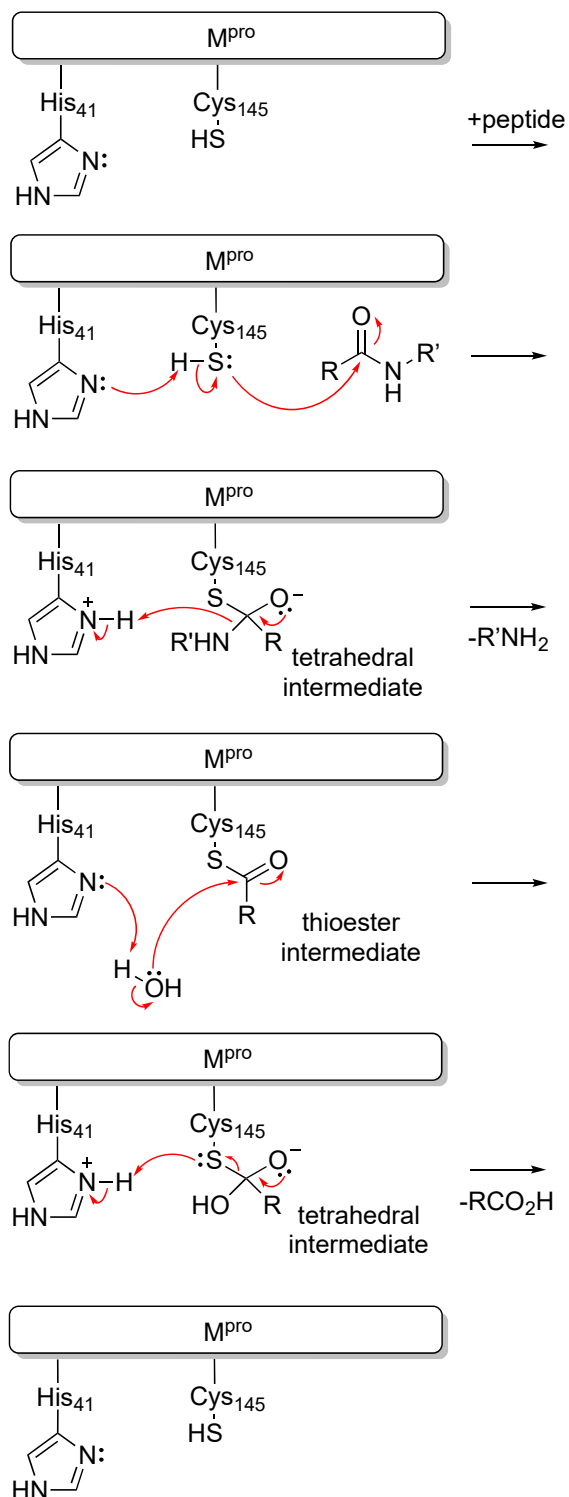


Figure 4.2. Proteolysis mechanism by the catalytic dyad of M^{pro}. This figure was prepared by Dr. Michael Morris.

In this chapter, we will use the X-ray crystallographic structure of the homologous SARS-CoV M^{pro} bound to a protein substrate to recapitulate the design of a cyclic peptide inhibitor of the SARS-CoV-2 M^{pro}.⁸ We will first use the molecular modeling software UCSF Chimera to visualize the X-ray crystallographic structure of the SARS-CoV M^{pro} bound to the protein substrate.⁹ We will then modify the protein substrate to create a model of the cyclic peptide inhibitor within the SARS-CoV M^{pro}. Finally, we will use AutoDock Vina to evaluate this model, by docking the inhibitor to SARS-CoV M^{pro} and then to SARS-CoV-2 M^{pro}.¹⁰ We have selected these software packages, because they can be downloaded without cost and are easy to learn.^{11–13} These and other molecular modeling studies helped our laboratory decide to pursue the synthesis of the cyclic peptide and experimentally evaluate its promise as an inhibitor of SARS-CoV-2 M^{pro}. In an accompanying paper, we describe the synthesis of the cyclic peptide and the experimental validation as an inhibitor of SARS-CoV-2 M^{pro}.⁸

Here, we provide the rationale and then overview the process of designing the inhibitor with UCSF Chimera and evaluating it with AutoDock Vina. In the supporting information, we provide an illustrated step-by-step protocol showing the inhibitor design process to teach others how to execute the design process. We anticipate this chapter will help students and scientists use free software to design their own drug candidates for COVID-19 and the coronaviruses that will cause future pandemics.

Results and Discussion

Selecting a starting structure for inhibitor design. The design of the cyclic peptide inhibitor begins with the X-ray crystallographic structure of SARS-CoV M^{pro} (C145A) [Protein

Data Bank (PDB) ID: 5B6O].¹⁴ The SARS-CoV M^{pro} is 96% identical to the SARS-CoV-2 M^{pro}, and thus provides a good starting point for the design of inhibitors of SARS-CoV-2 M^{pro}.⁷ In this crystal structure, the C-terminal fragment of one M^{pro} molecule extends into the active site of an adjacent M^{pro} molecule. The C-terminal fragment would normally be cleaved by SARS-CoV M^{pro}, and thus the inactive C145A mutant provides a snapshot of the enzyme bound to one of its substrates. Molecules that mimic the C-terminal fragment, but are resistant to proteolysis, may serve as inhibitors that block viral replication.

Modifying the C-terminal fragment of SARS-CoV M^{pro} to create a cyclic peptide inhibitor. We begin the procedures by displaying the C-terminal fragment of the M^{pro} (substrate) as sticks and the adjacent M^{pro} protein as a van der Waals surface, to visualize how the substrate fits into the binding pockets of the protein active site. The substrate adopts a kinked conformation, in which the phenyl group of Phe 309 points toward the backbone of Phe 305. The proximity of Phe 309 and Phe 305 inspired us to connect the phenyl group of the Phe 309 with the backbone of Phe 305 to form a cyclic peptide (Figure 4.3). By cyclizing the linear substrate, we aim to lock the peptide substrate into its bound conformation and increase its stability toward proteolysis. Furthermore, cyclic peptides often exhibit greater cell permeability than the corresponding linear analogues, which is critical because M^{pro} constitutes an intracellular target.^{15–20}

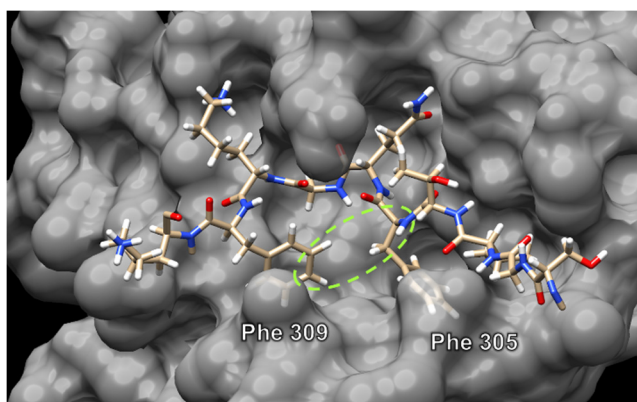
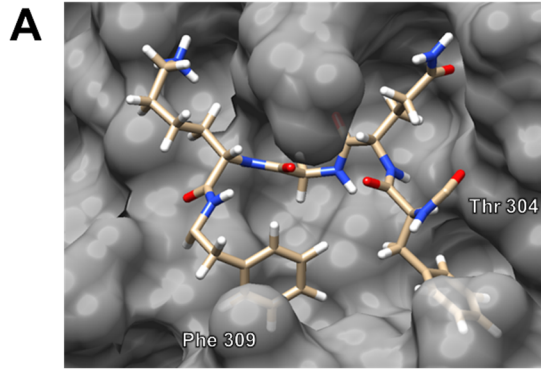


Figure 4.3. The interaction between the substrate (sticks) and the active site of the protein (grey surface). The green oval illustrates the concept of connecting the phenyl group of Phe 309 to the backbone of Phe 305.

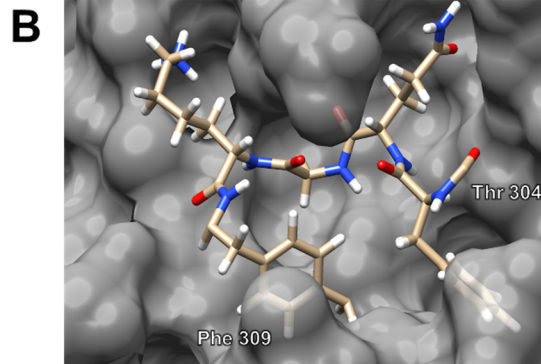
To create the cyclic peptide, we delete Ser 301, Gly 302, Val 303, Thr 304 (except for the carbonyl group), Lys 310, and the carbonyl group of Phe 309, as these fragments are not needed in the cyclic peptide (Figure 4.4A). We then add a methylene (CH₂) group at the *para* position of Phe 309 by building a tetrahedral methyl group (CH₃) in UCSF Chimera and then deleting one of the hydrogen atoms of the methyl group (Figure 4.4B).

We next prepare to connect the Thr 304 carbonyl carbon to the newly built CH₂ group, and thus cyclize the substrate. In UCSF Chimera, when the new bond is formed, it must not cross other atoms or bonds, otherwise subsequent structural minimization will fail. We rotate the backbone C α -N bond of Gln 306 to bring the Thr 304 carbonyl carbon close to the CH₂ group, to avoid crossing other atoms or bonds when building the new C-C bond (Figure 4.4C). We cyclize the substrate by building a C-C bond between the Thr 304 carbonyl carbon and the CH₂ carbon. In cyclizing the substrate, we have built an unnatural amino acid residue — [4-(2-aminoethyl)phenyl]-acetic acid (AEPA) — from Phe 309 and Thr 304. The resulting cyclic peptide contains a β -turn comprising Phe 305 and Gln 306 (Figure 4.4D). We envision that hydrogen bonding within this β -turn might provide additional conformational rigidity to the cyclic peptide.

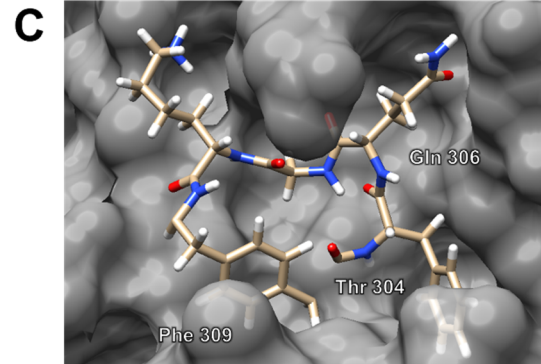
After Deleting Extra Fragments



Building a Methylene (CH₂) Group



Rotating the Backbone C–N Bond of Gln 306



Building a C–C Bond

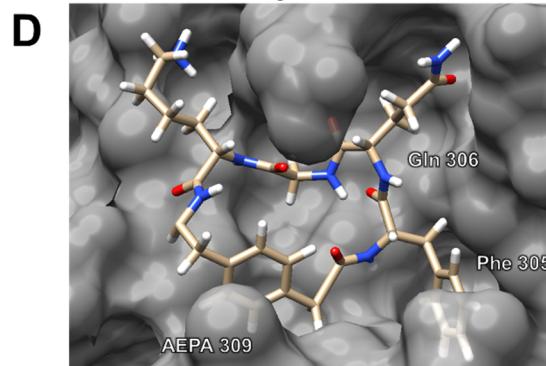


Figure 4.4. Building the cyclic peptide. A: The structure of the substrate after deleting extraneous fragments. B: Adding a CH₂ group at the *para* position of Phe 309. C: Rotating the backbone C α -N bond of Gln 306 to bring the Thr 304 carbonyl carbon close to the CH₂ group. D: Building a C-C bond between the Thr 304 carbonyl carbon and the CH₂ carbon.

Geometry optimization of the cyclic peptide inhibitor. At this point, the bond lengths, angles, and dihedral angles of the newly built cyclic peptide are not optimal. We are now ready to allow the cyclic peptide to relax to a low-energy conformation (local minimum) within the active site of the SARS-CoV M^{Pro}. We use the “minimize structure” tool to optimize the geometry of the cyclic peptide while holding the structure of M^{Pro} fixed.^a The minimized structure (Figure 4.5A) has more reasonable bond lengths, angles, and dihedral angles than the structure prior to minimization (Figure 4.4D), with Phe 305 and Gln 306 forming a hydrogen-bonded β -turn.

^a In preparing the structure for geometry optimization, hydrogens are added to the protein and the inhibitor. The addition of hydrogens causes the color of portions of the surface to change from grey to tan.

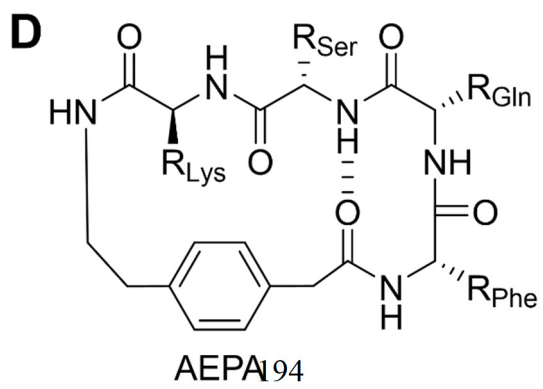
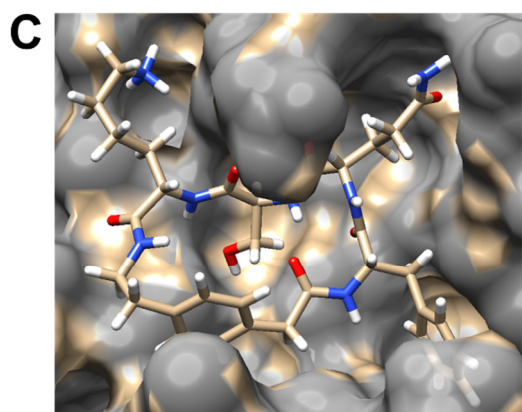
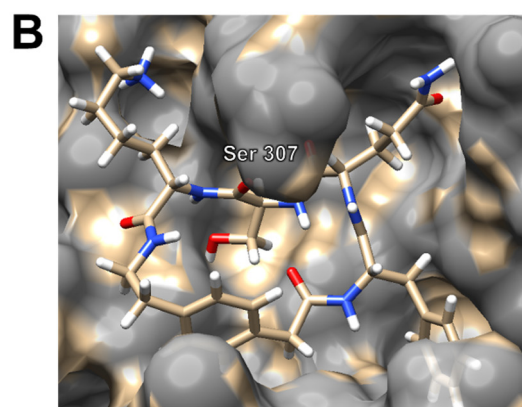
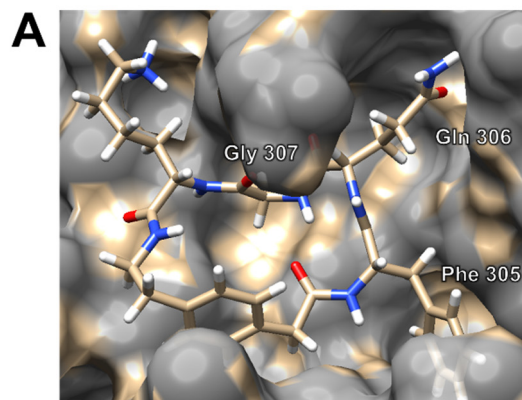


Figure 4.5. Geometry optimization of the cyclic peptide inhibitor. A: The structure of the Gly 307 cyclic peptide after geometry optimization.²¹ B: Gly 307 has been mutated to Ser. C: The structure of the Ser 307 cyclic peptide inhibitor after geometry optimization. D: The chemical structure of the Ser 307 cyclic peptide inhibitor.

To introduce additional conformational rigidity, we mutate Gly 307 to Ser, which is the most common residue at the P1' position of SARS-CoV-2 M^{pro} substrates (Figure 4.5B). UCSF Chimera allows this point mutation to be achieved with a single command. After the point mutation, we perform a second round of geometry optimization to clean up the structure and afford a hypothesized structure of the cyclic peptide inhibitor (Figure 4.5C). Figure 4.5D illustrates the chemical structure of the cyclic peptide inhibitor, which we term UCI-1 (University of California, Irvine Coronavirus Inhibitor-1).⁸

Docking the inhibitor to SARS-CoV M^{pro} and SARS-CoV-2 M^{pro}. In structure-based drug design, we would typically now synthesize the cyclic peptide inhibitor and evaluate its activity experimentally through studying its ability to block the cleavage of a fluorogenic peptide substrate by SARS-CoV-2 M^{pro}. We would also attempt to co-crystallize the inhibitor with the M^{pro} to experimentally evaluate the structure hypothesized in Figure 5C. Using the co-crystal structure and additional structure-activity studies, we would then carry out iterative rounds of modification and optimization of the cyclic peptide inhibitor to achieve higher affinity and specificity for SARS-CoV-2 M^{pro}.

Since this is exclusively a computational study, we will use the molecular docking software AutoDock Vina in place of these experimental studies. UCSF Chimera enables AutoDock Vina to be used as a plugin, which allows us to conveniently perform molecular docking and view the

docking results in UCSF Chimera.^a We will first evaluate the ability of the cyclic peptide inhibitor to bind the SARS-CoV M^{Pro} in silico and thus test our cyclic peptide inhibitor design. We will then evaluate the ability of the cyclic peptide inhibitor to bind SARS-CoV-2 M^{Pro} in silico to test our inhibitor against the relevant target of COVID-19.

In the first molecular docking exercise, we dock the geometry-optimized cyclic peptide inhibitor to the SARS-CoV M^{Pro} structure (PDB 5B6O), which we have already used for the inhibitor design.¹⁴ We start by defining a receptor search region to which AutoDock Vina will dock the inhibitor. The receptor search region should thus include the active site of the SARS-CoV M^{Pro}. To facilitate identification of the active site, we highlight several residues in the active site in red (Cys 38, Cys 44, Met 49, Met 165, and His 41) and then set a grid box which engulfs all of the active site as the search region (Figure 4.6A). After the molecular docking is complete, we get five docked structures, with energy scores of -10.5, -8.0, -7.8, -7.7, and -7.6 kcal/mol. In the lowest energy structure, the inhibitor fits well in the active site of SARS-CoV M^{Pro}. The P2 (Phe), P1 (Gln), P1' (Ser), and P2' (Lys) side chains of the inhibitor occupy the S2, S1, S1', and S2' pockets, and the AEPA residue occupies the S3' pocket (Figure 4.6B). This docking result demonstrates that the cyclic peptide inhibitor has the potential to bind to SARS-CoV M^{Pro}.

^a UCSF Chimera provides a graphical user interface for the AutoDock Vina plugin, which allows the user to avoid command-line programming required by the free-standing AutoDock Vina application.

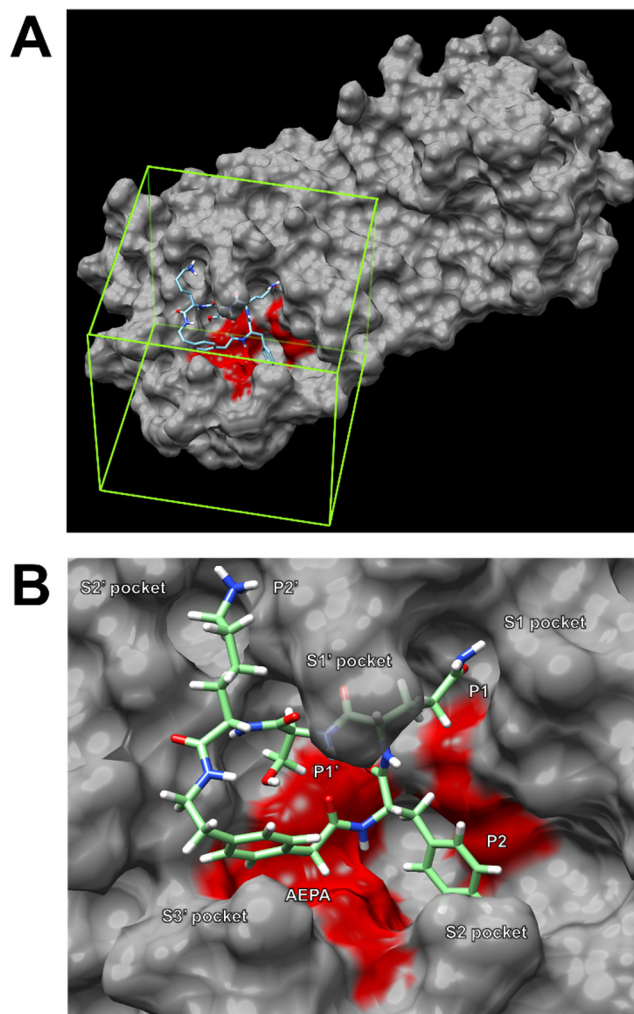


Figure 4.6. Molecular docking of the geometry-optimized cyclic peptide inhibitor to SARS-CoV M^{pro}. A: The region to which AutoDock Vina will perform molecular docking is defined using a grid box encompassing the active site of SARS-CoV M^{pro}. B: After molecular docking, the lowest energy conformation of the cyclic peptide inhibitor fits in the active site of SARS-CoV M^{pro}.

In the second molecular docking exercise, we dock the geometry-optimized cyclic peptide inhibitor to a recently published crystal structure of SARS-CoV-2 M^{pro} (PDB 6YB7).²¹ We load the SARS-CoV-2 M^{pro} structure using the “fetch PDB” function in UCSF Chimera, and conduct molecular docking in a similar fashion to the previous exercise (Figure 4.7A). After the molecular docking is complete, we get ten docked conformations with energy scores of -8.1, -7.8, -6.8, -6.5, -6.5, -6.4, -6.4, -6.4, -6.2, and -5.6 kcal/mol. Although the lowest energy structure only partially

fits into the active site of SARS-CoV-2 M^{pro}, the second lowest energy structure of the inhibitor fits better in the active site. The P2 (Phe), P1 (Gln), P1' (Ser), and P2' (Lys) side chains of the inhibitor occupy the S1, S1', S2, and S2' pockets, while the AEPA residue sits near the S3' pocket (Figure 4.7B). This docking result suggests that the cyclic peptide inhibitor that we designed based on SARS-CoV M^{pro} bound to a protein substrate might be repurposed to target SARS-CoV-2 M^{pro}.

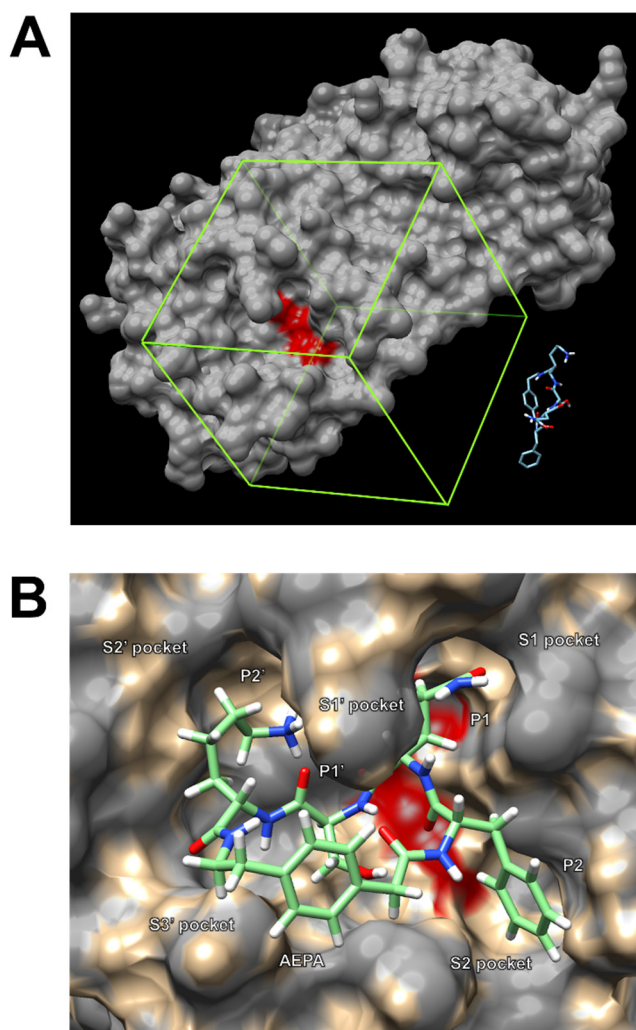


Figure 4.7. Molecular docking of the geometry-optimized cyclic peptide inhibitor to SARS-CoV-2 M^{pro}. A: The region to which AutoDock Vina will perform molecular docking is defined using a grid box encompassing the active site of SARS-CoV-2 M^{pro}. B: After molecular docking, the second lowest energy conformation of the cyclic peptide inhibitor fits in the active site of SARS-CoV-2 M^{pro}.

Conclusions

UCSF Chimera and AutoDock Vina allow the structure-based design of inhibitors of SARS-CoV-2 M^{Pro} as potential drug candidates. Using publicly available X-ray crystallographic structures and free software, anybody can unleash their imagination and try to invent new molecules that might help treat or prevent COVID-19 or other diseases. This chapter demonstrates the process and provides a simple example of how a published X-ray crystallographic structure can be modified and manipulated with the goal of creating molecules to bind and block a critical enzyme. This chapter can also be adapted to design inhibitors of other enzymes (e.g., HIV protease) from an X-ray crystallographic or NMR-based structure of an enzyme complex.^{22–28} We hope that this chapter will help students and scientists design their own inhibitors of SARS-CoV-2 M^{Pro} or other drug targets to help discover drugs for the treatment of COVID-19 and other diseases.

References and Notes

- (1) COVID-19 Map - Johns Hopkins Coronavirus Resource Center Website. <https://coronavirus.jhu.edu/map.html> (accessed Jun 20, 2021).
- (2) Dai, W.; Zhang, B.; Jiang, X. M.; Su, H.; Li, J.; Zhao, Y.; Xie, X.; Jin, Z.; Peng, J.; Liu, F.; Li, C.; Li, Y.; Bai, F.; Wang, H.; Cheng, X.; Cen, X.; Hu, S.; Yang, X.; Wang, J.; Liu, X.; Xiao, G.; Jiang, H.; Rao, Z.; Zhang, L. K.; Xu, Y.; Yang, H.; Liu, H. Structure-Based Design of Antiviral Drug Candidates Targeting the SARS-CoV-2 Main Protease. *Science*. **2020**, *368*, 1331–1335.
- (3) Douangamath, A.; Fearon, D.; Gehrtz, P.; Krojer, T.; Lukacik, P.; Owen, C. D.; Resnick, E.; Strain-Damerell, C.; Aimon, A.; Ábrányi-Balogh, P.; Brandaõ-Neto, J.; Carbery, A.;

- Davison, G.; Dias, A.; Downes, T. D.; Dunnett, L.; Fairhead, M.; Firth, J. D.; Jones, S. P.; Keely, A.; Keserü, G. M.; Klein, H. F.; Martin, M. P.; Noble, M. E. M.; O'Brien, P.; Powell, A.; Reddi, R.; Skyner, R.; Snee, M.; Waring, M. J.; Wild, C.; London, N.; Delft, F. von; Walsh, M. A. Crystallographic and Electrophilic Fragment Screening of the SARS-CoV-2 Main Protease. *Nat. Commun.* **2020**, *11*: 5047.
- (4) Vuong, W.; Khan, M. B.; Fischer, C.; Arutyunova, E.; Lamer, T.; Shields, J.; Saffran, H. A.; McKay, R. T.; van Belkum, M. J.; Joyce, M. A.; Young, H. S.; Tyrrell, D. L.; Vederas, J. C.; Lemieux, M. J. Feline Coronavirus Drug Inhibits the Main Protease of SARS-CoV-2 and Blocks Virus Replication. *Nat. Commun.* **2020**, *11*: 4282.
- (5) Zhang, L.; Lin, D.; Kusov, Y.; Nian, Y.; Ma, Q.; Wang, J.; Von Brunn, A.; Leyssen, P.; Lanko, K.; Neyts, J.; De Wilde, A.; Snijder, E. J.; Liu, H.; Hilgenfeld, R. α -Ketoamides as Broad-Spectrum Inhibitors of Coronavirus and Enterovirus Replication: Structure-Based Design, Synthesis, and Activity Assessment. *J. Med. Chem.* **2020**, *63*, 4562–4578.
- (6) Jin, Z.; Du, X.; Xu, Y.; Deng, Y.; Liu, M.; Zhao, Y.; Zhang, B.; Li, X.; Zhang, L.; Peng, C.; Duan, Y.; Yu, J.; Wang, L.; Yang, K.; Liu, F.; Jiang, R.; Yang, X.; You, T.; Liu, X.; Yang, X.; Bai, F.; Liu, H.; Liu, X.; Guddat, L. W.; Xu, W.; Xiao, G.; Qin, C.; Shi, Z.; Jiang, H.; Rao, Z.; Yang, H. Structure of Mpro from SARS-CoV-2 and Discovery of Its Inhibitors. *Nature*. **2020**, *582*, 289–293.
- (7) Zhang, L.; Lin, D.; Sun, X.; Curth, U.; Drosten, C.; Sauerhering, L.; Becker, S.; Rox, K.; Hilgenfeld, R. Crystal Structure of SARS-CoV-2 Main Protease Provides a Basis for Design of Improved α -Ketoamide Inhibitors. *Science*. **2020**, *368*, 409–412.
- (8) Kreutzer, A. G.; Krumberger, M.; Diessner, E. M.; Parrocha, C. M. T.; Morris, M. A.; Guaglianone, G.; Butts, C. T.; Nowick, J. S. A Cyclic Peptide Inhibitor of the SARS-CoV-2 Main Protease. *Eur. J. Med. Chem.* **2021**, *221*, 113530

- (9) Pettersen, E. F.; Goddard, T. D.; Huang, C. C.; Couch, G. S.; Greenblatt, D. M.; Meng, E. C.; Ferrin, T. E. UCSF Chimera - A Visualization System for Exploratory Research and Analysis. *J. Comput. Chem.* **2004**, *25*, 1605–1612.
- (10) Oleg, T.; Arthur J., O. AutoDock Vina: Improving the Speed and Accuracy of Docking with a New Scoring Function, Efficient Optimization, and Multithreading. *J. Comput. Chem.* **2010**, *31*, 2967–2970.
- (11) Price, G. W.; Gould, P. S.; Marsh, A. Use of Freely Available and Open Source Tools for in Silico Screening in Chemical Biology. *J. Chem. Educ.* **2014**, *91*, 602–604.
- (12) UCSF Chimera Home Page <https://www.cgl.ucsf.edu/chimera/> (accessed Aug 6, 2020).
- (13) Autodock Vina - molecular docking and virtual screening <http://vina.scripps.edu/index.html> (accessed Aug 6, 2020).
- (14) Muramatsu, T.; Takemoto, C.; Kim, Y. T.; Wang, H.; Nishii, W.; Terada, T.; Shirouzu, M.; Yokoyama, S. SARS-CoV 3CL Protease Cleaves Its C-Terminal Autoprocessing Site by Novel Subsite Cooperativity. *Proc. Natl. Acad. Sci. U. S. A.* **2016**, *113*, 12997–13002.
- (15) Dougherty, P. G.; Sahni, A.; Pei, D. Understanding Cell Penetration of Cyclic Peptides. *Chem. Rev.* **2019**, *119*, 10241–10287.
- (16) Morrison, C. Constrained Peptides' Time to Shine? *Nat. Rev. Drug Discov.* **2018**, *17*, 531–533.
- (17) Sawyer, T. K. Renaissance in Peptide Drug Discovery: The Third Wave. *Pept. Drug Discov. Challenges New Ther.* **2017**, *59*, 1–34.
- (18) Gang, D.; Kim, D. W.; Park, H. S. Cyclic Peptides: Promising Scaffolds for Biopharmaceuticals. *Genes.* **2018**, *9*, 557.
- (19) Vinogradov, A. A.; Yin, Y.; Suga, H. Macrocyclic Peptides as Drug Candidates: Recent

- Progress and Remaining Challenges. *J. Am. Chem. Soc.* **2019**, *141*, 4167–4181.
- (20) Guillen Schlippe, Y. V.; Hartman, M. C. T.; Josephson, K.; Szostak, J. W. In Vitro Selection of Highly Modified Cyclic Peptides That Act as Tight Binding Inhibitors. *J. Am. Chem. Soc.* **2012**, *134*, 10469–10477.
- (21) RCSB PDB - 6YB7: SARS-CoV-2 main protease with unliganded active site (2019-nCoV, coronavirus disease 2019, COVID-19) <https://www.rcsb.org/structure/6YB7> (accessed Aug 7, 2020).
- (22) Flexner, C. HIV-Protease Inhibitors. *N. Engl. J. Med.* **1998**, *338*, 1281–1292.
- (23) Ghosh, A. K.; Osswald, H. L.; Prato, G. Recent Progress in the Development of HIV-1 Protease Inhibitors for the Treatment of HIV/AIDS. *J. Med. Chem.* **2016**, *59*, 5172–5208.
- (24) Lv, Z.; Chu, Y.; Wang, Y. HIV Protease Inhibitors: A Review of Molecular Selectivity and Toxicity. *HIV/AIDS - Res. Palliat. Care* **2015**, *7*, 95–104.
- (25) Wlodawer, A.; Erickson, J. W. Structure-Based Inhibitors of HIV-1 Protease. *Annu. Rev. Biochem.* **1993**, *62*, 543–585.
- (26) Wlodawer, A.; Vondrasek, J. Inhibitors of HIV-1 Protease: A Major Success of Structure-Assisted Drug Design. *Annu. Rev. Biophys. Biomol. Struct.* **1998**, *27*, 249–284.
- (27) Arts, E. J.; Hazuda, D. J. HIV-1 Antiretroviral Drug Therapy. *Cold Spring Harb. Perspect. Med.* **2012**, *2*: a007161.
- (28) Paterson, D. L.; Swindells, S.; Mohr, J.; Brester, M.; Vergis, E. N.; Squier, C.; Wagener, M. M.; Singh, N.; Hudson, B. Adherence to Protease Inhibitor Therapy and Outcomes in Patients with HIV Infection. *Ann. Intern. Med.* **2000**, *133*, 21–30.

Supporting Information

Table of Contents

1. General notes	204
2. Selecting a starting structure for inhibitor design	205
3. Modifying the C-terminal fragment of SARS-CoV M ^{pro} to create a cyclic peptide inhibitor	206
3.1. Showing the substrate and the protein binding pocket	206
3.2. Deleting unnecessary residues, bonds, and atoms from the substrate	211
3.3. Mutating Phe 309 to [4-(2-aminoethyl)phenyl]-acetic acid (AEPA)	220
3.4. Creating a new bond to make the substrate a cyclic peptide	224
3.5. Renaming Thr 304	229
4. Geometry optimization of the cyclic peptide inhibitor	231
4.1. Changing the VDW radii used to create the surface	231
4.2. Minimize the cyclic peptide inhibitor while fixing the protein	234
4.3. Mutating Gly 307 to Ser 307	239
4.4. The second-round of minimization after mutating Gly 307 to Ser 307	240
5. Docking the inhibitor to SARS-CoV M ^{pro}	246
5.1. Saving the cyclic peptide inhibitor and the protein as separate PDB files	246
5.2. Installing AutoDock Vina and creating a folder for docking files	248
5.3. Opening the saved ligand and protein PDB files in the same view	249
5.4. Highlighting the active site of the protein	250
5.5. Running AutoDock Vina	254
5.6. Viewing the docking results	258
6. Docking the inhibitor to SARS-CoV-2 M ^{pro}	262

6.1.	Saving the cyclic peptide inhibitor as a PDB file	262
6.2.	Loading and modifying the SARS-COV-2 M ^{pro} structure	263
6.3.	Installing AutoDock Vina and creating a folder for docking files	267
6.4.	Opening the saved ligand and protein PDB files in the same view	268
6.5.	Highlighting the active site of the protein	268
6.6.	Running AutoDock Vina	273
6.7.	Viewing the docking results	2278
7.	Appendix: Generating a structure of SARS-CoV M ^{pro} bound to the C-terminal substrate (5B6O-S.pdb)	282
7.1.	Loading the SARS-CoV M ^{pro} crystal structure in UCSF Chimera	282
7.2.	Generating symmetry mates in the crystal lattice	284
7.3.	Deleting unnecessary parts	285
7.4.	Saving the modified PDB file	290
8.	References	291

1. General notes

- 1.1. Here we present the illustrated step-by-step protocol of our inhibitor design, geometry optimization, and molecular docking process. This protocol has been tested on both Windows (Windows 10) and Mac (MacOS Catalina) operating systems. The UCSF Chimera user interface is virtually identical between the two operating systems. This protocol includes steps and screenshots of operating UCSF Chimera in Windows 10 system, and MacOS Catalina-specific notes.^{1,2}

- 1.2. The following font style key will be used throughout the exercise to describe how to navigate and interact with the UCSF Chimera user interface using particular keystrokes or menu options:

Font style	Meaning	Example
bold	key on keyboard	up arrow, ctrl, shift, enter
<i>italics</i>	menu bar option in UCSF Chimera	<i>Actions → Surface → show</i>
“quotation”	on-screen window text in UCSF Chimera	“minimize structure”
<u>underlined</u>	on-screen button in UCSF Chimera	<u>minimize</u>

- 1.3. There is no general-purpose undo action in UCSF Chimera.³ For example, if you delete atoms, they are permanently gone and can only be recovered by reading the original structure file back into UCSF Chimera. It is therefore recommended to save the session after critical steps using *File → Save Session As*. To reopen a saved session, use *File → open*.

2. Selecting a starting structure for inhibitor design

- 2.1. We design the cyclic peptide inhibitor based on the X-ray crystallography structure of SARS-CoV M^{pro} (C145A) [Protein Data Bank (PDB) ID: 5B6O].⁴ To reduce the reader's workload, we simplified the SARS-CoV M^{pro} (C145A) structure (PDB 5B6O) using UCSF Chimera. The simplified structure contains only the portions that are relevant to this chapter: the C-terminal fragment of an M^{pro} molecule (substrate) and the adjacent M^{pro} molecule (protein) with the active site. We named the simplified PDB file as “5B6O-S.pdb”

and have provided it as an additional file with the Supporting Information (SI). Readers are encouraged to proceed to the next section using the “5B6O-S.pdb” file.

- 2.2. If you are interested in the process of simplifying the SARS-CoV M^{PRO} (C145A) structure (PDB: 5B6O) using UCSF Chimera, including generating symmetry mates and deleting unnecessary parts, the details can be found in the appendix of the SI.

3. **Modifying the C-terminal fragment of SARS-CoV M^{PRO} to create a cyclic peptide inhibitor**

- 3.1.1. Showing the substrate and the protein binding pocket

- 3.1.2. Download the “5B6O-S” PDB file from the SI.

- 3.1.3. Open the “5B6O-S” PDB file in UCSF Chimera.

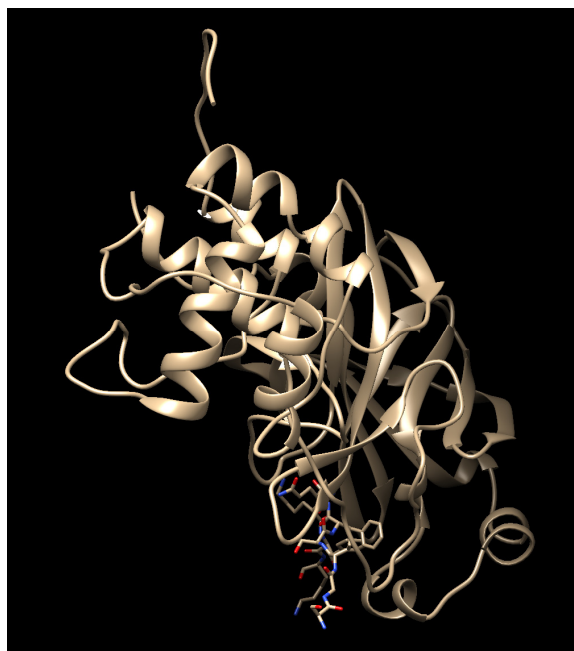
In the menu bar across the top of the UCSF Chimera window, click *File* → *Open*. Find the “5B6O-S” file, then click Open.

- 3.1.4. You can use the mouse to do basic model viewer controls.

Left mouse button (LMB): Rotate the view

Middle mouse button (MMB): Translate the view across screen

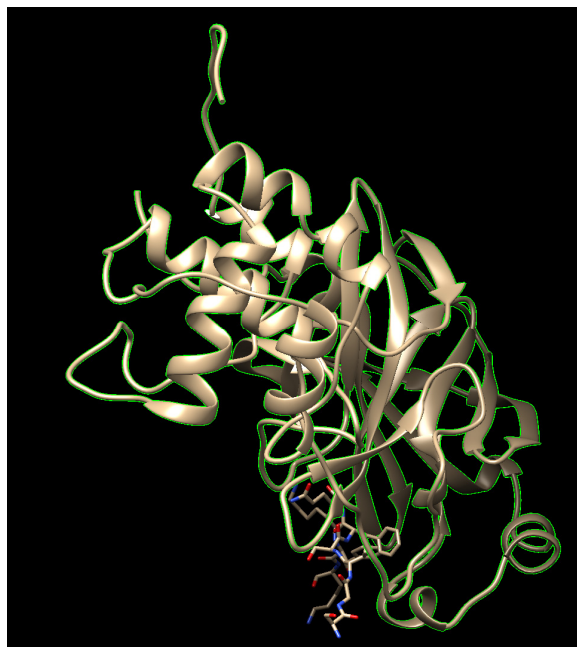
Right mouse button (RMB): Zoom in or out



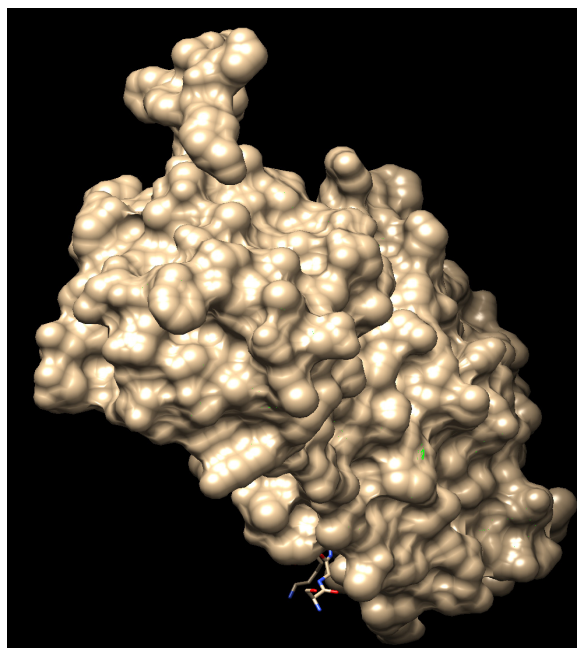
3.1.5. Visualize the protein as a van der Waals surface.

UCSF Chimera currently shows a ribbon representation of the protein. It is helpful to visualize the protein as a van der Waals surface in order to better interpret the shape of the binding pocket.

Select any part of the protein using **Ctrl+LMB**. Once an atom, residue, or secondary structure is selected, the **up** and **down** arrow keys will change the scope of a selection (e.g., atom → residue → secondary structure → entire model). To select the entire protein, press the **up** arrow key twice.



In the menu bar, click *Actions* → *Surface* → *show*.



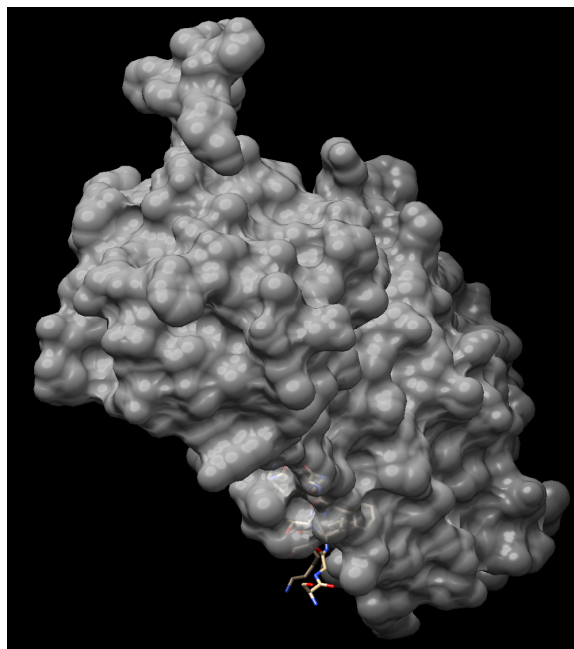
3.1.6. Change the color and transparency of the protein surface.

Sometimes it is helpful to add transparency to the protein surface in order to see through protrusions in the binding pocket, change the color of the surface, and remove other representations of the model from view:

Actions → Surface → transparency → 30%

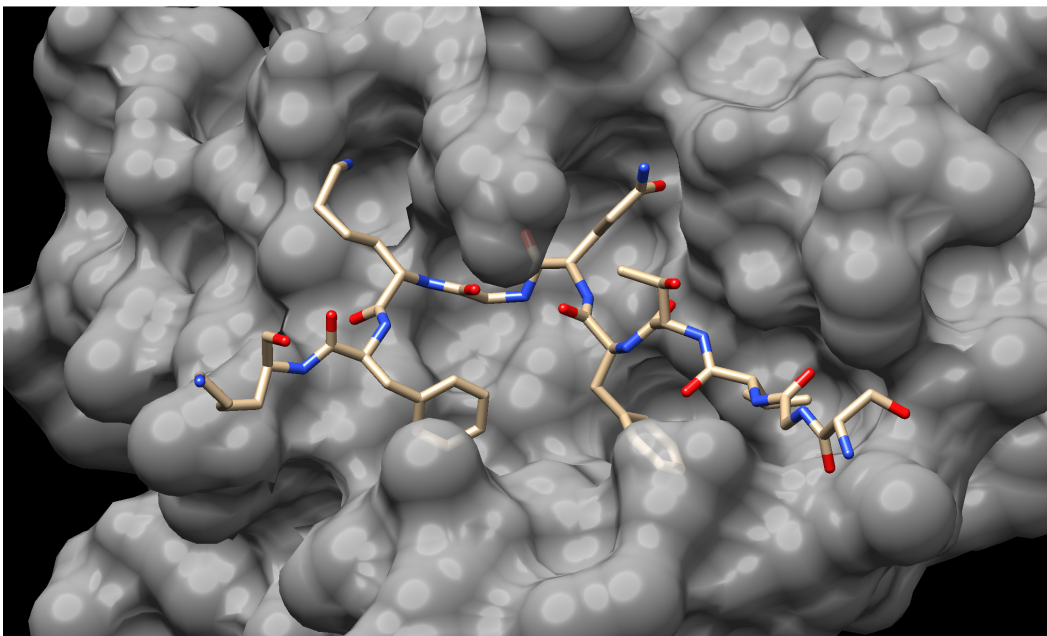
Actions → Color → Dark Grey

Actions → Ribbon → hide



3.1.7. Rotate and zoom in the view so the substrate and protein binding pocket are facing you.

Use LMB to rotate the view, MMB to translate view across screen, and RMB to zoom in, so that the substrate and protein binding pocket are facing you.



3.1.8. Add hydrogens to the substrate.

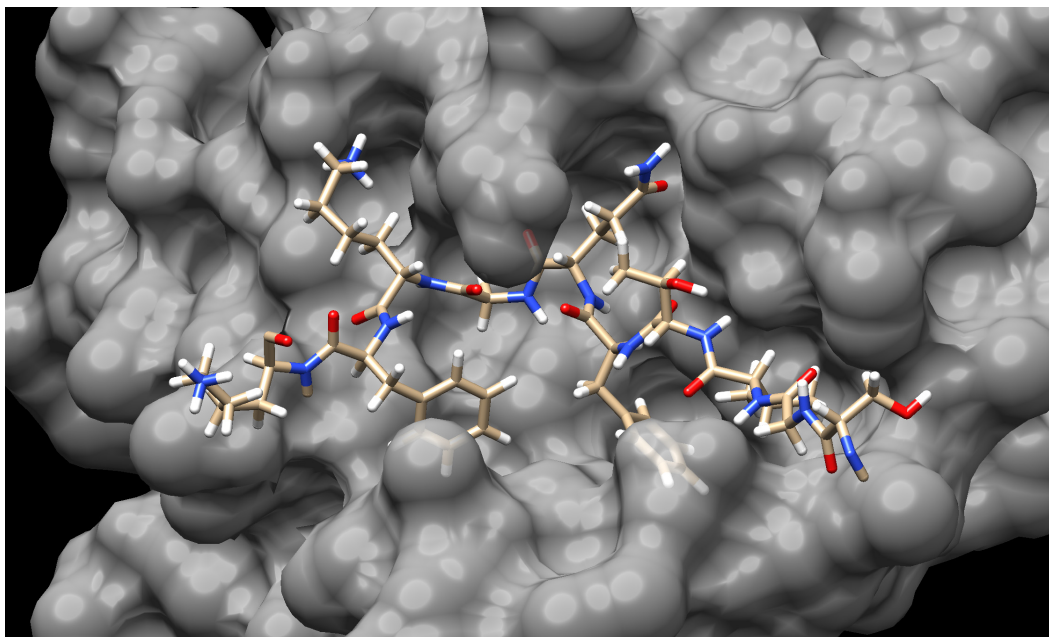
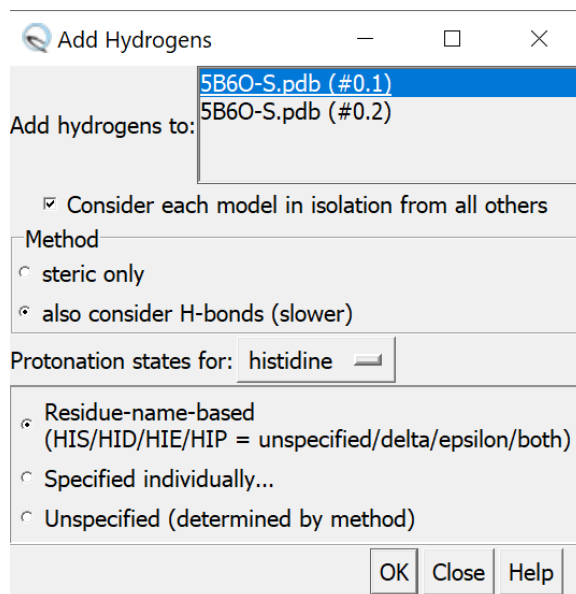
Based on the interactions between this substrate and the binding pocket, we now want to make some structural modifications to the substrate to create a cyclic peptide inhibitor that may be more conformationally rigid and resistant to proteolysis.

In order to simplify future structural modifications, we will add hydrogens to the substrate:

Tools → *Structure Editing* → *AddH*.

This will open the “Add Hydrogens” window. You will notice two possible models to add hydrogens to, “5B6O-S.pdb (#0.1)” and “5B6O-S.pdb (#0.2).” These two models are the substrate and protein, respectively.

Select “5B6O-S.pdb (#0.1)” (the substrate), then click OK.

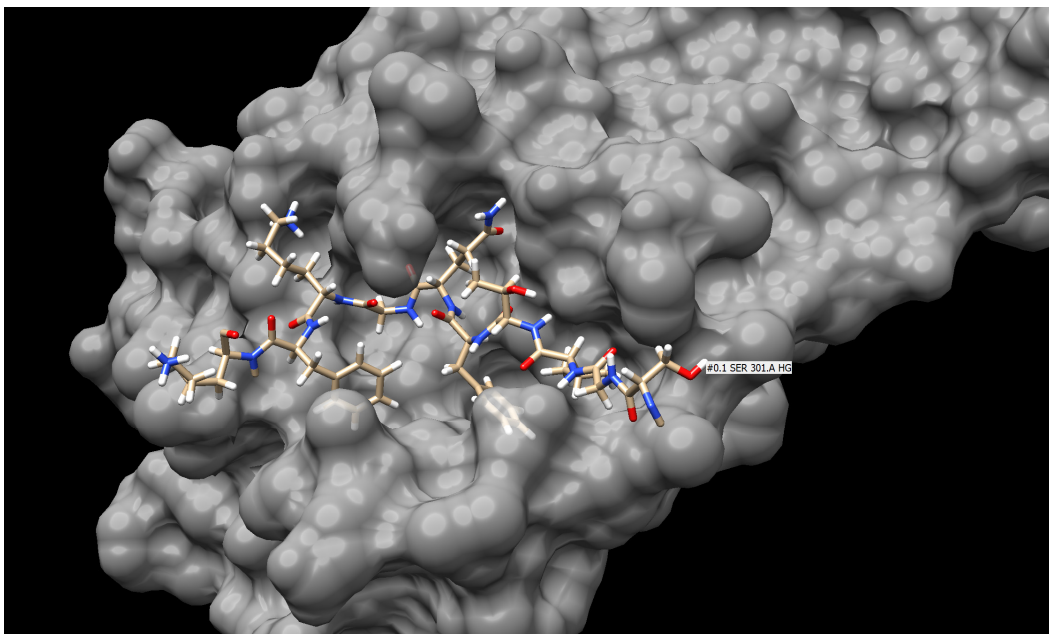


3.2. Deleting unnecessary residues, bonds, and atoms from the substrate

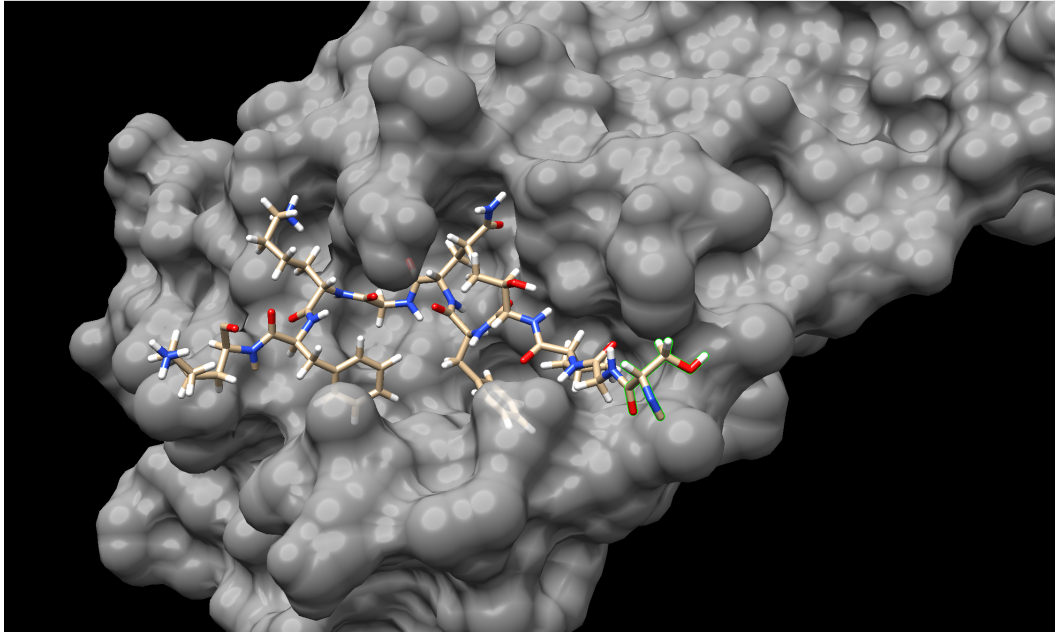
Constructing our inhibitor involves removing certain residues from the substrate, mutating others, and creating new bonds to form a macrocycle. We will begin by deleting unnecessary residues, bonds, and atoms.

3.2.1. First, we want to select Ser 301 in the substrate and delete it. There are two ways to find and select Ser 301 of the substrate.

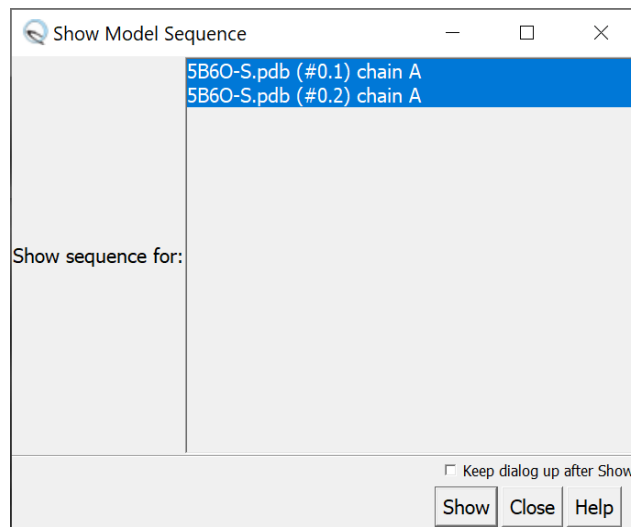
a. Hovering the mouse cursor over any atom in the structure will cause text to appear in the format [model number] [residue name] [residue number] [atom type]. Hover the cursor over the atoms of the substrate until you find Ser 301.



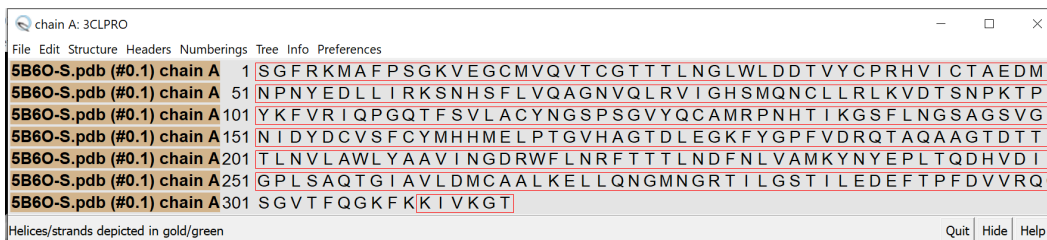
To select Ser 301, select any atom in the Ser 301 residue using **Ctrl**+**LMB**, then use the **up** arrow key once to expand the scope of the selection from a single atom to the entire Ser 301 residue.



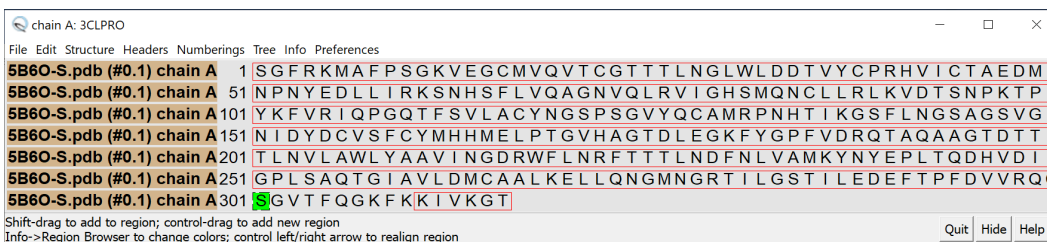
b. In the menu bar, *Favorite* → *sequence*. The following “Show Model Sequence” window will show up.



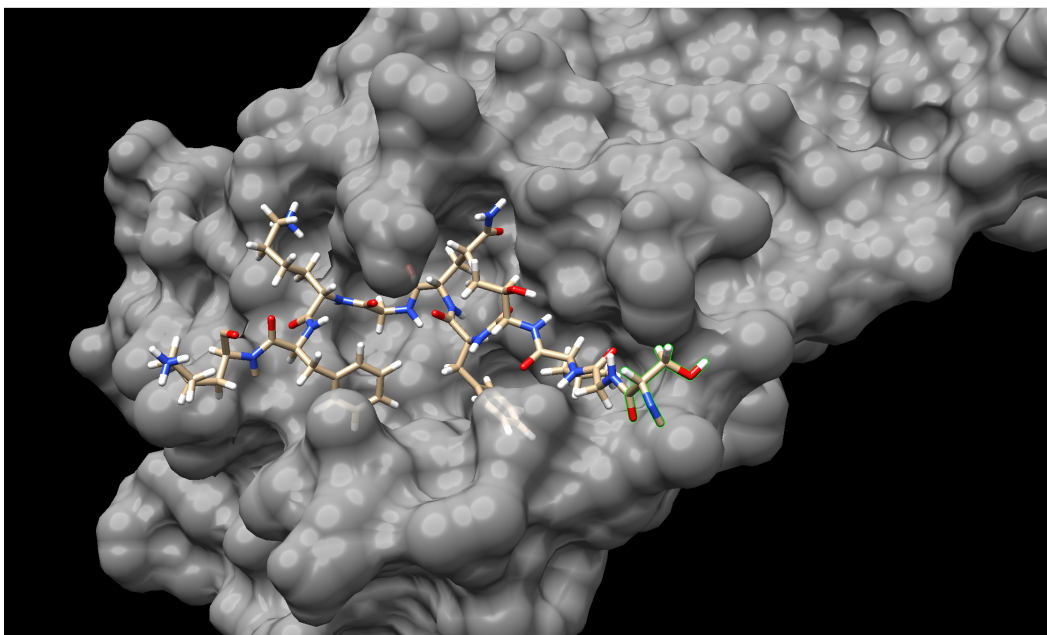
Highlight “5B6O-S.pdb (#0.1) chain A” only, click Show. The following “chain A: 3CLPRO” window will show up.



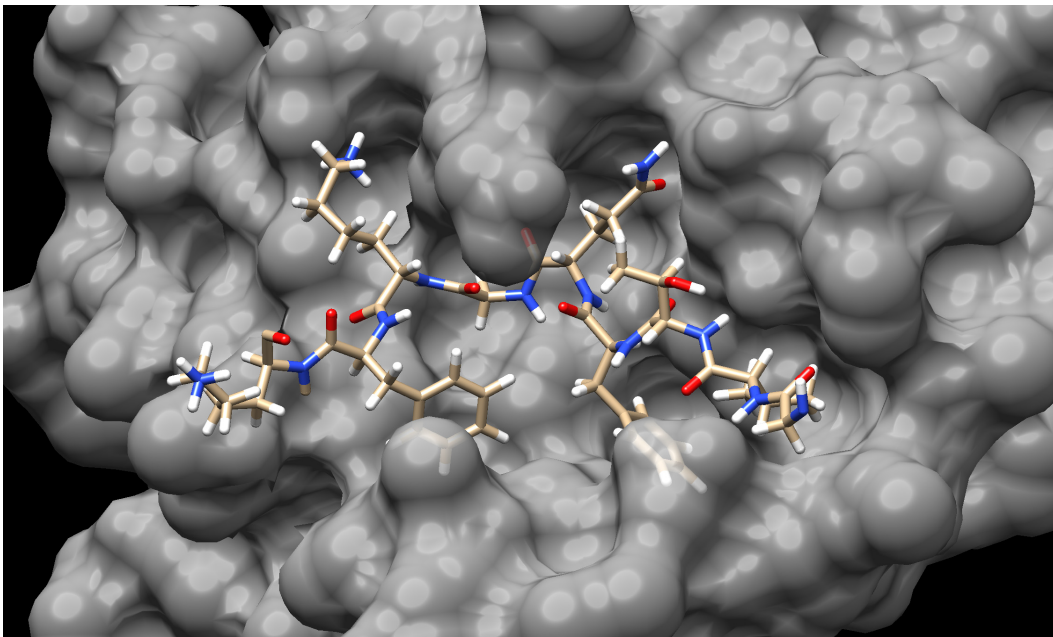
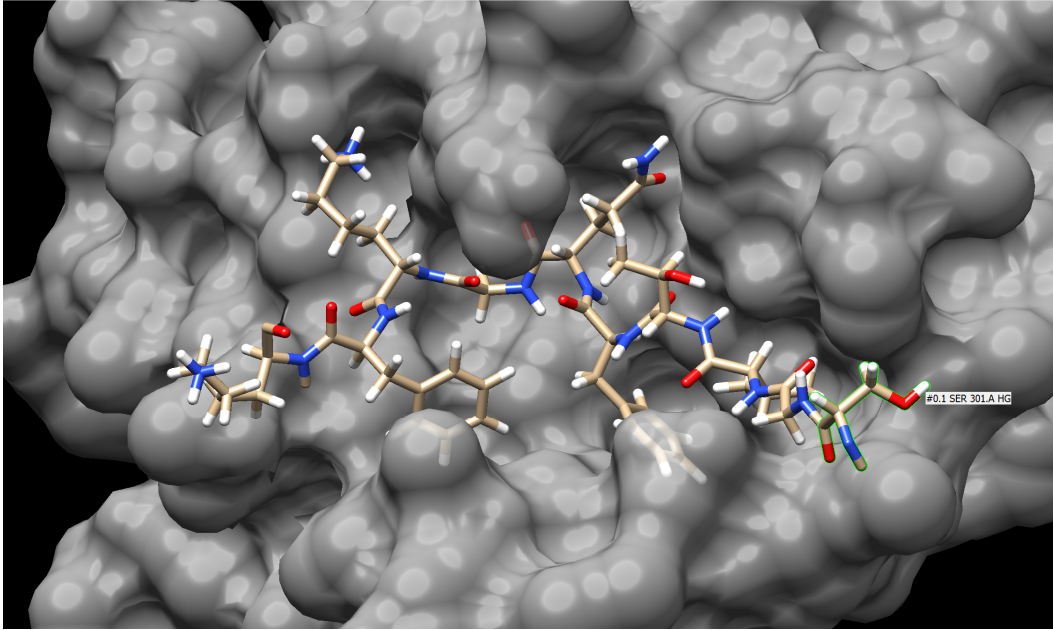
Find position 301, use LMB to click and drag to highlight the letter “S” representing Ser 301. Click Quit to close the window.



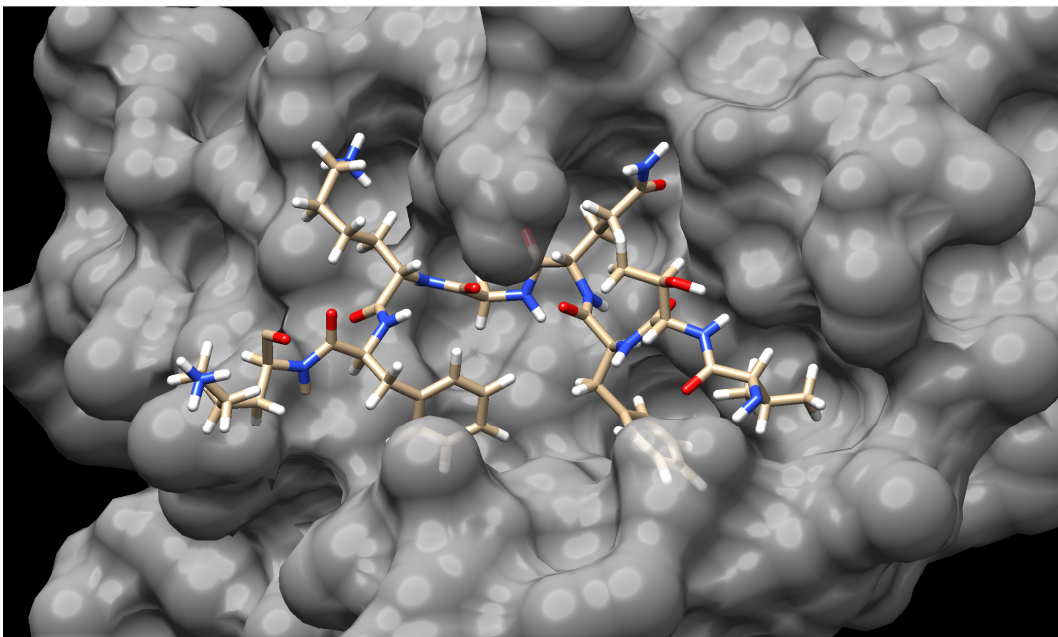
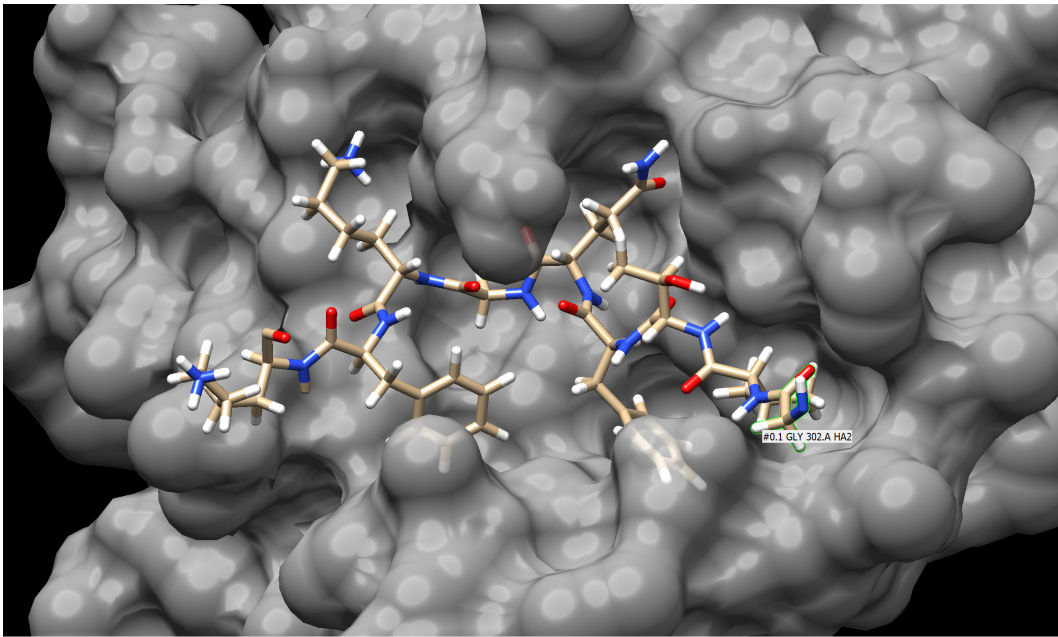
In the UCSF Chimera workspace, Ser 301 is selected.



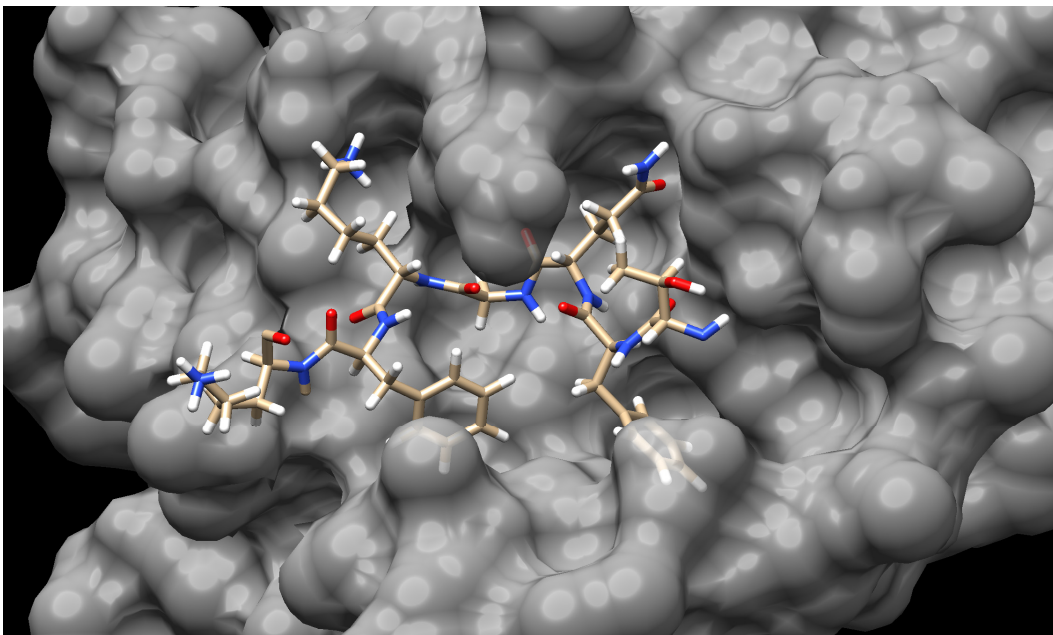
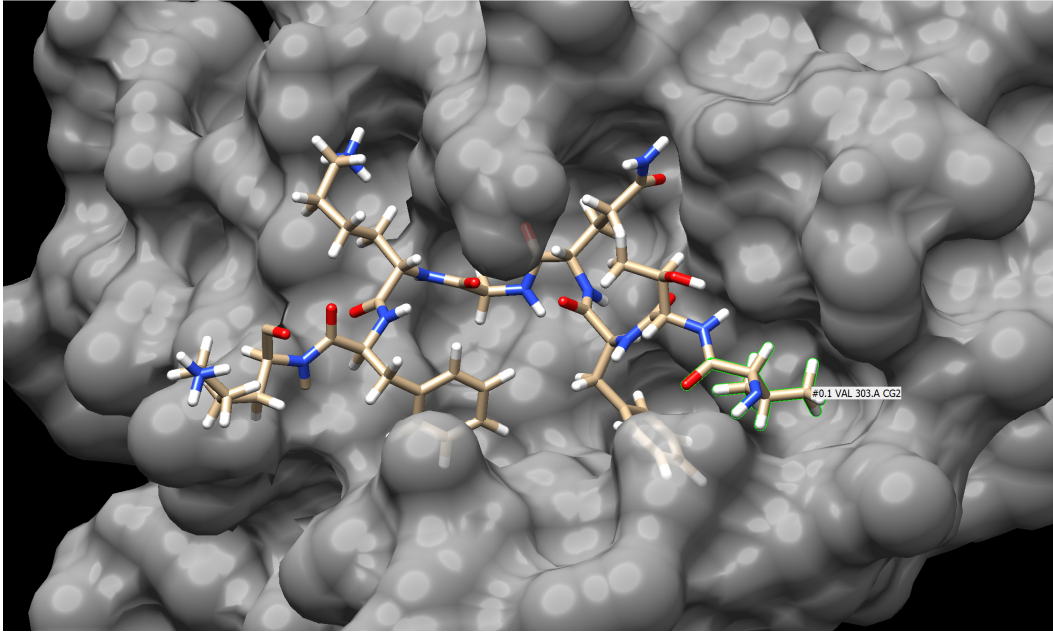
After using either way to select Ser 301, to delete the selected Ser 301, use *Actions* → *Atoms/Bonds* → *delete*.



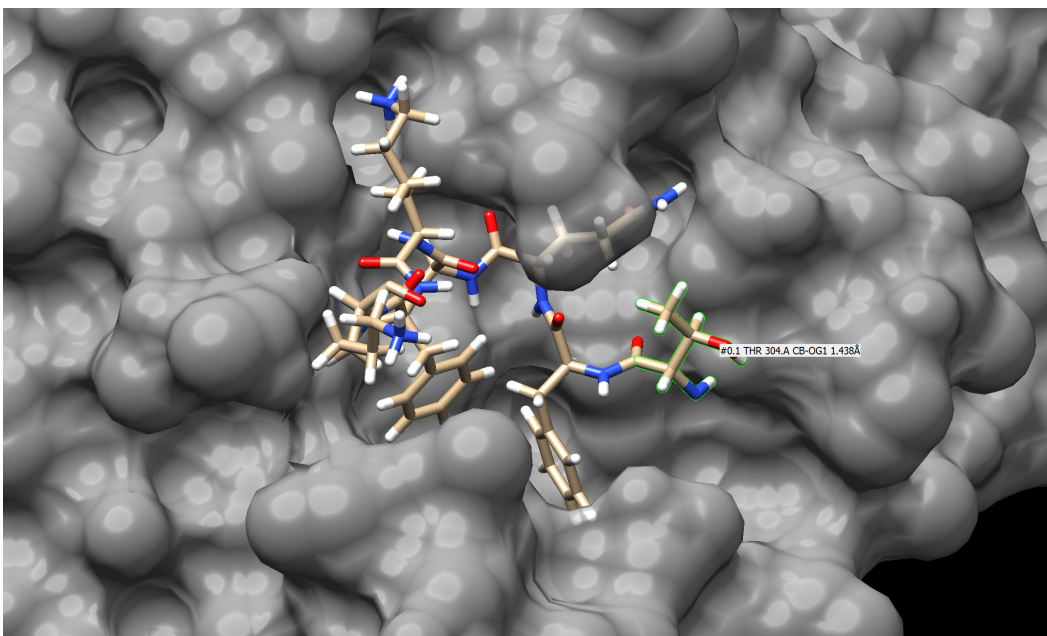
3.2.2. Now delete Gly 302, as above.



3.2.3. Delete Val 303.

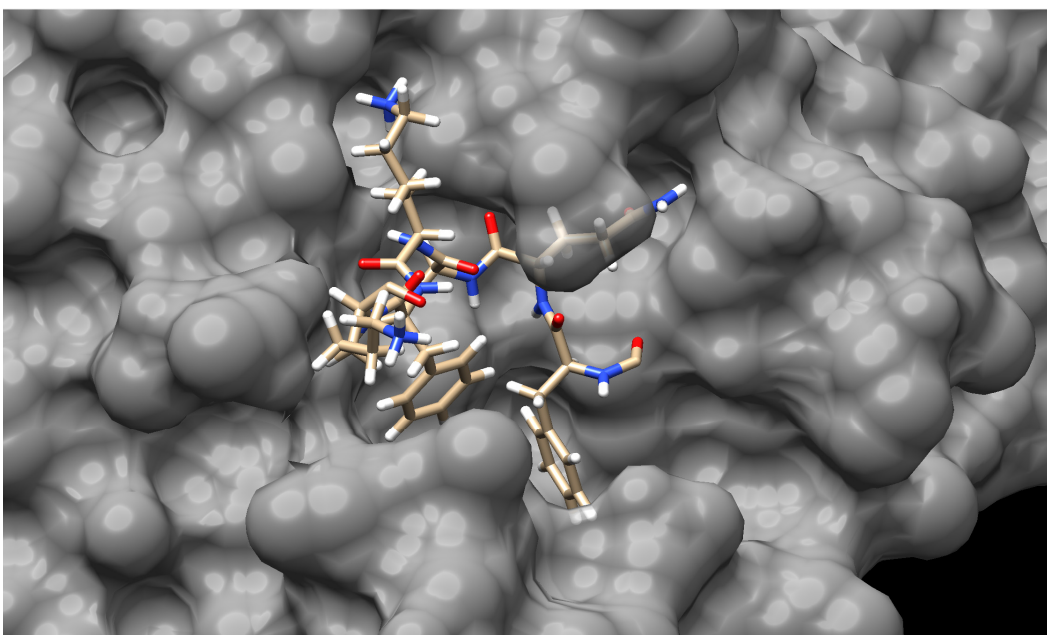


3.2.4. Rather than deleting Thr 304 in its entirety, we will only delete part of it. We will delete the side chain, the alpha carbon, and the amine, but leave the amide bond between Thr 304 and Phe 305 intact. Hover the cursor over the substrate until you find those atoms and bonds to delete. To select multiple atoms or bonds simultaneously, hold **Shift** while using **Ctrl+LMB** (i.e. **Ctrl+Shift+LMB**).

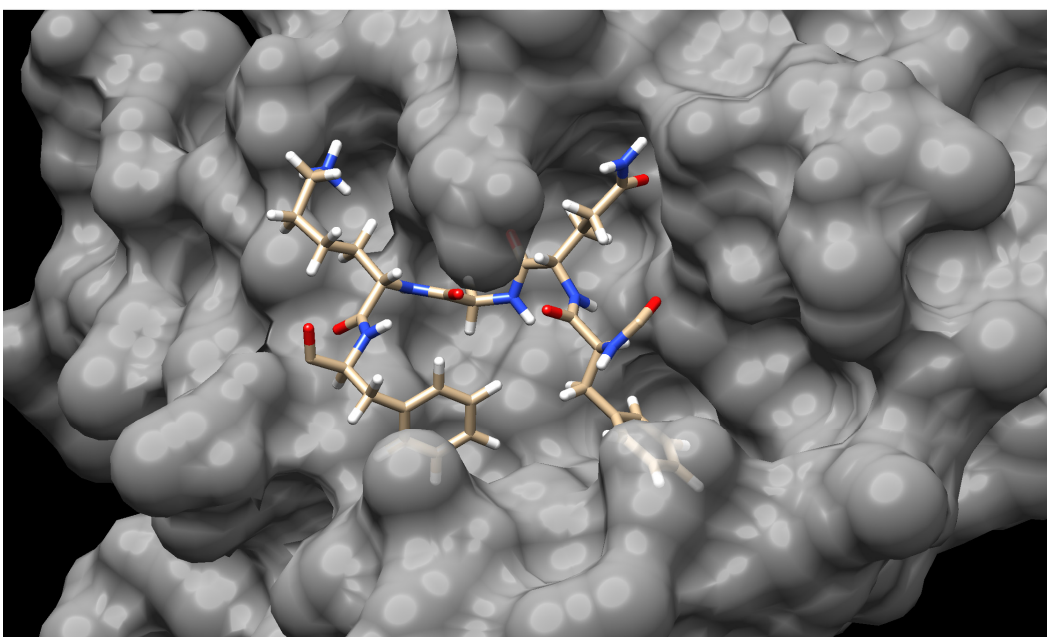
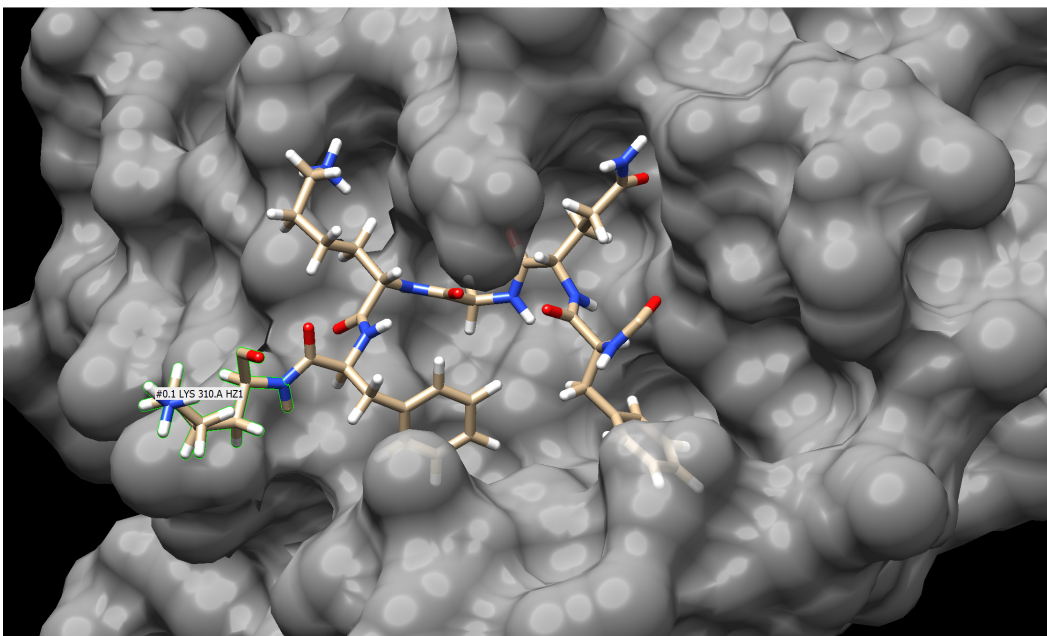


As before, delete this selection using *Actions* → *Atoms/Bonds* → *delete*.

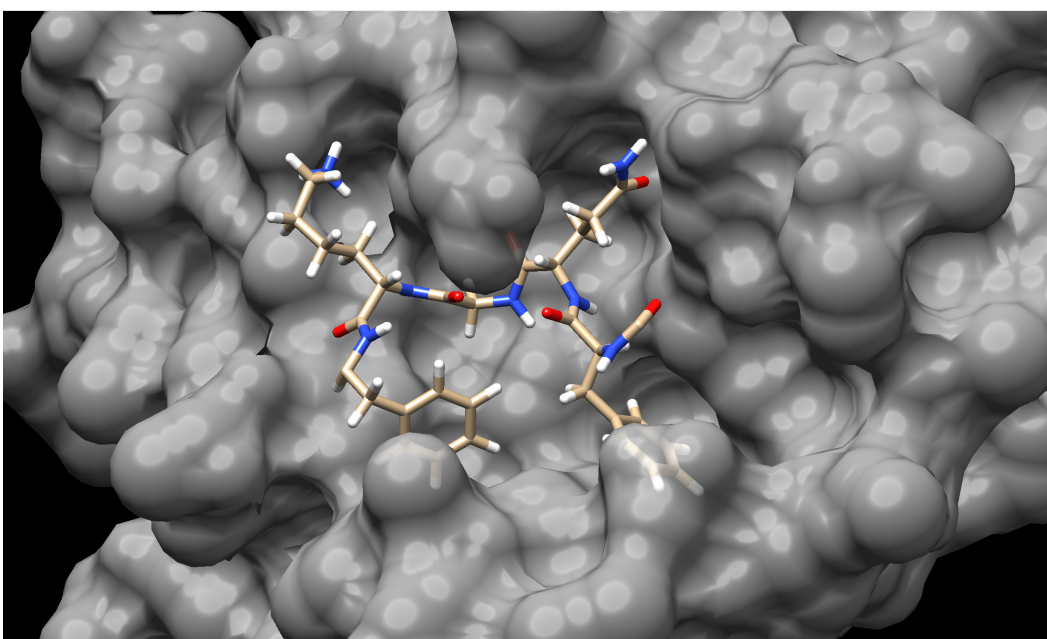
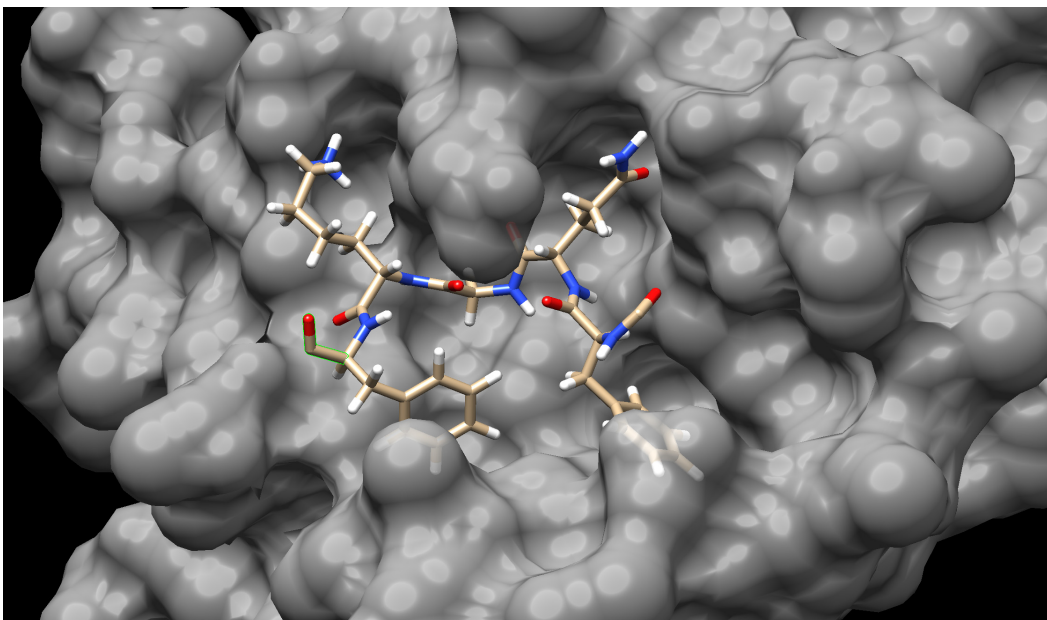
If there are any leftover atoms/bonds that you did not select the first time, use **Ctrl+Shift+LMB** to select them and delete. Now only the amide bond of Thr 304 remains.



3.2.5. Delete Lys 310 (the entire residue).



3.2.6. Delete the carbonyl of Phe 309. Use **Ctrl+Shift+LMB** to select the carbonyl oxygen, carbon-oxygen bond, carbonyl carbon, and carbon-carbon bond then *Actions* → *Atoms/Bonds* → *delete*.

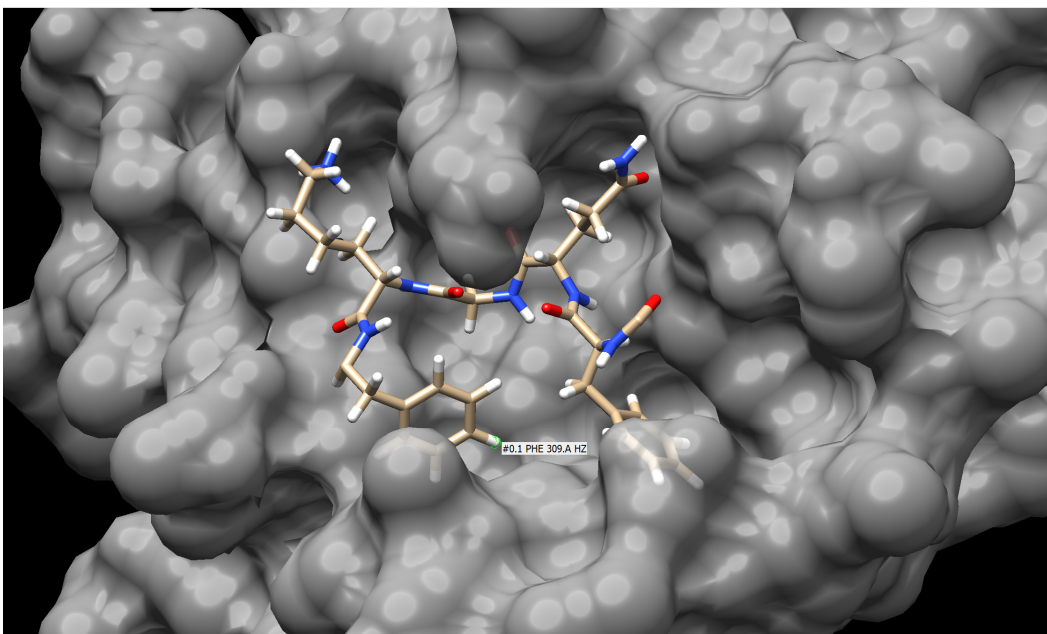


3.3. Mutating Phe 309 to [4-(2-aminoethyl)phenyl]-acetic acid (AEPA)

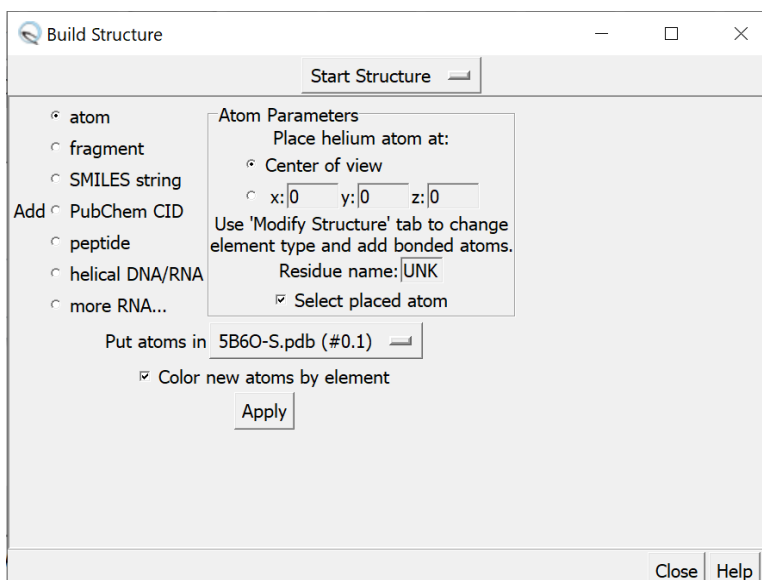
Our inhibitor design involves a mutation of Phe 309 to [4-(2-aminoethyl)phenyl]-acetic acid (AEPA) in order to form a macrocycle with the remaining amide bond of Thr 304.

This starts by adding a new tetrahedral methyl group (CH₃) to Phe 309 in the para position.

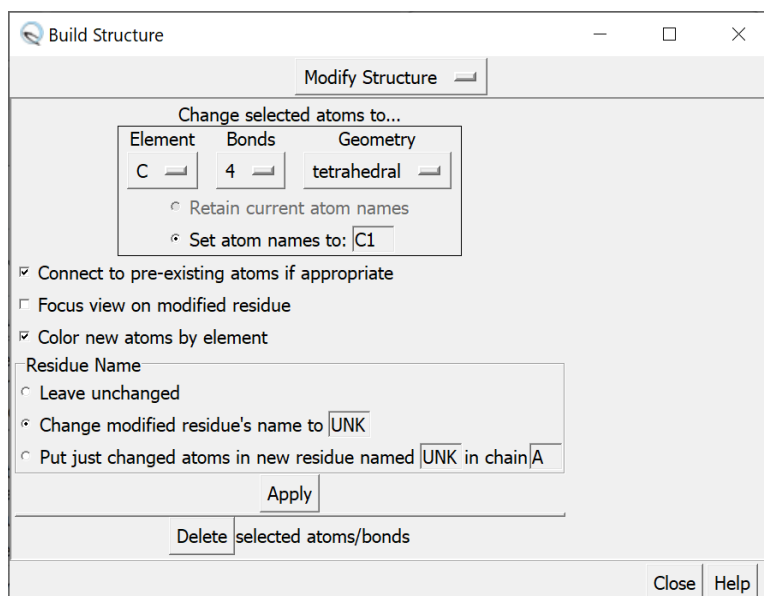
Select the para hydrogen using **Ctrl+LMB**.



Tools → *Structure Editing* → *Build Structure* will open the “Build Structure” window.

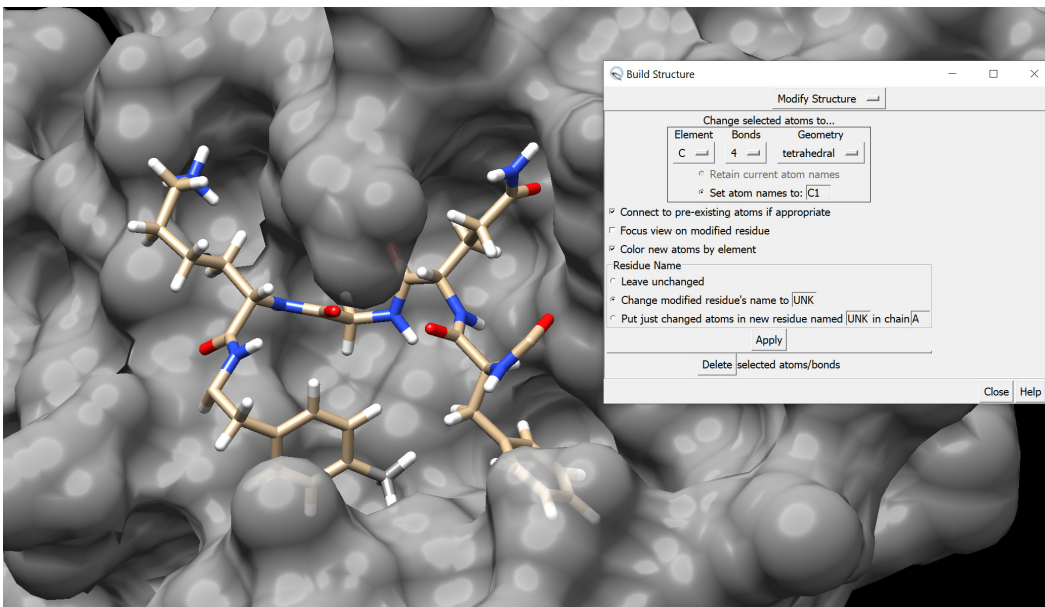


This window has multiple tabs for making structural modifications to atoms and bonds. These tabs can be navigated using the drop-down menu at the top-middle of the window; the initial tab is “Start Structure.” Navigate to the tab called “Modify Structure.” The window will change to show new options.



This window will allow you to modify selected atoms. (Keep this window open throughout the building process, or you will have to reopen it.) Currently, the para hydrogen of Phe 309 is selected, and we want to change it to a tetrahedral methyl group (CH₃). Under the heading “Change selected atoms to...”, make sure that the “Element,” “Bonds,” and “Geometry” options read “C,” “4,” and “tetrahedral,” respectively. Click Apply to make the indicated change.

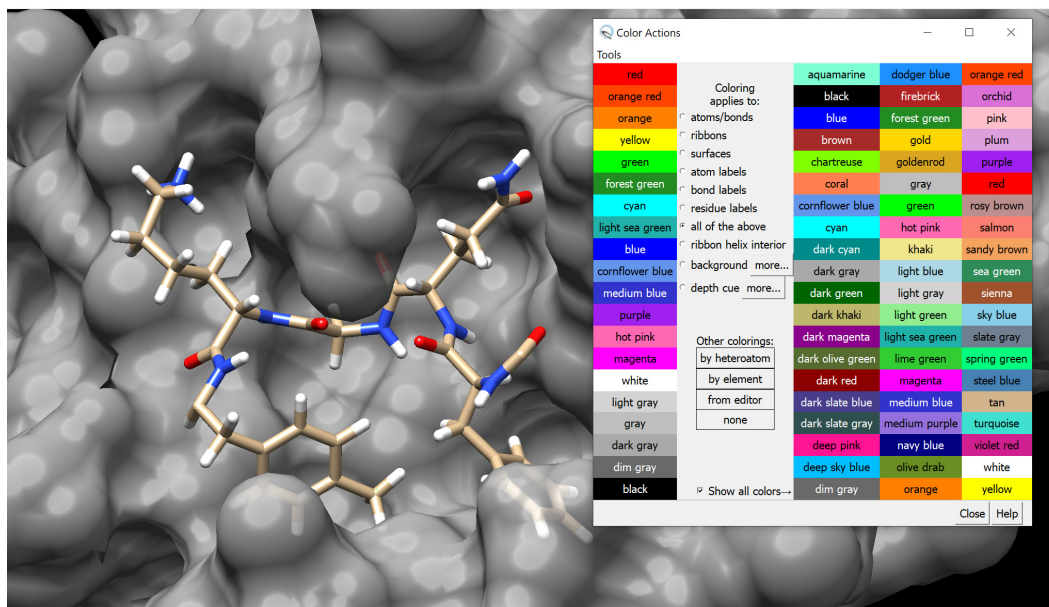
Note that under the header “Residue Name,” the radio button labeled “Change modified residue’s name to [UNK]” is selected. Because this is selected, when you changed the para hydrogen to a methyl, it also renamed Phe 309 to UNK 309. This is important for the upcoming minimization, and the reason why will be explained later.



Note that the new carbon is grey while the other carbons in the molecules remain tan. We want the color of the new carbon to be consistent with the rest of the substrate. Open the “Color Actions” window using:

Actions → *Color* → *all options*.

The grey carbon is already selected from the previous step; to change it to tan, check the box next to “Show all colors→” and click tan. Close the “Color Actions” window.

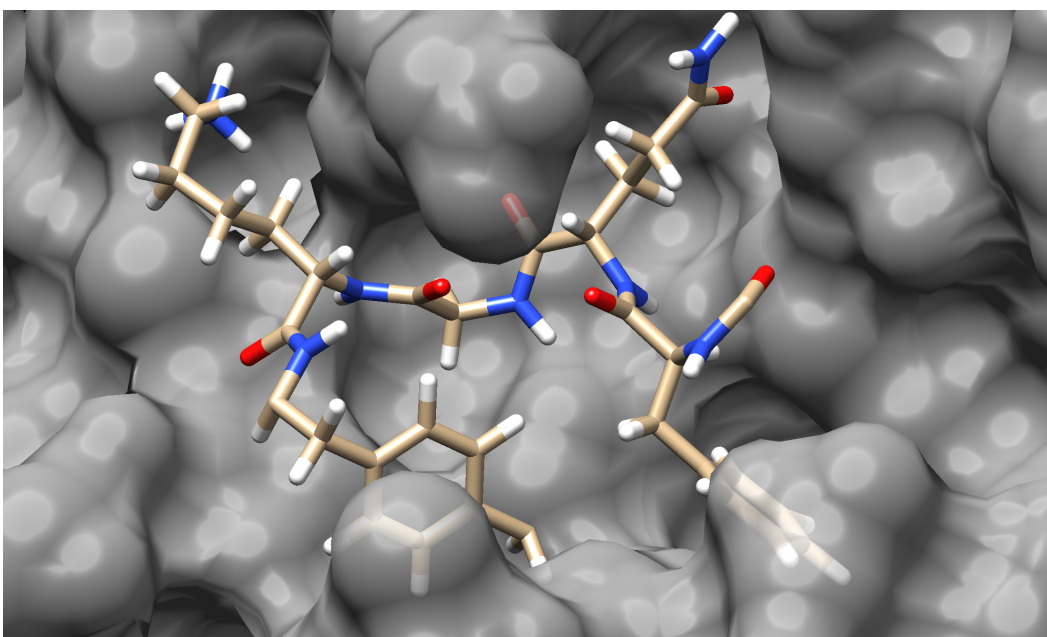
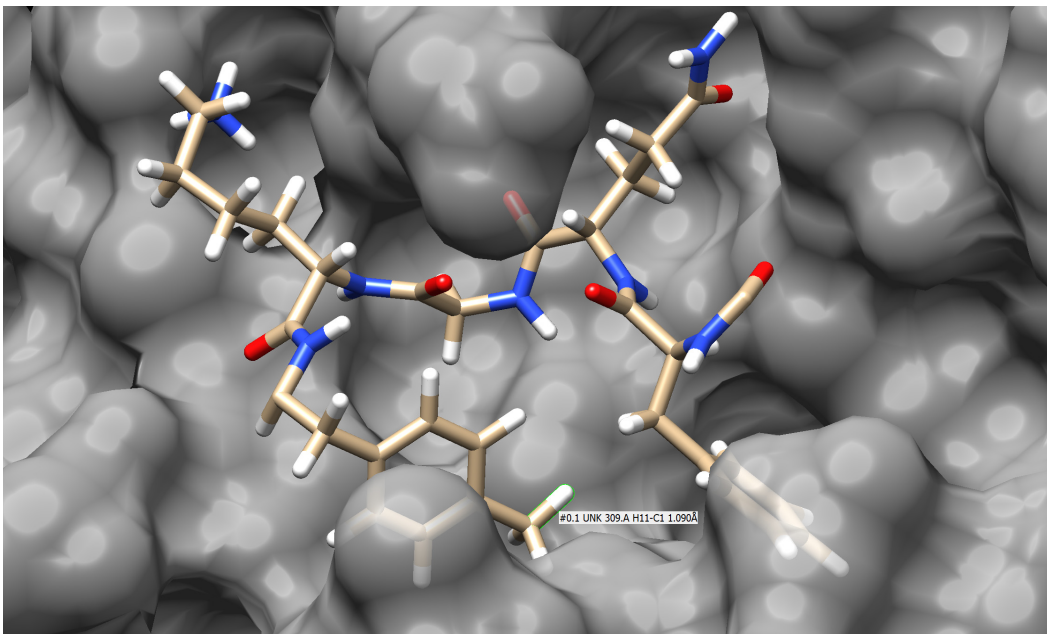


3.4. Creating a new bond to make the substrate a cyclic peptide

Now we want to form a bond between the carbonyl carbon of Thr 304 and the newly built methyl carbon to make this substrate a macrocycle. To do so, we first have to make room on the newly built methyl group (CH_3) by deleting one hydrogen. Clear the selection using

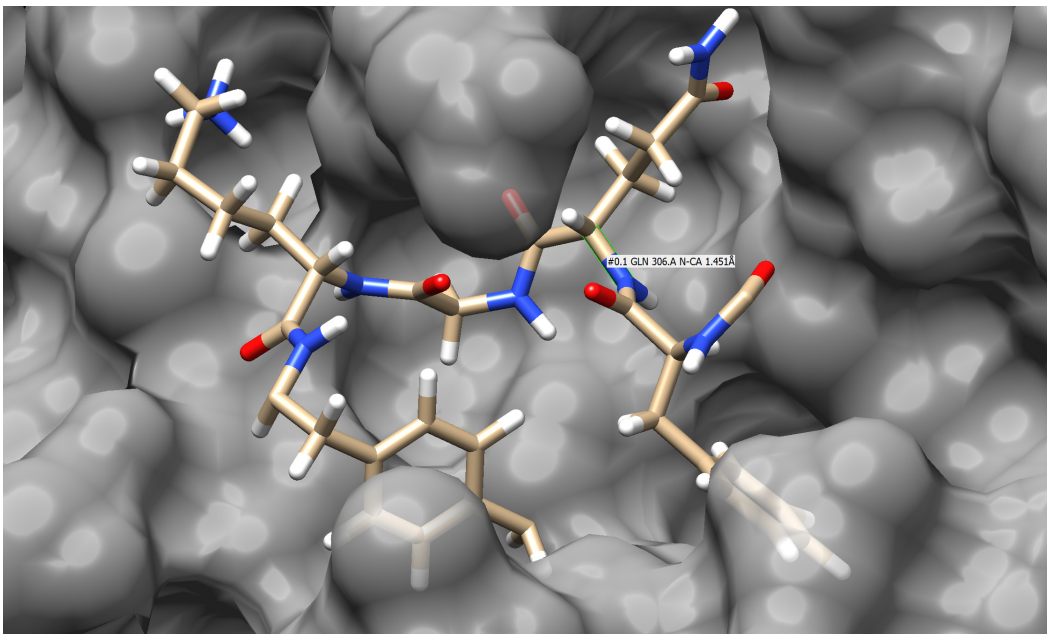
Select → *Clear Selection*

Simultaneously select one of the methyl hydrogens as well as its corresponding carbon-hydrogen bond using **Ctrl+Shift+LMB**, then delete that selection using *Actions* → *Atoms/Bonds* → *delete*. The methyl group (CH_3) becomes a methylene (CH_2) group.



To form a bond between the Thr 304 carbonyl carbon and the newly built methylene (CH₂) group carbon, we must rotate some bonds to put the atoms to be bonded into closer proximity. When the new bond is formed, it must not cross other atoms or bonds. Crossing other atoms or bonds will cause the later minimization to fail.

Select the backbone C α -N bond of Gln 306 using **Ctrl+LMB**.

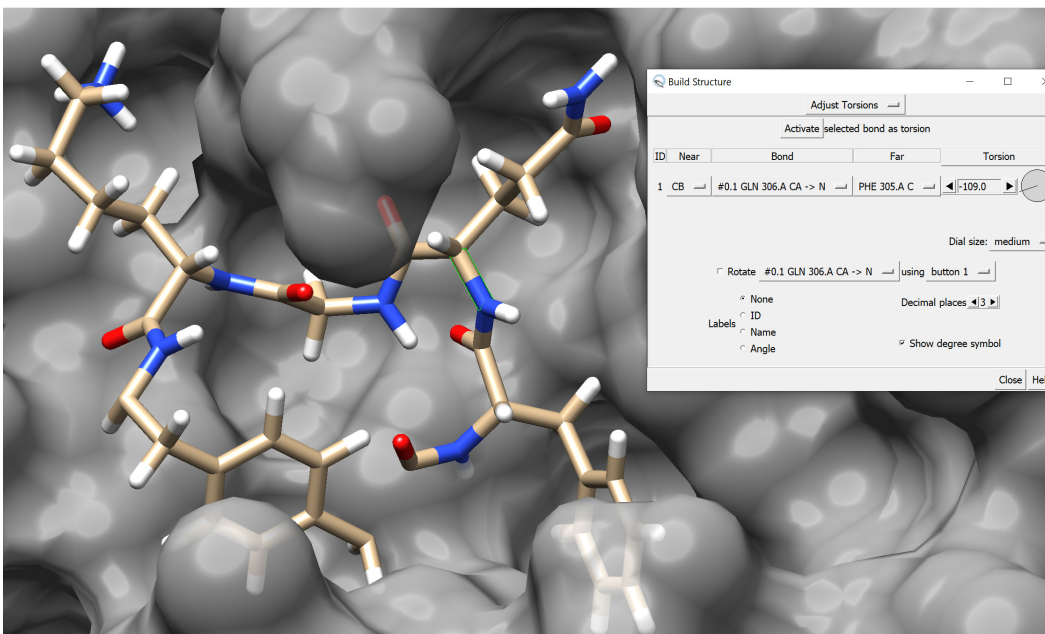


In the currently open “Build Structure” window, change from the “Modify Structure” tab to the “Adjust Torsions” tab. As the relevant bond in Gln 306 is already selected, click Activate to make it rotatable and bring up options for changing the bond torsion.

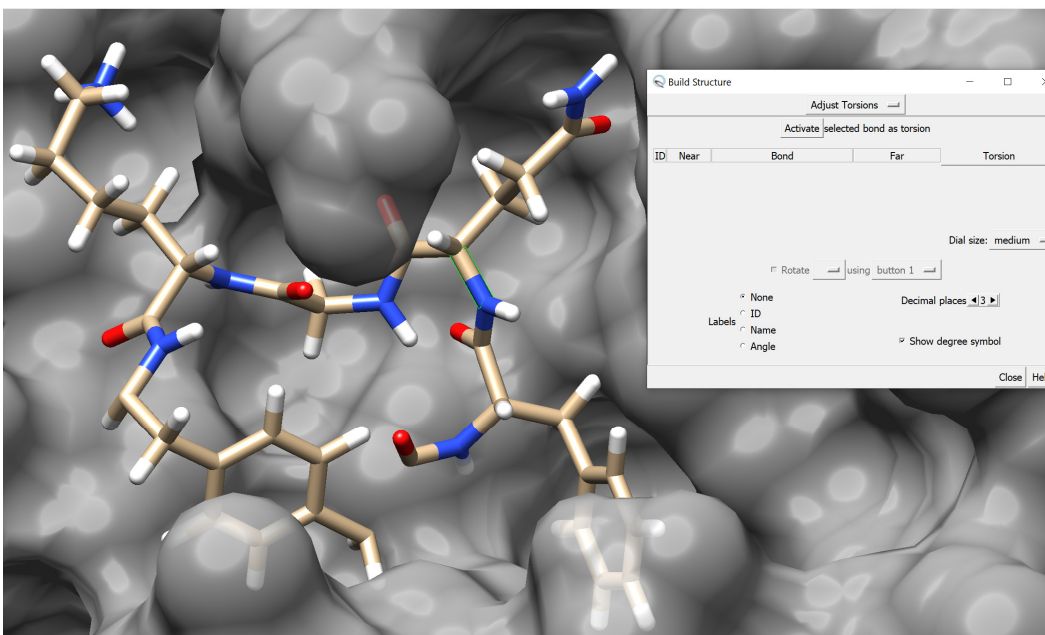
The bond can be rotated in three ways:

- a. Entering a new angle value and pressing **Enter**
- b. Clicking the arrow buttons to the left and right of the angle value
- c. Clicking and dragging the circular dial

Using the method of your choice, rotate the bond so the carbonyl carbon and the newly built methylene (CH₂) group carbon are as close to one another as possible. The goal is for there to be no intersections once a new bond is formed between these two atoms. In this case, we click the arrow button to the left of the angle value until the angle value shows -109.0.

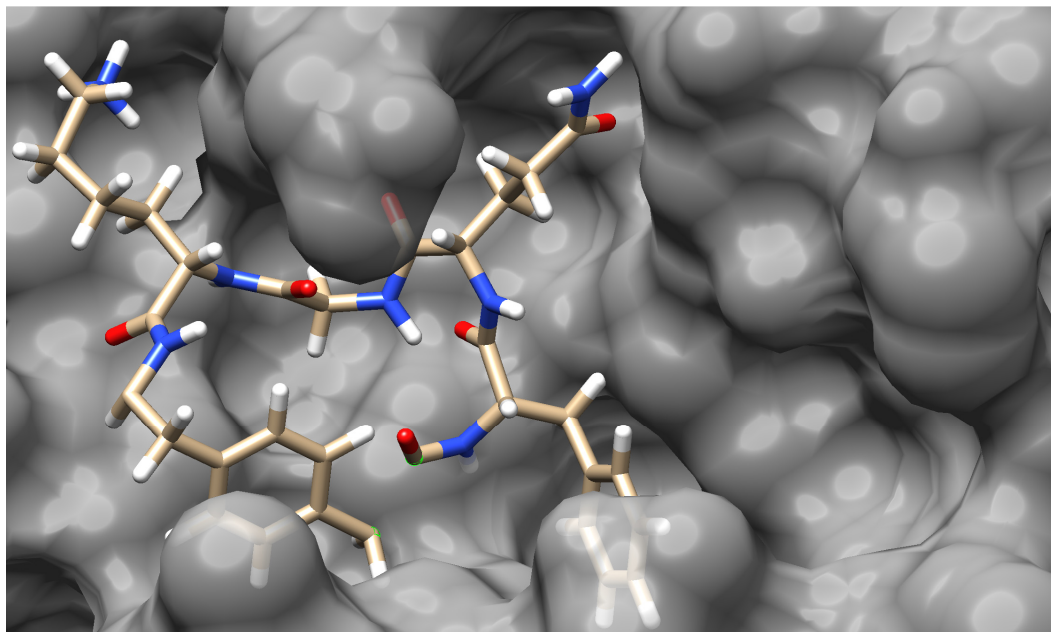


After you are done rotating, deactivate the bond torsion. To do so, click on #0.1 GLN 306.A CA -> N button and under the drop-down menu select Deactivate.

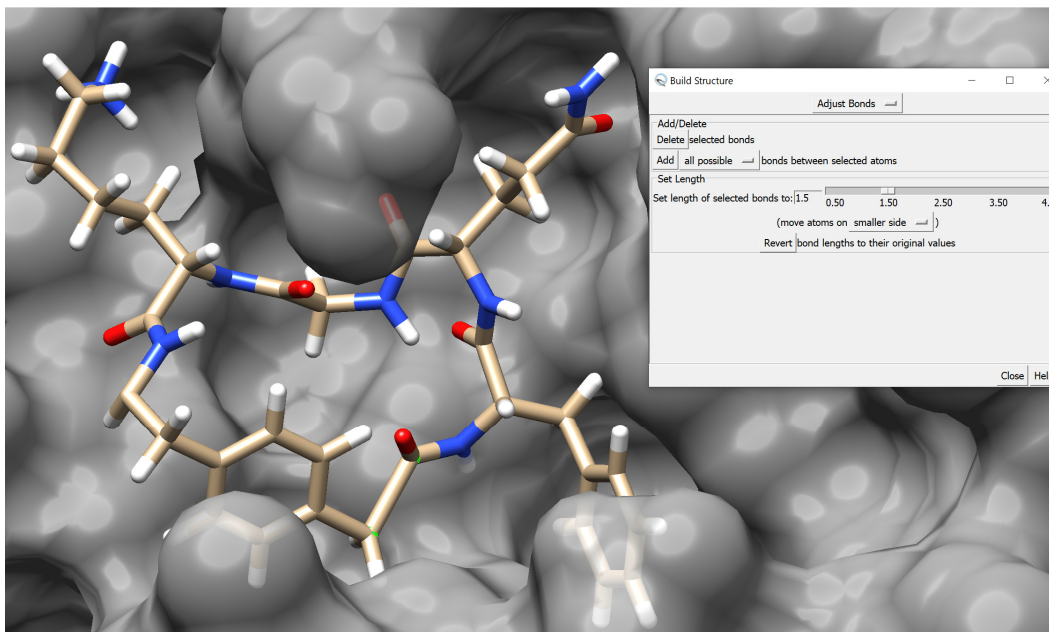


Now we want to build a C-C bond between the Thr 304 carbonyl carbon and the newly built methylene (CH₂) group carbon to cyclize the substrate. *Select* → *Clear Selection*. Use

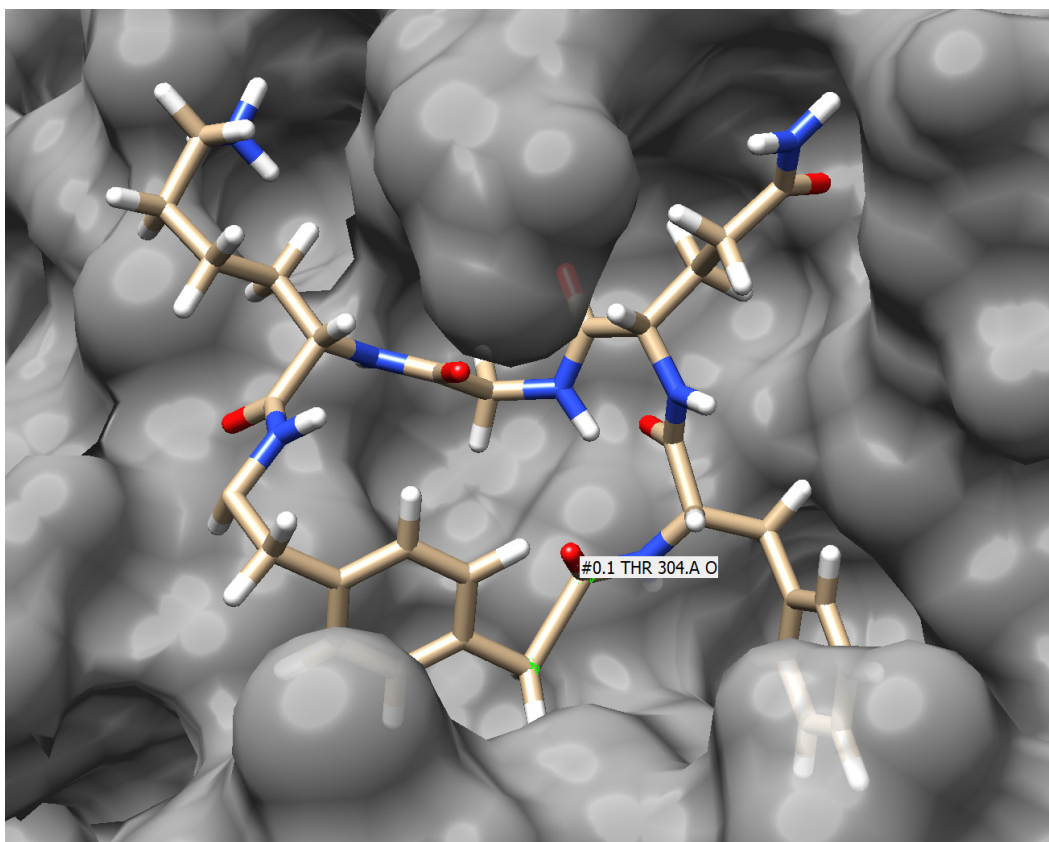
Ctrl+Shift+LMB to simultaneously select both the carbonyl carbon of Thr 304 and the CH₂ carbon.



In the currently open “Build Structure” window, change from the Adjust Torsions tab to the Adjust Bonds tab. Find the drop-down menu that says reasonable and change it to all possible. Because the selected carbon atoms are more than 1.5 Angstroms apart, the bond we are about to create is not ‘reasonable;’ however, the upcoming minimization will correct the bond length and make it reasonable. Click Add to form this new bond. Again check to make sure that this new bond is not crossing other atoms or bonds.



3.5. Renaming Thr 304



The last step we do before conducting structural minimization of the cyclic peptide inhibitor is renaming Thr 304. The minimization method we select in this chapter is the AMBER* force field, which is pre-programmed to recognize the canonical amino acids. However, if a modified amino acid has the name of a canonical amino acid, the force field will not recognize it and the minimization will fail. Thr 304 is no longer intact after we have deleted parts of it. We have to rename it so that the force field will treat it as a new object. The previously modified Phe 309 has already been renamed as “UNK” by UCSF Chimera when we were adding a methyl group to it, so we rename the modified Thr 304 as “UK2” using the command line. To open the command line:

Tools → General Controls → Command Line

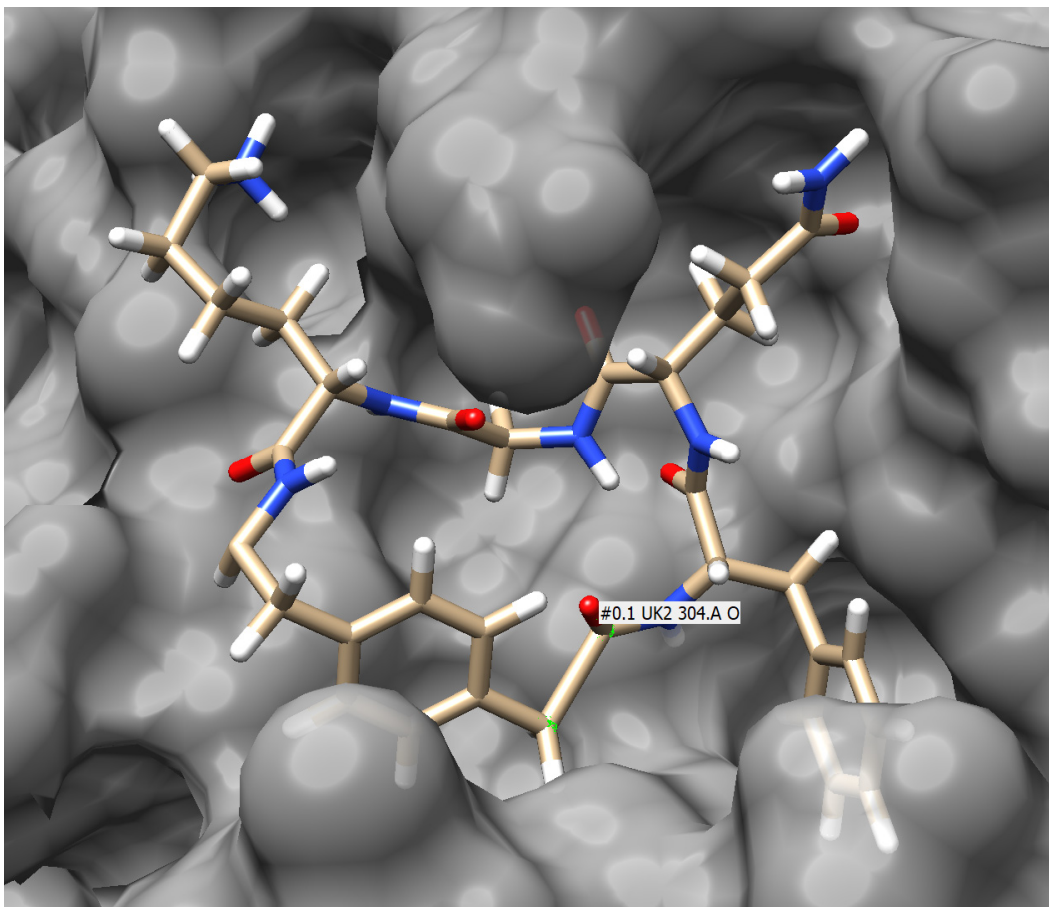
In the command line, type:

```
setattr r type UK2 :304.A
```

Then press **Enter**.

“setattr” stands for “Set Atttribute.” “r” means “residue,” “type” refers to the residue name, “UK2” is the new residue name, and “:304.A” is residue 304 on chain A (the “chain” is derived from the original PDB file).

Hover the cursor over Thr 304 to confirm that the name has been changed to “UK2.”

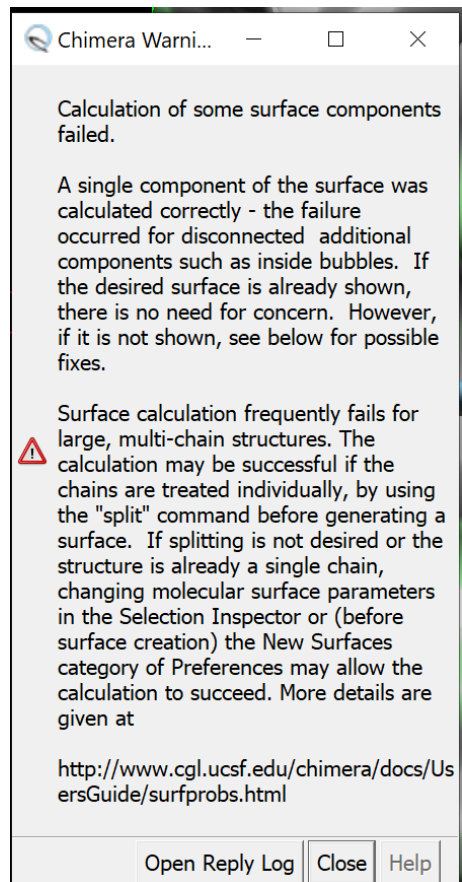


4. **Geometry optimization of the cyclic peptide inhibitor**

Since the bond lengths, angles, and dihedral angles of the newly built cyclic peptide are not optimal, we want to perform geometry optimization (structural minimization) to clean up the structure.

4.1. Changing the VDW radii used to create the surface

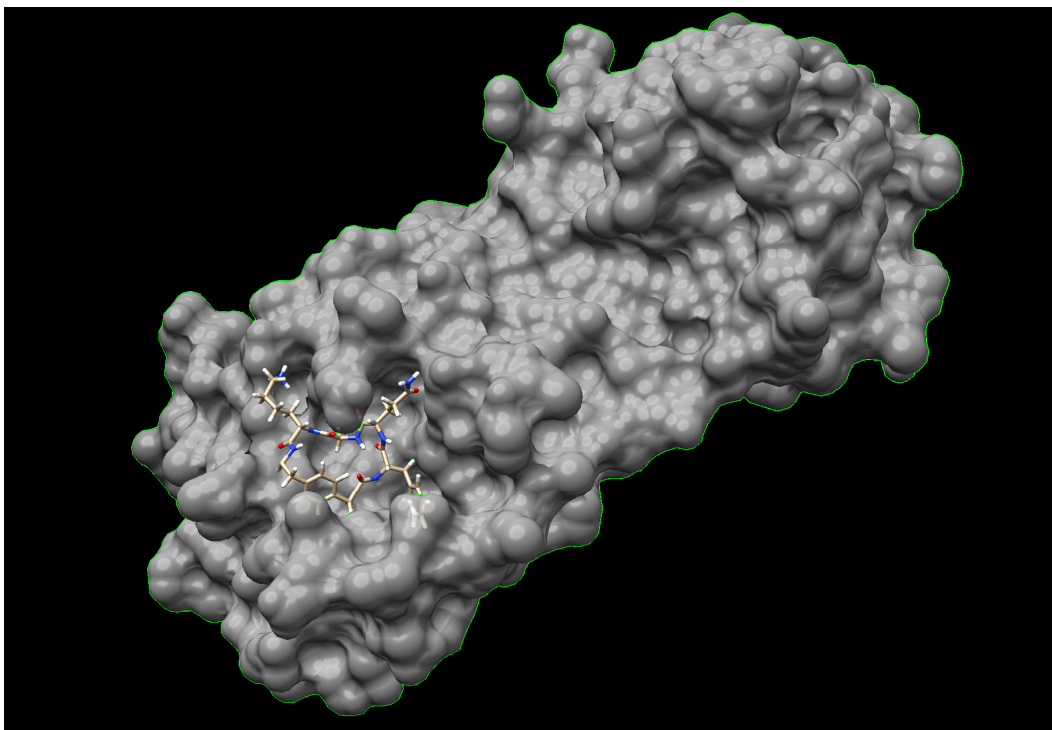
When minimizing, UCSF Chimera will be adding hydrogen atoms to both the cyclic peptide inhibitor as well as the protein. When hydrogens are added to a protein displayed in a surface representation, the following error message often pops up reflecting numerical failure of the embedded MSMS code in UCSF Chimera:⁵



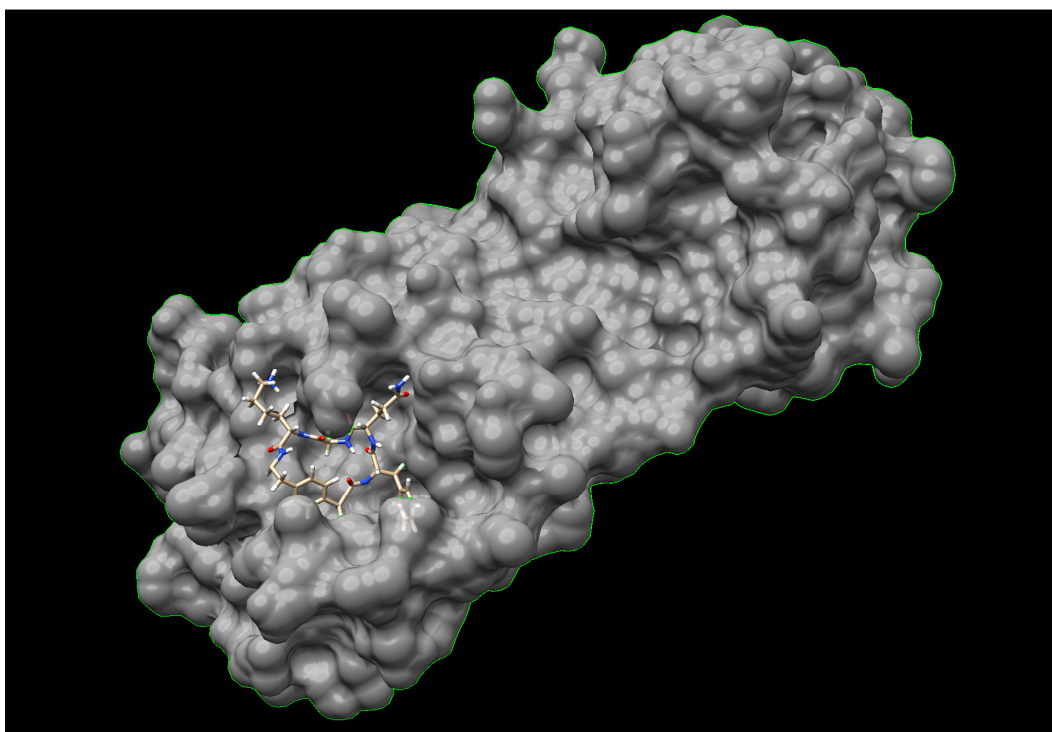
To avoid this error message, before adding hydrogens to the protein, we will slightly increase the van der Waals radii of all atoms. To do so:

Select → Clear Selection

Ctrl+LMB on any part of the surface to select the protein (you will see a green outline when the protein is selected).



In the currently open command line at the bottom of the workspace, type "vdwdefine +.05", then press **Enter**.⁵

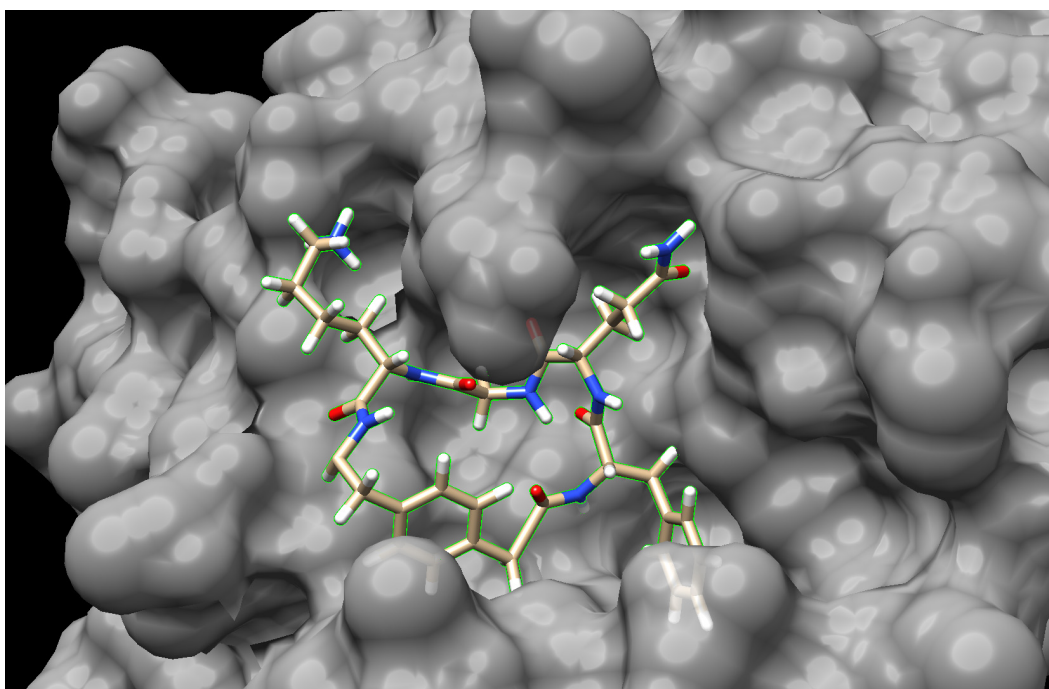


4.2. Minimize the cyclic peptide inhibitor while fixing the protein

We want to fix the protein and allow the cyclic peptide inhibitor to move freely during minimization. To do so:

Select → Clear Selection

Ctrl+LMB on any part of the cyclic peptide inhibitor, then press the **up** arrow key twice to select the entire cyclic peptide inhibitor.



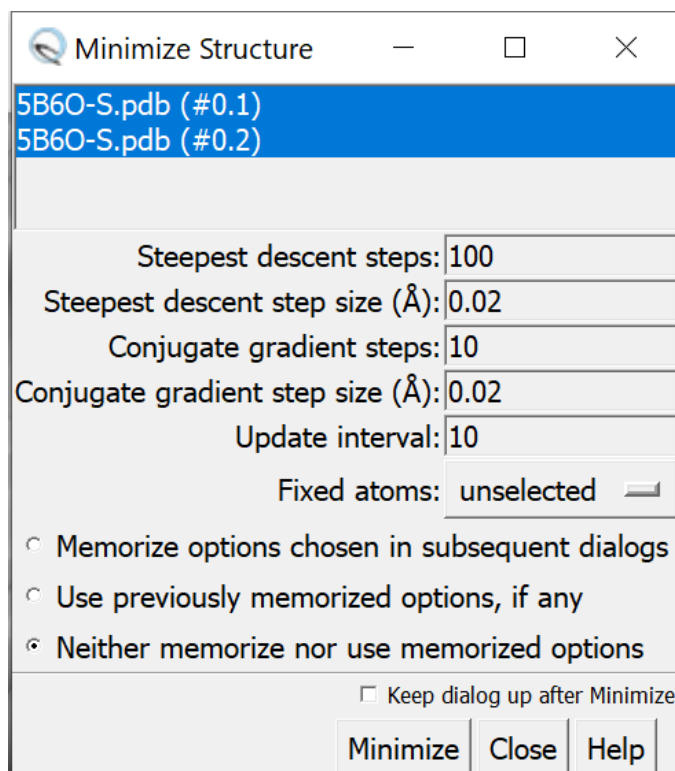
Open the “Minimize Structure” window using:

Tools → Structure Editing → Minimize Structure

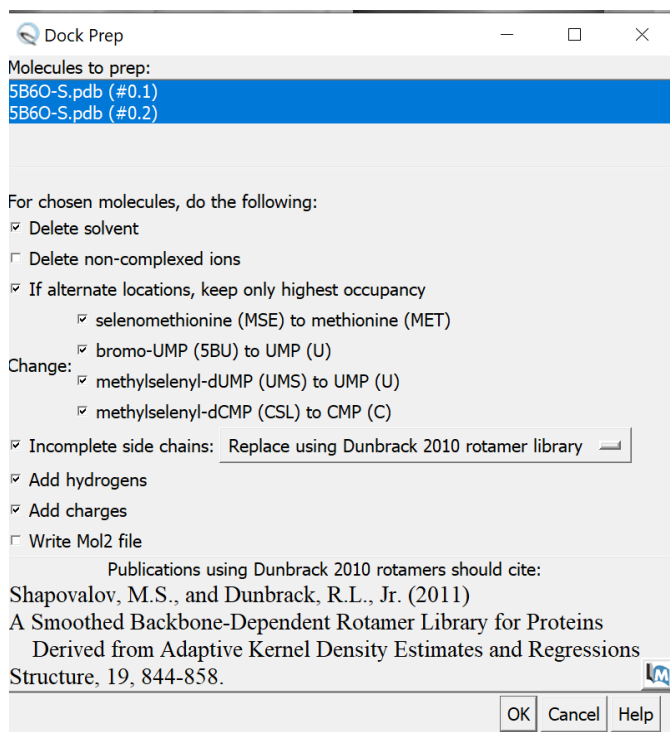
The following window will appear. Make sure that both “5B6O-S.pdb (#0.1)” and “5B6O-S.pdb (#0.2)” are highlighted so both the cyclic peptide inhibitor and the protein will be included in the minimization process.

Under the drop-down menu “Fixed atoms”, change from “none” to “unselected.” Doing so will fix the protein and allow the cyclic peptide inhibitor to move freely during minimization.

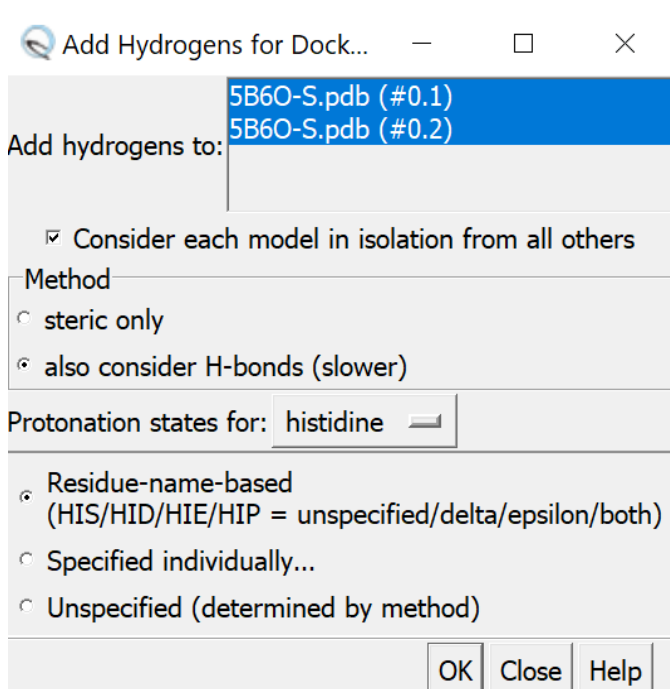
Select the radio button for “Neither memorize nor use memorized options” to prevent accidentally changing the upcoming minimization options.



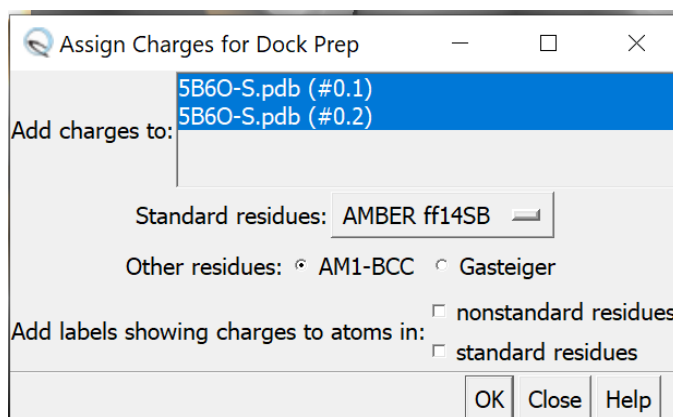
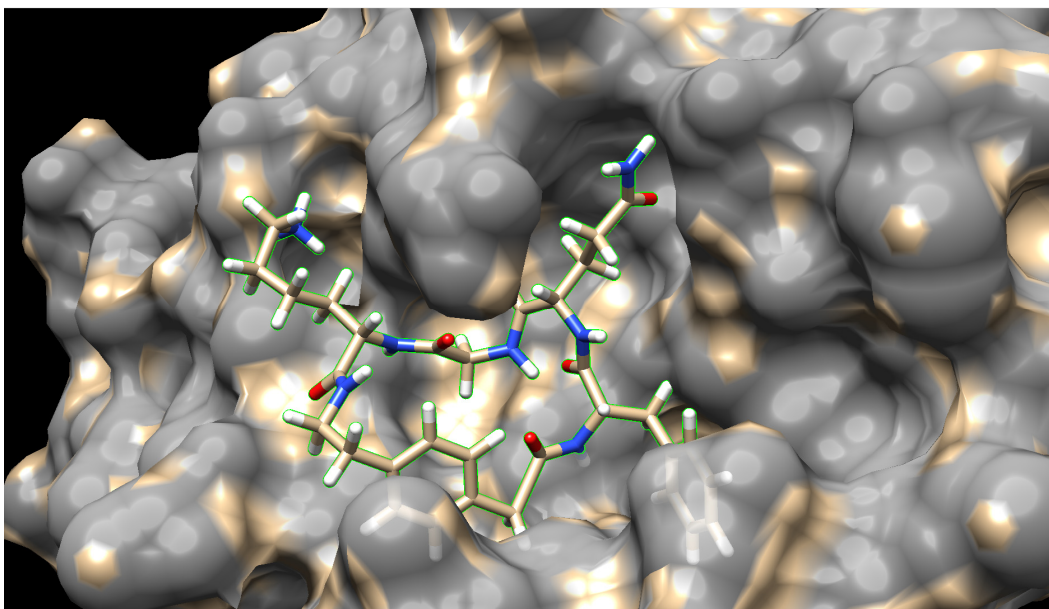
Click Minimize. The “Dock Prep” window will appear. Make sure that both “5B6O-S.pdb (#0.1)” and “5B6O-S.pdb (#0.2)” are highlighted, but leave the other settings as their defaults.⁶



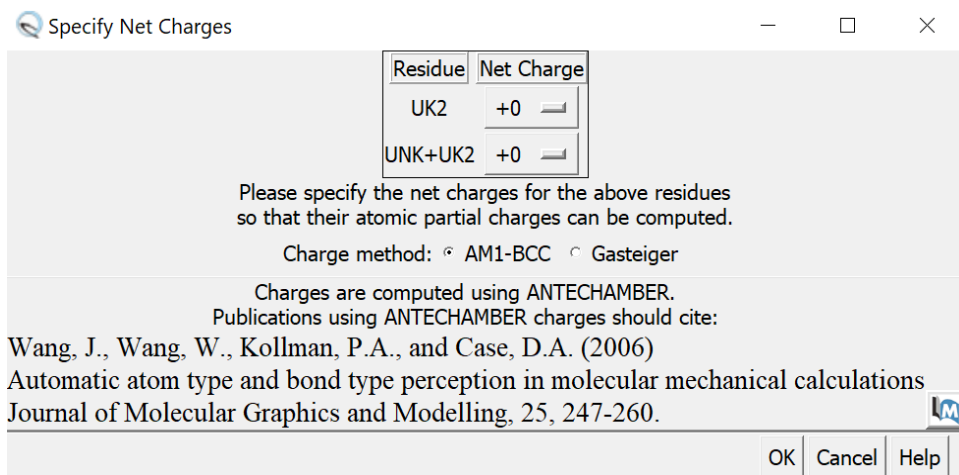
Click OK. The “Add Hydrogens for Dock Prep” window will appear. As before, make sure that both “5B6O-S.pdb (#0.1)” and “5B6O-S.pdb (#0.2)” are highlighted, but leave the other settings as their defaults.



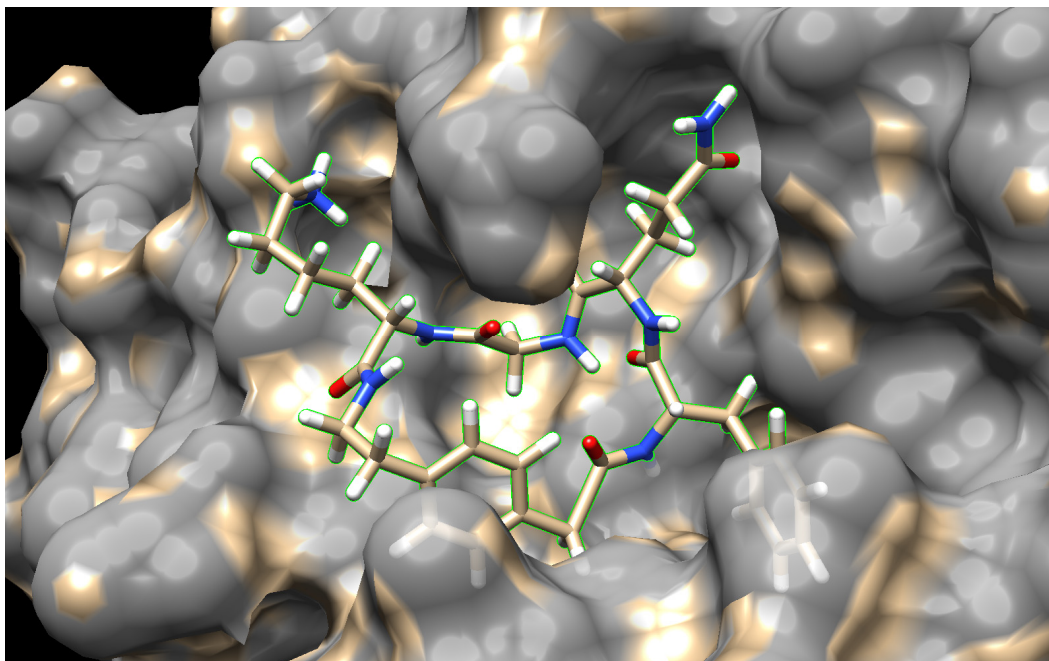
Click OK. Hydrogens have now been added to both the protein and the substrate. Note some of the newly added hydrogens on the substrate are not selected. In the UCSF Chimera window, press **up** arrow once to select the entire cyclic peptide substrate. In the “Assign Charges for Dock Prep” window, make sure that both “5B6O-S.pdb (#0.1)” and “5B6O-S.pdb (#0.2)” are highlighted, but leave the other settings as their defaults.



Click OK. The “Specify Net Charges” window will appear. The non-canonical amino acids UNK and UK2 that we built are not charged, so we use the default setting of net charge = 0. Leave the charge method as default: AM1-BCC.⁷

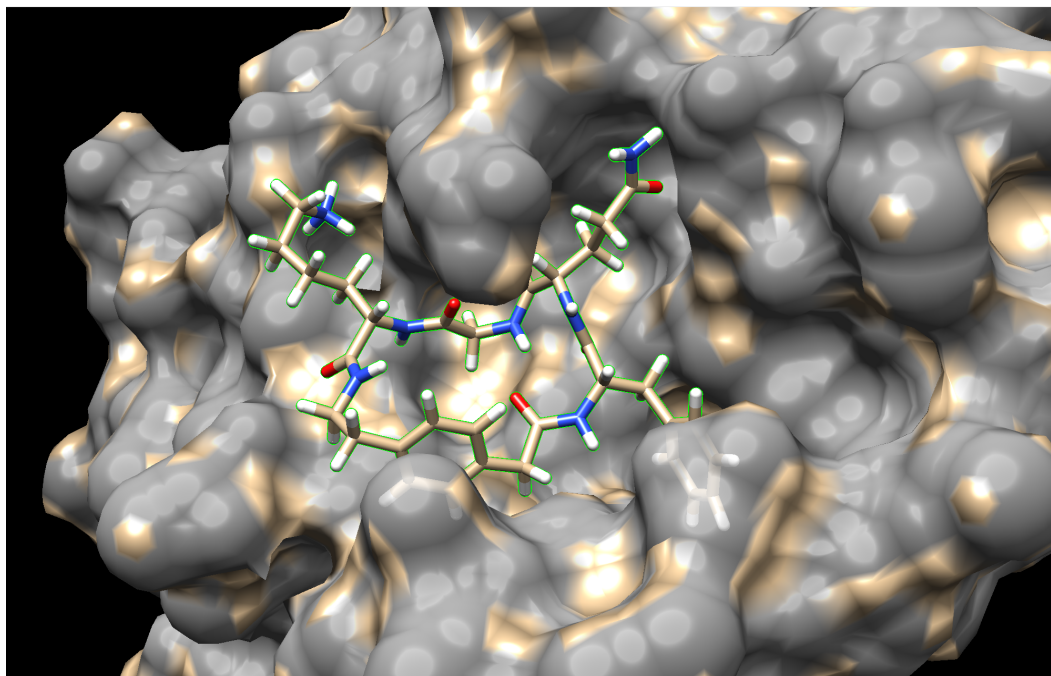


The following figure illustrates the cyclic peptide inhibitor structure before minimization.



Click OK in the “Specify Net Charges” window, and the minimization process will proceed in two steps: The first is “Steepest Descent”, during which you will be able to see subtle movements of the cyclic peptide inhibitor in increments of 10 steps. The second is “Conjugate Gradient”, which takes longer than “Steepest Descent”. “Finished 10 of 10

conjugate gradient minimization steps” will show at the bottom when the minimization is finished. The minimization should be complete in 2-5 minutes.



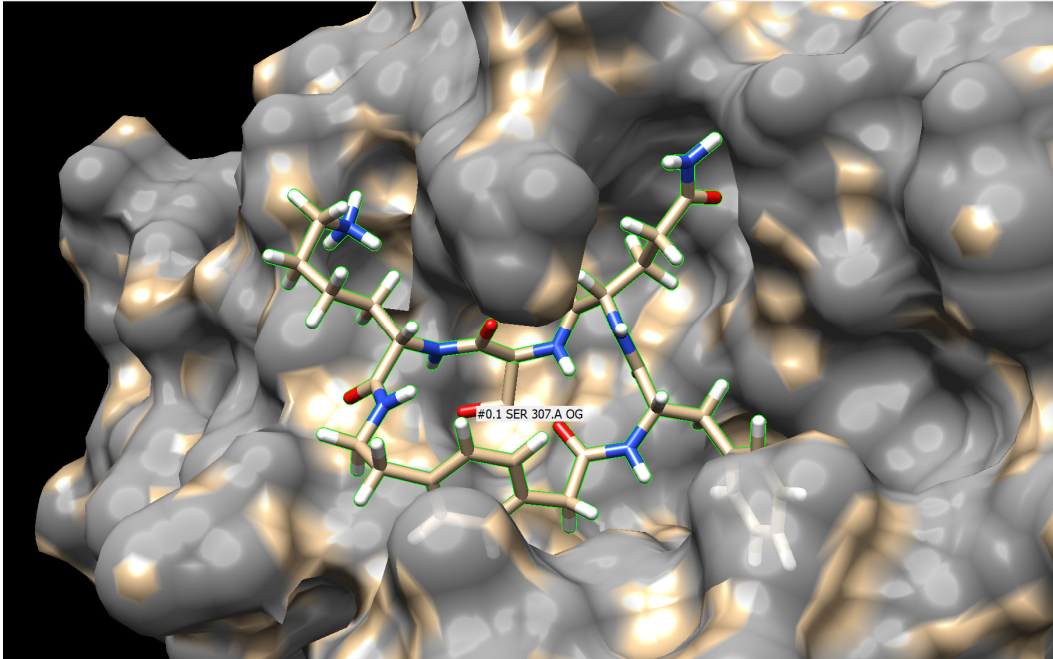
4.3. Mutating Gly 307 to Ser 307

We want to mutate Gly 307 to Ser to make the cyclic peptide inhibitor less flexible (i.e. more conformationally rigid). To do so, in the currently open command line at the bottom of the window, type

```
swapaa ser :307.a
```

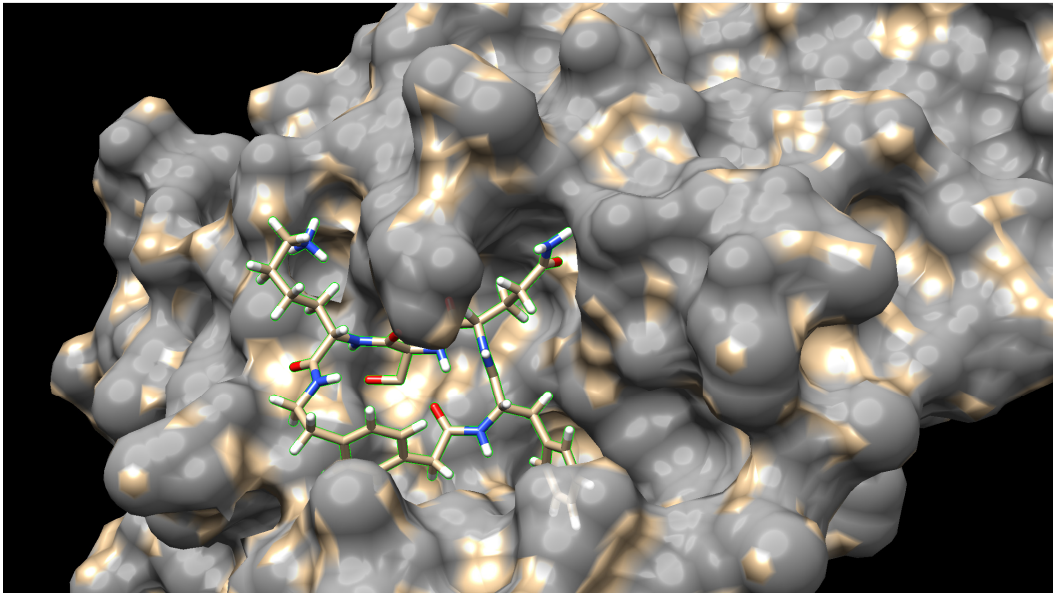
Then press **Enter**.

Gly 307 has now been mutated to Ser, and the name of that residue has also been changed to “Ser 307”.



4.4. The second-round of minimization after mutating Gly 307 to Ser 307

The side chain of Ser 307 is not selected. Press **up** arrow once to select the entire cyclic peptide inhibitor including the side chain of Ser 307.

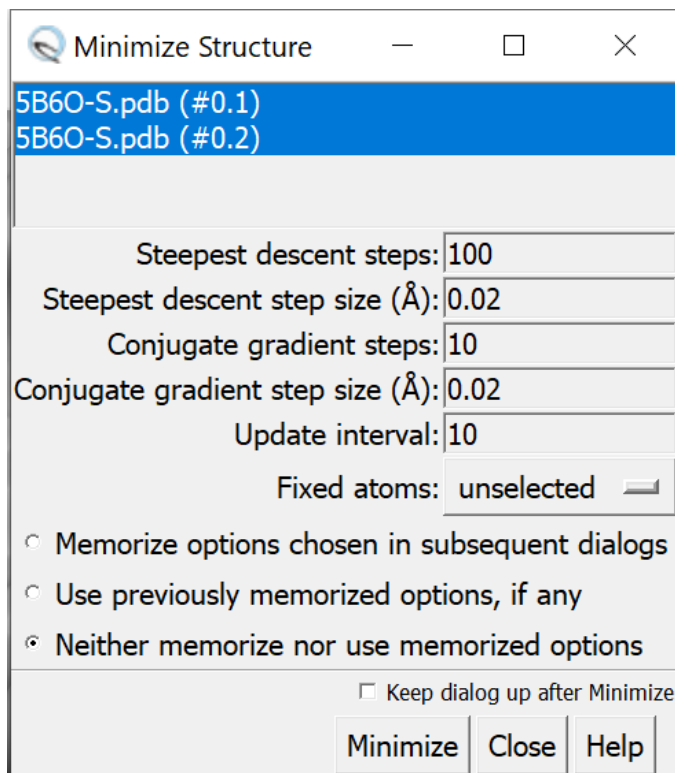


Open the “Minimize Structure” window using *Tools* → *Structure Editing* → *Minimize Structure*.

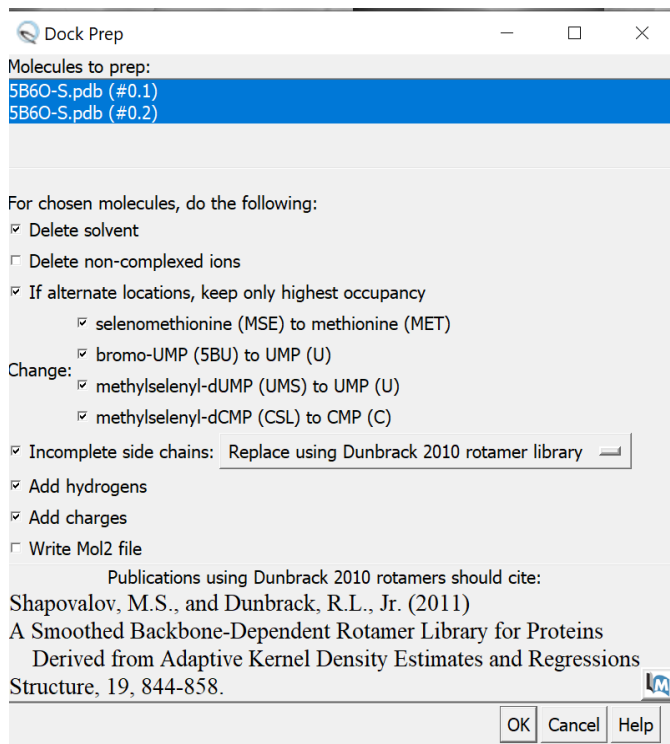
The following window will appear. Make sure that both “5B6O-S.pdb (#0.1)” and “5B6O-S.pdb (#0.2)” are highlighted so both the cyclic peptide inhibitor and the protein will be included in the minimization processes.

Under the drop-down menu “Fixed atoms”, change from “none” to “unselected.” This way we fix the protein and allow the cyclic peptide inhibitor to move freely during minimization.

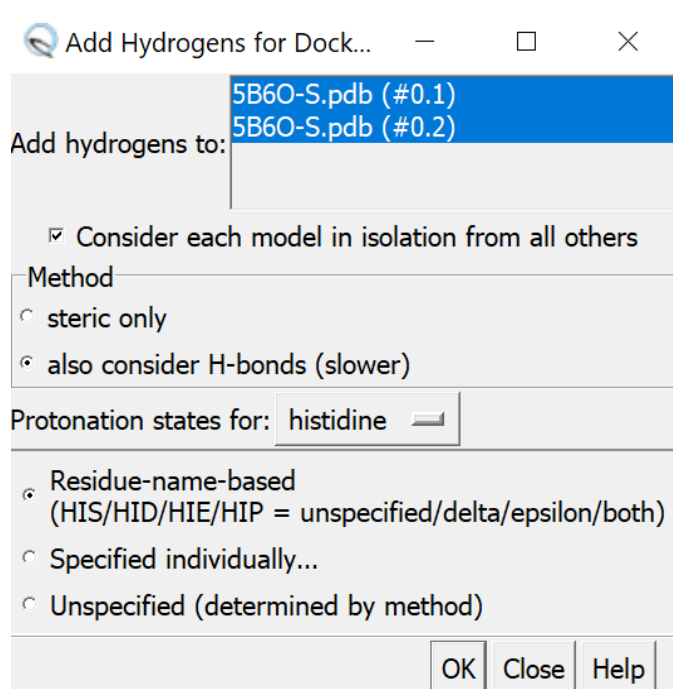
Select the radio button for “Neither memorize nor use memorized options” to prevent accidentally changing the upcoming minimization options.



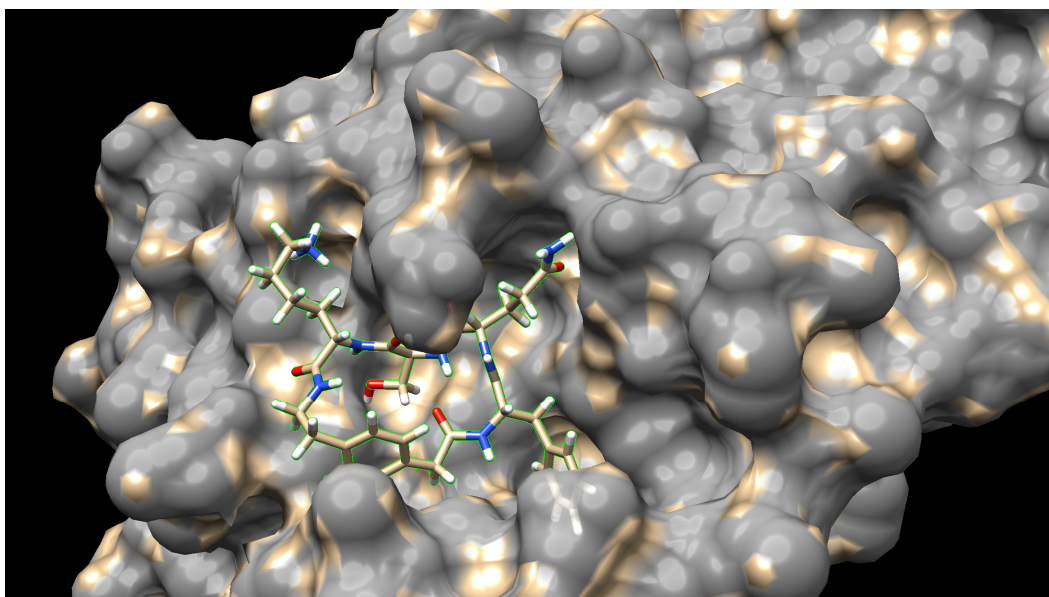
Click Minimize. The “Dock Prep” window will appear. Make sure that both “5B6O-S.pdb (#0.1)” and “5B6O-S.pdb (#0.2)” are highlighted, but leave the other settings as their defaults.⁶



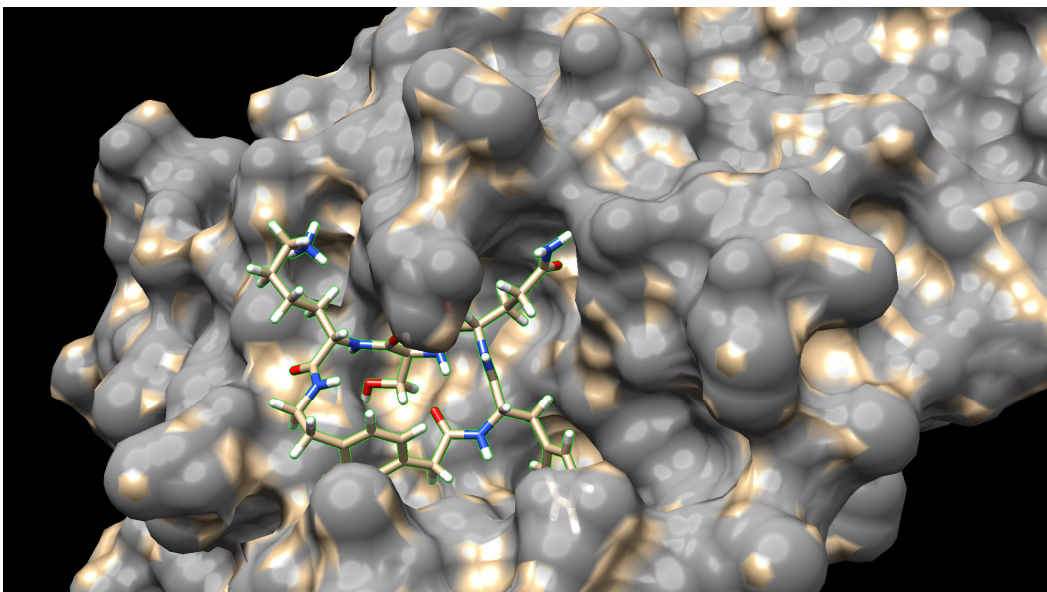
Click OK. The “Add Hydrogens for Dock Prep” window will appear. As before, make sure that both “5B6O-S.pdb (#0.1)” and “5B6O-S.pdb (#0.2)” are highlighted, but leave the other settings as their defaults.



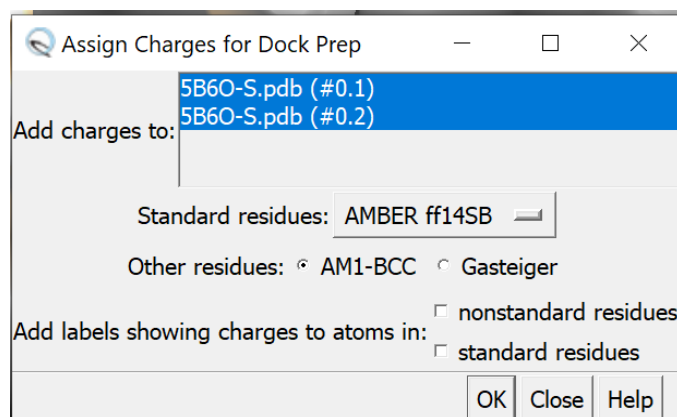
Click OK. Hydrogens have now been added to both the protein and the ligand.



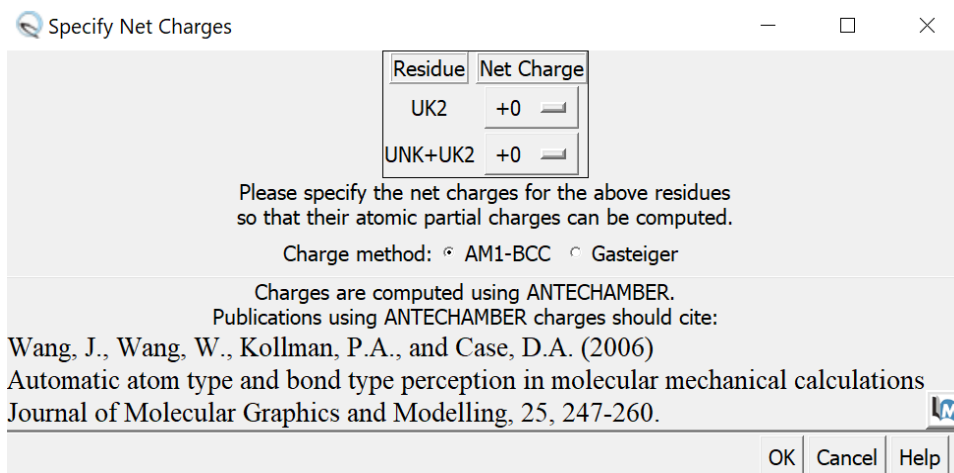
The hydrogens that just added to Ser 307 are not selected. Press **up** arrow once to select the entire cyclic peptide inhibitor including the hydrogens that was just added to Ser 307.



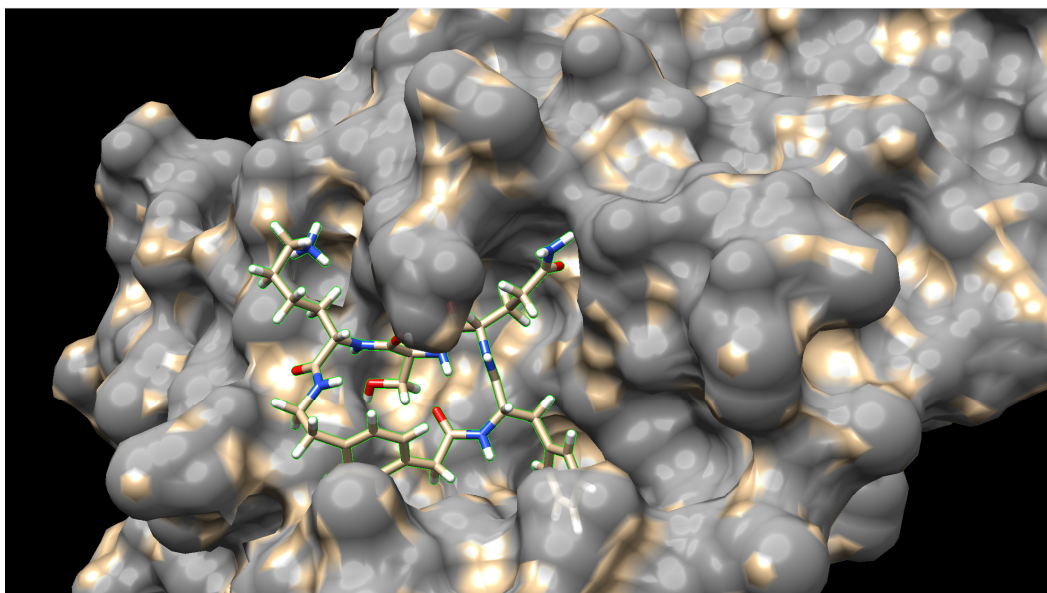
The “Assign Charges for Dock Prep” window will appear. Again, make sure that both “5B6O-S.pdb (#0.1)” and “5B6O-S.pdb (#0.2)” are highlighted, but leave the other settings as their defaults.



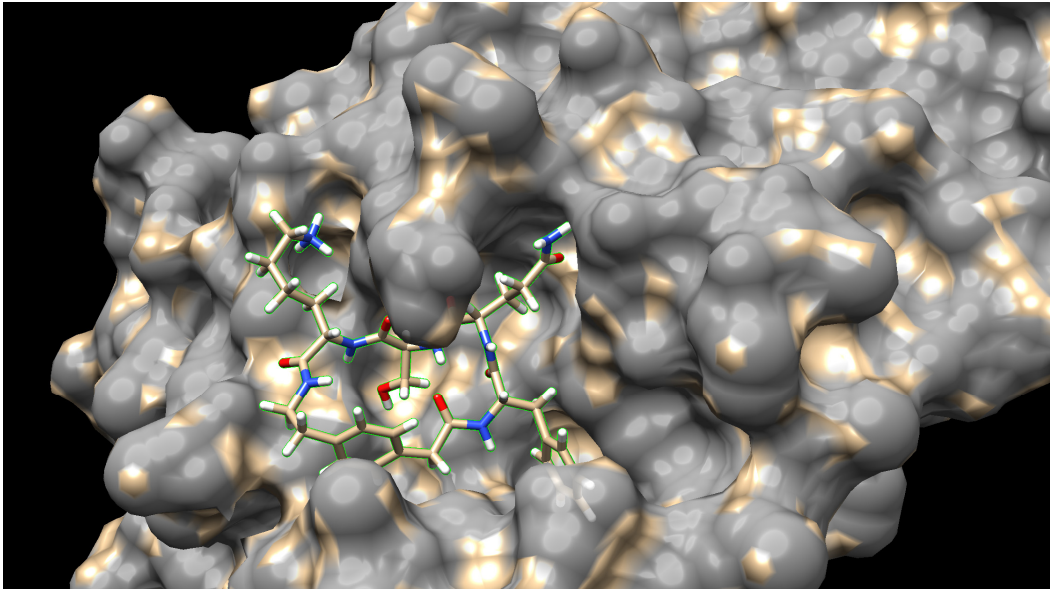
Click OK. The “Specify Net Charges” window will appear. The non-canonical amino acids UNK and UK2 are not charged, so we use the default setting of net charge = 0. Leave the charge method as default: AM1-BCC.⁷



The following figure illustrates the cyclic peptide inhibitor structure before minimization.



Click OK in the “Specify Net Charges” window, and the minimization process will proceed in two steps: The first is “Steepest Descent”, during which you will be able to see subtle movements of the cyclic peptide inhibitor in increments of 10 steps. The second is “Conjugate Gradient”, which takes longer than “Steepest Descent”. “Finished 10 of 10 conjugate gradient minimization steps” will show at the bottom when the minimization is finished. The minimization should be complete in 2-5 minutes.



5. Docking the inhibitor to SARS-CoV M^{pro}

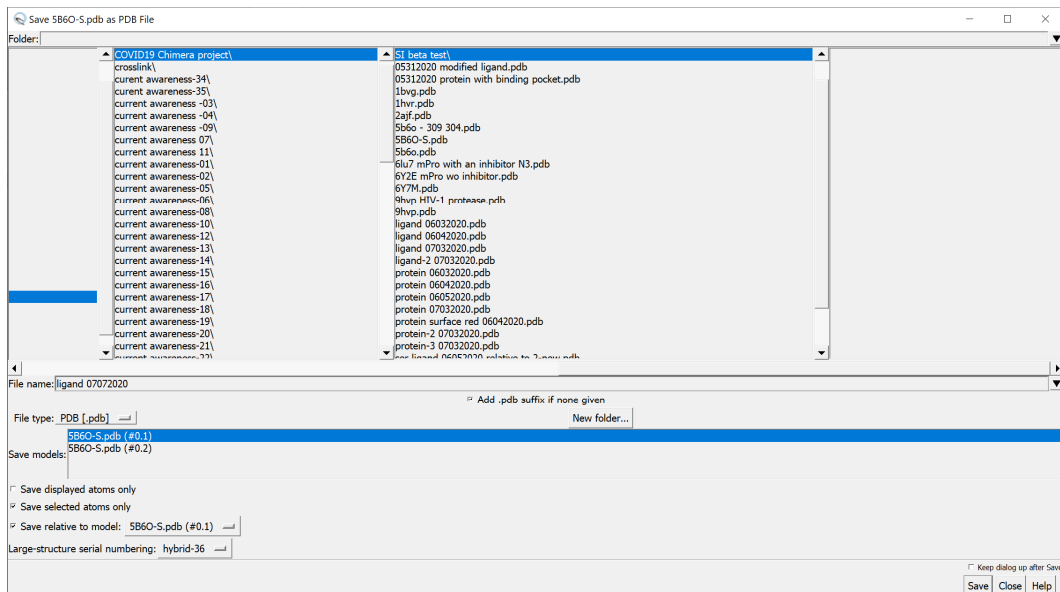
To evaluate the ability of the minimized cyclic peptide inhibitor binds to the SARS-CoV M^{pro}, we will dock the cyclic peptide inhibitor to the SARS-CoV M^{pro} structure (5B6O-S.pdb) using the AutoDock Vina plugin in UCSF Chimera.⁸⁻¹⁰

5.1. Saving the cyclic peptide inhibitor and the protein as separate PDB files

This step follows the “4. geometry optimization of the cyclic peptide inhibitor” section.

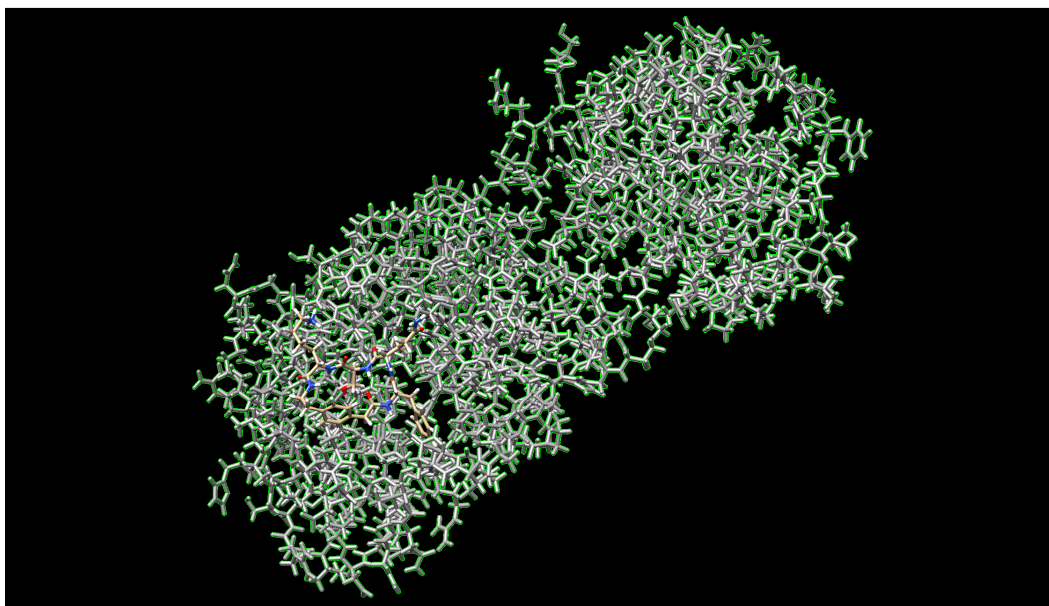
We want to save the cyclic peptide inhibitor and the protein as separate PDB files for AutoDock Vina to perform molecular docking.

To save the cyclic peptide inhibitor as a PDB file, we first make sure the cyclic peptide inhibitor is selected. Then in the menu bar, select *File* → *Save PDB*. In the pop-up window, select save models “5B6O-S.pdb (#0.1)”, select “save selected atoms only”, select “save relative to model “5B6O-S.pdb (#0.1)”, give a valid file name (example “ligand”) and click save.

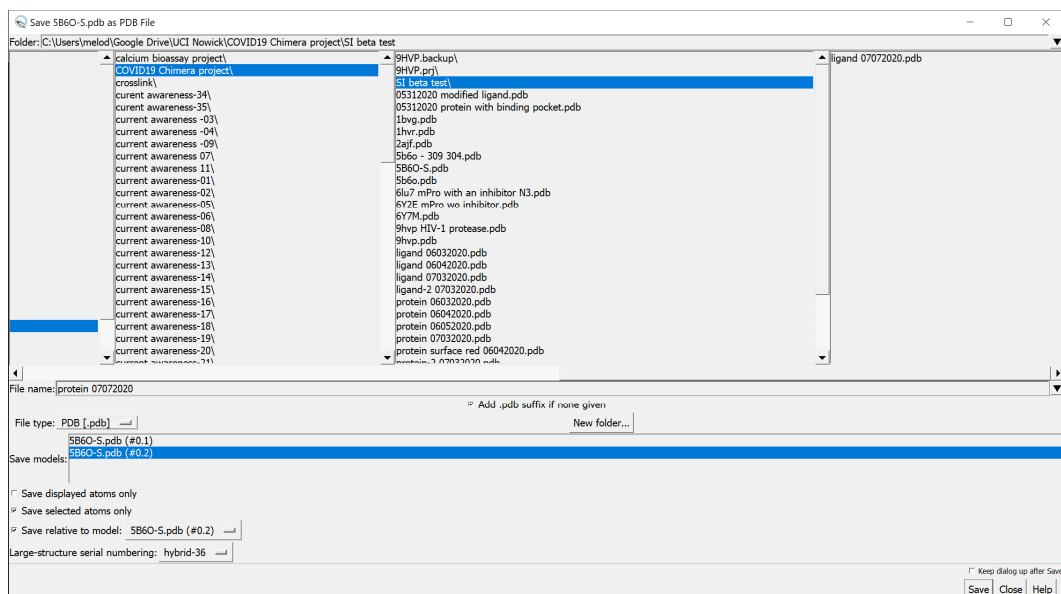


To save the protein (SARS-CoV M^{Pro}) as a PDB file:

Select → *invert (all models)*; *actions* → *surface* → *hide*; *actions* → *atoms/bonds* → *show*



File → *Save PDB*; select save models “5B6O-S.pdb (#0.2)”, select “save selected atoms only”, select “save relative to model “5B6O-S.pdb (#0.2)”, give a valid file name (example “protein”), click save.



5.2. Installing AutoDock Vina and creating a folder for docking files

5.2.1. Download and install AutoDock Vina (<http://vina.scripps.edu/download.html>).

5.2.2. Create a new folder on your desktop or a location you prefer and call it “docking” or a name you prefer.

5.2.3. Copy and paste both the ligand.pdb and protein.pdb that you just saved in the folder that you created on the desktop. Additionally, copy and paste vina.exe in this folder; Vina.exe can be found in your Program Files (X86) in the folder called “The Scripps Research Institute”.

For MacOS users, copy and paste vina linux executable file in this folder that you created on the desktop. The AutoDock Vina Unix executable file is located in the extracted folder that you downloaded from the AutoDock Vina website. Note for MacOS users: this may not happen to all MacOS users, but you might have to unlock permissions to run the AutoDock Vina Unix executable file. To do this, double click the Unix executable file, and

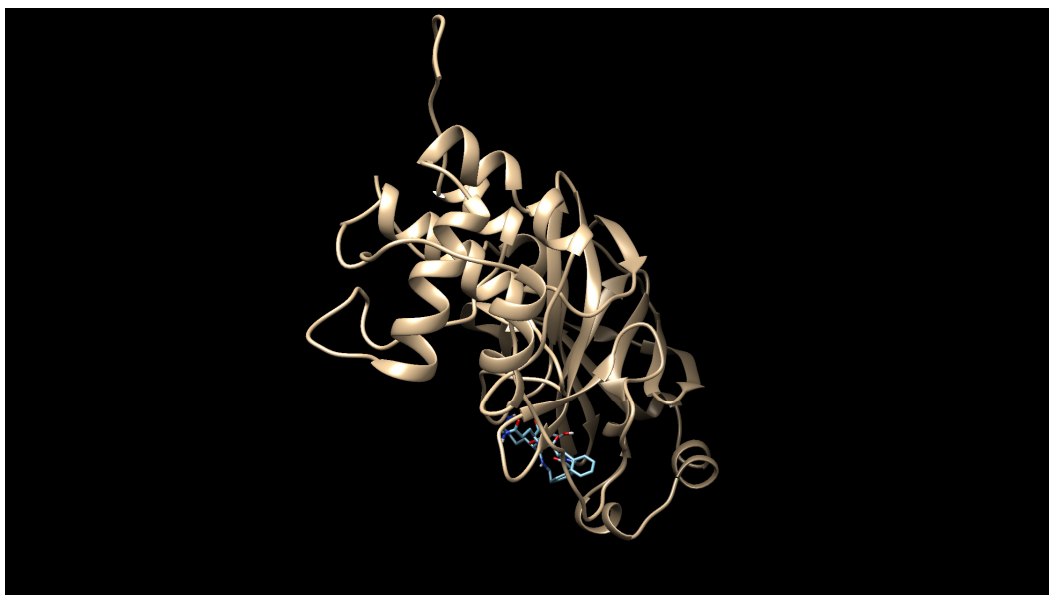
a pop-up window may show up stating that the software could be malware. If this window pops up, click on the “?” button, and then a help guide should load up. Click on the blue link and it should bring you to Security and Privacy preferences. Unlock permissions by entering your password to enable AutoDock Vina.

5.3. Opening the saved ligand and protein PDB files in the same view

File → *close session* to close the current session in UCSF Chimera (make sure that you have saved the important sessions).

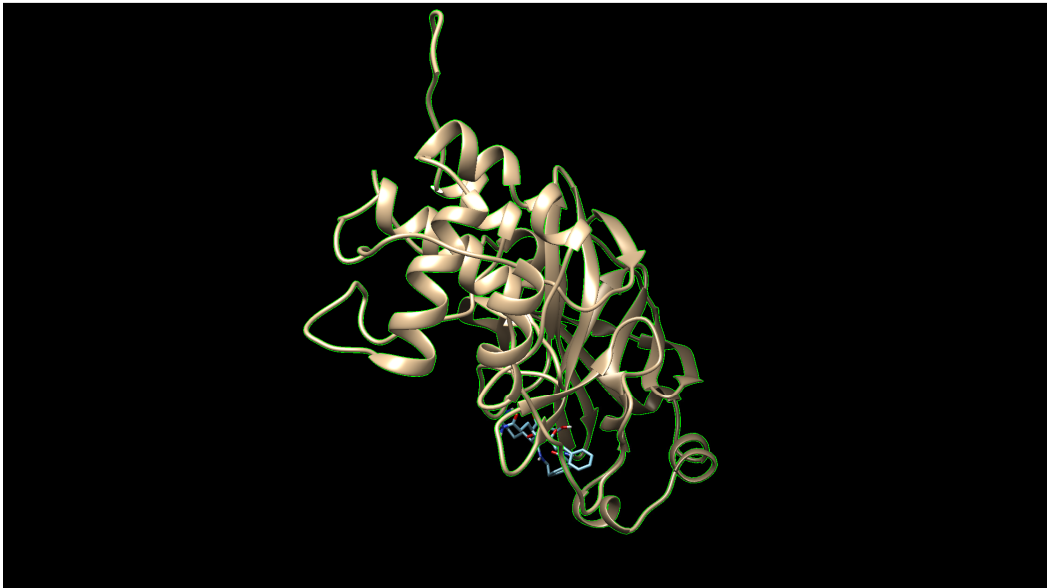
File → *Open*, find the protein.pdb file from the docking folder on your desktop and click open.

File → *Open*, find the ligand.pdb file from the docking folder on your desktop and click open.

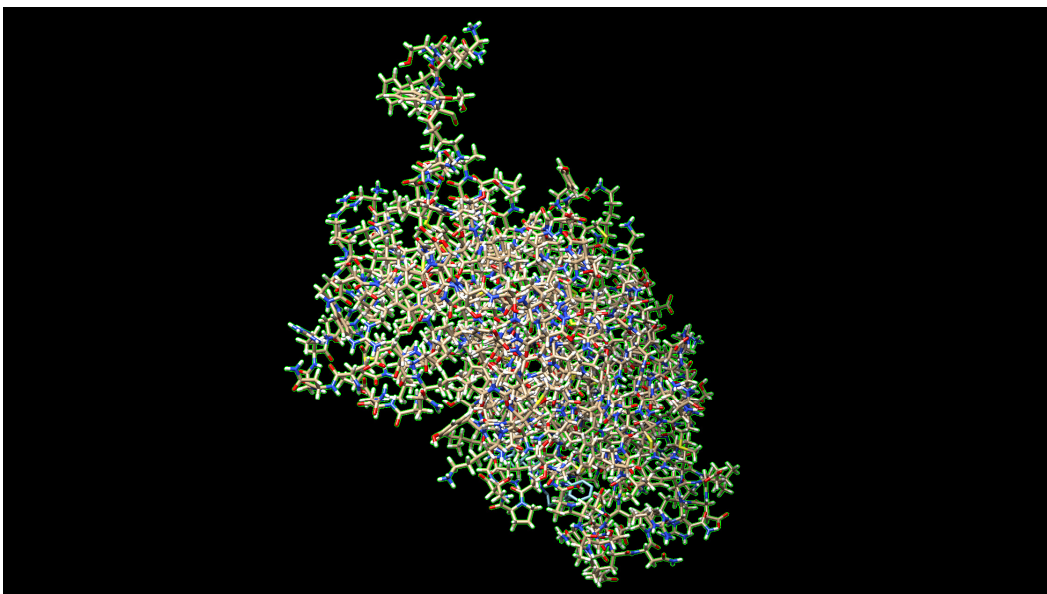


5.4. Highlighting the active site of the protein

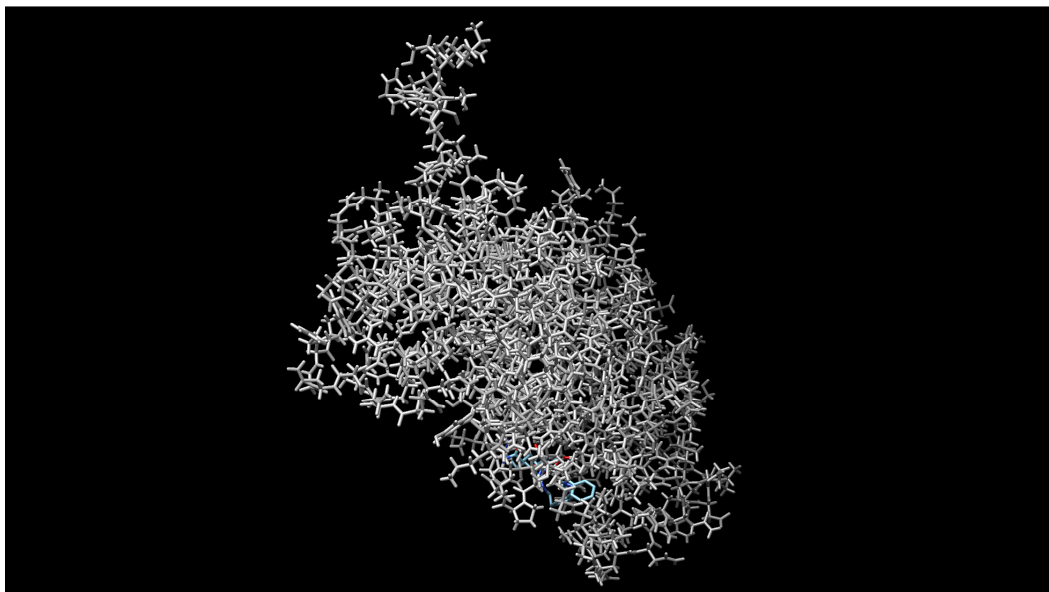
Select the protein by **Ctrl+LMB** any part of the protein, press up arrow twice.



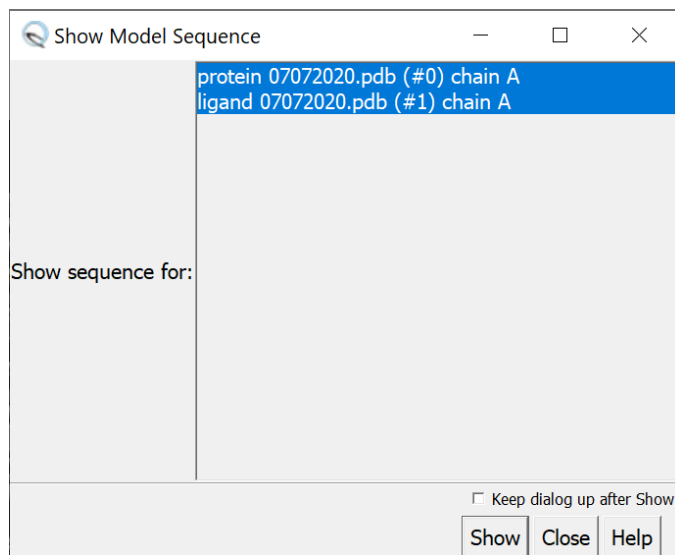
We want to change the preset to “stick” so we can locate the active site (binding pocket) easier. *Actions* → *Ribbon* → *Hide*; *Actions* → *Atoms/Bonds* → *stick*; *Actions* → *Atoms/bonds* → *show*



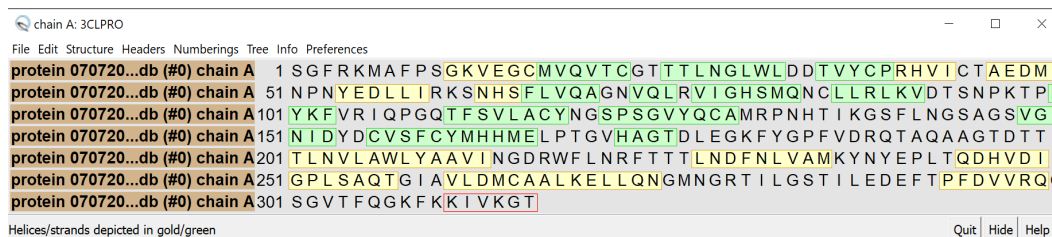
Actions → color → dark grey; Select → clear selection.



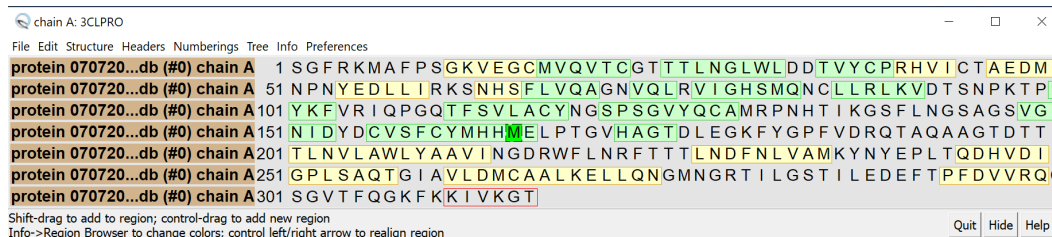
Locate the active site in the protein. It can most easily be found by looking for several residues in the active site, such as Cys 44, Cys 38, Met 49, Met 165, His 41. For example, to find Met 165, *Favorite → sequence*. The following “Show Model Sequence” window will show up.



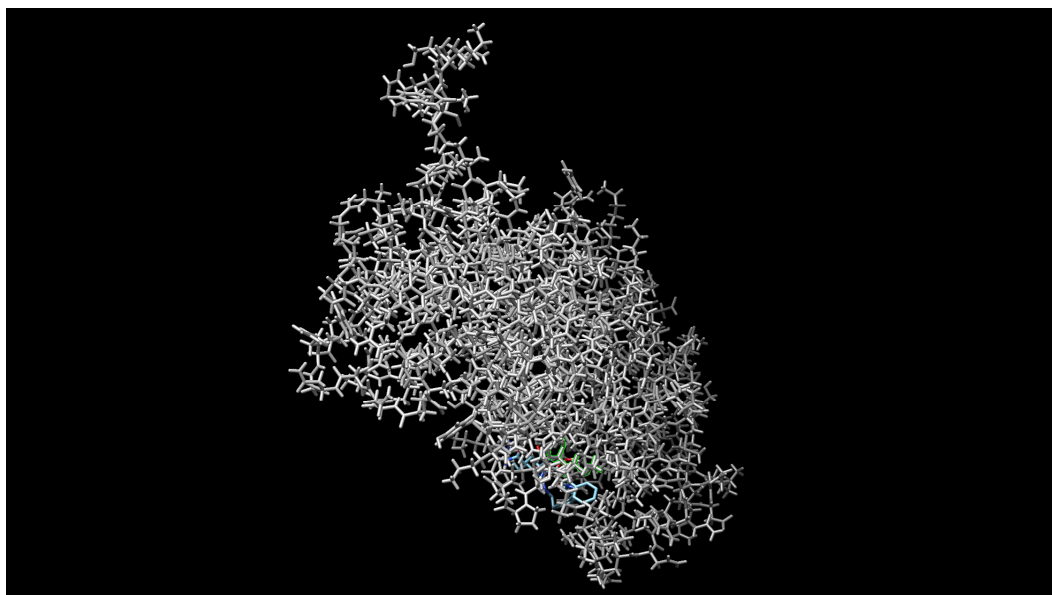
Highlight “protein 07072020.pdb (#0) chain A” only, click Show. The following “chain A: 3CLPRO” window will show up.



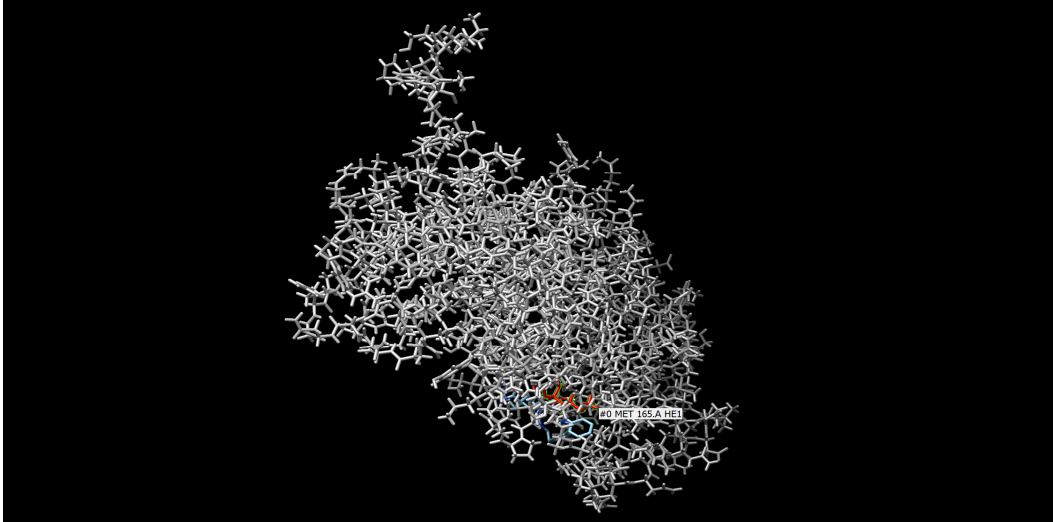
Find position 165, use LMB to click and drag to highlight the letter “M” representing Met 165. Click Quit to close the window.



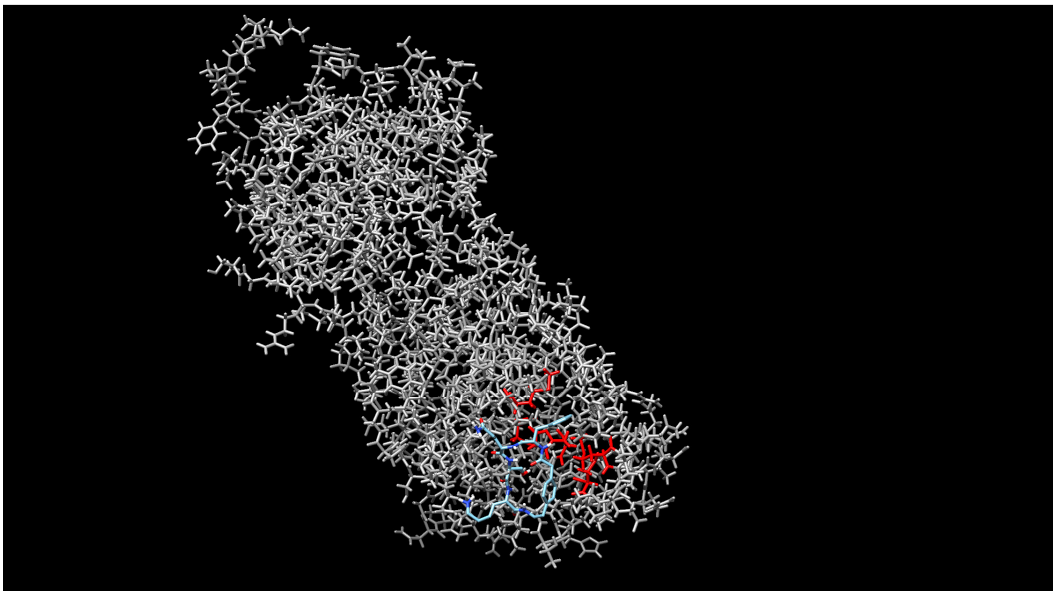
In the UCSF Chimera workspace, Met 165 is selected.



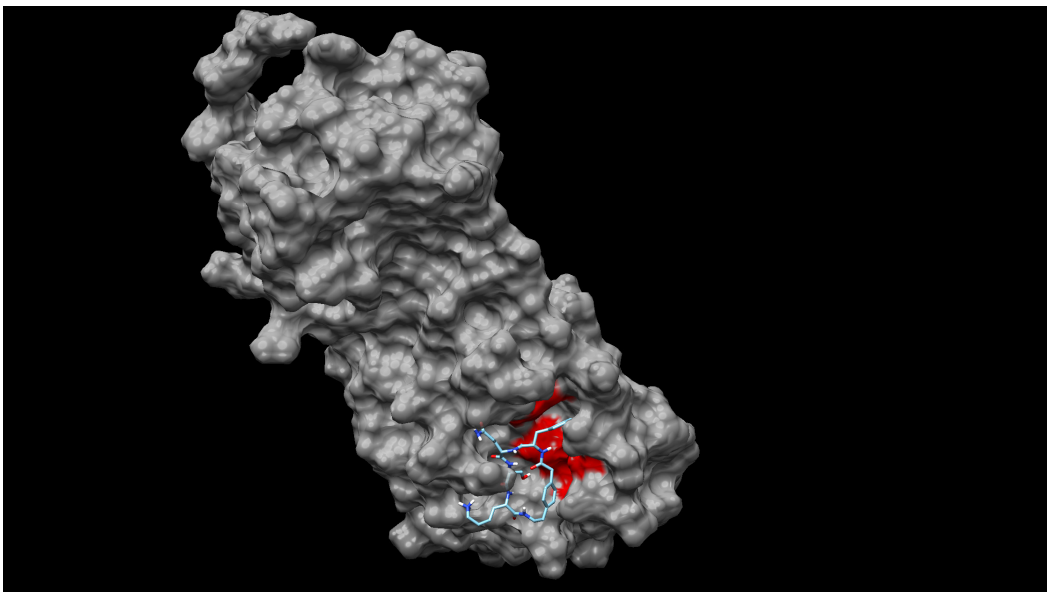
To color Met 165 in red, *Actions* → *color* → *red*.



Repeat the steps for Cys 44, Cys 38, Met 49, His 41. After that, *select* → *clear selection*.

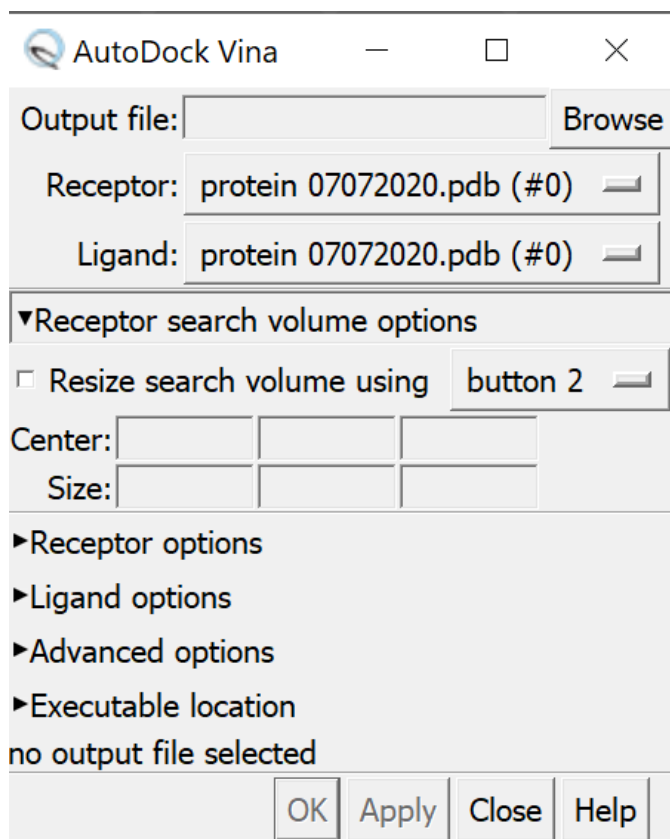


After highlighting several residues in the active site, we can show the protein as a van der Waals surface in order to better visualize the binding pockets in the active site. **Ctrl+LMB** on any part of the protein, press up arrow three times, *actions* → *surface* → *show*; *actions* → *atoms/bonds* → *hide*; *actions* → *surface* → *transparency* → 30%.



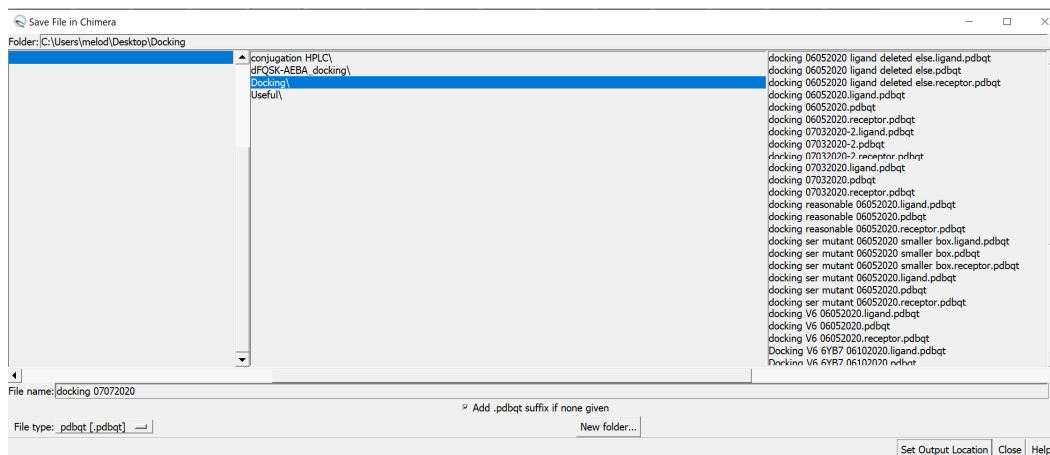
5.5. Running AutoDock Vina

Tools → *Surface/Binding Analysis* → *AutoDock Vina* (a new window will pop up).

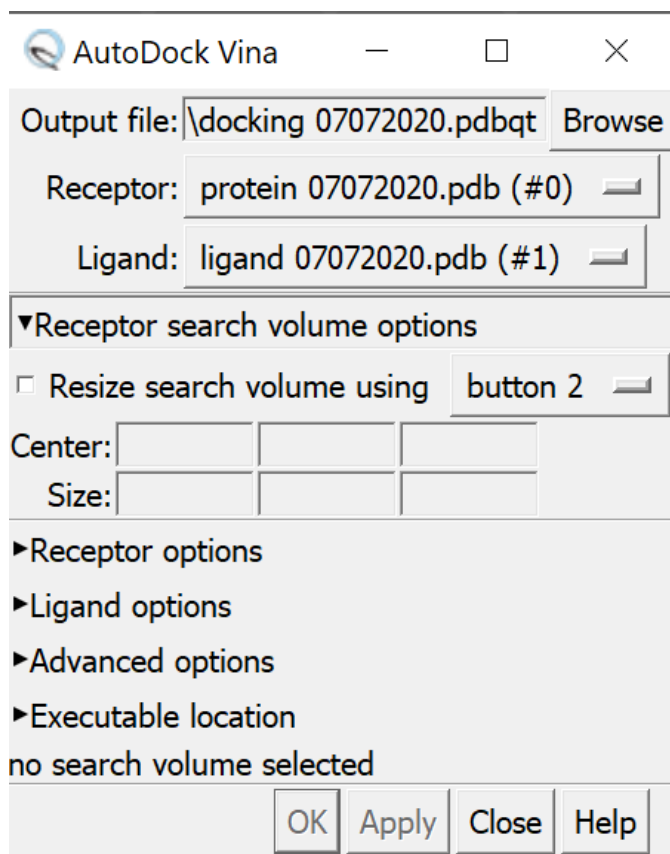


Click on Browse next to “Output file” and find the folder that you created on the desktop.

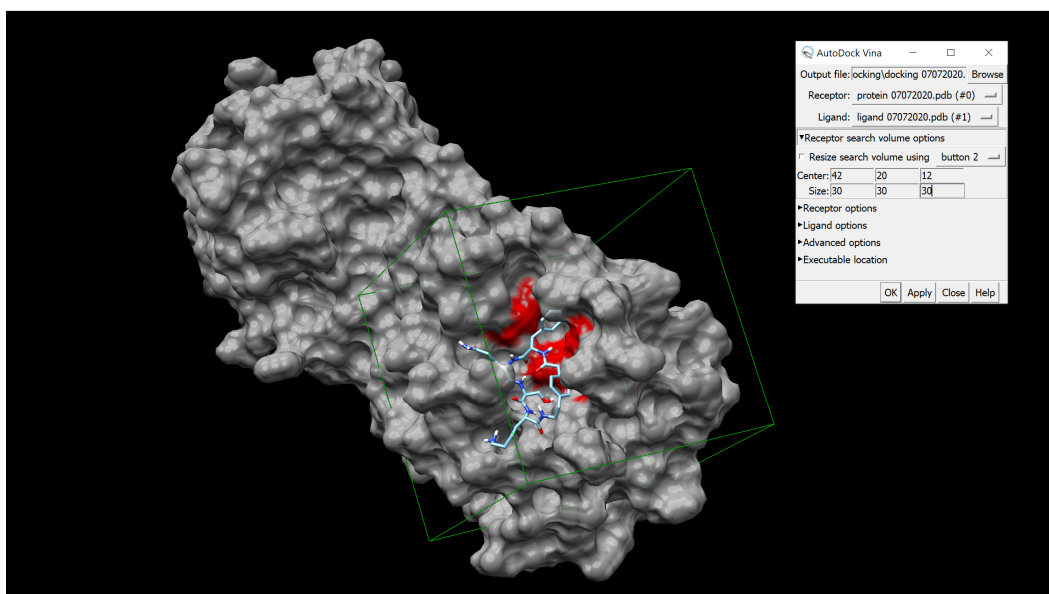
Under file name type “docking” or a name you prefer and press **enter** on your keyboard.



Select “protein.pdb” as the receptor and select “ligand.pdb” as the ligand.



You will now have to define the receptor search grid box (area where docking will be done) by typing in certain numbers in “Center” and “Size”. You have to play around with this so that your box engulfs all of the active site. The box must encompass all of the active site, but must not exceed 30 Å on an edge. You can also try to maneuver the box with your mouse by selecting the “Resize search volume using” and then selecting the mouse button that you want to use. Start off by typing 1, 1, 1 (x, y, z coordinates) for the center, and 30, 30, 30 (Å) for the size. Then, reposition the box so that the active site residues (Cys 44, Cys 38, Met 49, Met 165, His 41; colored in red) are in the center of the box. Do not make the box larger than 30, 30, 30. Rotate around to make sure the box is covering the active site. In this case, we use 42, 20, 12 for the center and 30, 30, 30 for the size.

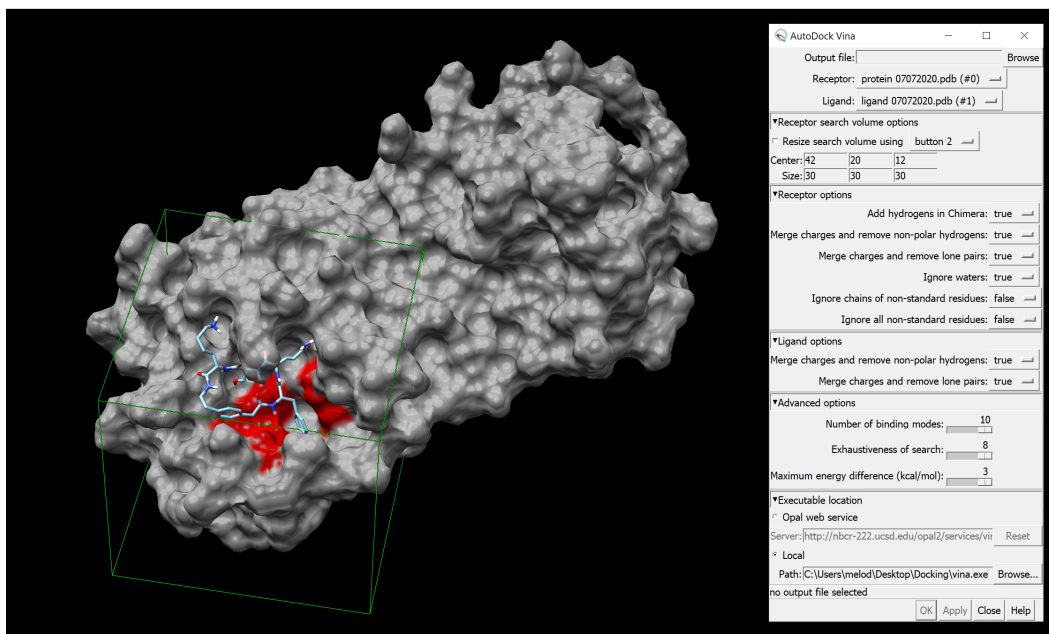


Once you have the receptor search grid box with appropriate size and position, you have to check that everything is set up for docking. Click on “Receptor options” and make sure that all of the options are set to “true” except for “Ignore chains of non-standard residues” and “Ignore all non-standard residues” which should be set to “false”.

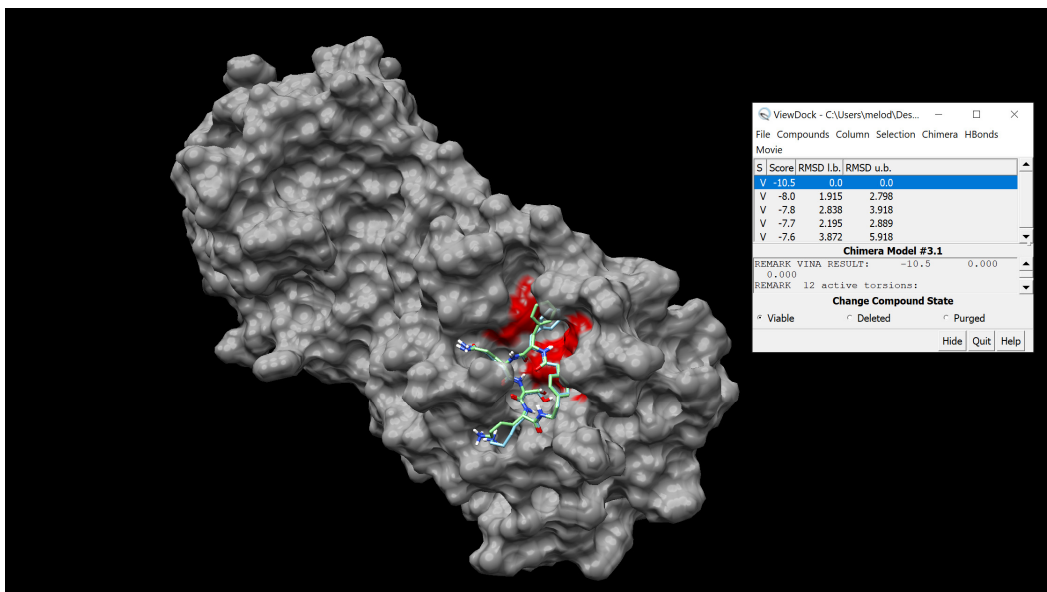
Click on “ligand options” and make sure that both options are set to “true”.

Click on “Advanced options” and make sure that the “Number of binding modes” is set to 10 (this is the maximum number of outputs that you will get per docking), “Exhaustiveness of search” is set to 8 (this determines how much of your CPU will be used and how good the search will be), and the “Maximum energy difference (kcal/mol) is set to 3.

Under “Executable location”, select “Local”, click Browse, and find the location of vina.exe in the folder that you created on the desktop.

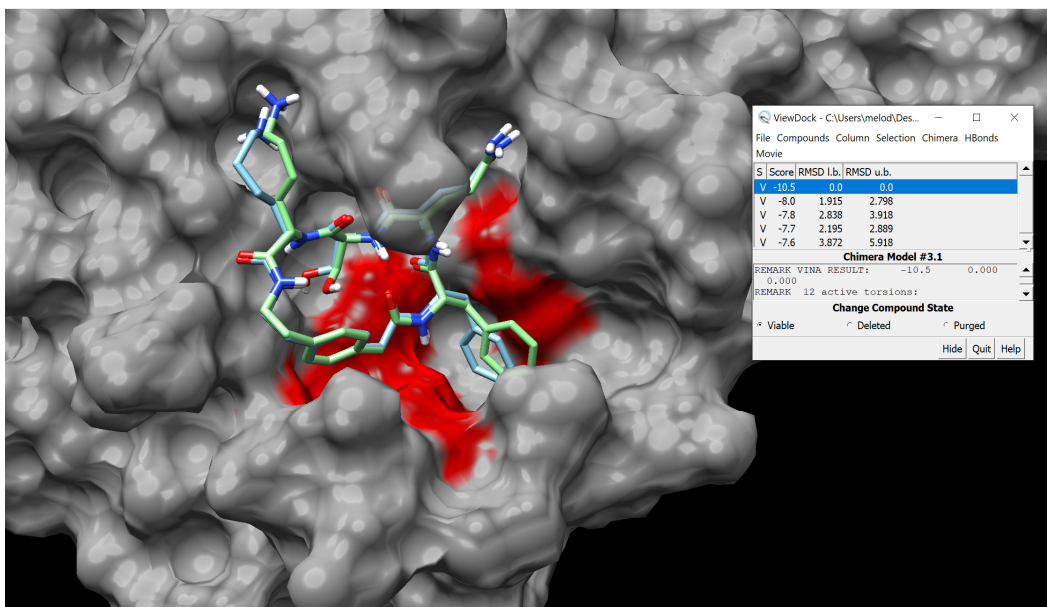


Click OK and wait. “Running” will show at the bottom. The docking will take approximately 2 minutes. Once the docking is done a new window will pop up called “ViewDock” and it will allow you to examine all of your docked structures. A “docking.pdbqt” file containing all of the docking results will be generated in your folder on the desktop.

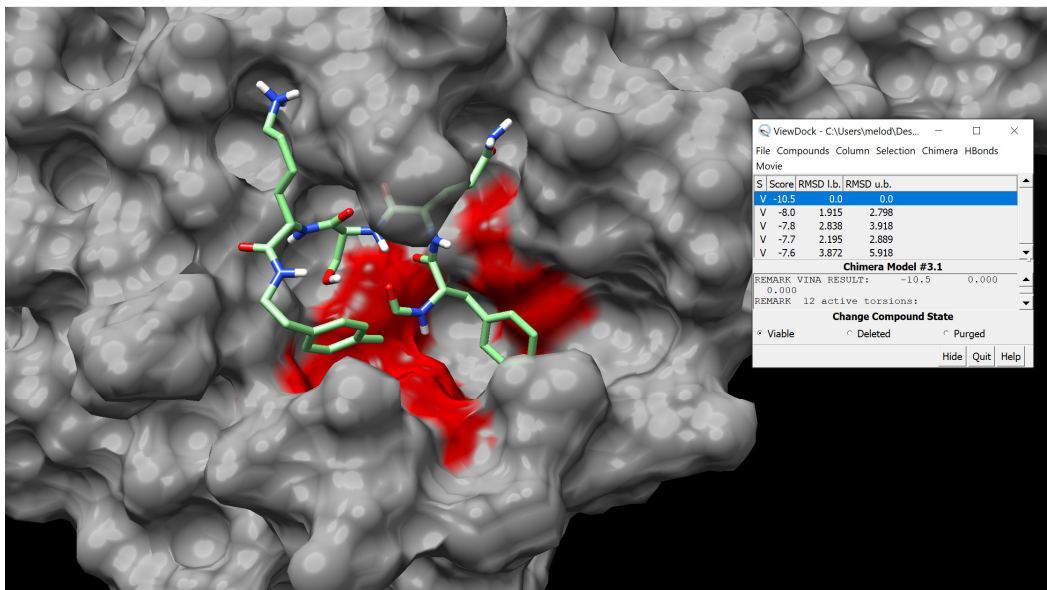


5.6. Viewing the docking results

Rotate until you find the binding pocket with key residues in red. You should find the docked cyclic peptide inhibitor (green) with the lowest energy structure (#3.1) falls into the binding pocket.



Ctrl+LMB on any part of the undocked inhibitor (blue), press **up** arrow twice; *actions* → *atoms/bonds* → *hide*.



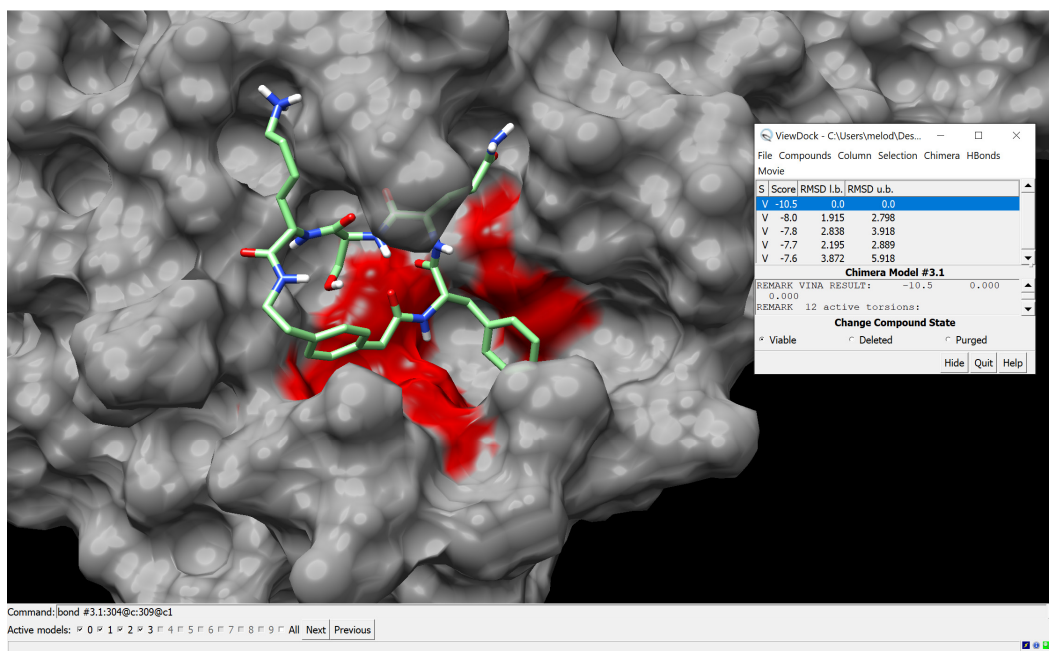
Note that in the docked inhibitor (green), the previously built C-C bond is missing. The docked ligand is created by reading the AutoDock Vina output, and that output is missing the ring-closing bond.¹⁰ You can easily re-establish the bond with the following command:

Tools → *general control* → *command line*

In the command line, type:

```
bond #3.1:304@c:309@c1
```

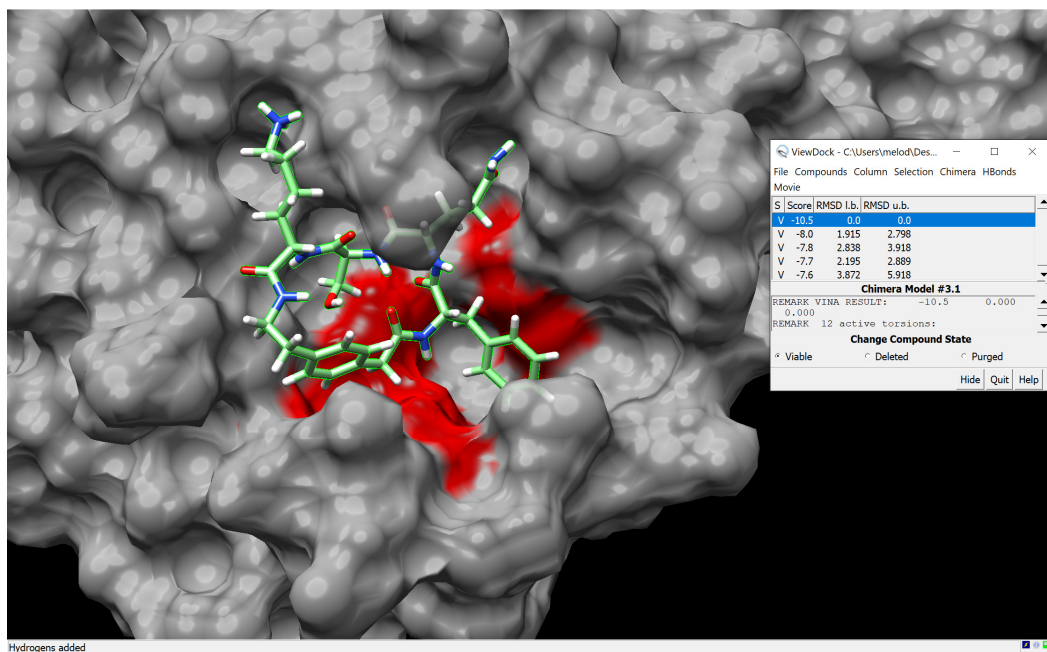
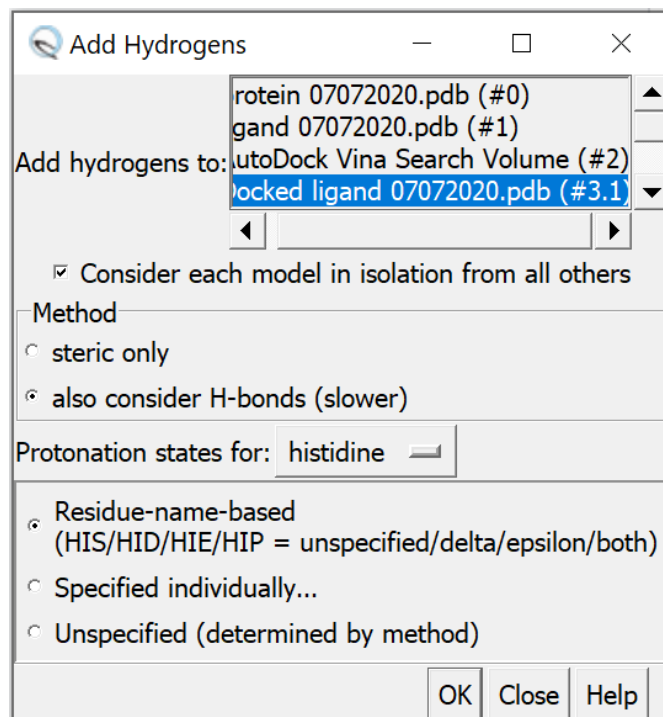
Press **Enter**



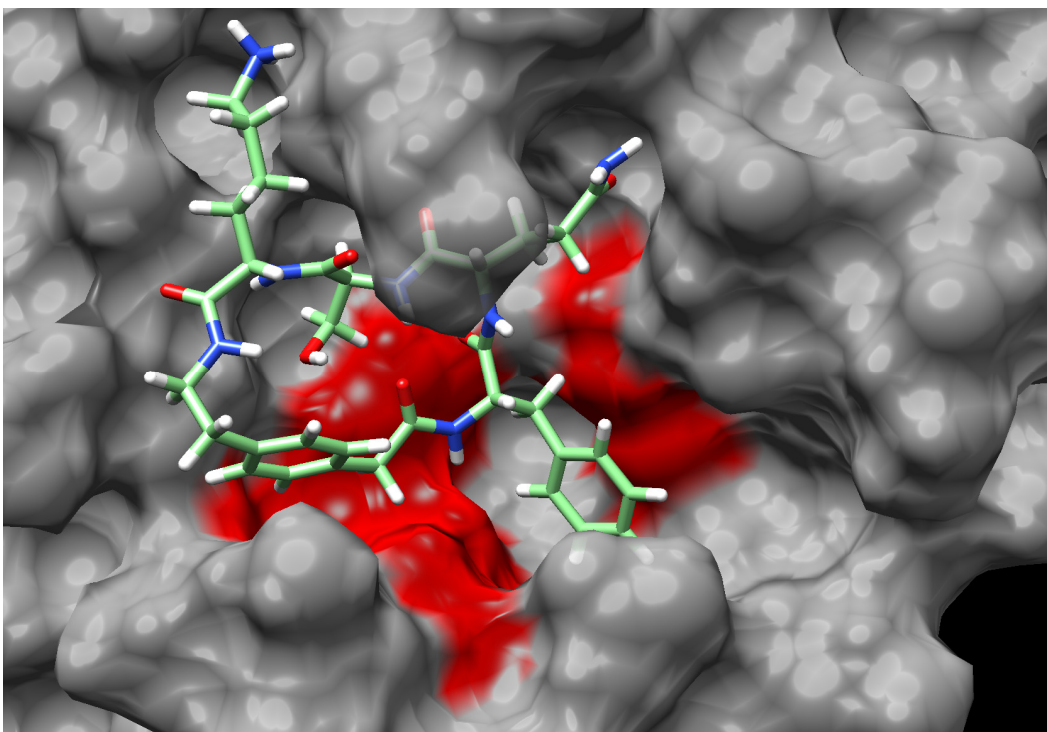
For other structures, use “bond #3.2:304@c:309@c1”, “bond #3.3:304@c:309@c1”, etc., to fix the missing bond issue.

To better view the lowest energy structure of the docked inhibitor (#3.1), we want to add hydrogens back to it. To do so, **Ctrl+LMB** on any part of the docked inhibitor, press **up** arrow twice. *Tools* → *Structure Editing* → *AddH*.

The “Add Hydrogens” window will appear. Make sure the lowest energy structure “docked ligand.pdb (#3.1)” is highlighted, and leave the other settings as their defaults. Click OK.



Select → *clear selection*. Use LMB to rotate view, MMB to translate view across screen, and RMB to zoom in.



6. Docking the inhibitor to SARS-CoV-2 M^{pro}

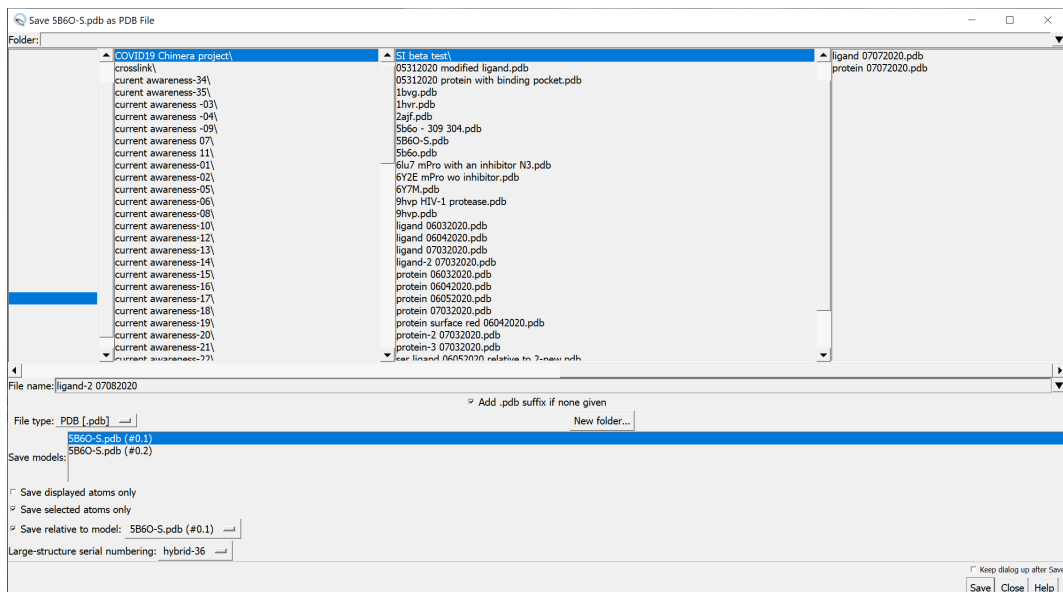
To evaluate the ability of the minimized cyclic peptide inhibitor binds to the SARS-CoV-2 M^{pro}, we will dock the cyclic peptide inhibitor to the SARS-CoV-2 M^{pro} structure (PDB ID: 6YB7) using the AutoDock Vina plugin in UCSF Chimera.⁸⁻¹¹

6.1. Saving the cyclic peptide inhibitor as a PDB file

This step follows the “4. geometry optimization of the cyclic peptide inhibitor” section.

To save the cyclic peptide inhibitor as a PDB file, we first make sure the cyclic peptide inhibitor is selected. Then in the menu bar, select *File* → *Save PDB*. In the pop-up window,

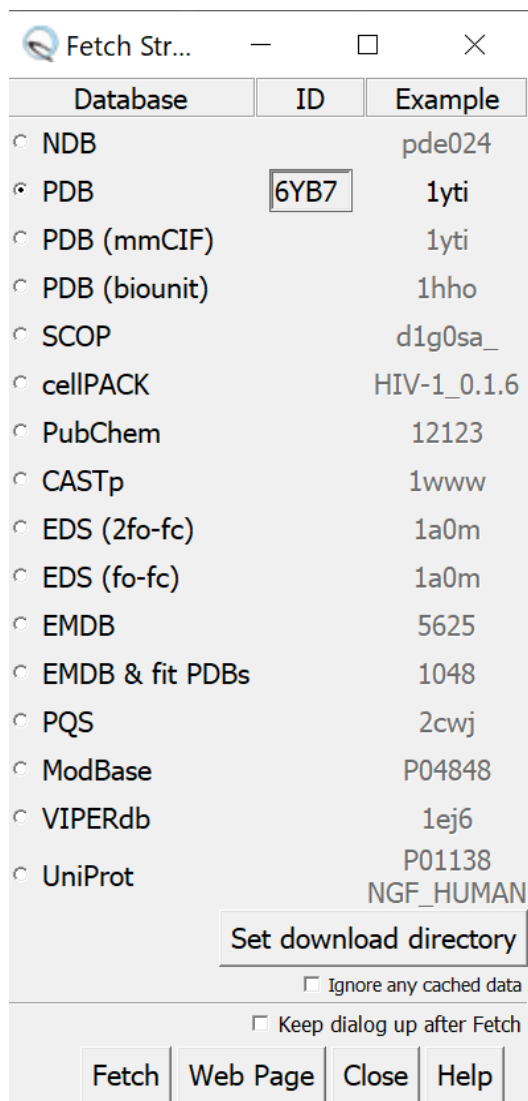
select save models “5B6O-S.pdb (#0.1)”, select “save selected atoms only”, select “save relative to model “5B6O-S.pdb (#0.1)”, give a valid file name (example “ligand”) and click save.

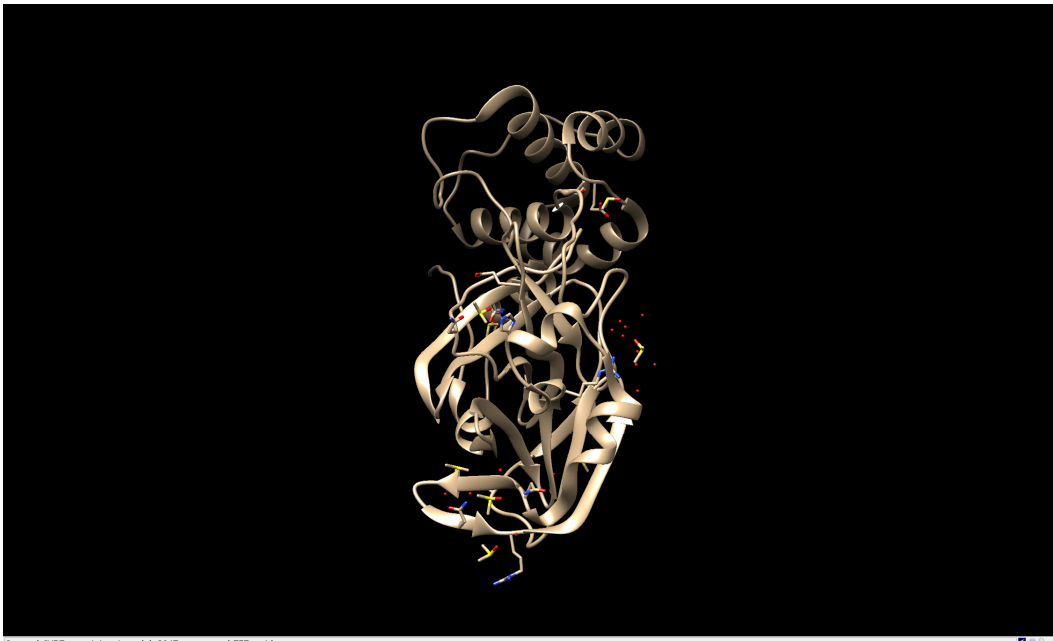


6.2. Loading and modifying the SARS-COV-2 M^{PRO} structure

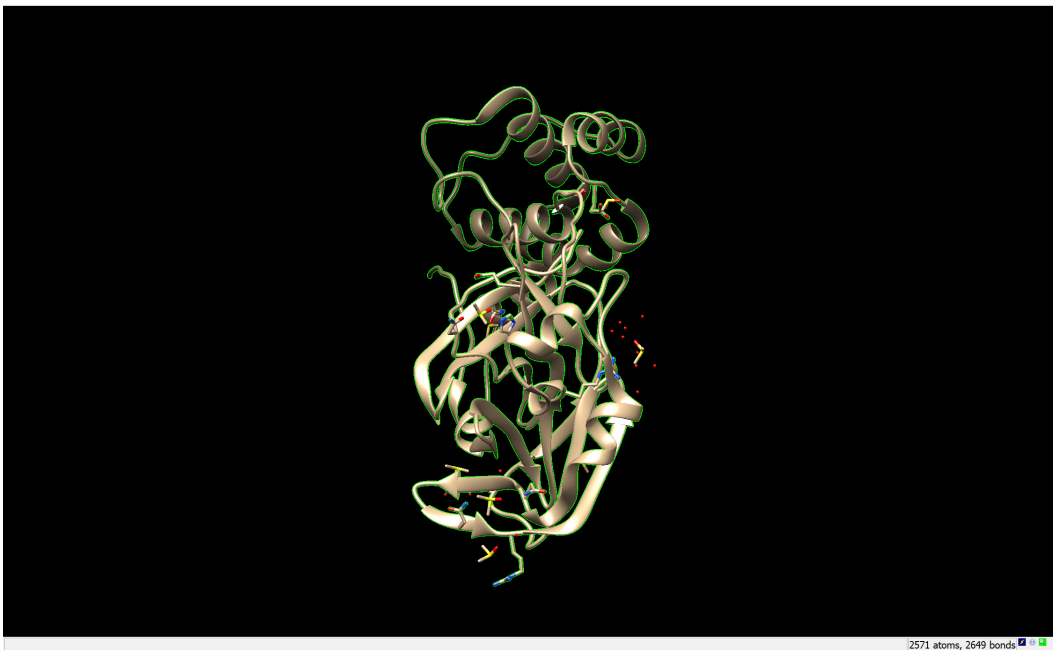
File → *close session* to close the current session in UCSF Chimera (make sure that you have saved the important sessions).

Protein X-ray crystallographic structure files can be retrieved from Protein Data Bank (PDB) and opened in UCSF Chimera with the “Fetch by ID” function. In the menu bar, select *File* → *fetch by ID* → select “PDB” → type in “6YB7” → click Fetch.¹¹

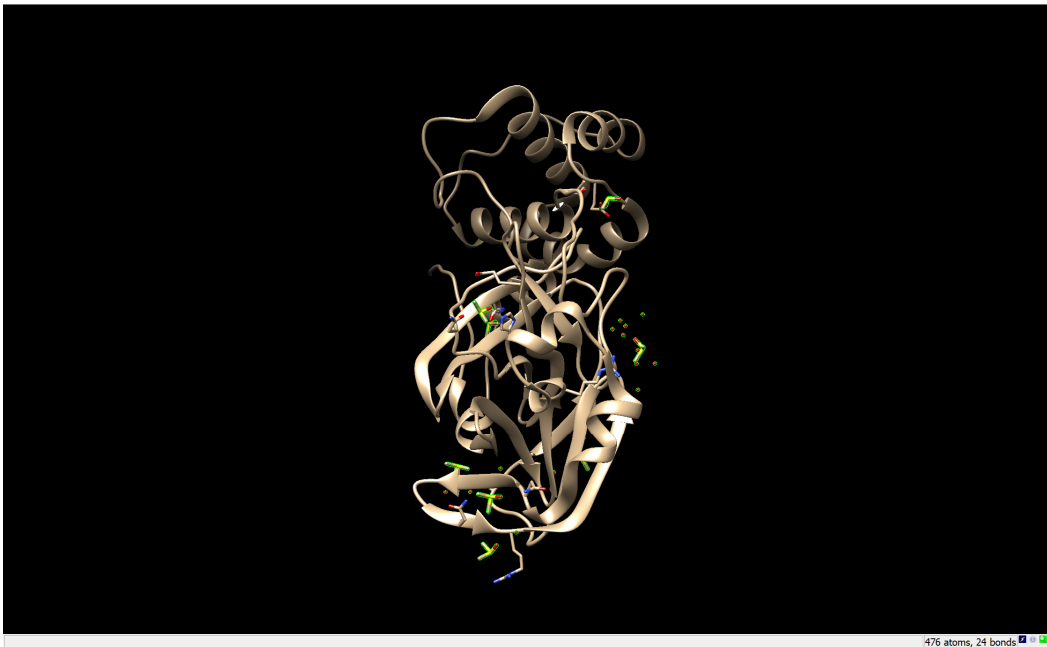




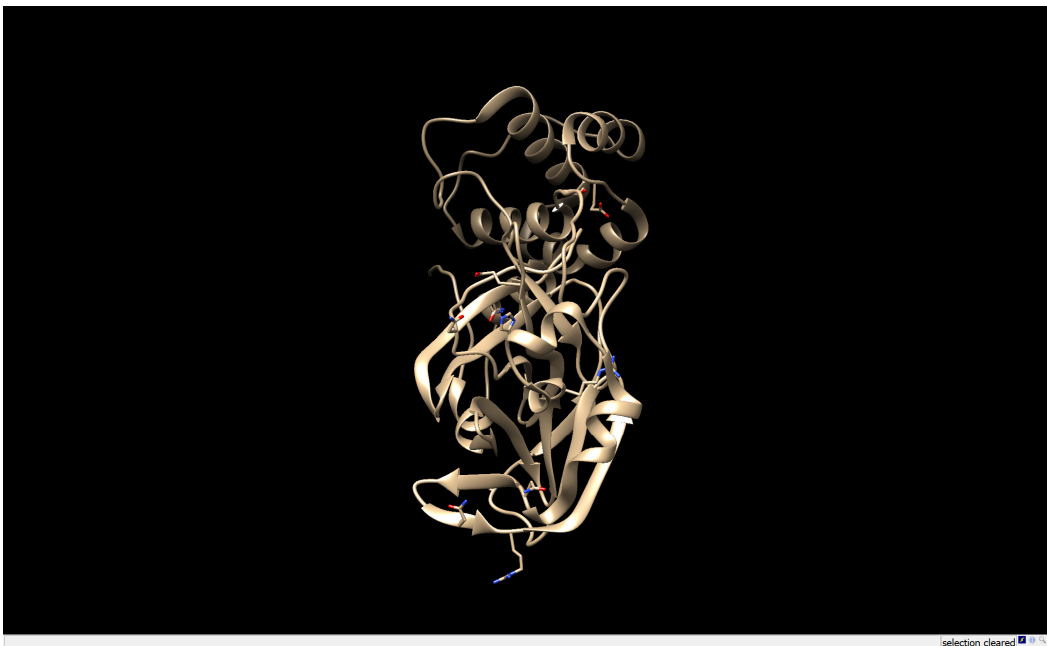
We want to delete the solvents (water, DMSO) in SARS-COV-2 M^{pro} structure (PDB 6YB7) as they are not necessary in the molecular docking process. **Ctrl+LMB** on any part of the protein, press up arrow twice to select the protein.



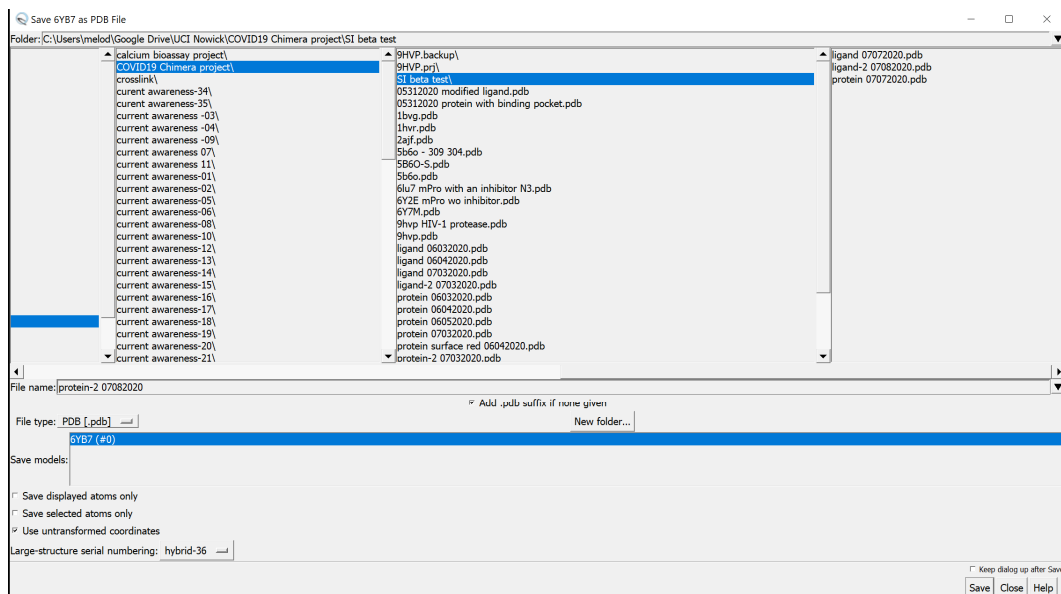
Select → invert (all models)



Actions → atoms/bond → delete



Now we want to save the solvent-deleted PDB file. *File → save PDB*; give a valid file name (example “protein”), click save.



6.3. Installing AutoDock Vina and creating a folder for docking files

6.3.1. Download and install AutoDock Vina (<http://vina.scripps.edu/download.html>).

6.3.2. Create a new folder on your desktop or a location you prefer and call it “docking” or a name you prefer.

6.3.3. Copy and paste both the ligand.pdb and protein.pdb that you just saved in the folder that you created on the desktop. Additionally, copy and paste vina.exe in this folder; Vina.exe can be found in your Program Files (X86) in the folder called “The Scripps Research Institute”.

For MacOS users, copy and paste vina linux executable file in this folder that you created on the desktop. The AutoDock Vina Unix executable file is located in the extracted folder that you downloaded from the AutoDock Vina website. Note for MacOS users: this may not happen to all MacOS users, but you might have to unlock permissions to run the AutoDock Vina Unix executable file. To do this, double click the Unix executable file, and a pop-up window may show up stating that the software could be malware. If this window

pops up, click on the “?” button, and then a help guide should load up. Click on the blue link and it should bring you to Security and Privacy preferences. Unlock permissions by entering your password to enable AutoDock Vina.

6.4. Opening the saved ligand and protein PDB files in the same view

File → *close session* to close the current session in UCSF Chimera (make sure that you have saved the important sessions).

File → *Open*, find the protein.pdb file from the docking folder on your desktop and click open.

File → *Open*, find the ligand.pdb file from the docking folder on your desktop and click open.

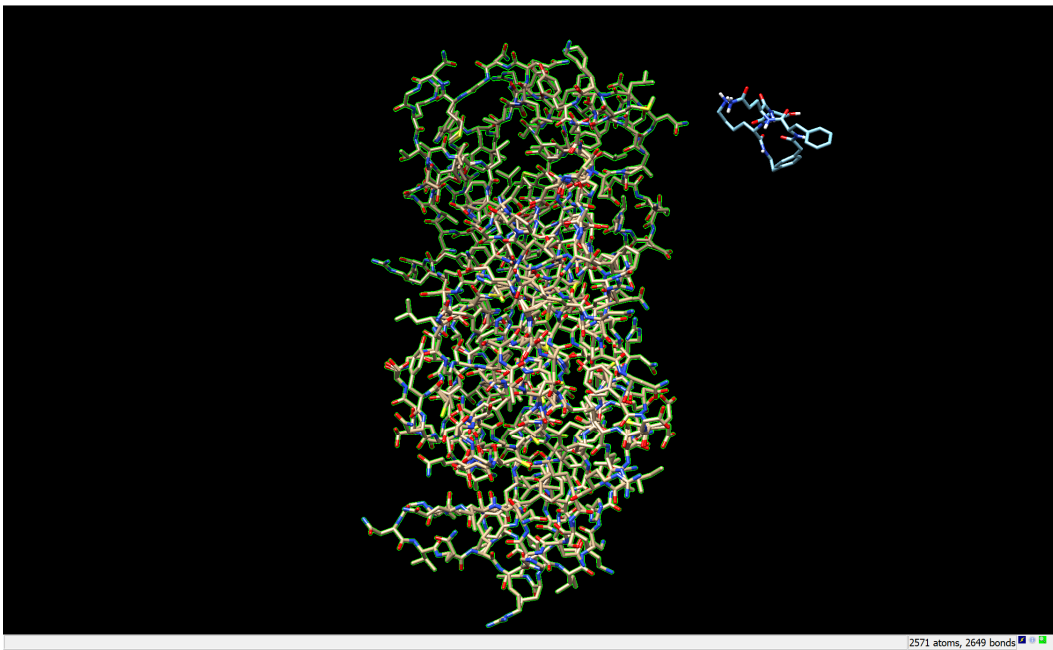


6.5. Highlighting the active site of the protein

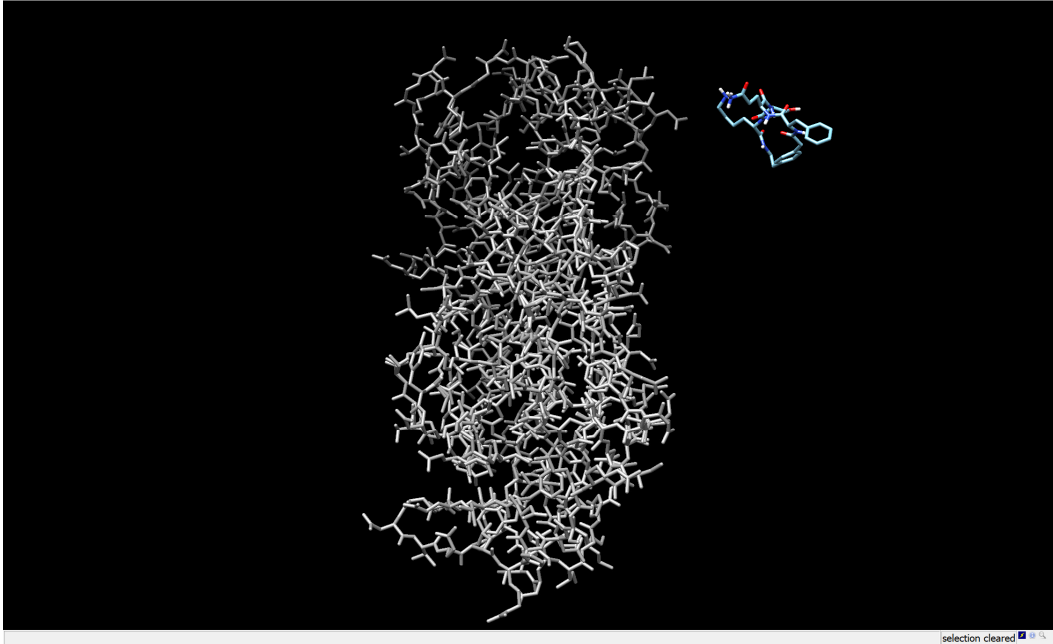
Select the protein by Ctrl+LMB any part of the protein, press up arrow twice.



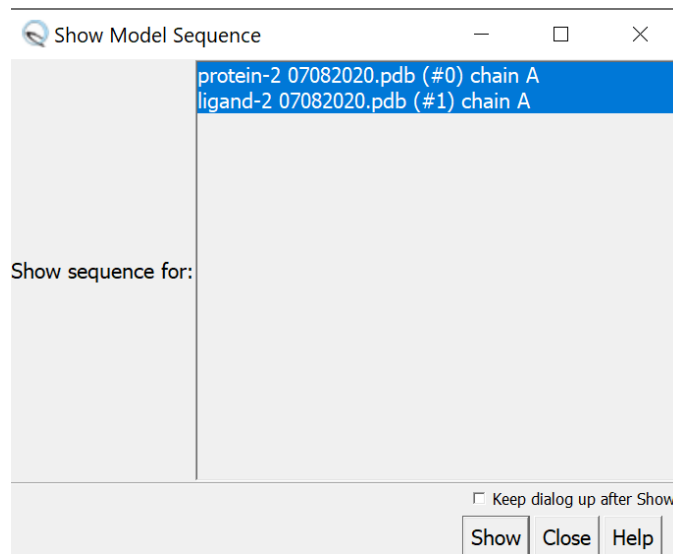
We want to change the preset to “stick” so we can locate the active site (binding pocket) easier. *Actions* → *Ribbon* → *Hide*; *Actions* → *Atoms/Bonds* → *stick*; *Actions* → *Atoms/bonds* → *show*



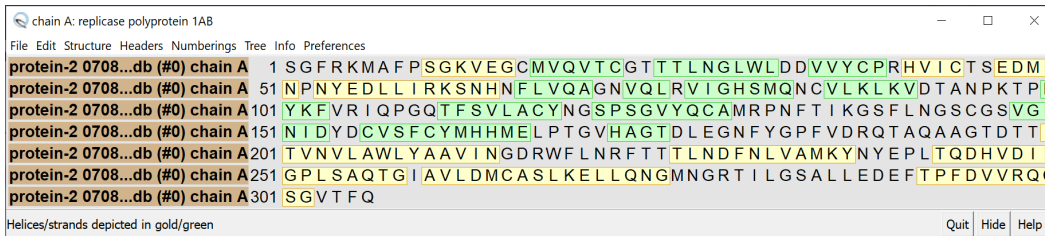
Actions → *color* → *dark grey*; *Select* → *clear selection*.



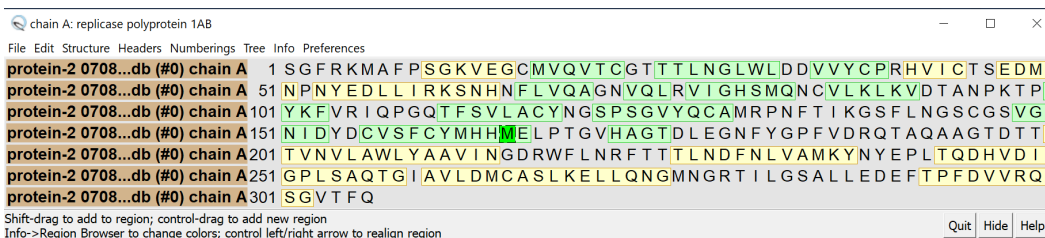
Locate the active site in the protein. It can most easily be found by looking for several residues in the active site, such as Cys 145, Met 165, His 164. For example, to find Met 165, *Favorite* → *sequence*. The following “Show Model Sequence” window will show up.



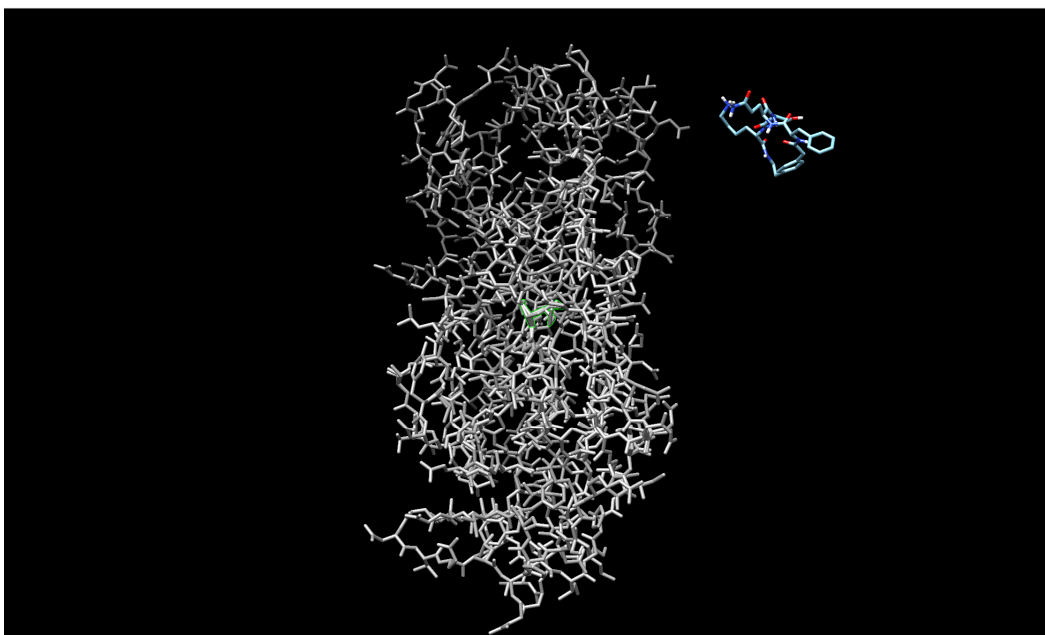
Highlight “protein-2 07092020.pdb (#0) chain A” only, click Show. The following “chain A: replicase polyprotein 1AB” window will show up.



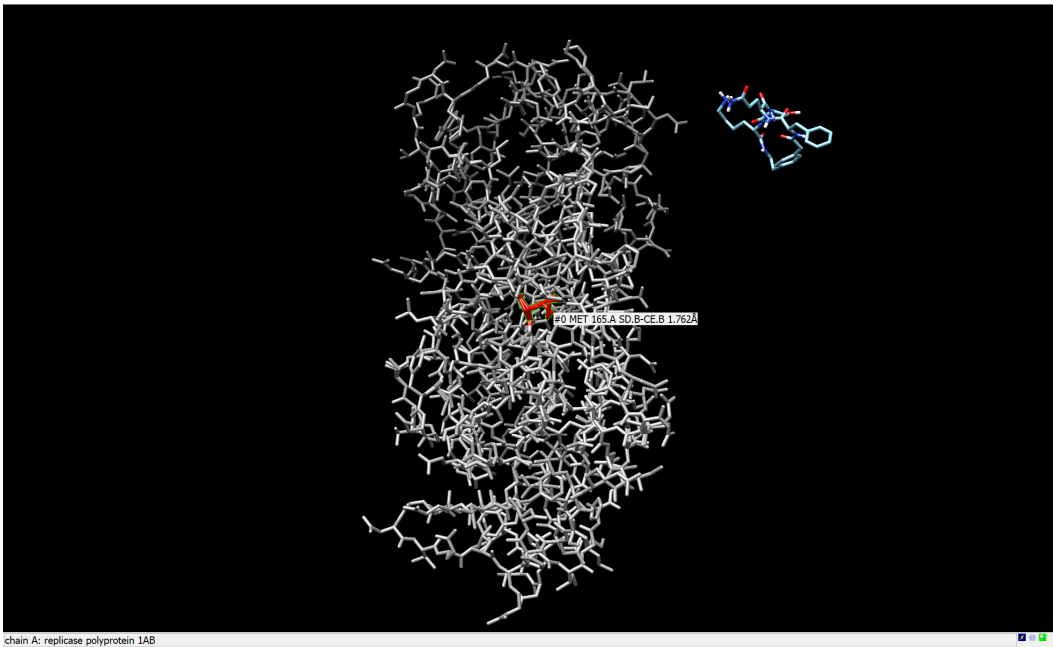
Find position 165, use LMB to click and drag to highlight the letter “M” representing Met 165. Click Quit to close the window.



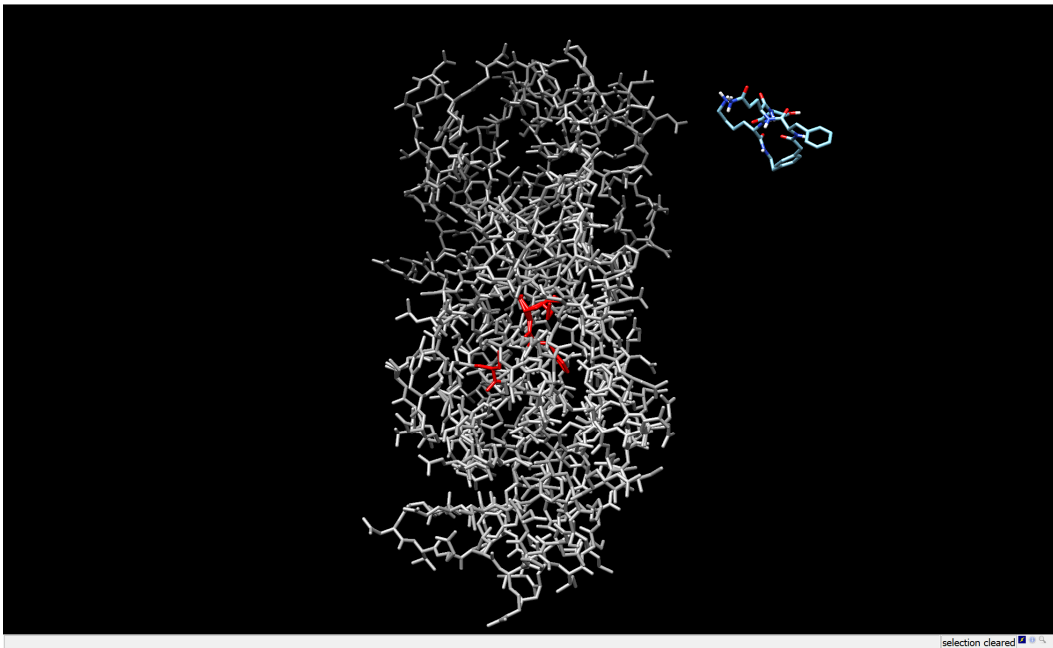
In the UCSF Chimera workspace, Met 165 is selected.



To color Met 165 in red, *Actions* → *color* → *red*.

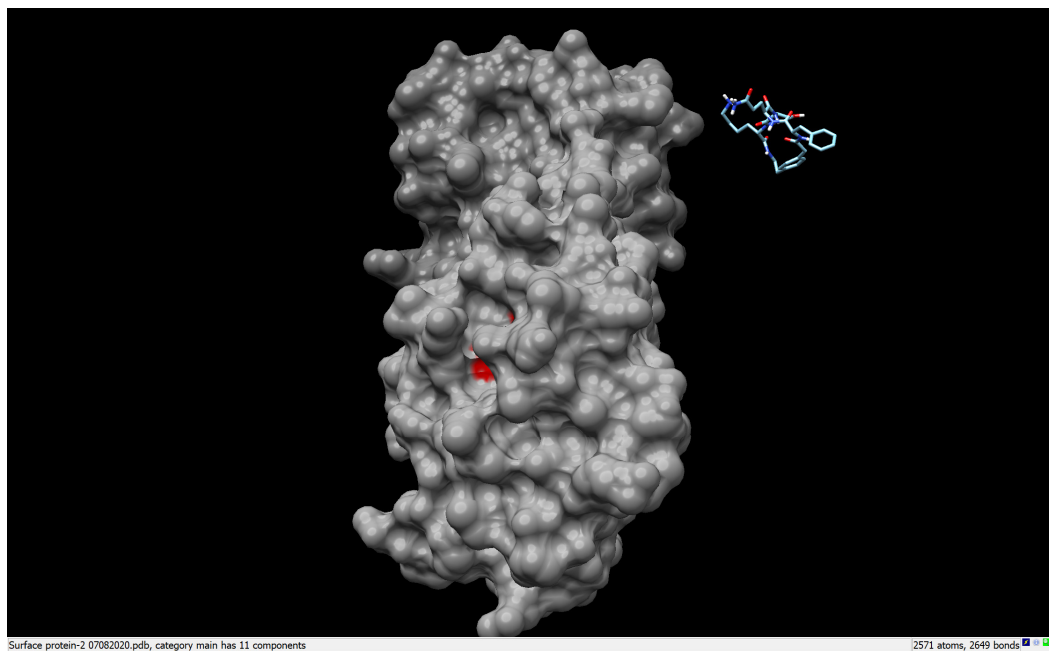


Repeat the steps for His 164 and Cys 145. After that, *select* → *clear selection*.



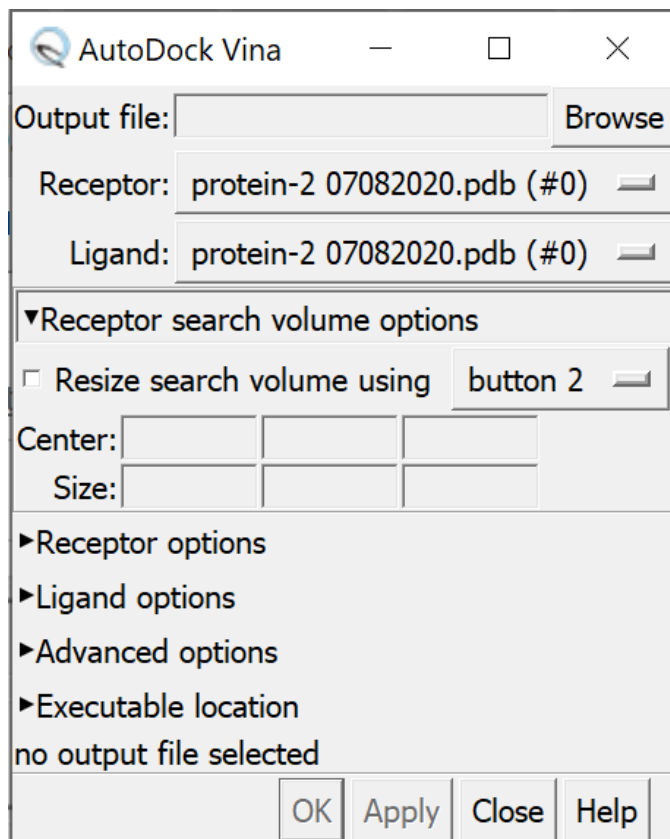
After highlighting several residues in the active site, we can show the protein as a van der Waals surface in order to better visualize the binding pockets in the active site. **Ctrl+LMB** on any part of the protein, press up arrow three times to select the entire protein, *actions*

→ *surface* → *show*; *actions* → *atoms/bonds* → *hide*; *actions* → *surface* → *transparency*
→ 30%.



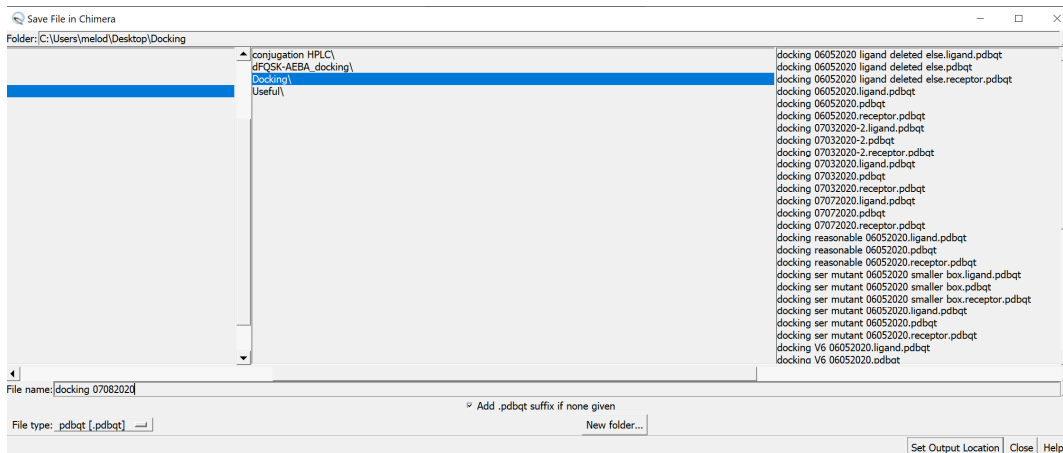
6.6. Running AutoDock Vina

Tools → *Surface/Binding Analysis* → *AutoDock Vina* (a new window will pop up).

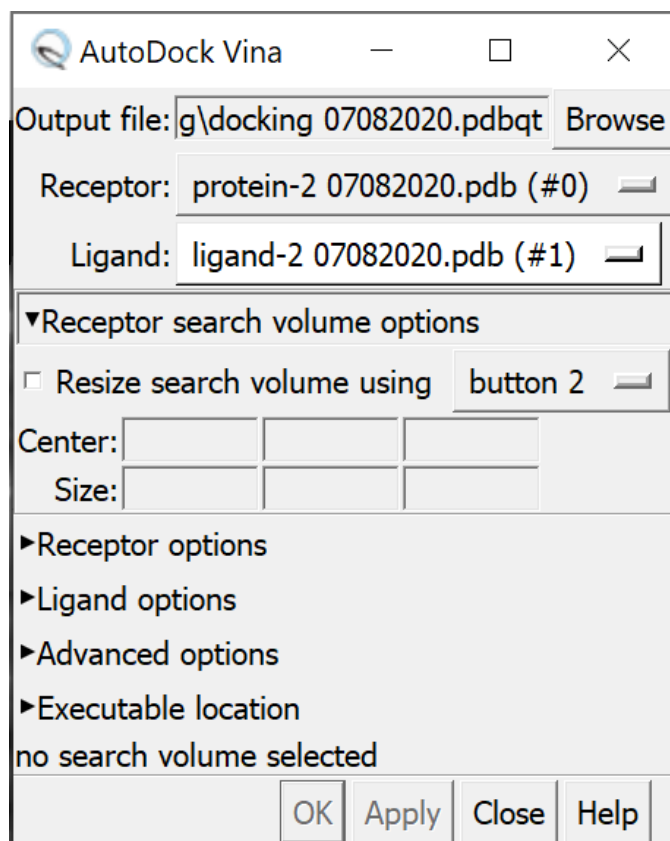


Click on Browse next to “Output file” and find the folder that you created on the desktop.

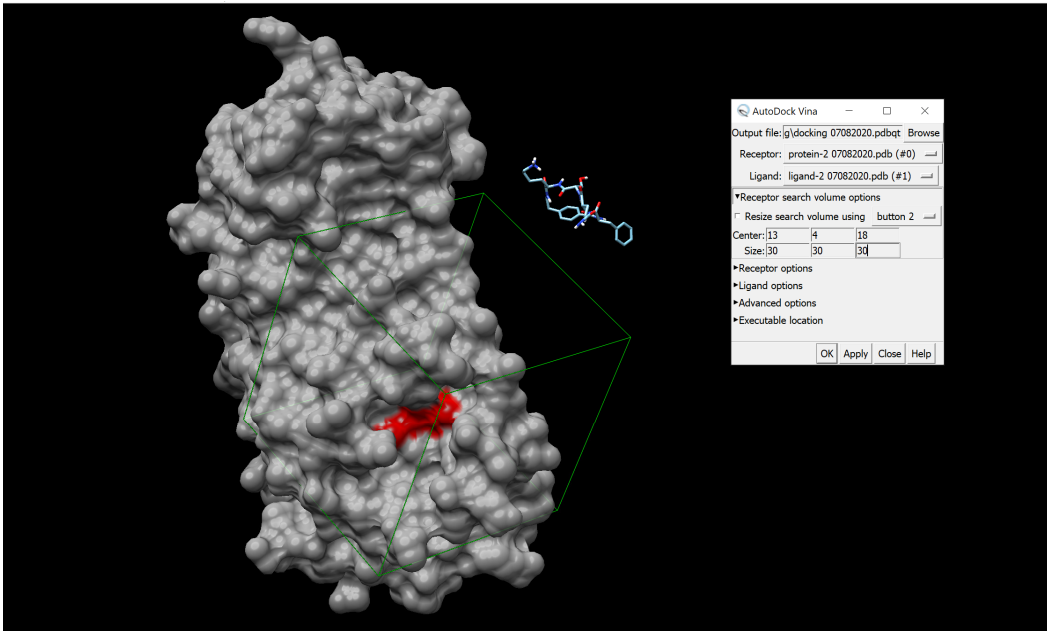
Under file name type “docking” or a name you presser and press **enter** on your keyboard.



Select “protein.pdb” as the receptor and select “ligand.pdb” as the ligand.



You will now have to define the receptor search grid box (area where docking will be done) by typing in certain numbers in “Center” and “Size”. You have to play around with this so that your box engulfs all of the active site. The box must encompass all of the active site, but must not exceed 30 Å on an edge. You can also try to maneuver the box with your mouse by selecting the “Resize search volume using” and then selecting the mouse button that you want to use. Start off by typing 1, 1, 1 (x, y, z coordinates) for the center, and 30, 30, 30 (Å) for the size. Then, reposition the box so that the active site residues (Cys 145, Met 165, His 164; colored in red) are in the center of the box. Do not make the box larger than 30, 30, 30. Rotate around to make sure the box is covering the active site. In this case, we use 13, 4, 18 for the center and 30, 30, 30 for the size.

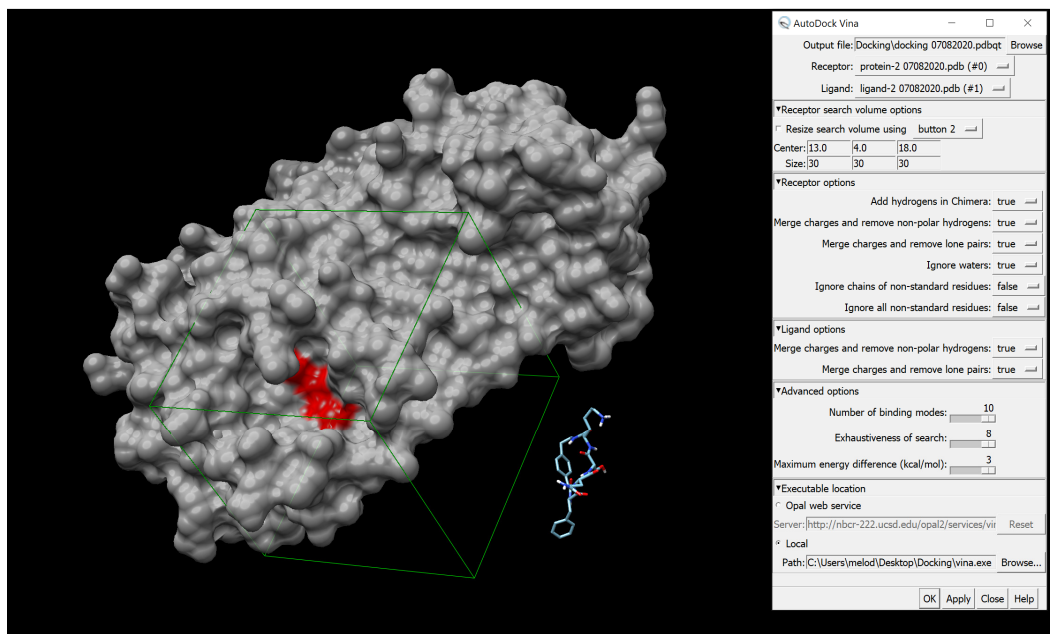


Once you have the box of the size and position that you would like you have to check that everything is set up for docking. Click on “Receptor options” and make sure that all of the options are set to “true” except for “Ignore chains of non-standard residues” and “Ignore all non-standard residues” which should be set to “false”.

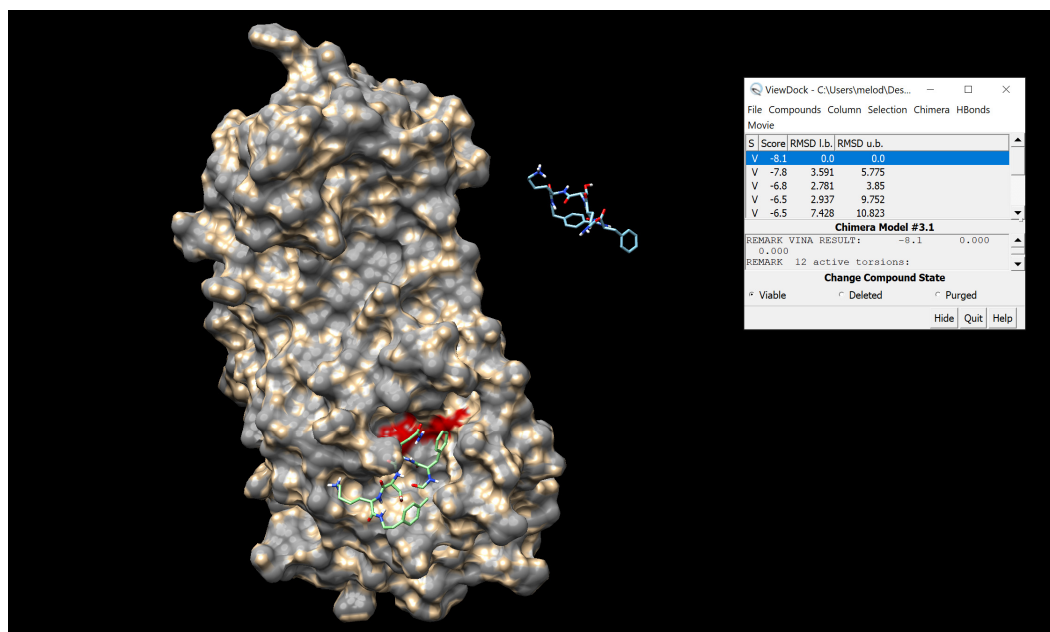
Click on “ligand options” and make sure that both options are set to “true”.

Click on “Advanced options” and make sure that the “Number of binding modes” is set to 10 (this is the maximum number of outputs that you will get per docking), “Exhaustiveness of search” is set to 8 (this determines how much of your CPU will be used and how good the search will be), and the “Maximum energy difference (kcal/mol) is set to 3.

Under “Executable location”, select “Local”, click Browse, and find the location of vina.exe in the folder that you created on the desktop.



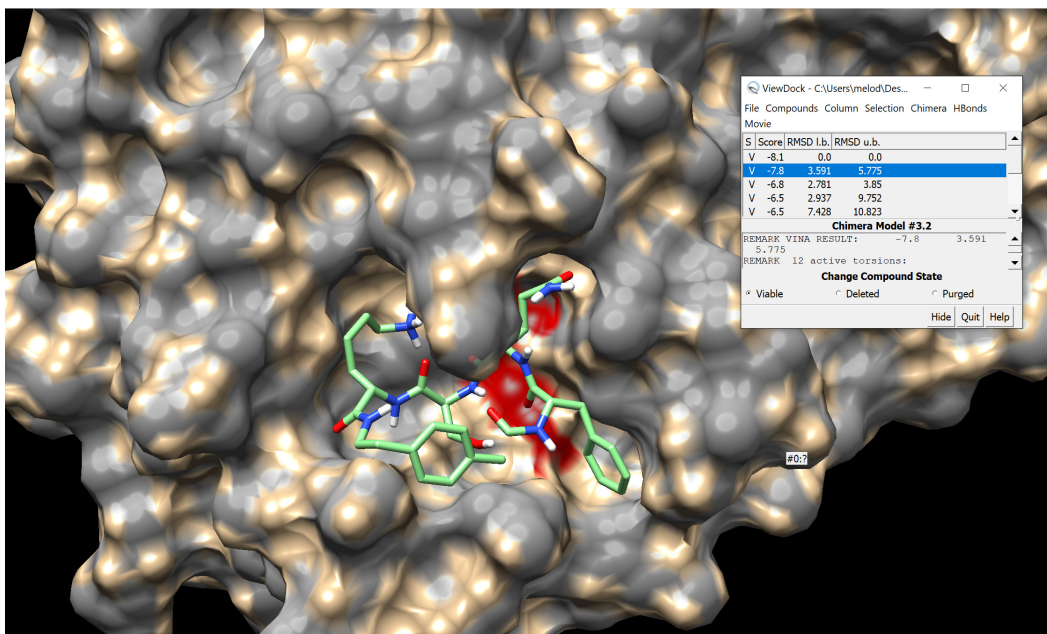
Click OK and wait. “Running” will show at the bottom. The docking will take approximately 3 minutes. Once the docking is done a new window will pop up called “ViewDock” and it will allow you to examine all of your docked structures. A “docking.pdbqt” file containing all of the docking results will be generated in your folder on the desktop.



6.7. Viewing the docking results

Rotate until you find the binding pocket with key residues in red. You should find the docked cyclic peptide inhibitor (green) with the second lowest energy (#3.2) falls into the binding pocket. (Alternatively, it may be the lowest energy structure, depending on how the docking was performed.)

Ctrl+LMB on any part of the undocked inhibitor (blue), press **up** arrow twice; *actions* → *atoms/bonds* → *hide*.



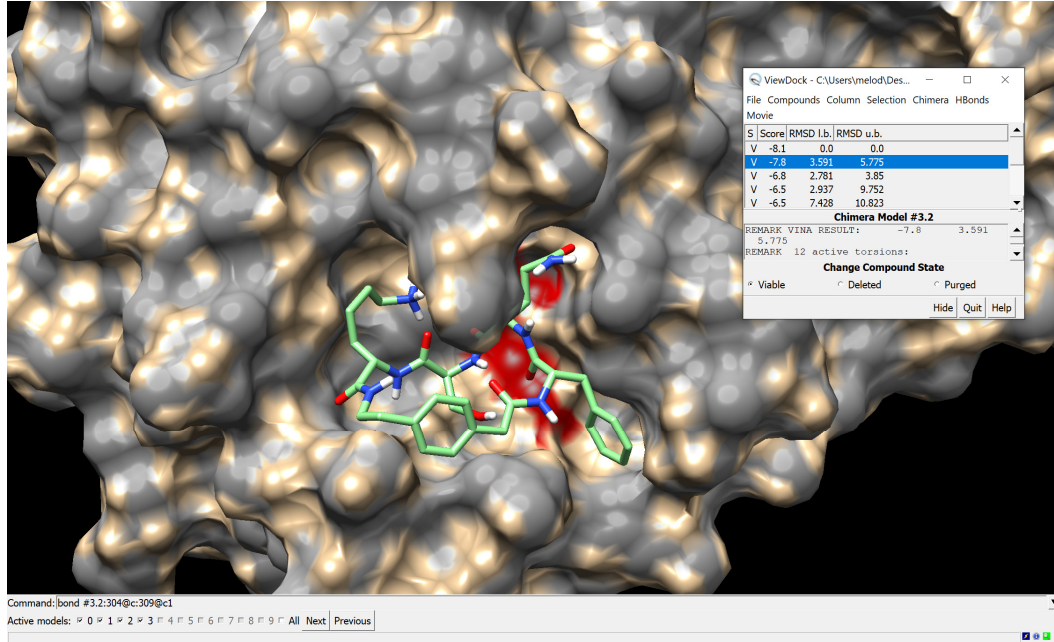
Note that in the green inhibitor (docked inhibitor), the previously built C-C bond is missing. The docked ligand is created by reading the AutoDock Vina output, and that output is missing the ring-closing bond.¹⁰ You can easily re-establish the bond with the following command:

Tools → *general control* → *command line*

In the command line, type:

bond #3.2:304@c:309@c1

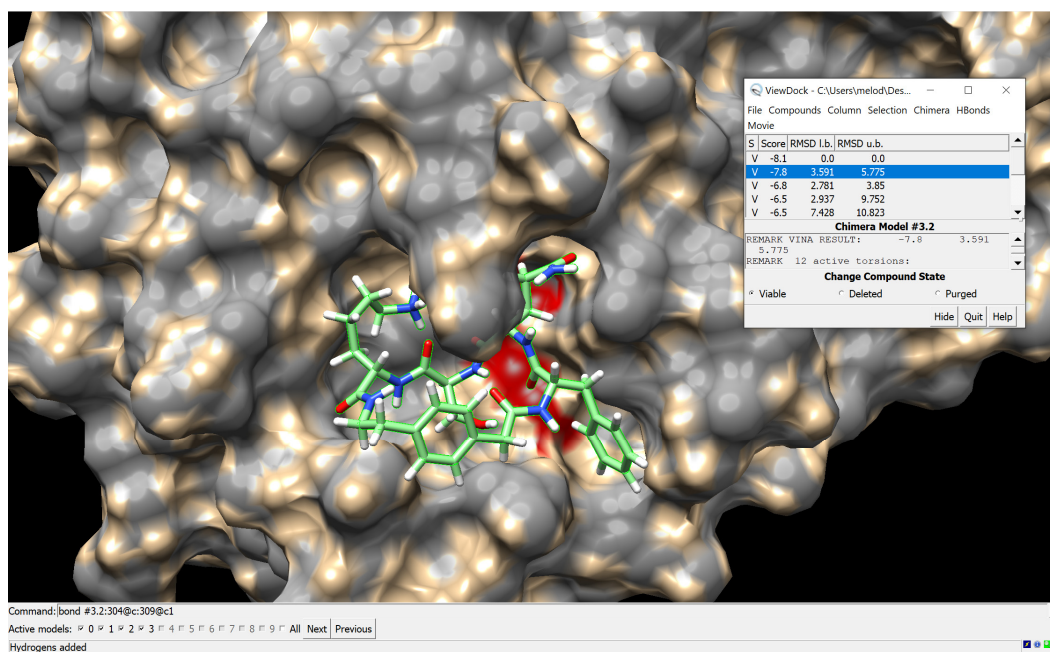
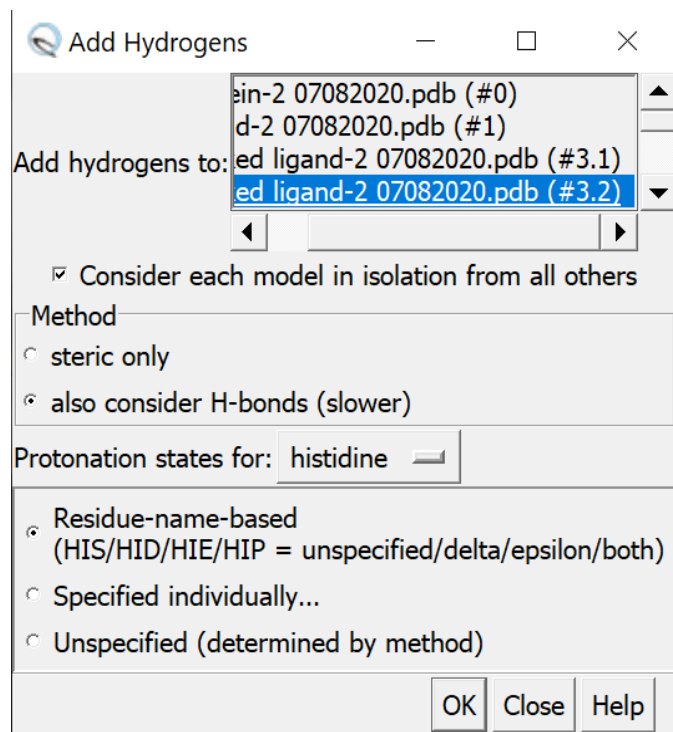
Press **Enter**



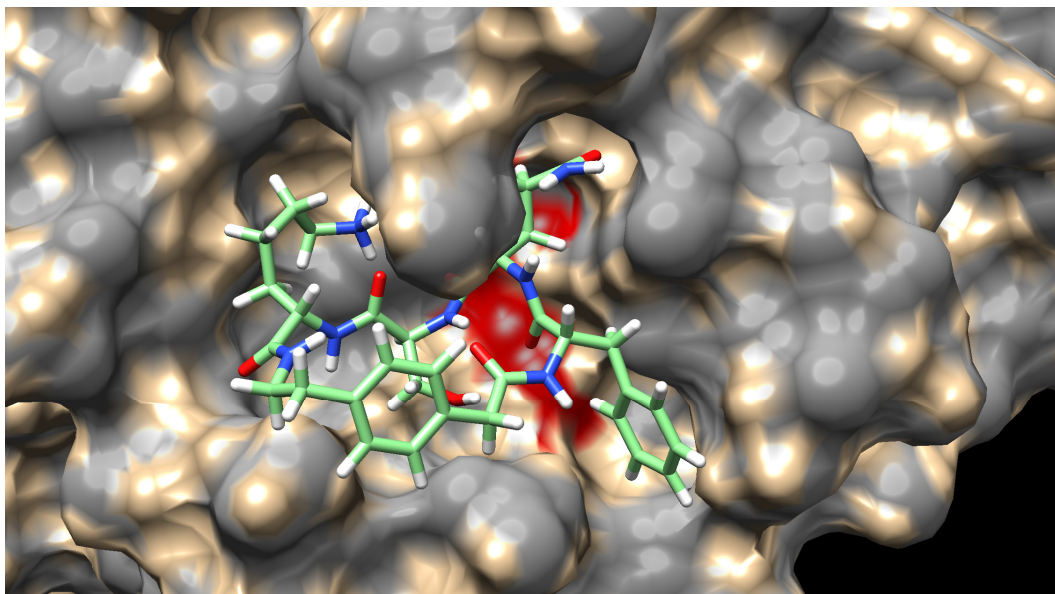
For other structures, use “bond #3.3:304@c:309@c1”, “bond #3.4:304@c:309@c1”, etc., to fix the missing bond issue.

To better view the second lowest energy structure of the docked inhibitor (#3.2), we want to add hydrogens back to it. To do so, **Ctrl**+**LMB** on any part of the docked inhibitor, press **up** arrow twice. *Tools* → *Structure Editing* → *AddH*.

The “Add Hydrogens” window will appear. Make sure the docked inhibitor structure with the second lowest energy structure “docked ligand.pdb (#3.2)” is highlighted, and leave the other settings as their defaults. Click OK.



Select → *clear selection*. Use LMB to rotate view, MMB to translate view across screen, and RMB to zoom in.

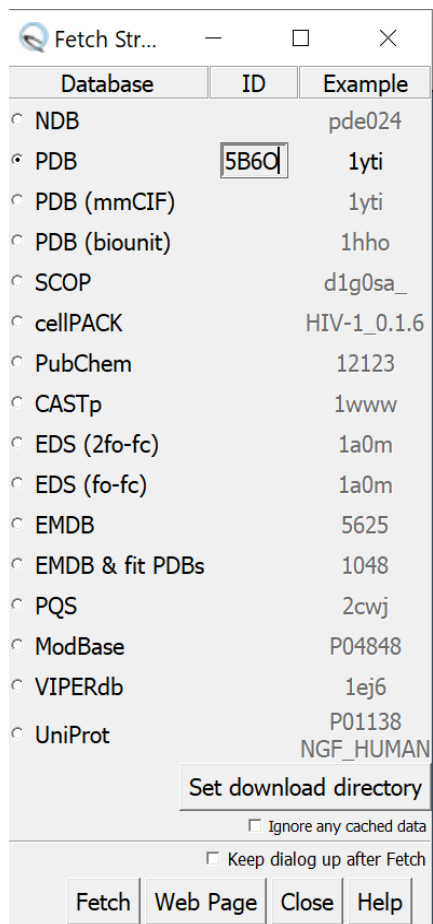


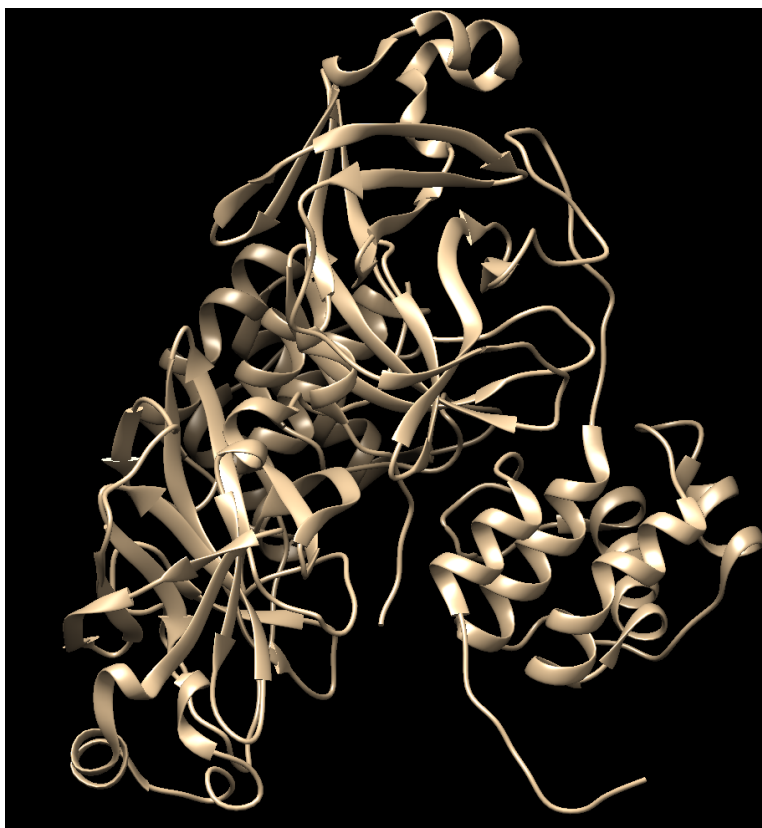
7. **Appendix: Generating a structure of SARS-CoV M^{pro} bound to the C-terminal substrate (5B6O-S.pdb)**

In this appendix, we will generate a structure of SARS-CoV M^{pro} bound to the C-terminal fragment of an M^{pro} molecule within the active site. We have already provided this file as “5B6O-S.pdb” as a separate Supporting Information document. Here we will go through the operations needed to generate 5B6O-S.pdb file from the publicly available PDB file 5B6O.

7.1. Loading the SARS-CoV M^{pro} crystal structure in UCSF Chimera

Protein X-ray crystallographic structure files can be retrieved from Protein Data Bank (PDB) and opened in UCSF Chimera with the “Fetch by ID” function. In the menu bar, select *File* → *fetch by ID* → select “PDB” → type in “5B6O” → click fetch

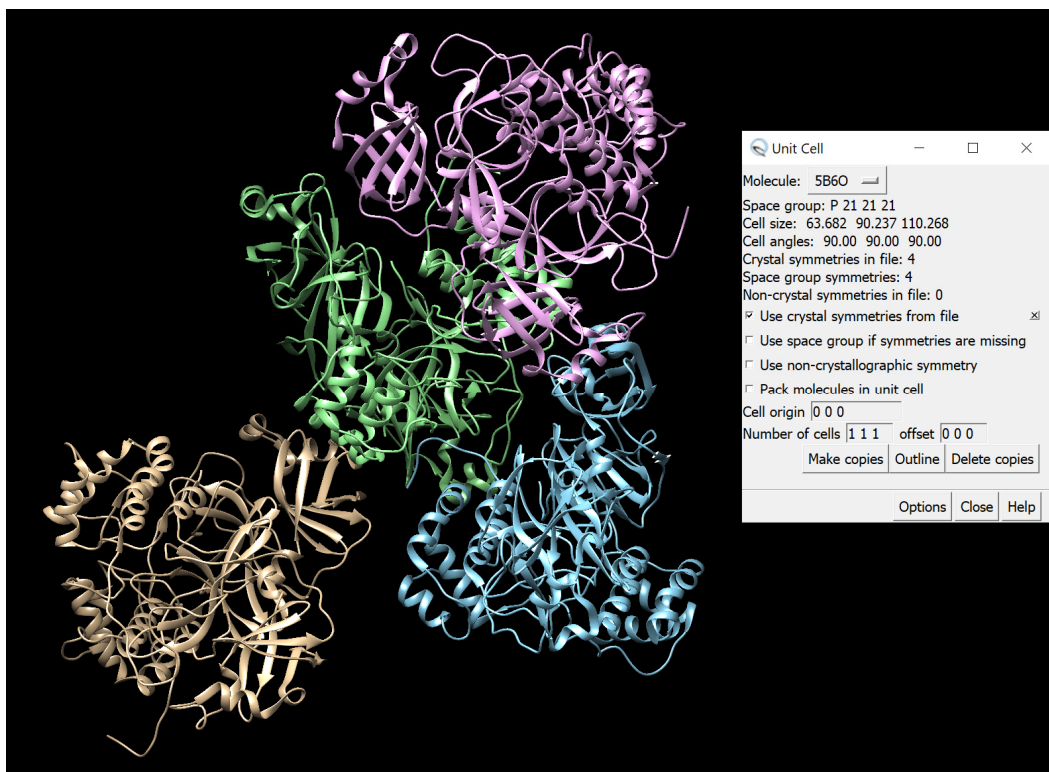




7.2. Generating symmetry mates in the crystal lattice

To visualize how the C-terminal fragment (substrate) interacts with the active site of the M^{pro} , we have to generate the symmetry mates in the crystal lattice. Doing so will allow us to see the C-terminal part of one M^{pro} molecule extending into the active site of another M^{pro} molecule in the adjacent asymmetric unit.

To do so, *Tools* → *Higher-order structure* → *unit cell*. A window will pop up: click options → check "use crystal symmetries from file" → uncheck "use space group if symmetries are missing", "use non-crystallographic symmetry", and "pack molecules in unit cell" → click make copies.



7.3. Deleting unnecessary parts

Close the “unit cell” window. Now we can see the *C*-terminus of the newly generated blue dimer extends into the binding pocket of the newly generated green dimer. To make the subsequent minimization and docking steps easier, we will only use the monomer of the green dimer containing the binding pocket and the *C*-terminus of the blue dimer in the exercise.

To delete the tan dimer, we **Ctrl**+**LMB** on any part of the tan dimer, press **up** arrow four times. Now we selected the tan dimer.



Actions → *atoms/bonds* → *delete*. Now we have deleted the selected tan dimer.



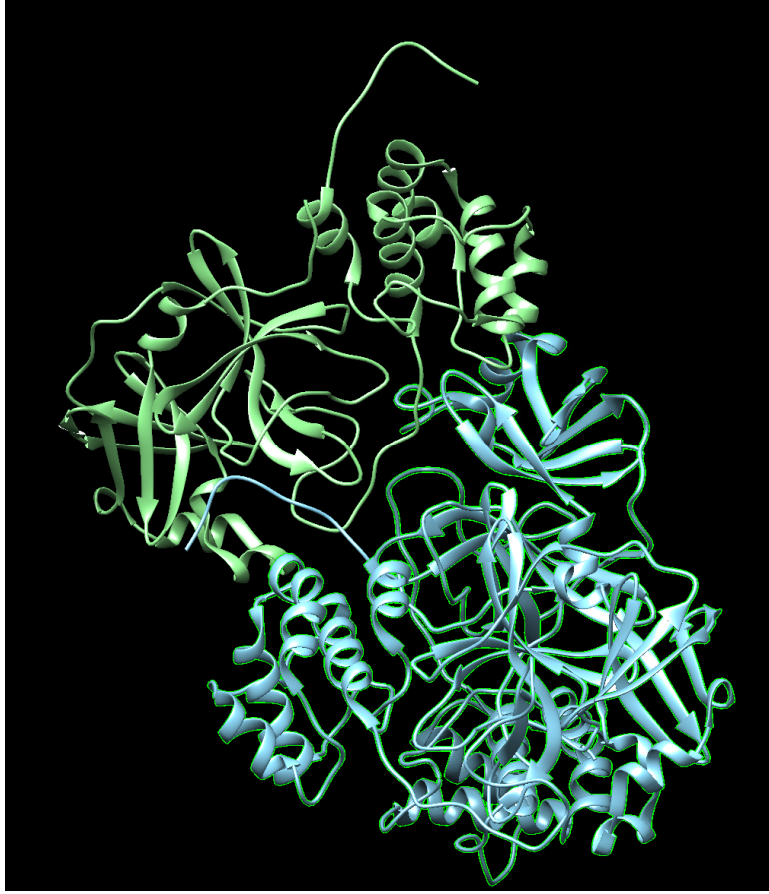
To delete the pink dimer, we **Ctrl+LMB** on any part of the pink dimer, press **up** arrow four times. Now we selected the pink dimer. *Actions* → *atoms/bonds* → *delete*.

To delete the monomer of the green dimer that does not interact with the blue dimer, we **Ctrl+LMB** on any part of the monomer of the green dimer that does not interact with the blue dimer, press **up** arrow twice. Now we selected the monomer of the green dimer that does not interact with the blue dimer. *Actions* → *atoms/bonds* → *delete*.

Now we want to keep the C-terminus substrate of the blue dimer and delete the rest parts of the blue dimer. First, we select the substrate. To select the substrate, find C-terminal lysine 310 on the blue dimer, **Ctrl+LMB** on the terminal Nitrogen, press **up** arrow once.



Select → *invert (selected models)*. This way you selected the non-substrate part of the blue dimer.



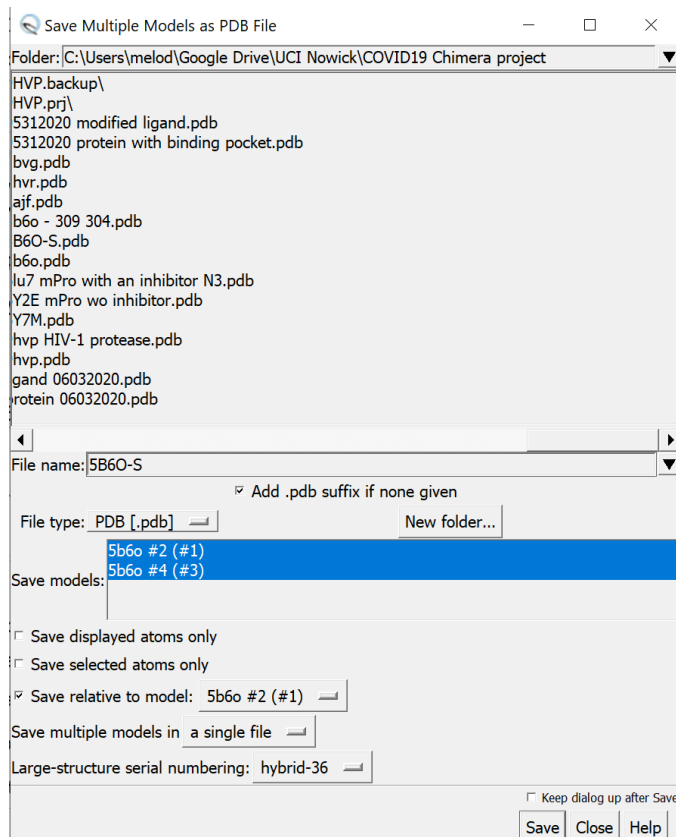
Actions → atoms/bonds → delete.



Now we should only have the monomer of the green dimer containing the binding pocket and C-terminal substrate of the blue dimer left. We can see the C-terminus of the blue dimer is interacting with the binding pocket of the green monomer.

7.4. Saving the modified PDB file

File → *save PDB* → select “save multiple models in a single file” → give the PDB file a valid file name (e.g., 5B6O-S) → save



8. References

- (1) Pettersen, E. F.; Goddard, T. D.; Huang, C. C.; Couch, G. S.; Greenblatt, D. M.; Meng, E. C.; Ferrin, T. E. UCSF Chimera - A Visualization System for Exploratory Research and Analysis. *J. Comput. Chem.* **2004**, *25*, 1605–1612.
- (2) UCSF Chimera Home Page <https://www.cgl.ucsf.edu/chimera/> (accessed Aug 6, 2020).
- (3) [Chimera-users] Is it possible to undo an action?
<http://plato.cgl.ucsf.edu/pipermail/chimera-users/2004-June/000172.html> (accessed Aug 6, 2020).

- (4) Muramatsu, T.; Takemoto, C.; Kim, Y. T.; Wang, H.; Nishii, W.; Terada, T.; Shirouzu, M.; Yokoyama, S. SARS-CoV 3CL Protease Cleaves Its C-Terminal Autoprocessing Site by Novel Subsite Cooperativity. *Proc. Natl. Acad. Sci. U. S. A.* **2016**, *113*, 12997–13002.
- (5) [Chimera-users] surface failures <http://plato.cgl.ucsf.edu/pipermail/chimera-users/2009-April/003816.html> (accessed Aug 6, 2020).
- (6) Shapovalov, M. V.; Dunbrack, R. L. A Smoothed Backbone-Dependent Rotamer Library for Proteins Derived from Adaptive Kernel Density Estimates and Regressions. *Structure* **2011**, *19*, 844–858.
- (7) Wang, J.; Wang, W.; Kollman, P. A.; Case, D. A. Automatic Atom Type and Bond Type Perception in Molecular Mechanical Calculations. *J. Mol. Graph. Model.* **2006**, *25*, 247–260.
- (8) Oleg, T.; Arthur J., O. AutoDock Vina: Improving the Speed and Accuracy of Docking with a New Scoring Function, Efficient Optimization, and Multithreading. *J. Comput. Chem.* **2010**, *31*, 2967–2970.
- (9) Autodock Vina - molecular docking and virtual screening <http://vina.scripps.edu/index.html> (accessed Aug 6, 2020).
- (10) Autodock Vina
<https://www.cgl.ucsf.edu/chimera/docs/ContributedSoftware/vina/vina.html> (accessed Aug 6, 2020).
- (11) RCSB PDB - 6YB7: SARS-CoV-2 main protease with unliganded active site (2019-nCoV, coronavirus disease 2019, COVID-19) <https://www.rcsb.org/structure/6YB7> (accessed Aug

7, 2020).